THE

LONDON, EDINBURGH, AND DUBLIN

PHILOSOPHICAL MAGAZINE

AND

JOURNAL OF SCIENCE.

[SEVENTH SERIES.]

MAY 1930.

LXXXII. *Dipoles in Relation to the Anomalous Properties of Dielectrics.* *By* S. WHITEHEAD, *M.A.*, *A.M.I.E.E.**

PREFACE.

IN studying the properties of ebonite as a dielectric at various frequencies it has been observed that the losses at low stresses expressed as power factor are practically constant over a range of frequencies from power frequencies up to millions per second, but there is an anomaly in the neighbourhood of 1000 cycles, in which part of the range the power factor is decreased.

Several hypothetical explanations have been suggested and are under consideration. This report covers the application of the Dipole Theory of Debye to anomalous properties of dielectrics.

CONTENTS.

		Page
I.	Introduction—The Dipole Theory	866
II.	Anomalous Properties (including Secondary Field)	868
III.	Anomalous Effects (neglecting Secondary Field)	873
IV.	Other Effects	875
V.	Experimental Work	875
	Appendix	876

* Report Ref. L/T 34 received from the British Electrical and Allied Industries Research Association.

I. Introduction—The Dipole Theory.

THE dipole theory was first introduced by Debye in order to explain the large temperature coefficients of the specific inductive capacities of the alcohols. Previous theories, such as those of Faraday, Mossotti, and Lorentz, which involved the assumption either of conducting particles or of an actual displacement of charges within the molecule or atom, were unable to account for the large variation of this induced polarization with temperature which is observed in some cases. Debye adopted Langevin's theory of paramagnetism. He assumed that there are dipoles of fixed electric moment in the medium, just as there are molecular or atomic magnets in a paramagnetic medium. Normally these dipoles have a random distribution, so that the component of density of electric moment in any direction, *i. e.*, the polarization, cancels out, and there is no resultant field. When, however, an electric field is applied the dipoles tend to orientate themselves in the direction of the field according to Boltzmann's law, since they have a potential energy depending on orientation. They may indeed have a definite orientation under exceptional circumstances without an electric field, as, for example, if an "electret" is solidified in an electric field. The dipoles move more easily when liquid than when solid, so that they align themselves while liquid and are caught in that position when solid. On removal of the field the "electret" continues to have a polarization which may continue for some months.

Generally, however, the dipoles do not align until an electric field is applied. The proportion in any direction can then be calculated, assuming Boltzmann's law as above. To a first approximation (at not very high field strengths) this distribution is given by

$$f = \mathrm{A}\left(1 + \frac{\mu \mathrm{F}}{k\mathrm{T}} \cos\theta\right). \quad . \quad . \quad . \quad . \quad . \quad (1)$$

(See Appendix (*a*) (2)),

where

$f d\Omega$ = number of dipoles per c.c. pointing in direction indicated in solid angle $d\Omega$,

μ = dipole moment,

k = Boltzmann's constant,

T = absolute temperature,

θ = angle of orientation of dipoles,

F = field strength.

From this the polarization or electric moment per c.c., P, can be calculated, since

$$P = 4\pi \int_0^{\pi} \mu f \cos\theta 2\pi \sin\theta d\theta, \quad . \quad . \quad . \quad (2)$$

where N = number of dipoles per c.c.

Thus we obtain the expression

$$P = 4\pi\mu^2 FN/3kT. \quad . \quad . \quad . \quad . \quad . \quad (3)$$

F is the total inducing field, that is, the external field together with that due to neighbouring molecules, so that, if ϵ is the specific inductive capacity,

$$\frac{\epsilon - 1}{\epsilon + 2} = b + 4\pi\mu^2 N/9kT. \quad . \quad . \quad . \quad . \quad (4)$$

(See Appendix (*a*) (4)),

where b = polarization arising from other causes, *e. g.*, a separation of charges, as in Lorentz's theory, or surface charges at different layers.

The form of variation of ϵ with temperature has been verified for a number of liquids and gases and some viscous materials. On the whole the theory has been satisfactorily verified qualitatively in those cases where dipoles might be expected. Quantitatively the theory is not so satisfactory, but the agreement is good in some instances. Certain refinements have been made to Debye's original theory, but no unquestioned improvement has resulted. The average values of the dipole moments work out of the order of 10^{-18} e.s.u.

In arriving at the above results it has been assumed that the dipoles are quite free to move, their directions being altered by collisions. In gases this is probably the case, but in liquids, and certainly in solids, retarding forces of a frictional nature will oppose the motion, and the movement of dipoles will result in heating, while they will not reach their most probable distribution for appreciable periods of time. Now this effect can be taken into account and brought in relation with the effective viscosity of the medium, and the following approximate equation is found for f:—

$$\rho \frac{\partial f}{\partial t} \frac{1}{\sin\theta} \frac{\partial}{\partial\theta} \left\{ \sin\theta \left(kT \frac{\partial f}{\partial\theta} + A\mu F \sin\theta \right) \right\} \quad . \quad (5)$$

(See Appendix (*b*), equation (8)),

where

ρ = frictional resistance coefficient = $8\pi\eta a^3$ for a fluid, if η = viscosity, a = radius of molecule,

t = time,

A = constant depending on number of dipoles, etc.

From the presence of this frictional resistance arise :

(1) A varying capacity current or absorption current.

(2) An energy loss in the dielectric, that is a power loss and power factor.

II. Anomalous Properties (including Secondary Field).

(a) *Absorption Current.*

If F is constant, then one of the solutions of (5) is

$$f = \mathrm{A}\left[1+\frac{\mathrm{A}\mu\mathrm{F}\cos\theta}{k\mathrm{T}}\left(1-e^{-\frac{2tk\mathrm{T}}{\rho}}\right)\right]. \quad . \quad . \quad (6)$$

(See Appendix (*c*), equation (10).)

From (6) the polarization can be found from (2), whence, as in (4), the following equation is obtained :—

$$\frac{\epsilon-1}{\epsilon+2} = b+\frac{4\pi\mu^2\mathrm{N}}{9k\mathrm{T}}\left(1-e^{-\frac{2tk\mathrm{T}}{\rho}}\right), \quad . \quad . \quad . \quad (7)$$

and

$$2+\epsilon = 3\Big/\left[1-b-a\left(1-e^{-\frac{2tk\mathrm{T}}{\rho}}\right)\right], \quad . \quad . \quad . \quad (8)$$

where

$$a = \frac{4\pi\mu^2\mathrm{N}}{9k\mathrm{T}}.$$

For a condenser of unit geometric capacity and unit thickness the capacity current is

$$i = \mathrm{F}\frac{\partial\epsilon}{\partial t}$$

$$= \mathrm{F}\frac{6k\mathrm{T}a}{\rho}e^{-\frac{2tk\mathrm{T}}{\rho}}\Big/\left\{1-b-a\left(1-e^{-\frac{2tk\mathrm{T}}{\rho}}\right)\right\}^2. \quad . \quad (9)$$

This gives an absorption current which decreases nearly

exponentially to zero with time, but not quite so rapidly (see fig. 1 (*a*)). The initial value is finite and given by

$$6\mathrm{F}k\mathrm{T}a/\rho(1-b)^2.$$

Returning to equation (6), it is seen that, after a field F_1 has been applied for t_0 seconds, the distribution f is given by

$$f = \mathrm{A}\left[1+\frac{\mu\mathrm{F}_1\cos\theta}{k\mathrm{T}}\left(1-e^{-\frac{2tk\mathrm{T}}{\rho}}\right)\right].$$

Fig. 1.

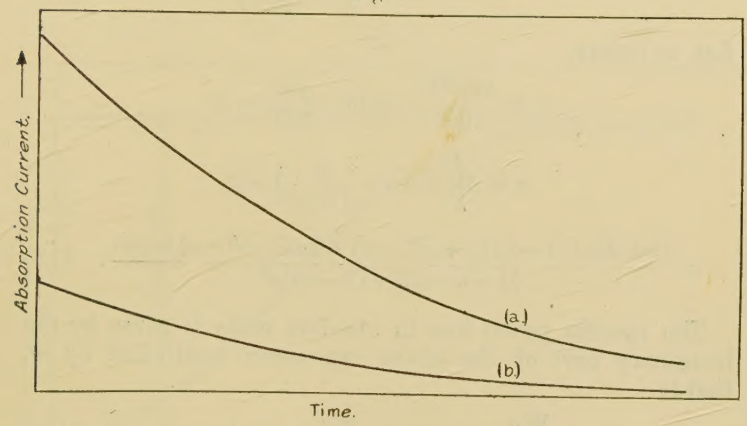

Absorption current/time curves.

If now a field F_2 is applied for a further t seconds a distribution which satisfies the differential equation and the conditions is given by

$$f = \mathrm{A}\left\{1+\frac{\mu\mathrm{F}_1\cos\theta}{k\mathrm{T}}\left(1-e^{-\frac{2(t+t_0)k\mathrm{T}}{\rho}}\right)+\frac{\mu(\mathrm{F}_2-\mathrm{F}_1)\cos\theta}{k\mathrm{T}}\left(1-e^{-\frac{2tk\mathrm{T}}{\rho}}\right)\right\} \quad . \quad . \quad . \quad (10)$$

(See Appendix (*d*), equation (14).)

From the form of equation (10) it would appear that the absorption current due to dipoles obeys the Super-position Principle.

(b) *Power Loss in Alternating Fields.*

It is here necessary to find a solution of (5) when

$$\mathrm{F} = \mathrm{F}_0 e^{j\omega t},$$

where $\omega = 2\pi$ frequency.

Such a solution is given by

$$f = A\left[1 + \frac{1}{\left(1 + \frac{j\rho\omega}{2kT}\right)} \frac{\mu}{kT} F\cos\theta\right] \quad . \quad . \quad . \quad (11)$$

(See Appendix, equation (15).)

Thus

$$\frac{\epsilon - 1}{\epsilon + 2} = b + \frac{4\pi\mu^2 N}{9kT\left(1 + \frac{j\rho\omega}{2kT}\right)} \quad . \quad . \quad . \quad . \quad (12)$$

Let, as before,

$$a = \frac{4\pi\mu^2 N}{9kT} \quad \text{and} \quad \frac{\rho\omega}{2kT} = x,$$

$$\epsilon = 3\Big/\left(1 - b - \frac{a}{1 + jx}\right) - 2$$

$$= \frac{(1+2b)\left[(1-b)(1+x^2) - a\right] + 2a(1-b-a) - jxa}{(1-b-a)^2 + (1-b)^2x^2} \quad . \quad (13)$$

The specific power loss in absolute units is given by the imaginary part of the above expression multiplied by ω, that is

$$\frac{W\rho}{2kT} = \frac{x^2 a}{(1-b-a)^2 + (1-b)^2x^2} \quad . \quad . \quad . \quad . \quad (14)$$

The power loss is zero at zero frequency, and then rises, as in fig. 2, and finally tends asymptotically to a maximum value at high frequencies given by

$$\frac{a2kT}{(1-b)^2\rho};$$

that is

$$W_{max.} = \frac{2kT}{\rho} \frac{P(\text{due to dipoles})}{(1 - P(\text{without dipoles}))^2} \quad . \quad . \quad (15)$$

P = polarization.

Again,

$$\frac{W}{W_{max.}} = 1\Big/1 + \left(1 - \frac{a}{1-b}\right)^2 \frac{1}{x^2}$$

$$= 1\Big/1 + \frac{1}{x^2}\left(\frac{\epsilon(\text{without dipoles}) + 2}{\epsilon(\text{D.C.}) + 2}\right)^2 . \quad (16)$$

Since a varies as 1/T, $W_{max.}$ should be independent of temperature. Since also $W/W_{max.}$ is a function of $\rho\omega/2kT$, W should decrease with temperature if ρ is constant. It is, however, highly probable that ρ varies with temperature, particularly with solids, and if, as is to be expected, ρ decreases with temperature, $W_{max.}$ will increase with temperature. Owing, however, to the fact that ω/T is a parameter in the expression for the loss, the latter will decrease with temperature for a given frequency. Such an effect is only occasionally observed, and then only over a limited range.

Fig. 2.

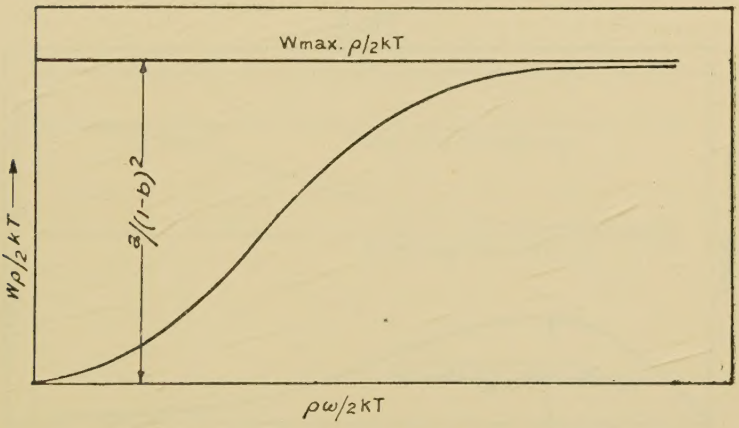

Variation of specific power loss with frequency.

(c) *Power Factor.*

If the loss angle is small, then $\tan\delta$ may be taken instead of $\sin\delta$. With this assumption the power factor becomes from (13)

$$\left.\begin{matrix}\text{Power}\\ \text{factor}\end{matrix}\right\} = \tan\delta = \frac{ax}{(1+2b)[(1-b)(1+x^2)-a]+2a(1-b-a)} \quad . \quad . \quad . \quad (17)$$

Thus the power factor increases with frequency up to a maximum for the frequency given by

$$\frac{\rho\omega}{2kT} = \sqrt{\left(1-\frac{a}{1-b}\right)\left(1+\frac{2a}{1+2b}\right)}, \quad . \quad . \quad (18)$$

and then decreases asymptotically towards zero (see fig. 3).

The maximum value of $\tan\delta$ is given by

$$(\tan\delta)_{\max.} = \frac{a}{2}\Big/(1-b)\sqrt{(1+2b)\left(1-\frac{a}{1-b}\right)(1+2b+2a)} \quad . \quad . \quad . \quad (19)$$

From the present result and from those concerning power loss it is probable that dipole losses occur alone only very rarely. It is nevertheless possible that the presence of a component of loss due to dipoles may account for some of the divergences from general relations such as Schweidler's laws. Maxima and minima in the power factor could be

Fig. 3.

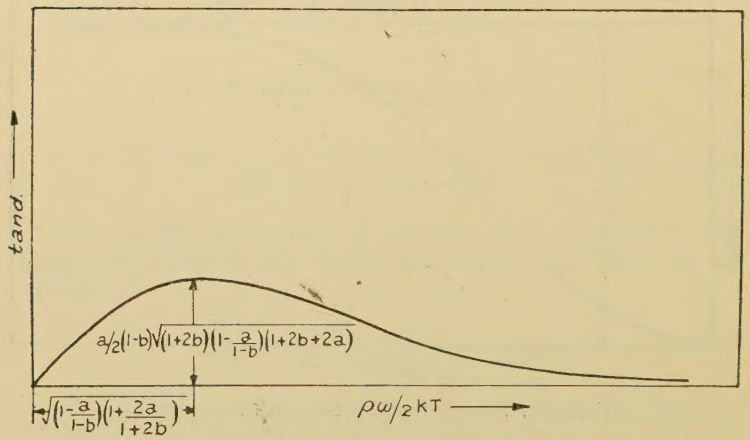

Variation of power factor with frequency.

explained by the effect of dipoles coming into action at different frequencies. It may be noted that

$$\omega = \frac{2k\mathrm{T}}{\rho}$$

is of the order of 10^{10} for water at normal temperatures. It would be much less for solids, owing to greater viscosity.

$$b = \frac{\epsilon-1}{\epsilon+2} \quad \text{(when there are no dipoles)},$$

$$a = \frac{\epsilon-1}{\epsilon+2} \quad \text{(when only dipoles are considered)} ;$$

a and b are thus always less than unity.

(d) *Permittivity.*

From equation (13) the following expression for the permittivity K is found :—

$$K = \frac{\sqrt{\{(1+2b)[(1-b)(1+x^2)-a]+2a(1-a-b)\}^2+a^2x^2}}{(1-a-b)^2+a^2x^2} \quad . \quad . \quad . \quad (20)$$

According to this equation the permittivity decreases with frequency from the value for the S. I. C. at zero frequency to the value when the dipoles no longer have any effect upon permittivity ; the reason being that for extremely high

Fig. 4.

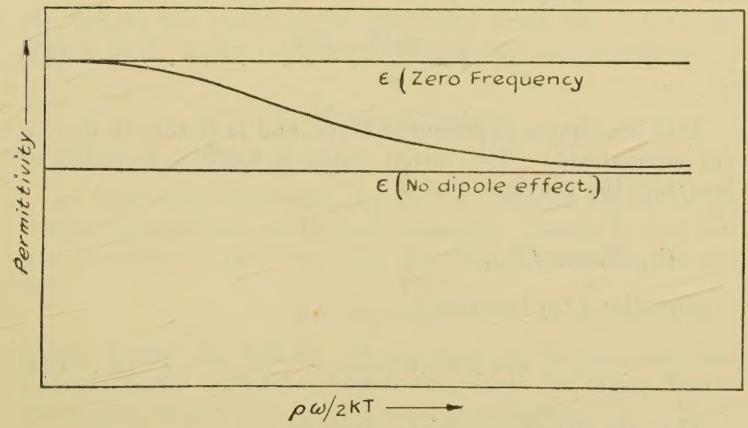

Variation of permittivity with frequency.

frequencies they hardly move at all during a cycle, and therefore contribute little to the capacity current. The form of variation of K is shown in fig. 4. It may be noted that for liquids little variation in frequency occurs up to the order of 10^6 p.p.s., but with solids, where the viscosity is much larger, variation should be observed at lower frequencies.

III. Anomalous Effects (neglecting Secondary Field).

Under Section I. above the field due to the induced polarization was taken into account when dealing with the field which tends to align the dipoles. The equations are

much simplified if only the impressed external field is supposed to affect the dipoles. Equation (4) becomes

$$\epsilon = 1+b+4\pi\mu^2 N/9kT, \quad . \quad . \quad . \quad . \quad (21)$$

since now $\epsilon = 1+P/F$. ϵ in the above equation refers to the S. I. C. in constant fields.

(a) *Absorption Current.*

Equation (8) now becomes

$$\epsilon = 1+b+a\left(1-e^{-\frac{2tkT}{\rho}}\right), \quad . \quad . \quad . \quad . \quad (22)$$

and the charging current is

$$i = \frac{2akT}{\rho} e^{-\frac{2tkT}{\rho}} \quad . \quad . \quad . \quad . \quad . \quad . \quad (23)$$

This is a simple exponential form, and is shown on fig. 1 *a* for comparison. The initial value is $2akT/\rho$, *i. e.*, 1/3 or less than the previous value.

(b) *Power Loss.*

Equation (13) becomes

$$\epsilon = 1+b+\frac{a}{1+x^2}-\frac{jax}{1+x^2}. \quad . \quad . \quad . \quad (24)$$

Thus the specific power is given by

$$W = \frac{ax^2}{1+x^2}\frac{2kT}{\rho}, \quad . \quad . \quad . \quad . \quad . \quad (25)$$

and the same remarks as in Section II. (*b*) apply here also:

$$W_{max.} = \frac{2akT}{\rho}, \quad . \quad . \quad . \quad . \quad . \quad (26)$$

$$\frac{W}{W_{max.}} = \frac{x^2}{1+x^2}. \quad . \quad . \quad . \quad . \quad . \quad (27)$$

These equations correspond to equations (15) and (16), but it now appears that $W/W_{max.}$ should be independent of the nature of the material except its effective viscosity towards dipole movements.

(c) *Power Factor*:

$$\tan\delta = \frac{ax}{(1+b)(1+x^2)+a}; \quad . \quad . \quad . \quad (28)$$

$\tan\delta$ increases to a maximum for

$$\frac{\rho\omega}{k\mathrm{T}} = \sqrt{\frac{1+a+b}{1+b}} = \sqrt{\frac{\epsilon_{\text{D.C.}}}{\epsilon_{\text{without dipoles}}}},$$

$$(\tan\delta)_{\max.} = a/2\sqrt{(1+b)(1+a+b)}. \quad . \quad . \quad (29)$$

(d) *Permittivity*:

$$\mathrm{K} = \sqrt{[(1+b)(1+x^2)+a]^2+a^2x^2}/1+x^2. \quad . \quad (30)$$

As before, the permittivity decreases from the S. I. C. for steady fields to the value when the dipoles have no effect.

IV. Other Effects.

(*a*) *High Field Strengths.*

At high field strengths the S. I. C. due to dipoles is no longer independent of the field strength. The S. I. C. ϵ and the permittivity decrease with the field F according to the law

$$\epsilon = \mathrm{A}_0 - \mathrm{A}_1\mathrm{F}^2. \quad . \quad . \quad . \quad . \quad . \quad (31)$$

The power loss would increase and no longer obey the Square Law. Evidence, however, even for cases where anomalous effects may be neglected is uncertain.

(b) *Magnetic Fields.*

If the dipole has also a comparable magnetic moment then the anomalous phenomena and the S. I. C. will be altered in the presence of a magnetic field. In most cases, however, the susceptibility of dielectrics would appear too small for an effect of this particular type to be of great consequence. It is, however, known that in some cases the properties of dielectrics are affected by a magnetic field.

V. Experimental Work.

As mentioned above, the effect of dipoles upon anomalous dispersion has for some years been known and investigated in the case of liquids. More recently the effect has been

applied to viscous dielectrics at commercial frequencies with some success (Kitchin and Muller, 'Physical Review,' pp. 979–987, xxxii. no. 6, Dec. 1928). These authors experimented with castor-oil and rosin, and obtained a variation of power factor and permittivity with temperature of a type predicted by theory.

The present paper was in manuscript form three years ago, and was received by the E. R. A. previous to the article referred to above. It is therefore felt that there is sufficient reason for issue at this date on this account, and because the treatment is slightly different from that given by the above authors. The latter take Debye's expression for the absorption coefficient α, and make use of the following relation for the power factor :

$$\text{power factor} = 2\alpha/(1-\alpha^2),$$

and find the maximum value of α and the power factor in terms of the permittivity ϵ at zero and infinity (ϵ_0 and ϵ_∞).

The present paper was rather intended to show the analogies and differences between the dipole theory and other theories (*e. g.*, Pellat, Schweidler, Wagner, and Décombe) of the anomalous properties of dielectrics.

Appendix.

(a) *Normal Dipole Effect.*

Let

μ = dipole moment,

f = number of dipoles pointing in directions θ contained in solid angle $d\Omega$,

F = field strength (supposed uniform),

P = polarization of medium,

E = field affecting dipoles (supposed uniform),

N = number of dipoles per c.c.,

k = Boltzmann's constant,

T = absolute temperature,

ϵ = specific inductive capacity.

Each dipole has a potential energy given by $\mu E \cos\theta$ with reference to the field E.

Thus

$$f = \mathrm{A}e^{\frac{\mu \mathrm{E}\cos\theta}{k\mathrm{T}}} \quad . \quad . \quad . \quad . \quad . \quad . \quad . \quad (1)$$

$$= \mathrm{A}\left(1 + \frac{\mu \mathrm{E}\cos\theta}{k\mathrm{T}}\right) \quad . \quad . \quad . \quad . \quad . \quad (2)$$

to a first approximation.

The total electric moment per c.c. in direction of E is

$$\mathrm{P} = 4\pi \int_0^\pi f \mu \cos\theta d\Omega$$

$$= 4\pi \int_0^\pi \mathrm{N}\left(1 + \frac{\mu \mathrm{E}\cos\theta}{k\mathrm{T}}\right)\cos\theta d(\cos\theta)$$

$$= 4\pi\mu^2 \mathrm{EN}/3k\mathrm{T}. \quad . \quad . \quad . \quad . \quad . \quad . \quad . \quad . \quad (3)$$

But $\mathrm{E} = \mathrm{F} + \mathrm{P}/3$ (Larmor's theory).

The total induction $= \mathrm{D} = \mathrm{F} + \mathrm{P} = \epsilon\mathrm{F}$.

$$\therefore \quad \mathrm{P} = (\epsilon - 1)\mathrm{F};$$

$$\therefore \quad \mathrm{E} = \mathrm{F}(\epsilon + 2)/3;$$

$$\therefore \quad \mathrm{P}/\mathrm{E} = 3\mathrm{P}/\mathrm{F}(\epsilon + 2)$$

$$= \frac{3(\epsilon - 1)}{(\epsilon + 2)}.$$

Thus

$$\left[\frac{\epsilon - 1}{\epsilon + 2}\right] = 4\pi\mu^2 \mathrm{N}/9k\mathrm{T}$$

when dipoles alone are considered.

To this must be added the polarization due to other causes, which in the present memorandum is taken, for convenience, to be independent of temperature and frequency, although in practice it will not usually be so.

Accordingly

$$\frac{\epsilon - 1}{\epsilon + 2} = b + \frac{4\pi\mu^2 \mathrm{N}}{9k\mathrm{T}}, \quad . \quad . \quad . \quad . \quad . \quad (4)$$

when all effects are considered where the additional polarization $= b\mathrm{E}$.

The right-hand side of (4) may be called the specific polarization, so that

$$b = \text{specific polarization without dipoles,}$$

$$\frac{4\pi\mu^2 N}{9kT} = a = \text{specific polarization due to dipoles.}$$

If the secondary field were neglected, and E taken as equal to F, then

$$\epsilon = 1 + P/F$$
$$= 1 + b + a. \quad . \quad . \quad . \quad . \quad . \quad . \quad (5)$$

(b) *Effect of Frictional Resistance.*

The moment tending to resist the motion of the dipole may be taken as

$$\rho \frac{d\theta}{dt} = M,$$

where ρ is the coefficient of internal friction. For a fluid we may put

$$\rho = 8\pi\eta a^3,$$

where a = radius of dipole, η = viscosity of medium.

The mean motion of the dipoles, which may be supposed as oscillating round varying positions of equilibrium, can be treated analogously with Einstein's equations for the Brownian movement, and by direct substitution in Einstein's equation it is found

$$\frac{\partial f}{\partial t} = \frac{\Delta}{4T \sin\theta} \frac{\partial}{\partial\theta}\left(\sin\theta \frac{\partial f}{\partial\theta}\right) - \frac{1}{\rho \sin\theta} \frac{\partial}{\partial\theta} f M \sin\theta, \quad (6)$$

where

Δ = mean square motion,

T = elementary interval of time considered.

Again Einstein's equation for Δ may also be adopted, which becomes in this case

$$\frac{\Delta}{T} = kT/\rho.$$

Thus, finally,

$$\rho \frac{\partial f}{\partial t} = \frac{1}{\sin\theta} \frac{\partial}{\partial\theta}\left[\sin\theta\left(kT \frac{\partial f}{\partial\theta} - fM\right)\right]. \quad . \quad . \quad (7)$$

Now the couple on the dipole due to the field F is $\mu F \sin\theta$. Thus, in order to find f, we may put for an average

$$f\rho\frac{d\theta}{dt} = Mf = -A\mu F\sin\theta,$$

so that

$$\rho\frac{\partial f}{\partial t} = \frac{1}{\sin\theta}\frac{\partial}{\partial\theta}\left[\sin\theta\left(kT\frac{\partial f}{\partial\theta} + A\mu F\sin\theta\right)\right]. \quad (8)$$

(c) *Constant Fields.*

Let F be independent of t. Then (8) reduces to

$$\rho\frac{\partial f}{\partial t} = \frac{1}{\sin\theta}\frac{\partial}{\partial\theta}\left(\sin\theta kT\frac{\partial f}{\partial\theta}\right) + 2A\mu F\cos\theta. \quad . \quad (9)$$

Let

$$f = f_1 + \frac{2A\mu F\cos\theta t}{\rho}.$$

Then

$$\rho\frac{\partial f_1}{\partial t} = \frac{kT}{\sin\theta}\frac{\partial}{\partial\theta}\sin\theta\frac{\partial f_1}{\partial\theta} - \frac{4A\mu Ft}{\rho}kT\cos\theta.$$

Let

$$f_1 = f_2 - \frac{4A\mu Ft^2\cos\theta}{2\rho^2}.$$

Then

$$\rho\frac{\partial f_2}{\partial t} = \frac{kT}{\sin\theta}\frac{\partial}{\partial\theta}\sin\theta\frac{\partial f_2}{\partial\theta} + \frac{8A\mu Ft^2\cos\theta(kT)^2}{2\rho^2}.$$

Thus by successive approximation it is found that

$$f = \frac{A\mu F\cos\theta}{kT}\left[\frac{2tkT}{\rho} - \frac{1}{2!}\left(\frac{2kTt}{\rho}\right)^2 + \frac{1}{3!}\left(\frac{2kTt}{\rho}\right)^3\cdots\right].$$

We may also add $f = A$, which does not affect the solution obtaining.

$$f = A\left[1 + \frac{\mu F\cos\theta}{kT}\left(1 - e^{-\frac{2tkT}{\rho}}\right)\right]. \quad . \quad . \quad (10)$$

On substituting in (3) and determining ϵ, it follows that

$$\frac{\epsilon - 1}{\epsilon + 2} = b + a\left(1 - e^{-\frac{2tkT}{\rho}}\right). \quad . \quad . \quad . \quad (11)$$

Suppose $F = F_1$ for a period t_0, then at the end of the interval

$$f = A\left[1 + \frac{\mu F\cos\theta}{kT}\left(1 - e^{-\frac{2tkT}{\rho}}\right)\right]. \quad . \quad . \quad (12)$$

If F_1 is changed to F_2, then, after a further period t, f may be assumed as made up of two parts, ϕ and ψ.

$$f = \phi + \psi$$

$$= A\left[1 + \frac{\mu F_1 \cos\theta}{kT}\left(1 - e^{-\frac{2(t+t_0)kT}{\rho}}\right)\right]$$

$$+ \frac{A\mu(F_2 - F_1)\cos\theta}{kT}\left(1 - e^{-\frac{2tkT}{\rho}}\right). \quad . \quad (13)$$

On substituting in (9), it is seen that

$$\rho\frac{\partial\phi}{\partial t} = \frac{kT}{\sin\theta}\frac{\partial}{\partial\theta}\sin\theta\frac{\partial\phi}{\partial\theta} + 2A\mu F_1\cos\theta$$

and

$$\rho\frac{\partial\psi}{\partial t} = \frac{kT}{\sin\theta}\frac{\partial}{\partial\theta}\sin\theta\frac{\partial\phi}{\partial\theta} + 2A\mu(F_2 - F_1)\cos\theta.$$

$$\therefore \quad \rho\frac{\partial(\phi+\psi)}{\partial t} = \frac{kT}{\sin\theta}\frac{\partial}{\partial\theta}\sin\theta\frac{\partial(\phi+\psi)}{\partial\theta} + 2A\mu F_2\cos\theta.$$

. . . (14)

Thus, over the period t_0 to $t_0 + t$ expression (13) satisfies the general condition (9). Further, when $t = 0$,

$$f = A\left[1 + \frac{\mu F_1\cos\theta}{kT}\left(1 - e^{-\frac{2t_0kT}{\rho}}\right)\right],$$

so that (13) satisfies the conditions of the problem.

(d) *Alternating Fields.*

In this case $F = F_0 e^{j\omega t}$ where $\omega = 2\pi$ frequency. Put

$$f = A(1 + \phi e^{j\omega t})$$

in (9). Then

$$\frac{\rho j\omega\phi}{kT} = \frac{1}{\sin\theta}\frac{d}{d\theta}\sin\theta\frac{d\phi}{d\theta} + 2\mu F_0\cos\theta. \quad . \quad . \quad (15)$$

The solution of this is

$$\phi = \frac{1}{1 + \frac{j\rho\omega}{2kT}}\frac{\mu F_0\cos\theta}{kT}.$$

Thus

$$f = A\left[1 + \frac{1}{1 + \frac{j\rho\omega}{2kT}}\frac{\mu}{kT}F_0 e^{j\omega t}\cos\theta\right]. \quad . \quad (16)$$

LXXXIII. *The Free and Forced Symmetrical Oscillations of Thin Bars, Circular Diaphragms, and Annuli.* *By* A. G. Warren, *M.Sc., M.I.E.E., F.Inst.P., Research Department, Woolwich* *.

THE use, within recent years, of circular diaphragms of considerable size as acoustic generators in wireless loud-speakers and in gramophones has awakened an extended interest in their operation. The case of the free edge rigid disk was investigated by Rayleigh ('Sound,' ii. p. 162 *et seq.*) ; recently that analysis has been extended by McLachlan (Proc. Roy. Soc. cxxii. p. 604 ; Phil. Mag. Suppl. June 1929, p. 1011). Such a generator is capable of excellent results over the lower portion of the musical scale, but the output falls off rapidly at high frequencies. The range of uniform reproduction may be extended by reduction of mass of the moving system, but mechanical rigidity is thereby lost, and the basic assumption of the theory is no longer applicable.

The present work arose in an attempt to extend the theory somewhat further. McLachlan has shown that over the upper portion of the musical scale the acoustic reaction is but a small percentage of the accelerational forces. It has been assumed in what follows that the acoustic reaction is negligible. The results are applicable over the whole of the audible range if the mass of the diaphragm is considerable, over a more restricted portion if the mass is small. Though the investigation is but a limited addition to the theory of the speaker, the problem is presented as one of considerable interest in itself. The case of reeds, or thin bars, is included because the equations, while bearing a general resemblance to those for diaphragms, are much simpler and are more easily followed physically. Further, it is believed that at least some of the results relating to thin bars are new.

General Conditions of Free and Forced Oscillations.

The periods of the natural vibrations of reeds or thin bars have been determined by Rayleigh ('Sound,' i. chap. viii.). He has also determined the natural periods of a disk clamped at its edge. The avenue of approach to the problems is here rather different. The motion of the system is determined under the action of a harmonic force. The ratio, force divided by acceleration, measured at the place of application

* Communicated by the Author.

of the force, is the apparent mass of the system. This apparent mass is zero for one type of symmetrical natural vibration; it is infinite for another type. The natural oscillations are thus included as particular cases in the more general problem.

Free and Forced Vibrations of Reed.

Unless the bending of a vibrating reed is great, the energy of rotation is negligible. The conditions of statical equilibrium with regard to curvature are therefore applicable. At any section the curvature is proportional to the bending moment; the linear acceleration of any element of the bar

Fig. 1.

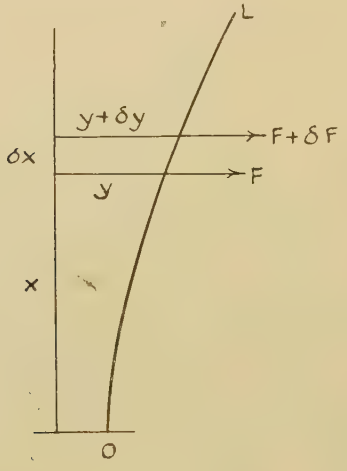

is proportional to the net force applied. Assuming a sinusoidal variation of all quantities, we have, therefore (fig. 1),

$$\frac{d^2y}{dx^2} = \mu \mathrm{M} \quad . \quad . \quad . \quad . \quad . \quad . \quad . \quad (1)$$

$$-\delta \mathrm{F} = m . \delta x . \frac{d^2y}{dt^2}, \quad . \quad . \quad . \quad . \quad . \quad . \quad (2)$$

where

M = bending moment at any section,
F = normal force at the section,
m = mass per unit length,
y = lateral displacement at a distance x,
μ = constant depending upon stiffness,
t = time.

Using $\frac{dM}{dx} = F$ and $\frac{d}{dt} \equiv j\omega$ (where $j = \sqrt{-1}$ and $\omega = 2\pi$. frequency), equations (1) and (2) become

$$\frac{d^2y}{dx^3} = \mu F, \quad . \quad . \quad . \quad . \quad . \quad . \quad (3)$$

and $$\frac{dF}{dx} = m\omega^2 y ; \quad . \quad . \quad . \quad . \quad . \quad . \quad (4)$$

or $$\frac{d^4y}{dx^4} = \mu\omega^2 m y$$

and $$\frac{d^4F}{dx^4} = \mu\omega^2 m F \Bigg\} ; \quad . \quad . \quad . \quad . \quad (5)$$

whence

$$y = X\cosh\gamma x + Y\sinh\gamma x + Z\cos\gamma x + W\sin\gamma x, \quad . \quad (6)$$

where $\gamma^4 = \mu\omega^2 m$.

The constants Y/X, Z/X, W/X are determined by the end conditions. If the oscillating force be applied at 0, the apparent mass M_a is given by

$$M_a = {}_{\mathrm{Lt}\, x=0} \left\{ -\frac{1}{\mu\omega^2}\frac{d^3y}{dx^3}\Big/ y \right\} = \frac{m}{\gamma} \cdot \frac{(W-Y)}{(X+Z)} \quad . \quad (7)$$

The range of γ is of interest. If we have a steel reed 1 cm. wide and $\frac{1}{2}$ mm. thick γ is approximately $1{\cdot}2 \times 10^{-2}\sqrt{\omega}$, or $3 \times 10^{-2}\sqrt{f}$. If the length l is 10 cm., γl varies from 1·8 to 30 between frequencies of 36 and 10,000.

Particular cases of interest are given by :—

(a) *End* L *free* ; *slope at* 0 *maintained unchanged.*

The constants of integration are determined by the conditions

$$\frac{d^3y}{dx^3} = 0 \quad \text{and} \quad \frac{d^2y}{dx^2} = 0 \text{ at } x = l \quad \text{and} \quad \frac{dy}{dx} = 0 \text{ at } x = 0,$$

giving

$$\left.\begin{aligned} \frac{Y}{X} &= -\frac{Cs+Sc}{1+Cc+Ss} \\ \frac{W}{X} &= \frac{Cs+Sc}{1+Cc+Ss} \\ \frac{Z}{X} &= \frac{1+Cc-Ss}{1+Cc+Ss} \end{aligned}\right\}, \quad . \quad . \quad . \quad . \quad (8)$$

where $C \equiv \cosh \gamma l$, $S \equiv \sinh \gamma l$, $c \equiv \cos \gamma l$, $s \equiv \sin \gamma l$, and the apparent mass

$$M_a = \frac{m}{\gamma} \cdot \frac{Cs + Sc}{1 + Cc}. \quad . \quad . \quad . \quad . \quad . \quad (9)$$

When γ is very small (9) reduces to ml, the mass of the reed. Fig. 2 shows the change of apparent mass with

Fig. 2.

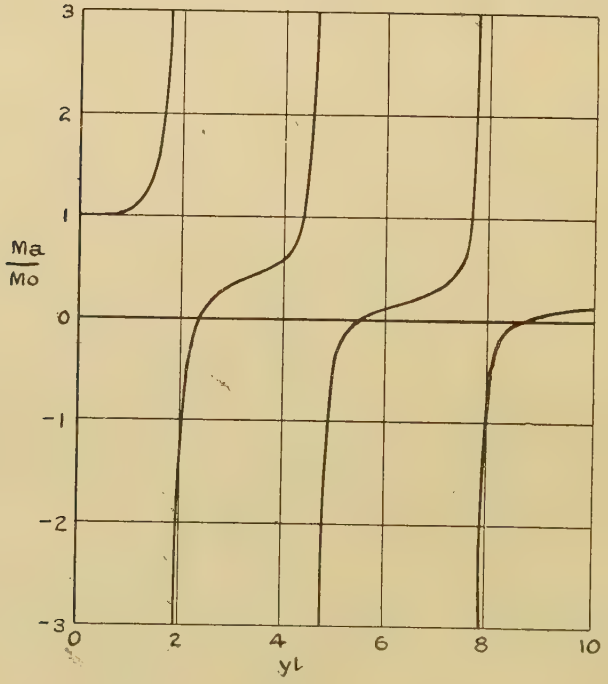

Showing change of apparent mass of reed with frequency.

frequency, and fig. 3 the form of the reed at various typical frequencies. The apparent mass is infinite when

$$Cc = -1. \quad . \quad . \quad . \quad . \quad . \quad . \quad . \quad . \quad (10)$$

The end 0 is then stationary, and equation (10) gives the natural frequencies of a reed clamped at one end. This condition is fulfilled by $\gamma l = 1\,875\ldots, 4{\cdot}694\ldots, 7{\cdot}854\ldots$, etc.

(Rayleigh, i. p. 278). It is easy to show that the displacement of the free end of the reed is then

$$y_l = \pm 2X. \quad . \quad . \quad . \quad . \quad . \quad . \quad (11)$$

At high frequencies, when 1/C becomes negligible, the apparent mass becomes

$$M_a = \frac{m}{\gamma}.(1 + \tan \gamma l). \quad . \quad . \quad . \quad . \quad (12)$$

Fig. 3.

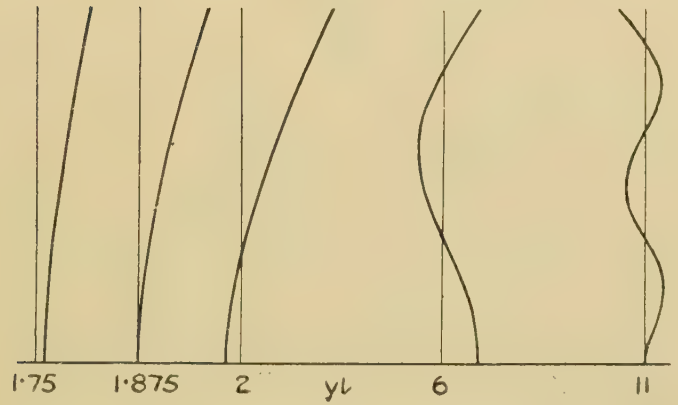

Showing form assumed by reed at various frequencies. The first three cases illustrate the changes consequent upon passing through a frequency of natural oscillations.

The apparent mass is zero when

$$Cs + Sc = 0. \quad . \quad . \quad . \quad . \quad . \quad . \quad (13)$$

This case is clearly that of the natural *symmetrical* vibrations of a reed $2l$ in length, free at both ends.

(b) *Both ends free.*

The constants of integration are determined from the conditions

$$\frac{d^3y}{dx^3} = 0 \quad \text{and} \quad \frac{d^2y}{dx^2} = 0 \text{ at } x = l \quad \text{and} \quad \frac{d^2y}{dx^2} = 0 \text{ at } x = 0,$$

giving

$$\left.\begin{aligned}\frac{Y}{X} &= \frac{-1+Cc-Ss}{Cs-Sc}\\ \frac{W}{X} &= \frac{1-Cc-Ss}{Cs-Sc}\\ \frac{X}{Z} &= 1\end{aligned}\right\}, \quad . \quad . \quad . \quad . \quad . \quad (14)$$

and the apparent mass

$$M_a = \frac{m}{\gamma}.(1-Cc). \quad . \quad . \quad . \quad . \quad . \quad (15)$$

The natural oscillations are given by

$$Cc = +1. \quad . \quad . \quad . \quad . \quad . \quad . \quad (16)$$

For a reed of length $2l$ the natural oscillations are similarly given by

$$\text{Cosh}\, 2\gamma l \,.\, \cos 2\gamma 1 = 1, \quad . \quad . \quad . \quad . \quad (17)$$

which may be written

$$(Cs+Sc)\,(Cs-Sc) = 0. \quad . \quad . \quad . \quad . \quad (18)$$

$Cs+Sc = 0$ (13) gives the symmetrical oscillations (see above).

$Cs-Sc = 0$ (19) gives the natural oscillations for which the centre of the reed is a point of inflexion. The symmetrical oscillations occur when $2\gamma l = 4{\cdot}730\ldots, 10{\cdot}995\ldots, 17{\cdot}278\ldots$, etc.; the asymmetrical oscillations when $2\gamma l = 7{\cdot}853\ldots$, $14{\cdot}137\ldots$, etc. (compare Rayleigh, i. pp. 277, 278).

(c) L *clamped, so that position and slope are maintained unchanged; slope at* 0 *maintained unchanged.*

The constants of integration are determined by the conditions

$$\frac{dy}{dx} = 0 \quad \text{and} \quad y = 0 \text{ at } x = l; \qquad \frac{dy}{dx} = 0 \text{ at } x = 0,$$

giving

$$\left.\begin{aligned}\frac{Y}{X} &= \frac{Cs+Sc}{1-Cc-Ss}\\ \frac{W}{X} &= -\frac{Cs+Sc}{1-Cc-Ss}\\ \frac{Z}{X} &= \frac{1-Cc+Ss}{1-Cc-Ss}\end{aligned}\right\}, \quad . \quad . \quad . \quad . \quad (20)$$

and the apparent mass

$$M_a = -\frac{m}{\gamma}\cdot\frac{Cs+Sc}{1-Cc}. \quad . \quad . \quad . \quad . \quad (21)$$

Hence the symmetrical natural vibrations of a reed of length $2l$, clamped at both ends, are given by

$$Cs+Sc=0, \quad . \quad . \quad . \quad . \quad . \quad . \quad (22)$$

and the complete system of natural vibrations is given by

$$\text{Cosh}\,2\gamma l\,.\cos 2\gamma l = 1, \quad . \quad . \quad . \quad . \quad (23)$$

or $$(Cs+Sc)\,(Cs-Sc)=0. \quad . \quad . \quad . \quad . \quad (24)$$

Fig. 4.

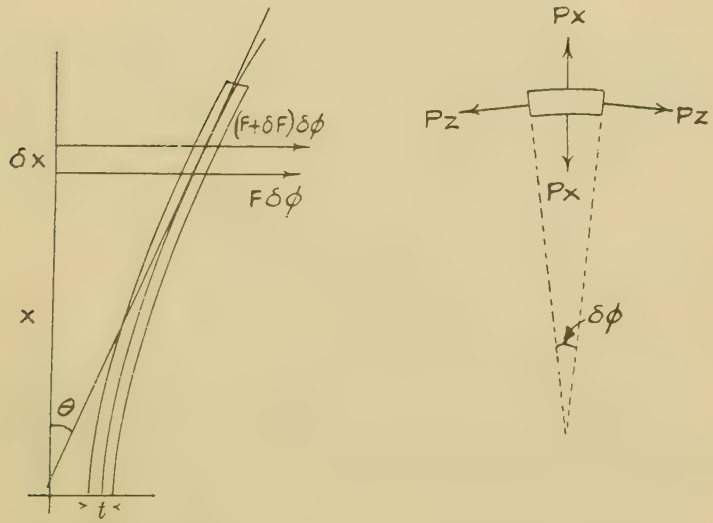

Equations (23) and (24) are identical with (17) and (18), showing that the natural periods of a reed *free* at both ends are the same as those of the same reed *clamped* at both ends (see Rayleigh, i. p. 275).

Free and Forced Vibrations of Diaphragm.

In this case, again, the rotational energy may be neglected and the form of an element of the diaphragm may be determined from the moments acting upon it. At unit distance from the neutral surface (fig. 4) the circumferential

strain is θ/x and the radial strain is $d\theta/dx$, giving the circumferential stress

$$p_z = \frac{E\sigma}{\sigma^2-1}\left(\sigma\frac{\theta}{x}+\frac{d\theta}{dx}\right), \quad . \quad . \quad . \quad . \quad (25)$$

and the radial stress

$$p_x = \frac{E\sigma}{\sigma^2-1}\left(\frac{\theta}{x}+\sigma\frac{d\theta}{dx}\right), \quad . \quad . \quad . \quad . \quad (26)$$

where E = Young's modulus.

σ = Poisson's ratio (expressed as a number greater than unity).

The moment on the element caused by the circumferential stress is

$$\frac{1}{12}\delta x\,.\,\delta\phi\,.\,t^3\,.\,\frac{E\sigma}{\sigma^2-1}\left(\sigma\frac{\theta}{x}+\frac{d\theta}{dx}\right).$$

The bending moment at a radius x caused by the radial stress is

$$\frac{1}{12}x\,.\,\delta\phi\,.\,t^3\,.\,\frac{E\sigma}{\sigma^2-1}\left(\frac{\theta}{x}+\sigma\frac{d\theta}{dx}\right),$$

and its contribution to the turning moment on the element is

$$\frac{1}{12}\delta x\,.\,\delta\phi\,.\,t^3\,.\,\frac{E\sigma}{\sigma^2-1}\left(\frac{d\theta}{dx}+\sigma\frac{d\theta}{dx}+\sigma x\frac{d^2\theta}{dx^2}\right).$$

From the equilibrium conditions we obtain

$$\frac{F\,.\,\delta\phi\,.\,\delta x}{2\pi} = \frac{1}{12}\delta x\,.\,\delta\phi\,.\,t^3\,.\,\frac{E\sigma^2}{\sigma^2-1}\left(x\frac{d^2\theta}{dx^2}+\frac{d\theta}{dx}-\frac{\theta}{x}\right). \quad (27)$$

where F is the total shearing force at a radius x.

Equation (27) may be rewritten

$$x\frac{d^3y}{dx^3}+\frac{d^2y}{dx^2}-\frac{1}{x}\frac{dy}{dx} = aF, \quad . \quad . \quad . \quad . \quad (28)$$

where $$\frac{1}{a} = \frac{\pi}{6}t^3\frac{E\sigma^2}{\sigma^2-1}.$$

If m is the mass of unit area of the diaphragm, we have

$$-\delta F = 2\pi x\,.\,\delta x\,.\,m\,.\,\frac{d^2y}{dt^2}, \quad . \quad . \quad . \quad . \quad (29)$$

or $$\frac{dF}{dx} = 2\pi\omega^2 mxy. \quad . \quad . \quad . \quad . \quad . \quad (30)$$

From (28) and (30) we obtain, writing $b = 2\pi\omega^2 m$,

$$\frac{d^4y}{dx^4} + \frac{2}{x}\frac{d^3y}{dx^3} - \frac{1}{x^2}\frac{d^2y}{dx^2} + \frac{1}{x^3}\frac{dy}{dx} - aby = 0, \quad . \quad (31)$$

which may be written

$$(\nabla^2 + k^2)(\nabla^2 - k^2)y = 0, \quad . \quad . \quad . \quad . \quad (32)$$

where $k^4 = ab$

(for the same material, of the same thickness, k has almost the same value as γ),

$$\text{and} \qquad \nabla^2 \equiv \frac{d^2}{dx^2} + \frac{1}{x}\frac{d}{dx}.$$

This is a Bessel equation, whose solution is

$$y = \mathrm{AJ}_0(kx) + \mathrm{BY}_0(kx) + \mathrm{CI}_0(kx) + \mathrm{DK}_0(kx). \quad . \quad (33)$$

In the case of an annular ring the constants of integration may be determined from the conditions obtaining at its inner and outer edges. Generally two equations are given by the conditions at the outer edge, and a third equation by the condition imposed at the inner edge by the method of attachment of the driving mechanism. These equations may be written respectively :

$$a_1\mathrm{A} + b_1\mathrm{B} + c_1\mathrm{C} + d_1\mathrm{D} = 0, \quad . \quad . \quad . \quad . \quad (34)$$

$$a_2\mathrm{A} + b_2\mathrm{B} + c_2\mathrm{C} + d_2\mathrm{D} = 0, \quad . \quad . \quad . \quad . \quad (35)$$

$$a_3\mathrm{A} + b_3\mathrm{B} + c_3\mathrm{C} + d_3\mathrm{D} = 0. \quad . \quad . \quad . \quad . \quad (36)$$

Their solution for B/A, C/A, D/A completely determines the motion for any value of k. For the natural oscillations a fourth equation (usually $\mathrm{F} = 0$ at $x = r$) is given by the extra condition postulated for the inner rim. It may be written

$$a_4\mathrm{A} + b_4\mathrm{B} + c_4\mathrm{C} + d_4\mathrm{D} = 0. \quad . \quad . \quad . \quad . \quad (37)$$

The frequencies of the natural vibrations are then given by

$$\begin{vmatrix} a_1 & b_1 & c_1 & d_1 \\ a_2 & b_2 & c_2 & d_2 \\ a_3 & b_3 & c_3 & d_3 \\ a_4 & b_4 & c_4 & d_4 \end{vmatrix} = 0. \quad . \quad . \quad (38)$$

When the annulus is driven at its inner rim the force exerted there is (from (28))

$$\mathrm{F} = \frac{k^3 r}{a}\{\mathrm{AJ}_1(kr) + \mathrm{BY}_1(kr) + \mathrm{CI}_1(kr) - \mathrm{DK}_1(kr)\}, \quad (39)$$

and the acceleration is

$$\frac{d^2y}{dt^2} = -\omega^2 y = -\omega^2\{AJ_0(kr) + BY_0(kr) + CI_0(kr) + DK_0(kr)\}. \quad . \quad . \quad . \quad . \quad (40)$$

Writing $\omega^2 a = k^4/2\pi m$, the apparent mass then becomes

$$M_a = -\frac{2\pi mr}{k}\left\{\frac{AJ_1(kr) + BY_1(kr) + CI_1(kr) - DK_1(kr)}{AJ_0(kr) + BY_0(kr) + CI_0(kr) + DK_0(kr)}\right\}. \quad . \quad . \quad . \quad . \quad (41)$$

Typical conditions which determine the coefficients in equations (34) to (36) may be considered. An edge (usually the outer) may be clamped in such a manner that its position and the slope in its neighbourhood are maintained ; or an edge (usually the inner) may be driven in such a way that as y changes dy/dx remains unaltered. In these cases no difficulty arises in expressing the conditions mathematically. The case of a free edge, however, has been a matter of discussion. One condition is, of course, that F disappears ; it is the other condition which is open to question. Here it is assumed that at a free edge (a) the radial stress disappears, (b) the expression for the radial stress given in equation (26) is applicable. Condition (b) is open to criticism. The diaphragms employed, however, are always thin and the distance from the edge at which condition (b) is fulfilled with practical accuracy must be but a small fraction of the radius of the disk. A similar assumption is made in connexion with the theory of beams, and then the error must be enormously greater. It seems reasonable to assume that any error introduced in the present case is negligible. We arrive, therefore, at the following equations for typical edge conditions. At radii where the displacement is zero we have

$$AJ_0(kx) + BY_0(kx) + CI_0(kx) + DK_0(kx) = 0 ; \quad (42)$$

where the slope is zero we have

$$AJ_1(kx) + BY_1(kx) - CI_1(kx) + DK_1(kx) = 0 ; \quad (43)$$

where F is zero we have

$$AJ_1(kx) + BY_1(kx) + CI_1(kx) - DK_1(kx) = 0 ; \quad (44)$$

and where the radial stress is zero

$$\frac{\sigma - 1}{\sigma . kx}\{AJ_1(kx) + BY_1(kx) - CI_1(kx) + DK_1(kx)\} - \{AJ_0(kx) + BY_0(kx) - CI_0(kx) - DK_0(kx)\} = 0. \quad (45)$$

Free Symmetrical Vibrations of Annulus or Disk with Clamped outside Edge, the Slope being maintained at the Inner Edge.

The particular example here considered is, in the case of the annulus, rather artificial. It has been chosen rather to illustrate the method, the equations being simpler than those of the annuli considered later, in which one or both of the edges are free. The diaphragm is supposed to be firmly clamped at its rim. The centre is clamped between two rigid plates of radius r, so that at this radius dy/dx must remain zero (fig. 5). An alternating harmonic force is applied at

Fig. 5

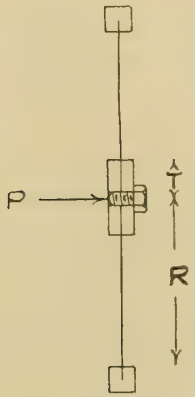

the centre, and the equations of motion determined. At certain frequencies the force P disappears for finite amplitudes of vibration. These are the natural frequencies under the conditions considered. When r is made indefinitely small the natural frequencies of the disk are obtained.

The conditions for the annulus are :—

$$dy/dx = 0 \quad \text{and} \quad y = 0 \text{ at } x = \mathrm{R}, \; dy/dx = 0 \text{ at } x = r,$$

giving

$$\mathrm{AJ}_1(k\mathrm{R}) + \mathrm{BY}_1(k\mathrm{R}) - \mathrm{CI}_1(k\mathrm{R}) + \mathrm{DK}_1(k\mathrm{R}) = 0, \quad (34\,a)$$

$$\mathrm{AJ}_0(k\mathrm{R}) + \mathrm{BY}_0(k\mathrm{R}) + \mathrm{CI}_0(k\mathrm{R}) + \mathrm{DK}_0(k\mathrm{R}) = 0, \quad (35\,a)$$

$$\mathrm{AJ}_1(kr) + \mathrm{BY}_1(kr) - \mathrm{CI}_1(kr) + \mathrm{DK}_1(kr) = 0. \quad (36\,a)$$

These equations completely determine the motion at all frequencies. At those frequencies at which the annulus vibrates naturally the shearing force is zero at radius r, or

$$AJ_1(kr)+BY_1(kr)+CI_1(kr)-DK_1(kr)=0, \quad (37\,a)$$

whence from (36a) and (37a)

$$\left.\begin{aligned} AJ_1(kr)+BY_1(kr)&=0\\ CI_1(kr)-DK_1(kr)&=0\end{aligned}\right\}. \quad . \quad . \quad . \quad (46)$$

Substituting from (46) in (34a) and (35a), we obtain

$$J_1(kR)-\frac{J_1(kr)}{Y_1(kr)}Y_1(kR)-\frac{D}{A}\left\{\frac{K_1(kr)}{I_1(kr)}I_1(kR)-K_1(kR)\right\}=0,$$

and . . . . (47)

$$J_0(kR)-\frac{J_1(kr)}{Y_1(kr)}Y_0(kR)+\frac{D}{A}\left\{\frac{K_1(kr)}{I_1(kr)}I_0(kr)+K_0(kR)\right\}=0,$$

. . . . (48)

whence

$$\frac{J_1(kR)Y_1(kr)-J_1(kr)Y_1(kR)}{J_0(kR)Y_1(kr)-J_1(kr)Y_0(kR)}+\frac{K_1(kr)I_1(kR)-K_1(kR)I_1(kr)}{K_1(kr)I_0(kR)+K_0(kR)I_1(kr)}=0. \quad (49)$$

Equation (49) gives the natural symmetrical vibrations of the annulus under the stated conditions.

If r is made vanishingly small, (49) reduces to

$$\frac{J_1(kR)}{J_0(kR)}+\frac{I_1(kR)}{I_0(kR)}=0. \quad . \quad . \quad . \quad . \quad (50)$$

(See Rayleigh, i. p. 366.)

This is the corresponding equation for the *disk*, and might have been obtained directly by putting $r=0$ in (34a) to (37a). The gravest mode of oscillation of the disk is given by $kR=3{\cdot}2$ approximately. Succeeding oscillations occur when kR is approximately 6·3, 9·4, 12·5 etc.

For the driven diaphragm general expressions embodying equations (34a) to (36a) may be deduced. It is, however, usually more convenient to work directly from the equations as they stand. When, however, the inner radius is very small considerable simplification is possible. Except for the free oscillations it is not permissible to consider the inner radius reduced to absolute zero, as the actuating force would

then produce an infinite stress. There is no objection, however, to considering the inner radius being made very small, the forces employed being correspondingly small. Putting equations (34a) and (35a) in the form of (34) and (35), that is, writing $a_1 = J_1(kR)$, $b_1 = Y_1(kR)$, $c_1 = -I_1(kR)$, $d_1 = K_1(kR)$; $a_2 = J_0(kR)$, $b_2 = Y_0(kR)$, $c_2 = I_0(kR)$, $d_2 = K_0(kR)$, and putting $kr = 0$ in equation (36a), we obtain

$$B = D, \quad . \quad . \quad . \quad . \quad . \quad . \quad . \quad . \quad (51)$$

$$\frac{B}{A} = \frac{D}{A} = \frac{a_2c_1 - a_1c_2}{c_2(b_1+d_1) - c_1(b_2+d_2)}$$

$$= -\frac{I_1J_0 + I_0J_1}{I_0(Y_1+K_1) + I_1(Y_0+K_0)}, \quad . \quad (52)$$

$$\frac{C}{A} = -\frac{a_2(b_1+d_1) - a_1(b_2+d_2)}{c_2(b_1+d_1) - c_1(b_2+d_2)}$$

$$= -\frac{J_0(Y_1+K_1) - J_1(Y_0+K_0)}{I_0(Y_1+K_1) + I_1(Y_0+K_0)}, \quad . \quad (53)$$

the arguments of the functions in (52) and (53) being kR. The motion of the centre of the disk is given by

$$y_0 = AJ_0(kr) + BY_0(kr) + CI_0(kr) + DK_0(kr). \quad . \quad (54)$$

In this equation two functions, $Y_0(kr)$ and $K_0(kr)$, become infinite as r vanishes, but their sum is finite. An examination of the simplification effected in equation (36a) shows that the difference between B and D is of such an order that when multiplied by $Y_0(kr)$ or $K_0(kr)$ the product becomes vanishingly small as r approaches zero. It therefore follows that the remainder terms in

$$y_0 = AJ_0(kr) + CI_0(kr) + B\{Y_0(kr) + K_0(kr)\} \quad . \quad (55)$$

are negligible.

From (41) and (36a) we see that the apparent mass for this case is

$$M_a = -\frac{4\pi mr}{k}\left\{\frac{AJ_1(kr) + BY_1(kr)}{AJ_0(kr) + BY_0(kr) + CI_0(kr) + DK_0(kr)}\right\}.$$

$$. \quad . \quad . \quad . \quad (56)$$

Putting in the limiting values,

$$J_0(kr) = 1, \quad I_0(kr) = 1,$$

$$Y_0(kr) + K_0(kr) = \log 2 - \gamma = \cdot 11593, \; J_1(kr) = kr/2,$$

$$Y_1(kr) = -1/kr, \; I_1(kr) = kr/2, \; K_1(kr) = 1/kr,$$

(56) reduces to

$$M_a = \frac{4\pi m}{k^3}\left\{\frac{B}{A + \cdot 11593\,B + C}\right\}. \quad . \quad . \quad (57)$$

The equivalent mass vanishes, and we obtain the natural oscillations, when $B = 0$ ((52) and (57)), a relation confirming equation (50). The disk may, however, vibrate with its centre fixed. The apparent mass is then infinite, and the natural frequencies of vibration are given by

$$A + \cdot 11593\,B + C = 0. \quad . \quad . \quad . \quad . \quad (58)$$

Fig. 6.

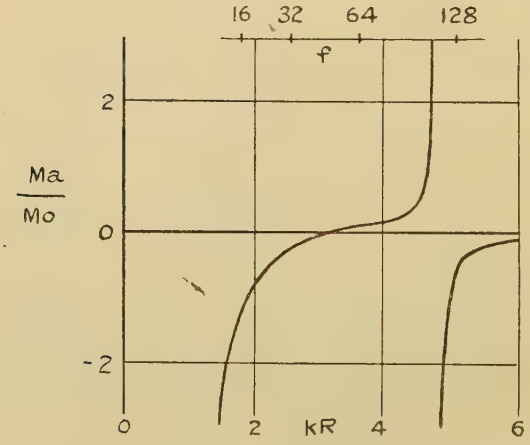

Variation of apparent mass of disk with clamped edge.

The variation of apparent mass at low frequencies, determined from (52), (53), and (57), is shown in fig. 6. (The frequency-scale shown on this and on various subsequent diagrams refers to an aluminium diaphragm having a mass of ·05 gm. per sq. cm., the radius R being 10 cm. Assuming $\sigma = 4$, we obtain $kR = \cdot 45\sqrt{f}$ approximately.)

Annulus or Disk with Free Outer Edge, the Slope being maintained at the Inner Edge.

If the outer rim of the diaphragm be free instead of clamped we approximate to the arrangement used in loud

speakers. For the diaphragm driven through a clamp at its centre equations (34) to (36) become

$$AJ_1(kR)+BY_1(kR)+CI_1(kR)-DK_1(kR)=0, \quad (34\,b)$$

$$\frac{\sigma-1}{\sigma.kR}\{AJ_1(kR)+BY_1(kR)-CI_1(kR)+DK_1(kR)\}$$
$$-\{AJ_0(kR)+BY_0(kR)-CI_0(kR)-DK_0(kR)\}=0, \quad (35\,b)$$
$$AJ_1(kr)+BY_1(kr)-CI_1(kr)+DK_1(kr)=0. \quad (36\,b)$$

These three equations determine the motion completely.

Fig. 7.

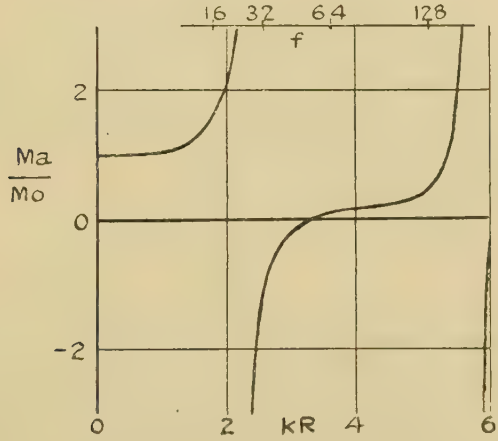

Variation of apparent mass of annulus with free edge.

Equation (36 *b*) is identical with (36 *a*) of the previous case, and hence the apparent mass is given by (56). It is easy to show that at low frequencies

$$M_0=\pi m(R^2-r^2), \quad . \quad . \quad . \quad . \quad . \quad (59)$$

the actual mass of the diaphragm. Fig. 7 has been plotted to show the variation of apparent mass of an aluminium diaphragm at low frequencies, assuming $m = \cdot 05$, $\sigma = 4$, $r = 2$ cm., $R = 10$ cm.

When the inner radius becomes vanishingly small we obtain the case of the disk. As in the previous example,

$$B = D, \quad . \quad . \quad . \quad . \quad . \quad . \quad (51a)$$

$$\frac{B}{A}=\frac{D}{A}=\frac{a_2c_1-a_1c_2}{c_2(b_1+d_1)-c_1(b_2+d_2)}, \quad . \quad . \quad (52a)$$

$$\frac{C}{A}=-\frac{a_2(b_1+d_1)-a_1(b_2+d_2)}{c_2(b_1+d_1)-c_1(b_2+d_2)}, \quad . \quad . \quad . \quad (53a)$$

where

$a_1=J_1(kR)$, $b_1=Y_1(kR)$, $c_1=I_1(kR)$, $d_1=-K_1(kR)$;

$a_2=\frac{2(\sigma-1)}{\sigma\,.\,kR}J_1(kR)-J_0(kR)$, $b_2=\frac{2(\sigma-1)}{\sigma\,.\,kR}Y_1(kR)-Y_0(kR)$

$c_2=I_0(kR)$, $d_2=K_0(kR)$.

Hence

$$M_a=\frac{4\pi m}{k_2}\left\{\frac{B}{A+\cdot11593\,B+C}\right\} \quad . \quad . \quad . \quad (57a)$$

This apparent mass has been plotted for various frequencies in fig. 8. Fig. 9 shows the form of the disk at various typical frequencies.

The natural symmetrical oscillations of the whole disk moving freely are given by B = 0, or

$$I_1(kR)\,.\,J_0(kR)+I_0(dR)\,.\,J_1(kR) = \frac{2(\sigma-1)}{\sigma\,.\,kR}J_1(kR)\,.\,I_1(kR). \quad . \quad (60)$$

The numerical values of kR fulfilling this relation depend to some extent upon the value of σ. When $\sigma=4$, the gravest mode of oscillation is given by $kR=3{\cdot}0$ approximately. It will be noticed that the frequencies of the gravest modes of the diaphragm with free and clamped edges are not greatly different ; the free and clamped reeds were shown to have the *same* natural frequencies. (Equations (17), (18), (23), (24).)

For the disk vibrating with its centre fixed the natural frequencies are given by

$$A+\cdot11593\,B+C=0, \quad . \quad . \quad . \quad . \quad (59a)$$

as before. Succeeding oscillations occur when kR is approximately 1·9, 4·6, 7·9, etc.

The natural oscillations with fixed centre have limited amplitudes determined by the magnitude of the applied alternating harmonic force. The amplitudes of the natural oscillations with free centre are, however, large, and are only limited by dissipation and radiation, the extent to which the limitation is operative being, of course, conditioned by the magnitude of the applied force.

Fig. 8.

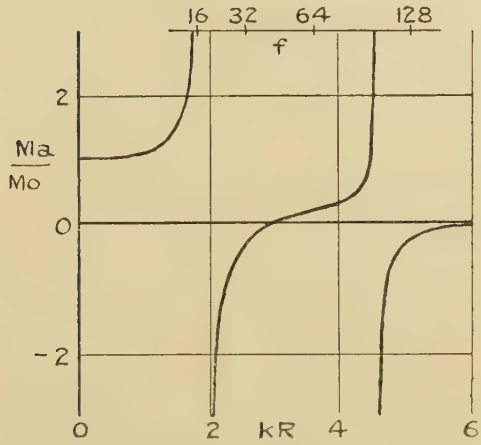

Variation of apparent mass of disk with free edge.

Fig. 9.

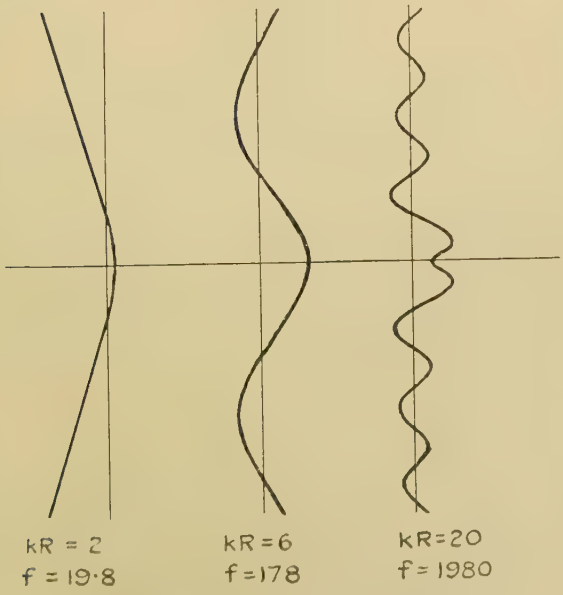

Form of free edge disk at typical frequencies.

Annulus or Disk with both Edges Free.

The general equations expressing the conditions are

$$AJ_1(kR)+BY_1(kR)+CI_1(kR)-DK_1(kR)=0, \quad (34\,c)$$

$$\frac{\sigma-1}{\sigma\,.\,kR}\{AJ_1(kR)+BY_1(kR)-CI_1(kR)+DK_1(kR)\}$$
$$-\{AJ_0(kR)+BY_0(kR)-CI_0(kR)-DK_0(kR)\}=0, \quad (35\,c)$$

$$\frac{\sigma-1}{\sigma\,.\,kr}\{AJ_1(kr)+BY_1(kr)-CI_1(kr)+DK_1(kr)\}$$
$$-\{AJ_0(kr)+BY_0(kr)-CI_0(kr)-DK_0(kr)\}=0. \quad (36\,c)$$

These equations completely determine the motion. For the natural vibrations we have

$$AJ_1(kr)+BY_1(kr)+CI_1(kr)-DK_1(kr)=0. \quad (37\,c)$$

The frequencies may be determined from these four equations.

If kr be made very small, (36 *c*) becomes

$$B-D=0, \quad . \quad . \quad . \quad . \quad . \quad . \quad (61)$$

and (37 *c*) becomes

$$B+D=0. \quad . \quad . \quad . \quad . \quad . \quad . \quad (62)$$

Hence

$$B=D=0. \quad . \quad . \quad . \quad . \quad . \quad . \quad (63)$$

Substituting in (34 *c*) and (35 *c*), we obtain

$$I_1(kR)\,.\,J_0(kR)+I_0(kR)\,.\,J_1(kR)=\frac{2(\sigma-1)}{\sigma\,.\,kR}J_1(kR)\,.\,I_1(kR),$$
$$. \quad . \quad . \quad . \quad (60\,a)$$

which is identical with (60). It will be noted that the assumptions involved in the two cases are fundamentally different. The identity of the results shows that the behaviour of the disk is unaltered by its being punctured at its centre, a result which is consistent with the fact that the curvature and radial stress disappear at the centre of the disk.

Asymptotic Conditions at High Frequencies.

Curves given so far have been plotted for values of the argument kR not exceeding 6. For the aluminium diaphragm already mentioned this corresponds to frequencies below 178 cycles per second. It is clear that for the major part of the musical scale the argument of the relevant functions, being proportional to the square of the frequency, assumes

fairly large values, and the asymptotic values of the functions themselves become applicable.

For the disk, whether free or clamped at its edge, we find approximately

$$\frac{B}{A} = \frac{D}{A} = -\frac{J_0+J_1}{Y_0+Y_1}, \quad . \quad . \quad . \quad . \quad . \quad (52\,b)$$

and

$$\frac{C}{A} = 0. \quad . \quad . \quad . \quad . \quad . \quad . \quad . \quad . \quad . \quad . \quad (53\,b)$$

The apparent mass therefore approximates to (from (57) and (57 *a*))

$$M_a = \frac{4\pi m}{k^2} \frac{J_0+J_1}{-(Y_0+Y_1)+(\log 2-\gamma)(J_0+J_1)}$$

$$= \frac{4\pi m}{k^2} \frac{J_0+J_1}{G_0+G_1} = \frac{8m}{k^2}\tan kR, \quad . \quad . \quad . \quad . \quad . \quad (57\,b)$$

(the argument being kR)

whence

$$\frac{M_a}{M_0} = \frac{8}{\pi}\frac{\tan kR}{k^2R^2}. \quad . \quad . \quad . \quad . \quad . \quad (64)$$

At high frequencies the natural oscillations are thus given by

$$kR = n\pi, \quad . \quad . \quad . \quad . \quad . \quad . \quad (65)$$

and the oscillations with fixed centre by

$$kR = (n+\tfrac{1}{2})\pi. \quad . \quad . \quad . \quad . \quad . \quad (66)$$

These conditions are approached for comparatively small values of kR.

Fig. 10 shows the asymptotic variations of apparent mass over the musical scale, together with the variations at low frequency for the free edge disk. The distribution of the natural oscillations of this disk is shown on the same figure.

For parts of the disk well removed from both centre and edge the displacement equation at very high frequencies becomes

$$y = AJ_0(kx)+BY_0(kx), \quad . \quad . \quad . \quad . \quad (67)$$

where

$$J_0 = \sqrt{\frac{1}{\pi x}}(\cos kx + \sin kx),$$

$$Y_0 = (\log 2-\gamma)\sqrt{\frac{1}{\pi x}}(\cos kx+\sin kx)$$

$$-\frac{1}{2}\sqrt{\frac{\pi}{x}}(\cos kx-\sin kx),$$

$$\frac{B}{A} = \frac{\tan kR}{\frac{\pi}{2} - (\log 2 - \gamma)\tan kR}.$$

There is therefore a decrescent sinusoidal variation of displacement along the axis of the disk, the amplitude at any radius x being proportional to $1/\sqrt{x}$; the wave-length λ is $2\pi/k$. It is towards this condition that the third curve of fig. 9 approximates.

Fig. 10.

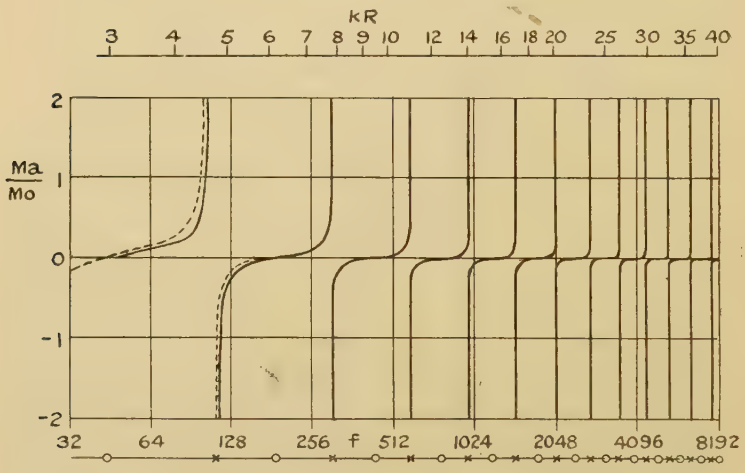

The full curve shows the variation of the apparent mass of either a free or clamped edge disk calculated from the asymptotic values of the functions. The broken line refers to a free edge disk using the true values of the functions.

⊙ Natural oscillations, centre free; amplitude limited only by dissipation and radiation.

× Natural oscillations, centre fixed; amplitude definitely limited.

Conclusion.

Present day practice in loud speaker design is based upon the theory of the rigid diaphragm, analysed by Rayleigh and others. It is true that to secure increased rigidity practical diaphragms are usually coned. Such a conformation affects not only the stiffness but also the acoustic output. The elastic equations of such diaphragms are different from those for flat disks. The differences, however, are not fundamental, but rather of degree. Other reasons must be sought for the

fact that in practice the reproduction of the upper portion of the musical scale is realized, although it is denied by the "rigid disk" theory. The analysis presented above cannot claim to be more than a contribution towards the more general solution of the problem. The effect of flexure of the diaphragm upon its acoustic output has not yet been examined, except roughly. But it is suggested that the "rigid disk" theory must be abandoned. It has served the useful practical purpose of securing good reproduction over the lower portion of the musical scale; in isolated cases empirical work has extended the range of quality over the greater part of the musical range. Till, however, the theory has been placed upon a sound basis design cannot be satisfactory.

That the types of vibrations suggested above actually occur is easily shown experimentally. The unsymmetrical vibrations have not been considered; they do not lend themselves so readily to analysis. But from the practical point of view they should be of little importance. They can only arise as highly damped transients or from bad design, and can be avoided. The symmetrical vibrations must occur at all frequencies; they are of importance over a considerable portion of the musical range.

LXXXIV. *Lag in a Thermometer when the Temperature of the External Medium is Varying.* *By* A. T. Starr, *B.A.* (*Cantab.*), *B.Sc.* (*London*)*.

1. *Introduction.*

A. R. McLeod† has discussed the lag in a thermometer with a spherical or cylindrical bulb in a medium whose temperature varies at a constant rate. Dr. Bromwich‡ has treated the same problem by the method of the Heaviside operational calculus. S. P. Owen§ has allowed for the containing glass vessel. It is here attempted to treat the problem for a more general variation of temperature of the external medium, the method being that of the operational calculus.

* Communicated by the Author.
† Phil. Mag. i. p. 134 (1919).
‡ Phil. Mag. i. p. 407 (1919).
§ Lond. Math. Soc. (1920).

It is very difficult, if not impossible, to obtain a theoretical expression for the rate of climb of an aeroplane, and hence for its height at any given time. But it is comparatively easy to take an actual curve between height and time and find an analytical expression for the height in terms of time. It is known that the temperature of the atmosphere decreases linearly with the height from the ground for the heights that aeroplanes attain at present, and hence we have a relation between the temperature of the external medium and the time which will fit the actual case as closely as we need.

2. *Determination of the Temperature of the Medium as a Function of the Time.*

We take the temperature of the air (which is here the external medium) at ground-level as the standard temperature, and call it the zero temperature.

Let u be the temperature of the atmosphere at height Z, and t the time to reach the height Z.

Then we have

$$u = -\alpha Z,$$

where α is a constant.

The curve connecting Z and t is given.

Let us take, as an example, the actual case of a supercharged "Liberty" engine, D.H.9.A.

The curve is fairly straight to begin with, showing a constant rate of climb, but then becomes concave downwards, showing a diminished rate of climb, as we should expect.

It is reasonable to assume that the curve can be expressed as Z in an ascending power series in t, viz. :—

$$Z = a_1 t + a_2 t^2 + a_3 t^3 + a_4 t^4 + \ldots$$

We find that the coefficients decrease rapidly, and we may stop at $a_4 t^4$.

We have the following values of height for time :—

t (in minutes) ...	0.	5.	10.	15.	20.	25.	30.	35.	40.
Z (in feet).....	0	4800	9300	14000	18500	23000	26900	30700	33500

Assuming that

$$Z = a_1 t + a_2 t^2 + a_3 t^3 + a_4 t^4, \quad . \quad . \quad . \quad . \quad (1)$$

and substituting for $t = 10, 20, 30, 40$, we get

$$a_1 = 919{\cdot}25, \quad a_2 = 1{\cdot}625, \quad a_2 = -{\cdot}0417, \quad a_4 = -{\cdot}00125.$$

These values fit the curve almost exactly at $t=10, 20, 30, 40$, and give $Z=4730, 13950, 22857$ respectively at $t=5, 15, 25$.

The fact that a_2 is positive shows that the best rate of climb is not at the ground-level, but at some higher level.

The value of t for the best rate of climb is given by

$$\frac{d^2Z}{dt^2} = 2a_2 + 6a_3t + 12a_4t = 0,$$

giving $t=8{\cdot}6$, corresponding to a height of about 8000 feet.

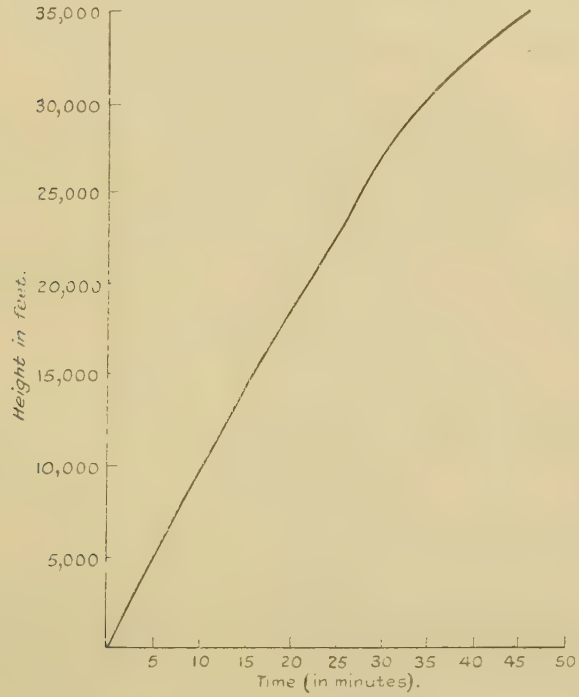

We thus have

$$u = -\alpha(919{\cdot}25\,t + 1{\cdot}625\,t^2 - {\cdot}0417\,t^3 - {\cdot}00125\,t^4)$$
$$= b_1t + b_2t^2 + b_3t^3 + b_4t^4.$$

3. *Thermometer with a Spherical Bulb and Infinite Surface Conductivity.*

Let us consider the case of a thermometer with a spherical bulb, neglecting the effect of the containing glass vessel and

assuming infinite conductivity at the surface, *i. e.*, the temperature at the surface of the sphere is always the temperature of the containing medium, u.

Let v be the temperature at a point inside the bulb at a distance r from the centre. The radius of the bulb is c. The equation of heat conduction is

$$a^2 \nabla^2 v = \frac{\partial v}{\partial t},$$

where $a^2 = K/\rho\sigma$, K = conductivity, ρ = density, and σ = specific heat.

By spherical symmetry, the equation becomes

$$\frac{\partial v}{\partial t} = a^2[\partial^2 v/\partial r^2 + 2/r \cdot \partial v/\partial r],$$

i. e.,
$$a^2 \frac{\partial^2}{\partial r^2}(rv) = prv,$$

p being Heaviside's operator $= \frac{\partial}{\partial t}$.

This gives

$$rv = A \sinh(qr/c) + B \cosh(qr/c),$$

where

$$p = a^2 q^2/c^2, \quad . \quad . \quad . \quad . \quad . \quad . \quad . \quad . \quad . \quad . \quad (2)$$

B must vanish, as v is finite at $r=0$.

Hence

$$rv = A \sinh(qr/c).$$

The condition at $r=c$ gives

$$\frac{rv}{c} = \frac{\sinh(qr/c)}{\sinh q} u. \quad . \quad . \quad . \quad . \quad . \quad (3)$$

(3) may be interpreted in the following way. Let $u=\phi(t)$. Then u can be expressed in operational form as

$$u = \phi(t) = \int_{-\infty}^{\infty} \phi(h) e^{-ph} p H(t)\, dh \,*,$$

where $H(t)$ is Heaviside's unit function, *i. e.*,

$$H(t) = 1, \text{ for } t > 0,$$

and

$$H(t) = 0, \text{ for } t < 0.$$

* H. Jeffreys, 'Operational Methods in Math. Physics,' p. 18.

We thus get

$$rv/c = \frac{\sinh(qr/c)}{\sinh q}\int_{-\infty}^{\infty}\phi(h)e^{-ph}p\mathrm{H}(t)\,dh,$$

which expresses v in operational form.

This can be translated back into ordinary form by Bromwich's method of the complex variable *, and we obtain

$$rv/c = \frac{1}{2\pi i}\int_{\mathrm{L}}e^{pt}\frac{\sinh(qr/c)}{\sinh q}dp\int_{-\infty}^{\infty}\phi(h)e^{-ph}\,dh$$

$$= \frac{1}{2\pi i}\int_{-\infty}^{\infty}\phi(h)\,dh\int_{\mathrm{L}}e^{p(t-h)}\frac{\sinh(qr/c)}{\sinh q}\,dp, \quad . \quad (4)$$

where p, in this last integral, is regarded as a complex variable, q is given by equation (2), and L is a curve from $c-i\alpha$ to $c+i\alpha$, where c is positive and finite, such that all the singularities of the integrand are on the left side of the path.

In (4) the range of h, which gives a contribution to the integral, is $0 \leq h \leq t$.

So

$$\frac{rv}{c} = \frac{1}{2\pi i}\int_{\mathrm{L}}e^{pt}\frac{\sinh(qr/c)}{\sinh q}dp\int_{0}^{t}e^{-ph}\phi(h)\,dh.$$

The poles of the integrand for the complex integration occur at $q = in\pi$, $n=0$ being excluded, *i. e.*, at $p = -n^2\pi^2a^2/c^2$. We then get for (4)

$$\frac{rv}{c} = -\frac{2\pi a^2}{c^2}\sum_{n=1}^{\infty}(-1)^n n\sin\frac{n\pi r}{c}\int_{\sigma}^{t}e^{-n^2\pi^2(t-h)/c^2}\phi(h)\,dh,$$

which is the expression that McLeod obtains.

The thermometer registers the average value of the temperature, viz.,

$$\bar{v} = (3/4\pi c^3)\int_0^a 4\pi r^2 v\,dr. \quad . \quad . \quad . \quad . \quad (5)$$

We can find $\bar{v}$ from (5), as Mc Leod does, but it is easiest to delay the interpretation of the operational form until the final stage; for example, here we first take the average, treating operators as ordinary numbers during this process, and then we interpret. This is one of the great advantages of the operational method, and very much labour is saved in this way.

* H. Jeffreys, *loc. cit.* p. 19, (2).

For the general case of $u=\phi(t)$ we get

$$\begin{aligned}\bar{v} &= 3\left(\frac{1}{q}\coth q-\frac{1}{q^2}\right)u \\ &= \frac{3}{2\pi i}\int_{\mathrm{L}} e^{pt}\left(\frac{1}{q}\coth q-\frac{1}{q^2}\right)dp\int_{-\infty}^{\infty}\phi(h)e^{-ph}\,dh \\ &= \frac{3}{2\pi i}\int_{\mathrm{L}} e^{pt}\left(\frac{1}{q}\coth q-\frac{1}{q^2}\right)dp\int_{0}^{t}\phi(h)e^{-ph}\,dh \\ &= 3\int_0^t\left[\phi(h)\,dh\times\text{residues of } e^{p(t-h)}\left(\frac{1}{q}\coth q-\frac{1}{q^2}\right)\right] \\ &= \frac{6a^2}{c^2}\sum_{n=1}^{\infty}\int_0^t\phi(h)e^{\frac{-n^2\pi^2a^2}{c^2}(t-h)}\,dh. \qquad\ldots\ldots\qquad (6)\end{aligned}$$

This gives the average temperature for a general variation of the temperature of the external medium.

If $\phi(t)=(\mathrm{G}t)$, (6) gives

$$\bar{v} = \mathrm{G}t-\frac{1}{15}\frac{c^2}{a^2}\mathrm{G}+6\mathrm{G}\frac{c^2}{\pi^4a^2}\sum_{n=1}^{\infty}n^{-4}e^{-n^2\pi^2a^2t/c}, \qquad (7)$$

agreeing with McLeod's particular result.

The lag is thus

$$\frac{1}{15}\frac{c^2}{a^2}\mathrm{G}-6\mathrm{G}\frac{c^2}{\pi^4a^2}\sum_{n=1}^{\infty}n^{-4}e^{-n^2\pi^2a^2t/c^2}. \qquad (8)$$

In our case u is easily transposable into operational form, and we have

$$u = b_1t+b_2t^2+b_3t^3+b_4t^4 = b_1\,1/p+b_2\,2\,!/p^2+b_3\,3\,!/p^3+b_4\,4\,!/p^4.$$

Hence

$$\bar{v} = 3\left(\frac{1}{q}\coth q-\frac{1}{q^2}\right)(b_1/p+b_2\,2\,!/p^2+b_3\,3\,!/p^3+b_4\,4\,!/p^4). \qquad (9)$$

But

$$\begin{aligned}\frac{1}{q}\coth q-\frac{1}{q^2} &= 2^2\mathrm{B}_2/2\,!+2^4\mathrm{B}_4q^2/4\,!+2^6\mathrm{B}_6q^4/6\,!+\ \ldots\text{ etc.} \\ &= \mathrm{A}_2+\mathrm{A}_4q^2+\mathrm{A}_6q^4+\ \ldots,\quad\text{say,}\end{aligned}$$

where $\mathrm{B}_2, \mathrm{B}_4, \ldots$ are Bernoulli's numbers. Hence

$$\left(\frac{1}{q}\coth q-\frac{1}{q^2}\right)t^n$$

has a polynomial contribution of

$$\begin{aligned}&(\mathrm{A}_2+\mathrm{A}_4p\,c^2/a^2+\mathrm{A}_6p^2\,c^4/a^4+\ \ldots)n\,!\,p^{-n} \\ &\quad=\mathrm{A}_2t^n+\mathrm{A}_4nt^{n-1}\,c^2/a^2+\mathrm{A}_6n(n-1)t^{n-2}\,c^4/a^4+\ \ldots\end{aligned}$$

Thus $\bar{v}$ has a polynomial contribution

$$\begin{aligned}
&3b_1\{A_2t + A_4\,c^2/a^2\} + 3b_2\{A_2t^3 + A_4\,2c^2t/a^2 + A_6\,2c^4/a^4\} \\
&\quad + 3b_3\{A_2t^3 + A_4\,3c^2t^2/a^2 + A_6.3.2.c^4t/a^4 + A_8.3.2.c^6/a^6\} \\
&\quad + 3b_4\{A_2t^4 + A_4\,4c^2t^3/a^2 + A_6\,4.3.c^4t^2/a^4 \\
&\qquad\qquad + A_8\,4.3.2.c^6t/a^6 + A_{10}\,4.3.2.c^8/a^8\} \\
&= 3A_2(b_1t + b_2t^2 + b_3t^3 + b_4t^4) \\
&\qquad\qquad + 3A_4\,(c^2/a^2)\,[b_1 + 2b_2t + 3b_3t^2 + 4b_4t^3] \\
&\quad + 3A_6\,(c^4/a^4)\,[2b_2 + 3.2b_3t + 4.3b_4t^2] \\
&\qquad\qquad + 3A_8\,(c^6/a^6)\,[3.2.1.b_3 + 4.3.2.b_4t] \\
&\quad + 3A_{10}\,(c^8/a^8)\,4.3.2.1.b_4 \\
&= 3A_2u + 3A_4c^2a^{-2}u' + 3A_6c^4a^{-4}u'' + 3A_8c^6a^{-6}u''' \\
&\qquad\qquad + 3A_{10}c^8a^{-8}u'''', \qquad (10)
\end{aligned}$$

where dashes denote differentiation with respect to t. It is obvious that expression (10), continued for the requisite number of terms, would hold when u is a finite polynomial in t.

We have

$$B_2 = \frac{1}{6}, \quad B_4 = -\frac{1}{30}, \quad B_6 = \frac{1}{42}, \quad B_8 = -\frac{1}{30}, \quad B_{10} = \frac{5}{66},$$

and hence

$$A_2 = \frac{1}{3}, \quad A_4 = \frac{1}{45}, \quad A_6 = \frac{2}{945}, \quad A_8 = -\frac{1}{4725}, \quad A_{10} = \frac{2}{93555}.$$

The polynomial contribution thus found is the contribution to the general sum by the residue at $p=0$, which is a pole of

$$\left(\frac{1}{q}\coth q - \frac{1}{q^2}\right)p^{-m},$$

if $m>0$. This is the part which predominates when $t\to\infty$, for then the other terms tend *exponentially* to zero. This is an example of the tendency that operators have of resembling ordinary numbers; for $p^{-1}=t$, and we see that the important part at $t=\infty$ is the part obtained at $p=0$.

$$\left(\frac{1}{q}\coth q - \frac{1}{q^2}\right)p^{-m}$$

has poles at $q = in\pi$, corresponding to $p = n^2\pi^2a^2c^{-2} = \alpha_n$, say.

$\bar{v}$ is $f(p)/\Delta(p)$, where $f(p)$ and $\Delta(p)$ are *polynomials* in p, given by

$$f(p) = (q\cosh q - \sinh q)/q^3,$$

and

$$\Delta(p) = p^m \sinh q/q.$$

$$f(\alpha_n) = (-1)^{\overline{n}-1} n^{-2}\pi^{-2}$$

and

$$\alpha_n\Delta'(\alpha_n) = \alpha_n{}^{m+1}\frac{1}{q}\frac{dq}{dp}\cosh q = (-1)^n \tfrac{1}{2}\alpha_n{}^m.$$

Hence the exponential terms given by

$$\left(\frac{1}{q}\coth q - \frac{1}{q^2}\right)p^{-m}$$

are

$$(-1)^{m+1}(2a^2/c^2)\sum_{n=1}^{\infty}(n^2\pi^2a^2/c^2)^{-m-1}\,e^{-n^2\pi^2a^2t/c^2}.$$

Thus the final expression for $\bar{v}$ is the expression (10) plus

$$\left.\begin{aligned} &6b_1\frac{a^2}{c^2}\sum_{n=1}^{\infty}\left(\frac{n^2\pi^2a^2}{c^2}\right)^{-2}e^{-n^2\pi^2a^2t/c^2},\\ &-12b_2\frac{a^2}{c^2}\sum_{n=1}^{\infty}\left(\frac{n^2\pi^2a^2}{c^2}\right)^{-3}e^{-n^2\pi^2a^2t/c^2},\\ &+36b_3\frac{a^2}{c^2}\sum_{n=1}^{\infty}\left(\frac{n^2\pi^2a^2}{c^2}\right)^{-4}e^{-n^2\pi^2a^2t/c^2},\\ &-144b_4\frac{a^2}{c^2}\sum_{n=1}^{\infty}\left(\frac{n^2\pi^2a^2}{c^2}\right)^{-5}e^{-n^2\pi^2a^2t/c^2}. \end{aligned}\right\} \quad . \quad . \quad (11)$$

The steady lag is

$$-3\{A_4c^2a^{-2}u' + A_6c^4a^{-4}u'' + A_8c^6a^{-6}u''' + A_{10}c^8a^{-8}u''''\}$$

$$= \frac{1}{15}\frac{c^2}{a^2}u' - \frac{2}{315}\frac{c^4}{a^4}u'' + \frac{1}{1575}\frac{c^6}{a^6}u''' - \frac{2}{31185}\frac{c^8}{a^8}u''''. \quad (12)$$

4. *The Sphere with Finite Conductivity at the Surface.*

The surface condition is now

$$K\frac{\partial v}{\partial r} = h(u-v), \quad \text{at } r = c.$$

Substituting in $rv = \mathrm{A}\sinh(qr/c)$, we obtain

$$\frac{rv}{c} = \frac{ch\sinh(qr/c)}{\mathrm{K}(q\cosh q - \sinh q) + ch\sinh q}\,u.$$

This gives

$$\bar{v} = \frac{3ch(q\cosh q - \sinh q)/q^2}{ch\sinh q + \mathrm{K}(q\cosh q - \sinh q)}\,u$$

$$= \frac{3\left(\frac{1}{q}\coth q - \frac{1}{q^2}\right)}{1 + \lambda q^2\left(\frac{1}{q}\coth q - \frac{1}{q^2}\right)}\,u, \quad . \quad . \quad . \quad . \quad . \quad (13)$$

where

$$\lambda = \frac{\mathrm{K}}{ch}.$$

The operator acting on u in (13), when expanded in ascending powers of q^2, gives

$$\begin{aligned}
&\mathrm{A}_2 + q^2(\mathrm{A}_4 - \lambda\mathrm{A}_2^2) + q^4(\mathrm{A}_6 - \lambda 2\mathrm{A}_2\mathrm{A}_4 + \lambda^2\mathrm{A}_2^3)\\
&\quad + q^6\left[\mathrm{A}_8 - \lambda(2\mathrm{A}_2\mathrm{A}_6 + \mathrm{A}_4^2) + \lambda^2 3\mathrm{A}_2^2\mathrm{A}_4 - \lambda^3\mathrm{A}_2^4\right]\\
&\quad + q^8\left[\mathrm{A}_{10} - \lambda(2\mathrm{A}_2\mathrm{A}_8 + 2\mathrm{A}_4\mathrm{A}_6) + \lambda^2(3\mathrm{A}_2^2\mathrm{A}_6 + 3\mathrm{A}_2\mathrm{A}_4^2)\right.\\
&\qquad\qquad \left. - \lambda^3 4\mathrm{A}_2^3\mathrm{A}_4 + \lambda^4\mathrm{A}_2^5\right]\\
&\quad + \text{higher powers of } q\\
&= \mathrm{A}_2 + \mathrm{A}_4'q^2 + \mathrm{A}_6'q^4 + \mathrm{A}_8'q^6 + \mathrm{A}_{10}'q^8 + \ldots, \quad \text{say.}
\end{aligned}$$

By (12) the steady lag is

$$-3\{\mathrm{A}_4'c^2a^{-2}u' + \mathrm{A}_6'c^4a^{-4}u'' + \mathrm{A}_8'c^6a^{-6}u''' + \mathrm{A}_{10}'c^8a^{-8}u''''\},$$

where

$$\mathrm{A}_4' = -\frac{1}{45} - \frac{\lambda}{9}, \qquad \mathrm{A}_6' = \frac{2}{945} + \frac{2\lambda}{135} + \frac{\lambda^2}{27},$$

$$\mathrm{A}_8' = -\frac{1}{4725} - \frac{8\lambda}{10125} - \frac{\lambda^2}{135} - \frac{\lambda^3}{81},$$

$$\mathrm{A}_{10}' = \frac{2}{93555} + \frac{2\lambda}{8505} + \frac{17\lambda^2}{14175} + \frac{4\lambda^3}{1215} + \frac{\lambda^4}{243},$$

giving for the steady lag the value

$$\left(\frac{1}{15}\frac{c^2}{a^2}u' - \frac{2}{315}\frac{c^4}{a^4}u'' + \frac{1}{1575}\frac{c^6}{a^6}u''' - \frac{2}{31185}\frac{c^8}{a^8}u''''\right)$$

$$+\lambda\left(\frac{1}{3}\frac{c^2}{a^2}u' - \frac{2}{45}\frac{c^4}{a^4}u'' + \frac{8}{3375}\frac{c^6}{a^6}u''' - \frac{2}{2835}\frac{c^8}{a^8}u''''\right)$$

$$+\lambda^2\left(-\frac{1}{9}\frac{c^4}{a^4}u''+\frac{1}{45}\frac{c^6}{a^6}u'''-\frac{17}{4725}u''''\right)$$

$$+\lambda^3\left(\frac{1}{27}\frac{c^6}{a^6}u'''-\frac{4}{405}\frac{c^8}{a^8}u''''\right)-\lambda^4\frac{1}{81}\frac{c^8}{a^8}u''''. \quad . \quad . \quad (14)$$

The poles of (13) are given by

$$1-\lambda+\lambda q\coth q=0,$$

i. e., by $q=i\omega$, where $\omega\cot\omega=1-1/\lambda$, ω being known to be real *.

Considering

$$3\left(\frac{1}{q}\coth q-\frac{1}{q^2}\right)p^{-n}\Big/\left\{1+\lambda q^2\left(\frac{1}{q}\coth q-\frac{1}{q^2}\right)\right\},$$

we have

$$F(p)=3(q\coth q-\sinh q)/q^3,$$

$$\Delta(p)=p^n\{\sinh q+\lambda(q\cosh q-\sinh q)\}/q,$$

whence

$$F(\alpha)/\alpha\Delta'(\alpha)=\frac{6a^2}{c^2}\frac{1}{(1-\lambda+\lambda^2\omega^2)\left(-\frac{a^2\omega^2}{c^2}\right)^{n+1}}.$$

Thus the lag is expression (14) plus the following:

$$\left.\begin{aligned}
&-\ 6b_1\frac{c^2}{a^2}\sum\frac{1}{(1-\lambda+\lambda^2\omega^2)\omega^4}e^{-a^2\omega^2t/c^2},\\
&+\ 12b_2\frac{c^4}{a^4}\sum\frac{1}{(1-\lambda+\lambda^2\omega^2)\omega^6}e^{-a^2\omega^2t/c^2},\\
&-\ 36b_3\frac{c^6}{a^6}\sum\frac{1}{(1-\lambda+\lambda^2\omega^2)\omega^8}e^{-a^2\omega^2t/c^2},\\
&+144b_4\frac{c^8}{a^8}\sum\frac{1}{(1-\lambda+\lambda^2\omega^2)\omega^{10}}e^{-a^2\omega^2t/c^2}.
\end{aligned}\right\} \quad . \quad . \quad (15)$$

5. *Cylindrical Bulb with Infinite Surface Conductivity.*

The equation of heat-conduction is now

$$\frac{1}{r}\frac{\partial}{\partial r}\left(r\frac{\partial v}{\partial r}\right)=\frac{1}{a^2}\frac{\partial v}{\partial t},$$

* *Vide* Bromwich, *loc. cit.*

leading to $I_0(qr/c)$ instead of $\{\sinh(qr/c)/(qr/c)\}$, where $I_0(x)$ is the modified Bessel function $J_0(ix)$. We obtain

$$\bar{v} = \frac{2}{c^2}\int_0^c rv\,dr = \frac{2}{q}\frac{I_0'(q)}{I_0(q)}u. \quad . \quad . \quad . \quad . \quad (16)$$

We have

$$\frac{2}{q}\frac{I_0'(q)}{I_0(q)} = 1 + C_4q^2 + C_6q^4 + C_8q^6 + \ldots,$$

where

$$C_4 = -\frac{1}{2.4}, \quad C_6 = \frac{4}{2.4^2.6}, \quad C_8 = \frac{-33}{2.4^2.6^2.8},$$

$$C_{10} = \frac{1026}{2.4^2.6^2.8^2.10}.$$

Hence, as in (10), the pole $p=0$ gives a steady lag of

$$-[C_4c^2a^{-2}u' + C_6c^4a^{-4}u'' + C_8c^6a^{-6}u''' + C_{10}c^8a^{-8}u''''']. \quad (17)$$

The other poles of (16) are given by

$$q = i\omega, \quad p = -a^2\omega^2/c^2,$$

where $J_0(\omega) = 0$.

$$\frac{2}{q}\frac{I_0'(q)}{I_0(q)}p^{-n} = \frac{4a^2}{c^2}\sum\left(-\frac{c^2}{a^2\omega^2}\right)^{n+1}e^{-a^2\omega^2t/c^2}.$$

Hence

$$\bar{v} = u - \frac{1}{8}\frac{c^2}{a^2}u' + \frac{4}{2.4^2.6}\frac{c^4}{a^4}u'' - \frac{33}{2.4^2.6^2.8}\frac{c^6}{a^6}u''' + \frac{1026}{2.4^2.6^2.8^2.10}\frac{c^8}{a^8}u''''$$

$$+ \frac{4c^2}{a^2}b_1\sum\frac{1}{\omega^4}e^{-a^2\omega^2t/c^2} - \frac{8c^4}{a^4}b_2\sum\frac{1}{\omega^6}e^{-a^2\omega^2t,c^2}$$

$$+ 24\frac{c^6}{a^6}b_2\sum\frac{1}{\omega^8}e^{-a^2\omega^2t/c^2} - 96\frac{c^8}{a^8}b_4\sum\frac{1}{\omega^{10}}e^{-a^2\omega^2t/c^2}. \quad (18)$$

6. *Cylindrical Bulb with Finite Surface Conductivity.*

Instead of equation (16), we obtain

$$\bar{v} = \frac{2}{q}\frac{I_0'(q)}{I_0 + \lambda q I_0'(q)}u \quad . \quad . \quad . \quad . \quad . \quad . \quad (19)$$

$$= \frac{\frac{2}{q}I_0'(q)/I_0(q)}{1 + \frac{1}{2}\lambda q^2\left\{\frac{2}{q}I_0'(q)/I_0(q)\right\}}u.$$

The operator in (19) when expanded is

$$(1 + C_4'q^2 + C_6'q^4 + C_8'q^6 + C_{10}'q^8),$$

where

$$C_4' = C_4 - \tfrac{1}{2}\lambda, \qquad C_6' = C_6 - \tfrac{1}{2}\lambda 2C_2C_4 + \tfrac{1}{4}\lambda^2,$$
$$C_8' = C_8 - \tfrac{1}{2}\lambda(2C_2C_6 + C_4^2) + \tfrac{1}{4}\lambda^2 3C_2C_4 - \tfrac{1}{8}\lambda^3,$$
$$C_{10}' = C_{10} - \tfrac{1}{2}\lambda(2C_2C_8 + 2C_4C_6) + \tfrac{1}{4}\lambda^2(3C_2^2C_6 + 3C_2C_4^2) - \tfrac{1}{8}\lambda^3 4C_2^3C_4 + \tfrac{1}{10}\lambda^4.$$

Hence the pole $p=0$ gives to $\bar{v}$ the expression

$$u + C_4'c^2a^{-2}u' + C_6'c^4a^{-4}u'' + C_8'c^6a^{-6}u''' + C_{10}'c^8a^{-8}u''''. \quad (20)$$

The other poles are at

$$q = i\omega, \qquad p = -a^2\omega^2/c^2,$$

where

$$J_0(\omega) + \lambda\omega J_0'(\omega) = 0.$$

We have

$$\left(\frac{\frac{2}{q} I_0'(q)/I_0(q)}{1 + \frac{1}{2}\lambda q^2 \left\{ \frac{2}{q} I_0'(q)/I_0(q) \right\}} \right) p^{-n}$$
$$= \frac{4a^2}{C^2} \sum \frac{(-c^2/a^2)^{n+1}}{(1+\lambda^2\omega^2)\omega^{n+1}} e^{-a^2\omega^2 t/c^2}.$$

Hence $\bar{v}$ = expression (20).

$$+ 4\frac{c^2}{a^2} b_1 \sum \frac{1}{\omega^4(1+\lambda^2\omega^2)} e^{-a^2\omega^2 t/c^2}$$
$$- 8\frac{c^4}{a^4} b_2 \sum \frac{1}{\omega^6(1+\lambda^2\omega^2)} e^{-a^2\omega^2 t/c^2}$$
$$+ 24\frac{c^6}{a^6} b_3 \sum \frac{1}{\omega^8} \frac{1}{1+\lambda^2\omega^2} e^{-a^2\omega^2 t/c^2}$$
$$- 96\frac{c^6}{a^6} b_4 \sum \frac{1}{\omega^{10}} \cdot \frac{1}{1+\lambda^2\omega^2} e^{-a^2\omega^2 t/c^2}.$$

I wish to thank the Department of Scientific and Industrial Research for their grant, which made this work possible.

LXXXV. *A Molecular Theory of Elastic Hysteresis.* *By* G. A. Tomlinson, *B.Sc.* (From The National Physical Laboratory.)*.

1. VARIOUS theories have been proposed to account for the phenomena of elastic hysteresis, though none has yet apparently received general acceptance, and for this reason a new theory put forward tentatively in the following paper may have some features worth consideration.

Earlier workers, and even some contemporary workers, have considered that some form of solid friction or viscosity always opposes an elastic strain, and so causes elastic hysteresis. Such an idea does not accord very well with present views regarding the nature of an elastic strain, unless it can be asserted that there is friction between two neighbouring atoms in a crystal lattice. Various recent workers are therefore inclined to attribute hysteresis to a loss of energy occurring in some way amongst the atoms at the crystal boundaries[1]. The term internal friction is still widely used, however, as the phenomena undoubtedly suggest the presence of some kind of friction.

In a previous paper[2] the writer has suggested an atomic theory of solid friction, based on the hypothesis that the atoms are subject to both an attraction and a repulsion, the latter having a considerably greater rate of change and a much smaller range than the former. It is now suggested that elastic hysteresis is due to the same atomic mechanism involving a loss of energy when a solid passes through a strain cycle. A brief *résumé* of the hypothesis advanced in the previous paper is necessary for the discussion of the present theory. It is not necessary to take into account the nature of the atomic forces, or to assume any mathematical relation between the forces and the atomic distances. It is assumed, however, that atomic equilibrium is obtained simply by the action of the two forces of attraction and repulsion, and the supposed forces are shown by the descriptive curves A and R of fig. 1, the abscissæ being the distance between the atom-centres. This distance is normally e or OJ in the unstrained material, when A and R are equal and opposite.

* Communicated by the Author.

At this point the atoms are in highly stable equilibrium, since $\frac{d\mathrm{R}}{dx}$ is much greater than $\frac{d\mathrm{A}}{dx}$, and on increasing the distance between them the equilibrium remains stable for some distance, but gradually changes into an unstable state at some separation OL at which $\frac{d\mathrm{R}}{dx} = \frac{d\mathrm{A}}{dx}$.

Fig. 1.

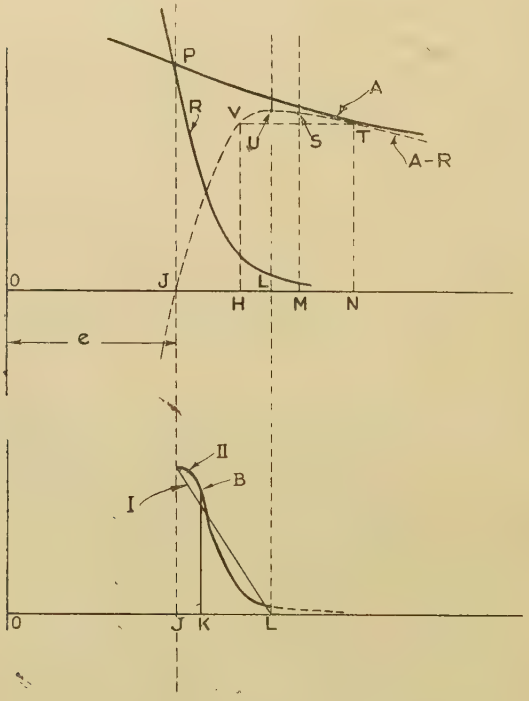

Consider a simple chain of three atoms originally in equilibrum, as shown by the point P, and suppose the outer ones to be gradually drawn away. The middle atom will remain equidistant from its neighbours in stable equilibrium so long as the separation of the atoms does not exceed OL. The atoms can be restored to their original position or beyond, or generally may go through any cycle of displacements for any number of times without loss of

energy, provided the range of stable equilibrium is not exceeded.

If we now suppose the chain of atoms to be further extended so that the separation of each pair exceeds OL, the equilibrium steadily changes from stable to unstable, and eventually the centre atom must leave its symmetrical position and attach itself to one or other of its neighbours in a condition of stable equilibrium again. Since the change in the condition of equilibrium is gradual and continuous, there is a certain probability that the centre atom may retain its symmetrical position halfway between the others for a very short distance, such as LM, beyond the point at which equilibrium is exactly neutral. It will at this point fly back to one of its attracting neighbours with additional kinetic energy or heat equal to the area LMSU, which is an irreversible stage in the cycle of displacements.

In the writer's theory of friction the surface atoms of two bodies in contact are supposed to form such chains temporarily at all points where the atoms approach close enough to come into repulsion and so support the load. On separating again the above process occurs, and results in what may be described as a plucking action of the atoms on each other, which is irreversible and involves a direct conversion of mechanical work into heat.

The same hypothesis may be applied to any phenomena in which relative motion in repeated cycles occurs amongst the atoms, such as stress-strain or magnetic cycles. The present paper is mainly concerned with the loss of energy accompanying a stress-strain cycle, and in a manner reverts to the view that elastic hysteresis is caused by internal solid friction, though only in the restricted sense in which friction has been treated in the previous paper—that is to say, it is not supposed that any gross tangential frictional forces operate on planes of slip within the solid, in the way that friction ordinarily manifests itself to the senses, but only that the process whereby individual atoms dissipate energy is identical in solid friction and in elastic hysteresis.

The hypothesis may be applied to suggest an interpretation of elastic hysteresis in the following way. It is quite improbable that the whole of the atoms of a solid are arranged throughout in the ideal condition of equilibrium corresponding to the atomic distance OJ of fig. 1.

It is far more likely to be the case that there are a large number of points at which small chains of contiguous atoms are slightly displaced either closer together or further apart than the ideal distance. Such local displacements may have any values between zero and JL in the one direction, and between zero and some indeterminate limit in the other direction, but we are only concerned for the present with the former. The magnitude of the maximum relative displacement JL which a pair of neighbour atoms may receive and yet remain in equilibrium is somewhat uncertain, but appears to be small compared with the distance between the atoms. Estimates based on the limiting elastic strain and on the limiting thermal expansion show the possible displacement to be of the order $\frac{1}{1000}$ to $\frac{1}{100}$ of the atomic dimensions respectively. It appears, therefore, that it is only necessary to assume a random distribution of distortion centres involving quite minute atomic displacements as premises for the present hypothesis.

If the material is now supposed to be strained in any manner by which the stretched chains are further extended, certain atoms by our hypothesis will in turn be drawn slightly into the unstable region and will fly back with added kinetic energy. On removing the stress the chains can reform in their original condition. Thus the strain may be quite elastic, in the sense that no atom is finally displaced permanently from its original position, or the dimensions and form of the specimen are exactly recovered, and yet even with very small stresses a loss of energy can occur with every strain cycle, which is found by experiment to be the case. Thus in some experiments described later the writer has found quite a measurable loss of energy when aluminium undergoes a stress cycle of maximum value only 2 lb. per sq. inch.

2. We shall now consider to what extent the theory briefly outlined above is in agreement with certain experimental data of elastic hysteresis. It is well known that the area of the stress-strain hysteresis loop, obtained by using a sensitive extensometer, increases rapidly with the range of stress applied. There are not many data available, however, as to the exact relation between the loss of energy per cycle and the stress range. This is

probably due to the limitations of the extensometer method, as the loss of energy on reducing the stress soon becomes too small for reliable measurement in terms of stress and strain. Some experiments have therefore been made by the writer with the object of finding the relation between the maximum stress and the internal loss per cycle for a number of different materials. A torsional oscillation method was used because of its greater sensitivity, and the loss of energy was found from the rate of decay of amplitude. A ground-steel disk about 6 in. in diameter was suspended in the field of a horizontal optical projector in such a way that a fine indicating point attached to the edge of the disk was in focus on the screen. The period of oscillation was adjusted by means of the length of the suspension to be 4 secs. As the motion of the indicating point was magnified 50 times, only quite a small angular movement was required, the maximum amplitude being less than 5°. This, together with the long period and the smooth form of the disk led to the great advantage that the correction for loss of energy in air resistance was always small and sometimes negligible compared with the hysteresis loss. The actual air resistance of the disk at different amplitudes was fairly well known when oscillating with a period of 4 secs., having been determined experimentally some time previously in the course of some experiments on rolling friction.

The successive amplitudes of the indicating point were marked off at the screen. In some cases a definite number of oscillations were allowed between marking the amplitudes, when the hysteresis damping was small. From these measurements can be found the decrement $\delta\theta$ per oscillation for any amplitude θ. The loss of energy per cycle is then $\lambda\theta \cdot \delta\theta$, if λ is the torsional stiffness of the suspension. Since the system has a constant moment of inertia and a constant period, λ is the same for all the materials. The maximum stress in any cycle can be calculated from the equation

$$f_{\max.} = \frac{C\theta r}{l}, \quad . \quad . \quad (1)$$

where C = modulus of rigidity,
r = radius of suspension wire,
l = length.

This, however, involves a knowledge of C for all the materials, and the following method was actually used. If T is the twisting couple and J the polar moment of inertia of the cross-section of the wire,

$$f_{\max.} = \frac{Tr}{J} = \frac{\lambda\theta r}{J} = \frac{2\lambda\theta}{\pi r^3}. \quad . \quad . \quad . \quad . \quad . \quad (2)$$

For the series of materials λ is constant; hence, if $f_{\max.}$ is calculated by equation (1) for any one material such as steel having a well-established value for C, it is only necessary to know the radii of all the specimens to be able to calculate the stresses in all other cases by simple proportion from equation (2).

The results that have been obtained from such measurements show that the loss of energy per c.c. per cycle, denoted by h, is given by

$$h = k(f_{\max.})^n, \quad . \quad . \quad . \quad . \quad . \quad . \quad (3)$$

in which k is a constant for each material, and the index n is found to be always about 2, but in a number of metals it is rather greater than 2. In no material tested has an index less than 2 been found.

Since the strain applied is torsional the range of stress to which any element of the specimen is subjected varies from zero to the surface stress $f_{\max.}$ It can be shown, however, that within the elastic limit the hysteresis loss under uniform shear stress for any maximum stress f is also proportional to $(f)^n$.

Thus, let us assume the loss per c.c. to be kf^n, then the total loss is given by

$$E = \Sigma k(f)^n \delta V,$$

if δV is an element of volume for which the maximum stress in the cycle is f, or

$$E = \int_0^a k(f)^n 2\pi r l \, dr,$$

where r is the radius of any cylindrical shell of thickness dr, l is the length, and a the radius of the specimen.

At a radius r the stress $f = \frac{f_{\max.}}{a} r$. Hence

$$E = 2\pi k l \int_0^a \frac{(f_{\max.})^n}{a^n} r^{n+1} \, dr$$

$$= \frac{2}{n+2} k\pi a^2 l (f_{\max.})^n$$

$$= \frac{2}{n+2} k V (f_{\max.})^n,$$

or hysteresis loss per unit volume

$$h = \frac{2}{n+2} k (f_{\max.})^n. \quad . \quad . \quad . \quad . \quad . \quad (4)$$

Hence, when the hysteresis loss of a torsion specimen is found to be proportional to a power of the maximum stress at the surface, it follows that the same power law applies

Fig. 2.

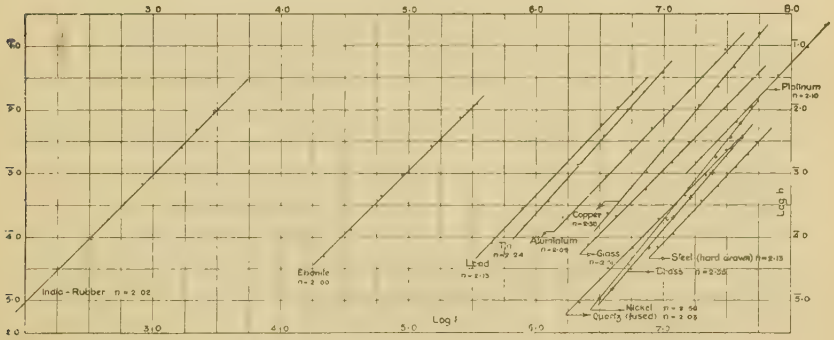

to the case of a uniform stress, but the constant in the latter case is greater in the ratio $\frac{n+2}{2}$.

The results of the measurements are shown by the curves of fig. 2. These show in c.g.s. units the hysteresis loss per unit volume of the torsion specimens plotted against maximum stress, logarithmic plotting being employed. It will be seen that all the curves are fairly closely linear, and there are slight variations in slope, the index n being given in brackets for each material. The maximum stress applied is comparatively low, and except for the platinum specimen does not exceed about 1000 lb. per sq. inch, and is as small as 140 lb. per sq. inch for the softer metals tin and lead. There is therefore little doubt that the stresses are well within the ordinary elastic range of the materials.

These results may be compared with those of Kimball and Lovell [3], who give a general formula for the internal friction loss per unit volume similar to the above, but with a uniform index 2. They state, however, that the formula is not given as an exact relation, but merely as the nearest all round statement of results obtained.

Reverting to the theory, it can be shown that such a result as the above would in general be expected. In the first place the loss of energy entailed in the supposed plucking process is liable to vary considerably, as different atoms may be drawn different distances into the unstable region. A great number of atoms are involved, however, and there will be a statistical average value ε for this loss of energy. The atoms to be affected first in an elastic strain are those already displaced by the maximum amount JL of fig. 1. Other atoms initially displaced by an amount such as JK will contribute to the loss of energy at a stage when the applied strain is equal to KL. Thus in any strain the total loss of energy depends on the statistical average value of ε and on the numerical distribution of the initial displacements of the atoms according to the magnitude of the displacement.

Since the normal distance between the atoms is e or OJ, corresponding to equilibrium between the repulsion and attraction, it is reasonable to suppose that of the atoms further apart than this there will be the greatest number in the neighbourhood of OJ and the least in the neighbourhood of OL. There should be none at all at greater distances than OL. If, then, the ordinate KB of the distribution curve shown at the foot of fig. 1 represents the number of atoms displaced by an amount JK, a curve having a maximum at J and approaching zero at L would be expected. If we now use the same diagram to represent the elastic displacement of the atoms due to an applied strain, taking the point L as origin and proceeding in the direction of J for an extension of the atom chain, it is clear that the amount of energy lost in a strain such as LK will be proportional to the area under the distribution curve from L to K.

Two types of distribution curve are shown in fig. 1, the first of which is linear, corresponding to a distribution in which the number of atoms having a particular displacement decreases uniformly as the displacement increases. The chief interest of this curve lies in the fact that it

evidently leads to the result that the loss of energy in a strain cycle is proportional to the square of the maximum strain or stress, as found by experiment in some materials.

As the phenomenon of hysteresis must involve very large numbers of atoms, it would appear more reasonable to expect a distribution of displacements determined by statistical considerations, and curve II. in fig. 1 therefore shows the probability curve of the type $y=e^{-x^2}$. This curve approaches the axis of x asymptotically, and at the same time in our hypothesis no displacements exceed JL, while the number which has the limiting value JL is supposed to approach zero, to avoid a discontinuity at

Fig. 3.

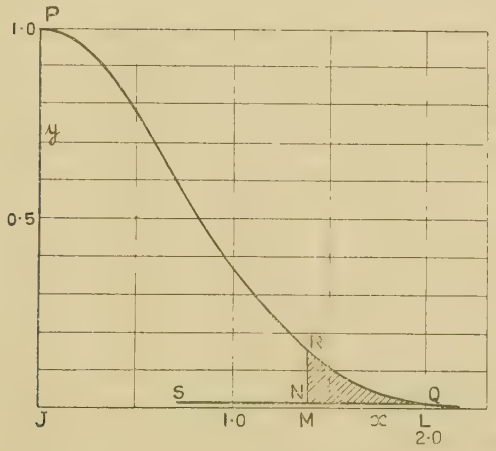

this point in the law of distribution. We shall therefore attempt to satisfy all these conditions by taking an arbitrary point such as Q in fig. 3 low down on the curve, and shall assume the ordinates of the curve, taken from the base line S Q, to represent the numerical distribution of displacements.

It is interesting that with such a distribution the theory indicates that the loss of energy in hysteresis would be given by a relation $h=k\ (f_{\max.})^n$, with an exponent n having a value somewhat greater than 2, as found experimentally for various metals.

Referring to fig. 3, in which the probability curve is drawn to scale, the hysteresis loss for a strain proportional

to LM is proportional to the area RQN. Having chosen an arbitrary value for x_0, the abscissa of the point Q, the relation between the area, and the value of LM can be readily computed numerically by means of the tabulated values of the probability integral. The results of this calculation for three different positions of the point Q, corresponding to values 1·6, 1·8, and 2·1 for x_0, are shown in fig. 4. These cover the complete range of the distribu-

Fig. 4.

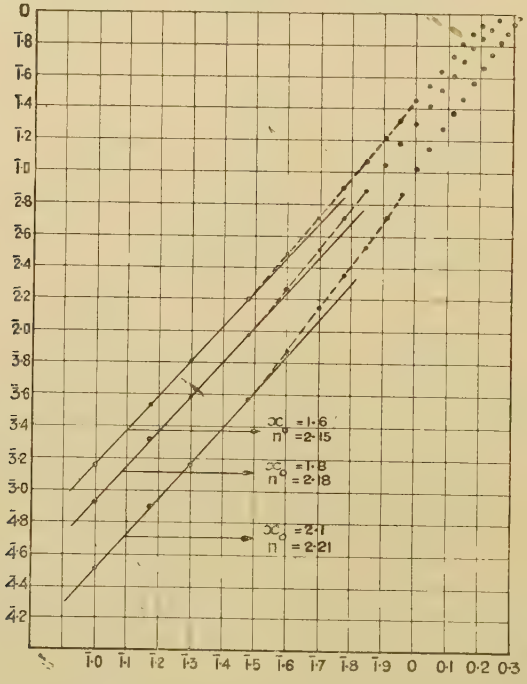

tion curve from Q to P, and the results are plotted logarithmically. The units employed in this diagram are quite arbitrary, and simply depend on the numerical values of the coordinates in fig. 3. It is clear that for a comparison with the hysteresis measurements of fig. 2 the lower part only of these curves need be considered, in view of the small range of strains concerned in the experiments. It will be seen in fig. 4 that the lower part of each curve is closely linear, indicating that the theory would give a

simple power law for the hysteresis loss of energy, and the values of the exponent in the three cases taken are 2·15, 2·18, and 2·21 respectively. The suggested theory, on assuming a reasonable type of distribution of displacements, thus appears to offer an explanation of the empirical power law which is well established by the experiments.

3. The theory proposed will now be considered from some other points of view. It is of some interest to notice, firstly, that the theory quite well accounts for the fact that elastic hysteresis is a process which is perfectly reversible in the elastic sense but quite irreversible thermodynamically. Thus, in passing through a strain cycle the increment of kinetic energy assumed to be gained by certain atoms is completely irreversible. On the other hand, the original arrangement of the atoms can recur exactly on removing the strain, as by this theory the production of heat energy is accounted for without having to consider any internal slip motion as taking place attended by some form of friction very similar to ordinary solid friction. The theory thus affords a satisfactory explanation of the perplexing fact, now well established, that under certain circumstances a solid can continue to dissipate energy by repetition of strain cycles apparently indefinitely, without any cumulative effect such as change in size or shape or internal structure.

The assumed mechanism by which the atom receives kinetic energy is itself irreversible, in the sense that it can only occur during a strain which causes an extension in the atomic chains. It would follow from the present theory that the instantaneous rate of loss of energy in the course of a stress-strain cycle would be very variable. Considering a symmetrical cycle, such as occurs in a torsional oscillation, as shown in fig. 5, the rate would be zero throughout the period of decreasing stress. During the period of rising stress the rate would commence at zero, increasing rather rapidly as the stress increased.

In this connexion some experiments made by Constant[4] are of much interest. In these experiments the rate of generation of heat in a magnetic hysteresis cycle was determined by a series of temperature measurements of the specimen. It was found that all the rise of temperature occurs in the stage of the cycle during

which the magnetic induction is increasing, and the rate of rise of temperature increases with the induction. During the stage of decreasing induction the temperature remains at a steady value. The rate of dissipation of energy thus exhibits quite closely the variations which should be found according to the theory in an elastic hysteresis cycle, if it were possible to make similar experimental observations. It is not impossible that the phenomena of magnetic and elastic hysteresis are more than merely analogous, and may each depend on a similar atomic mechanism. The magnitude of the loss of energy in the two cases is of the same order, and the occurrence of magneto-striction demonstrates the existence of small

Fig. 5.

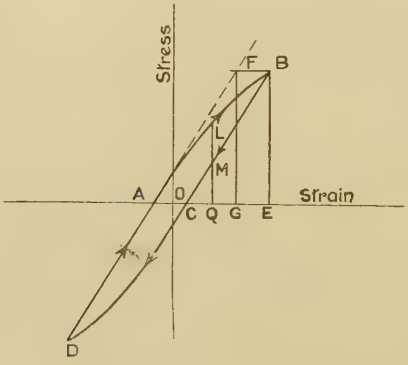

relative motions amongst the atoms during magnetization. Such a suggestion, in the absence of more substantial evidence, must be regarded as very tentative, but it does not seem unreasonable to imagine that all modes of dissipation of energy associated with minute relative motions of the atoms may have a common mechanism depending entirely on the nature of the atomic attraction and repulsion. The present theory already offers a common interpretation of many of the phenomena observed in solid friction, rolling friction, and elastic hysteresis—that is, in three different modes of relative atomic movement.

Reverting to the typical hysteresis cycle shown in fig. 5, the above remarks concerning the variations in the rate of loss of energy as deduced from the theory are

fully compatible with the observed form of the loop. It is found that when the stress is increasing from zero to the maximum, along the portion AB or CD of the cycle, the stress-strain relation is not quite linear, and the curve bends over more and more as the stress increases. On decreasing the stress the return portion BC of the cycle is found to be almost exactly linear and parallel to the initial slope of AB. The work done in straining the material along AB is represented by the area ABE, and the energy returned on coming back along the path BC is BCE, which is equal to AFG, the work that would be necessary to strain the material had the stress and strain remained proportional. Hence the path AB requires more energy than the return path BC by the amount ABC. In the theory proposed such a distinction between the condition of increasing and decreasing stress is definitely necessary, and this feature of the theory appears to be in good accordance with the form of the hysteresis loop found by the extensometer.

Since the theory indicates that a dissipation of energy occurs only in the course of a strain which involves an extension of the atom chains, it would follow that in a uniform compression, in which there can only be a compression of the chains everywhere, there should be an absence of hysteresis. It is significant that Bridgman[5] states that solids are found to behave with perfect elasticity under hydrostatic pressure even up to pressures of 12,000 atmospheres. There is not in general a strictly linear relation between stress and strain, but there is found to be no measurable departure from true elasticity on applying and removing the pressure.

The theory is found to be qualitatively in agreement with experiment as regards the effect on the hysteresis loss of overstrain and annealing. If the energy loss occurs as supposed entirely at certain points at which the atom chains are stretched by local distortion, and these points are scattered in a random way throughout the mass, it is reasonable to infer that by overstraining the material the total number of atoms displaced from the true equilibrium position would be increased. Some direct evidence of this is provided by the fact that overstraining a metal generally diminishes its density. In annealing, on the other hand, the atoms are set into more violent motion, and are then allowed to settle down slowly.

Initially some groups of atoms are nearer together than the equilibrium distance and others are further apart, and the process of annealing provides the atoms with an opportunity to re-arrange themselves slightly, aided by their own intrinsic forces, so that their final disposition is a closer approximation to the ideal formation. The hysteresis loss would therefore be expected to increase on overstraining a material and to decrease on annealing it. The above argument carries more weight if there is any reason to consider the strained atom chain to be quite an abnormal condition only occurring very sparsely

Fig. 6.

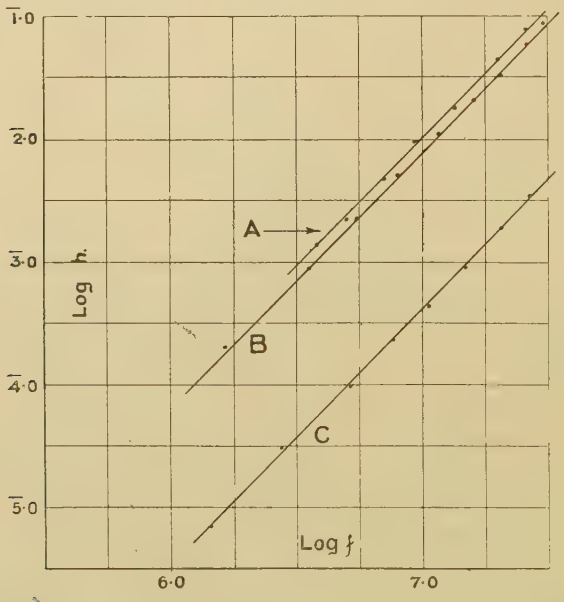

distributed. This point is discussed in a subsequent section of the paper, where reasons are given for thinking that the number of displaced atoms is only an extremely small proportion of the total number.

The above deductions are found to be well substantiated by the following experiment. An aluminium specimen was overstrained by twisting beyond its elastic limit, and the relation between hysteresis loss and maximum stress was then determined. The result obtained is shown by curve A of fig. 6 plotted logarithmically. Curve B is the

similar relation for the original material. The specimen was then annealed in a somewhat crude but effective way by passing a flame up and down its length a number of times, after which the result shown by curve C was obtained.

The three curves are closely parallel straight lines, showing that the hysteresis in each condition follows the same law $h = k(f_{\max})^n$, only the constant k being affected. In terms of the theory the statistical distribution of the atoms is not altered, but only the total number of displaced atoms. The difference in the latter or in the value of k is greater than appears from the logarithmic plotting. Thus the vertical distance between curves A and C is 1·4 on the logarithmic scale used—that is, the loss of energy in hysteresis after annealing is only about $\frac{1}{25}$ of that found after overstraining. A similar effect was found on annealing a brass wire specimen, the hysteresis being reduced to $\frac{1}{4}$ of the amount found in the unannealed state. Such results seem to indicate fairly definitely that hysteresis is a consequence of the presence of internal strains.

Certain results of other workers on internal friction will next be considered briefly as regards their bearing on the present theory. Kimball and Lovell[3] have quite established the fact that the energy loss per cycle is independent of the frequency of the cycles over a wide experimental range. Such a result was indicated, but not so completely confirmed, by the results of Hopkinson and Williams[6] and Rowett[7], working actually on a different aspect of the subject. This fact is difficult to reconcile with the views of some who prefer to regard hysteresis as a viscous phenomenon of the solid state, but is, on the other hand, a result to be expected by the proposed atomic theory, at least as regards ordinary frequencies attainable by experiment.

Another experimental result found by Guye[8] is that the internal friction of metals depends on the temperature, generally decreasing considerably as the temperature is reduced. Such a result has a simple explanation in the present theory and may be regarded as a consequence of the thermal contraction of the metal. The average distance between the atoms is slightly reduced, causing a general diminution in the displacements in the strained atom chains, as a result of which the numerical scale of the

distribution curve becomes reduced, and less energy is dissipated in any given strain cycle. Such an explanation, of course, involves the assumption that the force-fields of the atom are unaffected by the temperature of an aggregation of atoms.

4. If the view that both friction and elastic hysteresis have the same origin is provisionally accepted, it becomes possible to derive some further information about the process by combining data found experimentally as to the loss of energy in rolling friction and in hysteresis. The actual amount of energy involved on the average in each atomic separation can be estimated, and from this it can be shown that only an extremely small fraction of the atoms are concerned in the hysteresis loss in a stress-strain cycle.

The following data are taken from the previous paper[2], and concern the loss of energy in the rolling friction of a highly lapped steel cylinder rolling on a lapped steel plane surface:—

Diameter of cylinder = 0·254 cm.

Length of cylinder in rolling contact = 0·254 cm.

Load on cylinder = 300 gm. (M).

Coefficient of rolling friction = 0·000044 (λ).

Width of elastic contact area between cylinder and plane = $8{\cdot}28 \times 10^{-4}$ cm. ($2a$).

Mean contact stress $f = 0{\cdot}14 \times 10^{10}$ dynes per sq. cm.

Maximum contact stress $f_m = 0{\cdot}21 \times 10^{10}$ dynes per sq. cm.

In rolling through unit distance a total area of 0·254 sq. cm. comes into contact, and is subject at some moment to the maximum normal stress f_m. The loss of energy amounts to

$$E = \lambda M g \text{ ergs},$$

and, if we can estimate the total number N of atomic separations involved, an estimate of $\varepsilon = \frac{E}{N}$, the energy lost in the separation of one pair of atoms can be derived.

Unfortunately we can do no more than find two limits within which N most probably falls. An upper limit N_1 may be estimated by making the simple assumption that

the contact area of 0·254 sq. cm. is packed with atoms every one of which comes into repulsive contact with a corresponding atom in the other body. If e denotes the average distance between the atoms, for which the lattice constant $2{\cdot}86\times10^{-8}$ cm. will be assumed as a probable value, we have approximately

$$N_1=\frac{0{\cdot}254}{e^2}=3{\cdot}1\times10^{14}.$$

And the loss of energy involved in one atomic separation has a lower limit ϵ_1, given by

$$\epsilon_1=\frac{E}{N_1}=\frac{0{\cdot}000044\times300\times981}{3{\cdot}1\times10^{14}}=4{\cdot}1\times10^{-14}\text{ erg.}$$

The above estimate of N_1 is almost certainly too large, and it is more probable that in an elastic contact where the maximum stress has the comparatively low value $0{\cdot}21\times10^{10}$, the total number of atoms under repulsion is considerably less than the maximum possible number. In the writer's opinion, as described more fully in the previous paper on friction, the range of the repulsion is so small compared even with atomic dimensions that the atoms gradually come into repulsion to an extent which adjusts itself by the elastic strain to the normal stress, at least during the range of elastic contact. If the stress is further increased a point is reached at which the metal flows, and it may be reasonably assumed that then all the possible atoms are in active repulsion and are individually exerting the maximum repulsion that the strength of the lattice permits. For hard steel this flow stress is known to be about $7{\cdot}5\times10^{10}$ dynes per sq. cm., from which it may be inferred that the maximum atomic repulsion is about

$$7{\cdot}5\times10^{10}\times e^2=6{\cdot}15\times10^{-5}\text{ dyne.}$$

To derive a lower limit N_2 we can assume that the stress $0{\cdot}21\times10^{10}$ acting on the area 0·254 sq. cm. is supported by N_2 atoms repelling with forces having all possible values between zero and the maximum value of $6{\cdot}15\times10^{-5}$ dyne. In this way we have

$$N_2=\frac{0{\cdot}21\times10^{10}\times0{\cdot}254}{3{\cdot}07\times10^{-5}}$$

$$=1{\cdot}74\times10^{13}$$

and $$\epsilon_2=7{\cdot}4\times10^{-13}\text{ erg.}$$

This estimate N_2 is almost as certainly too small as N_1 is too large, since we have assumed that under a stress of only about $\frac{1}{3.5}$ of the flow stress there is an equal probability of all values of the repulsion right up to the maximum occurring with the flow stress.

The loss of energy in elastic hysteresis for steel piano-wire was found by experiment to be as follows :—

Maximum Stress.	Hysteresis loss per cycle.
Dynes per sq. cm.	Ergs per c. c.
$5{\cdot}4\times10^7$	3·00
4·68	2·02
3·72	1·285
2·68	0·63
1·97	0·40
$1{\cdot}57^5$	0·212
1·19	0·113
$0{\cdot}84^5$	0·067

Taking the first value in the Table of 3 ergs per c.c., even with the smaller estimate ϵ_1 the number of atoms involved in this loss of energy will be only

$$\frac{3}{4{\cdot}15\times10^{-14}} = 0{\cdot}725\times10^{14}.$$

The total number of atoms in 1 c.c. of iron is of the order $0{\cdot}8\times10^{23}$; hence, at the highest estimate only about 1 in 10^9 of the total atoms contributes to this loss of energy, although the whole number concerned in the hysteresis is very great, approximately 10^{14}. Thus it appears probable that the conditions of locally stretched atomic chains we have assumed to exist are quite sparsely scattered throughout the metal.

5. Certain of the well-known phenomena of hysteresis can be accounted for by the present theory. We have already seen how the general shape of the stress-strain loop may be deduced from the theory, and the formation of a loop will now be considered briefly from a somewhat different standpoint. For any given strains, such as OQ

in fig. 5, the rising stress LQ is always greater than the falling stress MQ, and this can be explained by the supposition that it is only with an extending atom chain that atoms can be displaced at all into the region of unstable equilibrium. In fig. 7 three atoms are shown diagrammatically: (*a*) as extended slightly beyond the critical distance as C moves to the right in an elastic strain, and (*b*) as distributed later after B has returned to a stable position and C is returning towards A. A reference to fig. 1 shows that the net attraction A—R between the atoms in case (*a*) is MS, while in case (*b*) it will be HV between A and B and NT between B and C, these being necessarily equal. It is clear that in case (*a*) this force must be greater than it is in case (*b*). With a rising stress

Fig. 7.

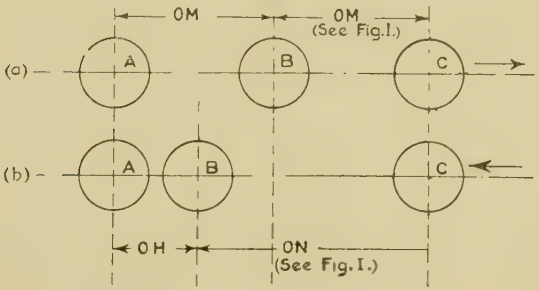

there are by our hypothesis a number of atoms passing through the condition corresponding to case (*a*). Regarding stress as the aggregate of the atomic forces, such atoms contribute a larger element of force with rising stress than the same atoms disposed as shown by case (*b*) when the stress is diminishing, and we should therefore expect the rising stress to exceed the falling stress for the same strain.

It is well known that in many metals if a stress-strain cycle is repeated a large number of times the loss of energy per cycle is found to diminish fairly rapidly at first, and then more and more slowly, becoming finally approximately constant. If the stress range is not great enough to induce a condition of fatigue, the final state

of hysteresis apparently may persist indefinitely. Gough and Hanson[9], for example, have subjected iron to no less than a hundred million cycles. This diminution in the hysteresis may be observed either by measurements of the stress-strain loop with an extensometer or by thermal measurement of the energy dissipated, a method successfully developed by Haigh. The effect is so marked that it has been suggested that there are two or even three different types of hysteresis. The initial stage, in which a rapid diminution of the lost energy occurs, has been called primary or transient hysteresis, leading to the second stage, which may be regarded as true elastic hysteresis, and is a stable condition of imperfect elasticity. If a sufficiently great stress range is employed, the second type of hysteresis gradually merges into what has been distinguished as a third type. In this there occurs a slow increase in the loss of energy, together with the development of a state of fatigue, and this phase ends in fracture of the material.

As regards the first and second types of hysteresis, a possible explanation of the observed phenomena can be given by the present theory. It may be suggested that the observed diminution in the energy dissipated per cycle from the primitive state to the final cyclic elastic condition is due to a process of auto-annealing, by which the displaced atoms are gradually enabled to adjust themselves in relation to their near neighbours, and arrive at a disposition more and more like the ideal condition of equilibrium. In a previous section the marked reduction in hysteresis produced by annealing has been attributed to a general tendency of the atoms at the strain centres to redistribute themselves more in equilibrium with their neighbours, this tendency being facilitated by the increased energy of motion imparted temporarily during annealing. It will now be shown that the momentary increase in the energy of those atoms, which by the theory give rise to the hysteresis, is itself a quantity comparable with the increased thermal energy of the atom in annealing. This leads to the view now suggested as a possibility, namely, that the hysteresis loss of energy dissipated in heat itself produces the gradual effect of internally annealing the material. The total amount of heat energy concerned is only enough to raise the whole mass very slightly in temperature, but this heat is primarily generated by only

a very small fraction of the total number of atoms, and the temporary access of energy of any atom may reasonably be supposed to assist in the tendency to a better adjustment of position in just the same way as in annealing. On this view the atoms which actually need the aid of annealing are just those which receive the extra energy in each stress-strain cycle No appreciable accumulation of energy from one cycle to the next will occur, as the time required to disperse the heat by conduction through the minute distances concerned is very small by comparison with the interval of time elapsing between successive cycles. The supposed process recurs, however, with every cycle until as many as possible of the displaced atoms are one by one assisted to take up a more normal arrangement with their neighbours, and by minute stages the distorted local condition becomes relieved. At the same time the energy dissipated becomes less and less, and a stage is reached at which no further readjustment occurs, a stage corresponding to the elastic or second type of hysteresis.

In a previous section we have given estimates of upper and lower limits of the energy lost per atom. These estimates are 74×10^{-14} and $4{\cdot}15\times10^{-14}$ erg, and from the manner of deriving them it is probable that they are decidedly too high and too low respectively. For our present purpose we shall take the geometric mean of the two $17{\cdot}5\times10^{-14}$ as a probable value, thereby assuming that each limit has the same probable percentage error. The average amount of energy possessed by one atom of iron at 15° C. can be computed approximately from the mass of the atom and specific heat data, and is about 10×10^{-14} erg. Hence, if we accept $17{\cdot}5\times10^{-14}$ as a probable value for the average quantity of energy added, this corresponds to the energy increment of a temperature rise amounting to 400–500° C. Even if the estimate of $17{\cdot}5\times10^{-14}$ should be high for the average value, the individual increments of energy of different atoms are probably very variable, and a certain proportion of the atoms may in every cycle receive sufficient heat energy to produce in time the local annealing effect in the way suggested.

If the present view is substantially correct, it follows that there is no physical distinction at all between the first and second phases of hysteresis, and the observed

difference is merely a numerical difference in the total number of displaced atoms involved.

6. The relative behaviour as regards hysteresis of the metals and non-metals deserves a brief discussion, as it involves the important question of whether a crystal unit is liable to elastic hysteresis, to which, unfortunately, no very conclusive answer can be given at present.

It was found that in the case of all the metals, which are composed of crystal aggregates, the index n had a value exceeding 2, whereas the non-metals, glass, quartz (fused), ebonite, and indiarubber, which have an amorphous atomic structure, all give an index which is closely equal to 2. Apart from this, however, there is no difference in behaviour as regards hysteresis between the crystalline and the amorphous materials. An inspection of fig. 2 shows how completely the curves for glass and quartz fit in with those of the metals. As the atoms constituting any crystal unit are arranged in a nearly perfect geometrical lattice, it is almost certain that the groups of bonding atoms between two crystals which are differently orientated must be disposed in some irregular manner. If the view expressed in this paper concerning the minute range of the atomic repulsion force is correct, the border-line between a lattice formation and an amorphous grouping of the atoms is fairly sharply defined, and any small cluster of atoms only need extremely small displacements to disturb completely the normal condition of equilibrium and result in an amorphous arrangement. It seems probable, therefore, that this is the condition of the bonding atoms, as Rosenhain supposes for other reasons in his well-known theory of inter-crystalline cement. The occurrence of strained atom chains therefore appears likely to be much more frequent among the bonding atoms than among those forming the regular lattice of the crystal unit, and it might be expected on general grounds that the hysteresis loss under low stresses would therefore be largely or even wholly confined to the former atoms.

On the other hand, there is the experimental fact that the hysteresis of glass and fused quartz, which are amorphous throughout, is very similar to that of the group of metals, which can contain only a very small proportion of probable amorphous material. If, therefore, the

hysteresis in the crystal aggregate is confined to the bonding atoms, it would follow that the loss of energy per unit mass of amorphous material must be far greater for the metals than for the non-metals, a conclusion which is difficult to accept. Furthermore, although little work has yet been attempted on the elastic hysteresis of single crystals, the experiments that have been made show that single crystal specimens display much the same hysteresis phenomena as ordinary aggregates.

The theory suggested in this paper perhaps helps to reconcile the apparent conflict with reason which arises if it must be accepted that hysteresis occurs in a strained crystal lattice. It has been estimated above that only about 1 in 10^9 of the atoms is involved in the loss of energy, and if this is the case it becomes clear that quite minute imperfections or discontinuities in the lattice structure, such as might be caused by impurities or submicroscopic fissures, would be sufficient to lead to hysteresis. In this connexion it may also be repeated that the theory requires only extremely small displacements of the atoms, and it is on all points quite compatible with the occurrence of hysteresis in a crystal unit.

The author is indebted to Sir J. E. Petavel, Director of the National Physical Laboratory, for the experimental facilities and permission to publish the paper, and to Mr. J. E. Sears for his continued interest in the work. Useful help has also been received from his colleagues Dr. Gough and Messrs. Wright and Cox in the course of discussion of the subject.

References.

(1) Trans. Farad. Soc. "Discussion on Cohesion," xxiv. p. 53 (1928).
(2) Phil. Mag. vii. p. 905 (1929).
(3) Phys. Rev. xxx. p. 948 (1927).
(4) Phys. Rev. xxxii. p. 486 (1928).
(5) Proc. 2nd International Congr. for App. Mechanics, Zurich (1926).
(6) Proc. Roy. Soc. lxxxvii. p. 502 (1912).
(7) Proc. Roy. Soc. lxxxix. p. 528 (1913).
(8) *Comptes Rendus*, p. 1066 (1909); p. 964 (1910).
(9) Proc. Roy. Soc. civ. p. 538 (1923).

LXXXVI. *Redshift and Relativistic Cosmology.* *By* Hermann Weyl, *Zurich (Switzerland)**.

Abstract.

1. The de Sitter hyperboloid as homogeneous state of the world. Besides, on this solution of the gravitational equations, the cosmology depends on additional assumptions concerning the question which part of the hyperboloid corresponds to the real world, and, in connexion with this, concerning the undisturbed state of motion of the stars. The static coordinates used by most authors represent only a cuneiform sector.

2. Hypothesis of common origin in the infinitely distant past. The range of influence of a star covers only half the hyperboloid. ∞^3 stars have their range of influence in common with it. Assumption that this half is the entire universe.

3. The universe then has the same topological character as in the special theory of relativity. Introduction of Robertson's coordinates. Computation of the redshift by means of these coordinates.

4. A homogeneous distribution of mass of infinitely small density is possible by which no point in space and time is distinguished. Computation of the density in static coordinates. Space is open, the total mass infinite.

RECENT observations made on spiral nebulæ have ascertained their extra-gallactic nature and confirmed the redshift of their spectral lines as systematic and increasing with the distance †. By these facts the cosmological questions about the structure of the world as a whole, to which the general theory of relativity gave rise in purely speculative form, have acquired an augmented and empirical interest. It is not my opinion that we can vouch for the correctness of the "geometrical" explanation which relativistic cosmology offers for this strange phenomenon with any amount of certainty at this time. Perhaps it will have to be interpreted in a more physical manner, in correspondence

* Communicated by the Author.

† E. Hubble, Proc. Nat. Ac. xv. p. 168 (1929).

with the ideas of F. Zwicky *. But the cosmologic-geometrical conception must on any account be examined seriously as a possibility. And this is my motive for saying a few words about the more recent discussion of the question by H. P. Robertson † and R. C. Tolman ‡ : firstly, to show that the cosmology proposed by Robertson is identical with the one proposed by me—this is the result of a conference with Professor Robertson at Princeton ; and, secondly, to clarify and defend my or our point of view as opposed to the assertions of Professor Tolman §.

Like Mr. Tolman, I start from de Sitter's solution: the world, according to its metric constitution, has the character of a four-dimensional "sphere" (hyperboloid)

$$x_1^2+x_2^2+x_3^2+x_4^2-x_5^2=a^2 \quad . \quad . \quad . \quad . \quad (1)$$

in a five-dimensional quasi-euclidean space, with the line element

$$ds^2=dx_1^2+dx_2^2+dx_3^2+dx_4^2-dx_5^2. \quad . \quad . \quad (2)$$

The sphere has the same degree of metric homogeneity as the world of the special theory of relativity, which can be conceived as a four-dimensional "plane" in the same space. The plane, however, has only one connected infinitely distant "seam," while it is the most prominent topological property of the sphere to be endowed with two—the infinitely distant past and the infinitely distant future. In this sense one may say that space is closed in de Sitter's solution. On the other hand, however, it is distinguished from the well-known Einstein solution, which is based on a homogeneous distribution of mass, by the fact that the null cone of future belonging to a world-point does not overlap with itself; in this causal sense, the de Sitter space is open.

Tolman's careful investigation shows anew that nothing like a systematic redshift can be derived solely on the basis of the constitution of the metric field in its undisturbed state, *i. e.*, from the de Sitter solution of the gravitational equations. I believe, however, that in a complete cosmology supplementary assumptions must be added :—(1) assumptions of topological character, which determine whether the entire

* Phys. Rev. xxxiii. p. 1077 (1929). A detailed communication will appear in the Proc. Nat. Ac.

† Phil. Mag. v. Suppl. p. 835 (1928).

‡ Astroph. Journ. lxix. p. 245 (1929).

§ Besides, in the fifth edition of 'Raum Zeit Materie' (Berlin, 1923), I have exposed my opinion in 'Was ist Materie?,' p. 71 (Berlin, 1924), and defended it against L. Silberstein in Phil. Mag. [6] xlviii. p. 348 (1924).

de Sitter sphere or which part of it corresponds to the real world, and (2) closely connected with these an assumption about the "undisturbed" motion of the stars by which ∞^3 geodesic world-lines are set off from the manifold of all these lines. As regards the first point, the static coordinates, *e. g.*, which belong to a star (the "observer"), and with which Mr. Tolman works by preference, represent only a cuneiform sector of the entire sphere.

The world-line of the observer A shall be given by

$$x_1 = x_2 = x_3 = 0, \qquad x_4 > 0. \quad . \quad . \quad . \quad . \quad (3)$$

Let us put

$$x_4 = z \,.\, \mathrm{ch}\, t/a, \qquad x_5 = z \,.\, \mathrm{sh}\, t/a. \quad . \quad . \quad . \quad (4)$$

Then we obtain

$$ds^2 = (dx_1^2 + dx_2^2 + dx_3^2 + dz^2) - \frac{z^2}{a^2}\, dt^2 \quad . \quad . \quad (5)$$

with the relation

$$x_1^2 + x_2^2 + x_3^2 + z^2 = a^2. \quad . \quad . \quad . \quad . \quad . \quad (6)$$

Space and time fall apart ; space, with regard to its metric constitution, is the three-dimensional sphere (6) of radius a in a four-dimensional euclidean space with coordinates $x_1\, x_2\, x_3\, z$, or rather the hemisphere $z > 0$. Our representation only exhibits the sector of the hyperboloid

$$x_4 + x_5 > 0, \qquad x_4 - x_5 > 0. \quad . \quad . \quad . \quad . \quad (7)$$

The geodesics are cut out of the sphere by the two-dimensional planes passing through the origin in the five-dimensional space with the coordinates x_a. The null cones opening into the future, which issue from all the points of such a geodesic with time-like direction, from the world-line of a star, fill a region of the world which I shall call the *range of influence of the star*. It is a highly remarkable feature of the de Sitter cosmology that this range of influence covers only half the hyperboloid (while it coincides with the entire "plane" in the special theory of relativity). In the case of the observer star A, for example, the range of influence is characterized by $x_4 + x_5 > 0$. (The sector represented by the corresponding static coordinates is again only part of the range of influence, and more precisely that part which is accessible to observation from A.) There are ∞^3 stars or geodesics to which the same range of influence belongs as to the arbitrarily chosen star A ; they form a *system that has been causally interconnected since eternity.*

Stars that do not belong to it lie beyond the range of influence of A during their early history. On the other hand, it is true that if A′ is a star of the system, A ceases to act upon A′ from a certain moment of its history on, even though conversely A′ remains in the range of influence of A during its entire history. Therefore the stars of the system may be described as stars "of common origin," but the common origin lies in an infinitely distant past. *Our assumption is that in the undisturbed state the stars form such a system of common origin.* Clearly this means neither continuous formation nor continuous entry in the sense of the two hypotheses mainly discussed by Mr. Tolman. By the assumption of the common range of influence the future acquires a different significance from the past. Moreover, it can be shown that this assumption (and the contrary one that results from it by the interchange of past and future) is the only one which sets off a system of ∞^3 geodesics from the entire manifold of these lines in such a manner that all time moments remain equivalent.

If this hypothesis of common origin, according to which the stars have stood in a connexion of mutual interaction since eternity, is the correct one, it will be natural to consider only that part of the sphere which they cover, *i. e.*, that half of the hyperboloid which represents their common sphere of influence as the real world. This is surely the smallest part of the hyperboloid that can be taken into consideration as the real world: a star existing from eternity to eternity and the propagation of the light emitted by it must have room in the universe. By the perfectly natural topological assumption that the world does not project over this minimum, the ∞^3 geodesics referred to are immediately distinguished as those lines which have taken their course in the real world since eternity, which, therefore, demand neither formation of stars nor "entry from the border of the world" at a finite moment of time. Only when referring to the entire hyperboloid is it appropriate to describe the pencil of ∞^3 world-lines of our system of stars as one that concentrates on an infinitely small part of the total extent of the sphere towards the infinitely distant past, while it spreads over it more and more towards the future.

But if only that half which is covered by the world-lines has real significance, it is convenient to follow Professor Robertson in introducing coordinates τ, ξ_1, ξ_2, ξ_3, such that the world-lines expressed in terms of them appear as "parallel vertical straight lines" on which the three "spacial coordinates" ξ_1, ξ_2, ξ_3 are constant and only the "time" τ

varies *. All four coordinates are capable of the values from $-\infty$ to $+\infty$ independently of one another; the world has again exactly the same topological constitution as in the special theory of relativity, so that one can no longer reasonably speak of a "closed space." The introduction of these coordinates can be performed in such a manner that the line element assumes the form

$$ds^2 = e^{-2\tau/a}(d\xi_1^2 + d\xi_2^2 + d\xi_3^2) - d\tau^2. \quad . \quad . \quad (8)$$

If one asks for all the transformations which not only leave this expression of the metric field invariant but carry the system of the world-lines of our stars into itself, the answer reads: all euclidean motions of the space $(\xi_1\,\xi_2\,\xi_3)$ combined with the transformation $\tau \longrightarrow \tau + \tau_0$, $\xi_i \longrightarrow e^{\tau_0/a}\,.\,\xi_i$ (τ_0 an arbitrary constant). Thus full homogeneity prevails also with regard to the stellar motions. a cannot very well be regarded as the radius of space any longer; according to (8) its simplest interpretation is that of being the standard of measurement for the scattering of the stars or the redshift which corresponds to it as Doppler effect.

To arrive at the Robertson coordinates, we bear in mind that the world-line of a star in our system is defined by a set of equations

$$x_i = \xi_i(x_4 + x_5)/a \qquad [i = 1, 2, 3]$$

with constant ξ_i (two-dimensional plane that goes through the line

$$x_1 = x_2 = x_3 = 0, \qquad x_4 + x_5 = 0).$$

Let us add the definition

$$x_4 + x_5 = a\,.\,e^{\tau/a},$$

which takes account of the restriction $x_4 + x_5 > 0$. The transformation can then be summed up in the form

$$x_i = \xi_i\,.\,e^{\tau/a} \quad [i = 1, 2, 3], \qquad x_4 + x_5 = a\,.\,e^{\tau/a}. \quad . \quad (9)$$

On account of equation (1),

$$x_1^2 + x_2^2 + x_3^2 + (x_4 + x_5)(x_4 - x_5) = a^2,$$

$x_4 - x_5$ can then be expressed in the Greek coordinates. For ds^2 one easily obtains the desired result (8). If one puts

$$x_1^2 + x_2^2 + x_3^2 = r^2, \qquad \xi_1^2 + \xi_2^2 + \xi_3^2 = \rho^2,$$

then

$$z = \sqrt{a^2 - r^2}$$

* The same coordinates have already been discovered by G. Lemaitre, Journ. Math. Massach. iv. p. 188 (1925).

in that region which can be referred to the static coordinates of the observer, and according to (4) the equations (9) furnish

$$r=\rho\,.\,e^{\tau/a}, \qquad \sqrt{1-\left(\frac{r}{a}\right)^2}\,.\,e^{t/a}=e^{\tau/a} \quad . \quad . \quad (10)$$

for the connexion which Robertson himself indicated as prevailing between his own and the static coordinates. But it is essential to take into consideration not only this part but the entire range of influence of the observer star. For the cosmology which regards it as the real world the coordinates introduced by Mr. Robertson are by far the most appropriate.

Since Mr. Tolman finds the derivation of my formula for the redshift unclear, it shall quickly be repeated here in the Greek coordinates. The final result, of course, depends on what one means by the distance of the observed star from the observer. If the equation of the infinitely small null cone issuing from an arbitrary point is written in the form

$$d\xi_1^2+d\xi_2^2+d\xi_3^2-a^2(de^{-\tau/a})^2=0,$$

it is immediately seen that the equation of the finite null cone issuing from the point

$$\xi_1=\xi_2=\xi_3=0, \qquad \tau=\tau_0,$$

is the following :

$$\xi_1^2+\xi_2^2+\xi_3^2-a^2(e^{-\tau/a}-e^{-\tau_0 a})^2=0,$$

or the time τ at which a light-signal must be dispatched from a star at the distance ρ in order to reach the observer at the moment τ_0 is given by

$$\rho=a(e^{-\tau/a}-e^{-\tau_0/a}).$$

To the radiation period $d\tau$ therefore corresponds the observation period $d\tau_0$, which is furnished by

$$d(e^{-\tau/a}-e^{-\tau_0/a})=0 \qquad \text{or} \qquad e^{-\tau/a}d\tau=e^{-\tau_0 a}d\tau_0.$$

A radiation frequency ν is observed as the distinct frequency ν_0:

$$\frac{\nu_0}{\nu}=\frac{d\tau}{d\tau_0}=e^{(\tau-\tau_0)/a}.$$

This may be written

$$\frac{\nu_0}{\nu} = e^{\tau/a} \cdot e^{-\tau_0/a} = e^{\tau/a}\left(e^{-\tau/a} - \frac{\rho}{a}\right) = 1 - \frac{\rho}{a} e^{\tau/a}.$$

If the r of the star has the value r at the moment of light emission, then, according to (10),

$$\frac{\nu_0}{\nu} = 1 - \frac{r}{a}, \qquad \frac{\Delta\nu}{\nu} = -\frac{r}{a}.$$

r is the projection of the natural distance d on the sphere (6) onto the equatorial plane $z=0$; therefore

$$\frac{r}{a} = \sin\frac{d}{a},$$

and we have the formula

$$\frac{\Delta\nu}{\nu} = -\sin d/a.$$

Mr. Tolman asks why I got the tan instead of the sin. The reason for this is as follows. In my earlier paper d meant the naturally measured distance of the star in the static space *at the same moment t at which the observation takes place* ; t is the static time of the observer. We have

$$\frac{\nu}{\nu_0} = e^{\tau_0/a} \cdot e^{-\tau/a} = e^{\tau_0/a}\left(e^{-\tau_0/a} + \frac{\rho}{a}\right)$$

$$= 1 + \frac{\rho}{a} e^{\tau_0/a}. \quad . \quad . \quad . \quad . \quad (11)$$

The time t of observation is $=\tau_0$. According to (10)

$$\frac{r}{\sqrt{a^2 - r^2}} = \frac{\rho}{a} \cdot e^{t/a}$$

holds. At the moment of observation $t=\tau_0$, the star ρ therefore has the distance r which is given by this equation with $t=\tau_0$, and one obtains from (11)

$$\frac{\nu}{\nu_0} = 1 + \frac{r}{\sqrt{a^2 - r^2}} = 1 + \tan d/a.$$

So long as one is only dealing with distances that are small compared with a the precise definition is of no consequence, and one obtains the law for the linear increase of

the redshift with the distance; but as soon as the order of magnitude of a is approached, an exact discussion is required as to which distance is determined by the indirect astronomical methods.

The de Sitter solution corresponds to an empty world or to an infinitely small density of the stars. Can this density be chosen so that the distribution of the stars distinguishes neither a definite centre in space nor a definite moment in time? This is actually possible; the density need only be assumed constant, say $=\beta$, in the Robertson coordinates. The total mass of the universe then becomes infinite. This shows clearly how impossible it has become to speak of a closed space. It is, of course, easy to reduce this density to static coordinates. We determine the mass which is contained at the static time t in the region $r \leqq r_0$ of static space. The world-lines of this mass cover that part of the world which is described by $\rho \leqq \rho_0$ in Robertson's coordinates,

$$\rho_0 = -\frac{ar_0}{\sqrt{a^2 - r_0^2}} \cdot e^{-t/a}.$$

The desired mass is therefore

$$= \beta \cdot \frac{4\pi}{3} \rho_0^3 = \frac{4\pi\beta}{3} \left(\frac{r_0}{\sqrt{1 - r_0^2/a^2}} \right)^3 \cdot e^{-3t/a}.$$

In the region in which r lies between r and $r+dr$ we consequently at the time t find the mass

$$4\pi\beta r^2 dr \cdot \frac{e^{-3t/a}}{(1 - r^2/a^2)^{5/2}}.$$

The naturally measured volume of this zone is

$$4\pi r^2 dr \,:\, (1 - r^2/a^2)^{1/2},$$

so that the quantity

$$\beta \cdot \frac{e^{-3t/a}}{(1 - r^2/a^2)^2}$$

is to be regarded as the density at the distance r and at the time t.

Berkeley, California,
July 1929.

LXXXVII. *The Equilibrium of Dense Stars.* *By* EDMUND C. STONER, *Ph.D. (Camb.), Reader in Physics, University of Leeds* *.

Introduction.

IN white dwarf stars the last stages of the ionization process are reached, so that at least in the central parts the molecules consist almost entirely of atomic nuclei and free electrons. Under these conditions very high densities are possible. The mean densities deduced from observations, though large (of the order 50 to 100 thousand), fall very far short of those corresponding to a "close-packed" arrangement, if a naive view of the "sizes" of electrons and nuclei is taken. It was suggested that some limitation might be introduced by the "jamming" of a few remaining atoms with K-ring electrons. In a previous paper †, however, it was shown that a limitation is imposed by the exclusion principle applying to free electrons, as embodied in the Fermi statistics. The number of electrons with momenta within a definite range cannot exceed a certain maximum. Any increase in density involves an increase of energy. In the limiting case, at absolute zero, the star can contract until the decrease in gravitational energy becomes insufficient to balance the increase of kinetic energy of the electrons. With a few simplifying assumptions, an expression was derived which indicated that the maximum density varied as the square of the mass of the star. It has been pointed out by Anderson ‡ that in this calculation the effect of the relativity change of mass was neglected. He has taken this effect into account, but in a manner which seems open to criticism. His general conclusions, which seem to be correct, are that the simple expression holds provided the electron densities are not too large, but that the mass corresponding to large electron densities is smaller than that previously calculated, and that it reaches a limit. The correction becomes important for stars of mass about half that of the Sun, and so for the white dwarfs which were actually considered. The main purpose of this paper is to calculate the effect of the relativity change of mass, using a method which seems more rigorous than

* Communicated by Prof. R. Whiddington, F.R.S.

† E. C. Stoner, Phil. Mag. vii. p. 63 (1929). (This paper will be referred to as I.)

‡ W. Anderson, *Zeits. für Phys.* lvi. p. 851 (1929).

that of Anderson. The conclusion drawn is that the range in which the simple expression holds approximately is wider than that indicated by Anderson's results, the "limiting mass" being somewhat greater, so that there is still an equilibrium state, under the particular conditions, for the stars under consideration. The significance of the results for very dense stars is discussed, and the effect of the electron gas following the Fermi statistics at the smaller densities found in normal stars is briefly considered.

Effect of the Relativity Change of Mass on the Zero-point Energy of Electron Gas.

Let E_G be the gravitational energy of the idealized star, E_K the total kinetic energy of the electrons, n the number of electrons per unit volume. Then, as previously shown, the equilibrium condition is given by

$$\frac{d}{dn}(E_G+E_K)=0. \quad . \quad . \quad . \quad . \quad . \quad . \quad (1)$$

Let ϵ be the mean kinetic energy of the electrons at absolute zero, V the volume of the star, supposed to be of uniform density. (The distribution of density will be considered later.) When the relativity change of mass is neglected, the total kinetic energy at absolute zero is given by

$$E_K=nV\bar{\epsilon}=nV\frac{3}{40}\left(\frac{3}{\pi}\right)^{2/3}\frac{h^2n^{2/3}}{m_0}. \quad . \quad . \quad . \quad (2)$$

It is this expression which has to be modified.

In Anderson's treatment m_0 is replaced by m, where m is derived from the equation

$$c^2(m-m_0)=\frac{3}{40}\left(\frac{3}{\pi}\right)^{2/3}\frac{h^2n^{2/3}}{m}. \quad . \quad . \quad . \quad . \quad (3)$$

It is thus assumed that the total kinetic energy can be expressed in the alternative forms

$$nVc^2(m-m_0) \quad \text{and} \quad nV\frac{3}{40}\left(\frac{3}{\pi}\right)^{2/3}\frac{h^2n^{2/3}}{m},$$

where m has the same value in both expressions, being a "mean" mass; further, that this mean mass can be employed in subsequent calculations in place of m_0. The value of a mean mass, however, depends on the manner in which the mass enters into the particular expressions for which the appropriate mean value is being derived, and it is not legitimate to use one particular mean value indiscriminately

in more general calculations. (Perhaps the simplest illustration is that the arithmetic mean is not in general equal to the root mean square. The objection to Anderson's treatment has a similar basis.) It seems more satisfactory to attack the problem of determining the zero-point energy without introducing the idea of mean mass at all.

Let ϵ be the kinetic energy of an electron, p the momentum, and let $\beta = v/c$,

$$\epsilon = (m - m_0)c^2 = m_0c^2\left(\frac{1}{\sqrt{1-\beta^2}} - 1\right), \quad . \quad . \quad (4)$$

$$p^2 = (m\beta c)^2 = m_0{}^2c^2\left(\frac{1}{1-\beta^2} - 1\right). \quad . \quad . \quad . \quad . \quad . \quad (5)$$

Substituting for $1/\sqrt{1-\beta^2}$ in (4),

$$\epsilon = m_0c^2\left[\left(1 + \frac{p^2}{m_0{}^2c^2}\right)^{1/2} - 1\right]. \quad . \quad . \quad . \quad . \quad (6)$$

In the completely condensed state there are two electrons in each cell of the 6-dimensional phase-space (of 6-volume h^3), so that the number of electrons in a volume V with momenta between p and $p + dp$ is equal to

$$2 \times \frac{4\pi p^2 dp}{h^3} \times \mathrm{V}.$$

Thus for the total energy $\mathrm{E_K}$ of the electrons in a condensed state with maximum momentum p_0

$$\mathrm{E_K} = \int_0^{p_0} 2m_0c^2\left[\left(1 + \frac{p^2}{m_0{}^2c^2}\right)^{1/2} - 1\right]\frac{4\pi p^2 dp\,\mathrm{V}}{h^3}. \quad . \quad (7)$$

Since $n\mathrm{V}$ is the total number of electrons (double the number of cells), the maximum momentum p_0 is related to n by

$$(\mathrm{V}/h^3)\int_0^{p_0} 4\pi p^2\,dp = \tfrac{1}{2}\,n\mathrm{V}.$$

Let

$$\left.\begin{aligned} n &= \frac{8\pi p_0{}^3}{h^3}, & p_0 &= \left(\frac{3h^3n}{8\pi}\right)^{1/3}. \\ y &= \frac{p}{m_0c}, & x &= \frac{p_0}{m_0c}. \end{aligned}\right\} \quad . \quad . \quad (8)$$

Then

$$E_K = \frac{8\pi V m_0 c^2}{h^3} \times (m_0 c)^3 \int_0^x \{(1+y^2)^{1/2} - 1\} y^2 \, dy,$$

$$= \frac{8\pi V m_0^4 c^5}{h^3} \left[-\frac{x^3}{3} + \int_0^x (1+y^2)^{1/2} y^2 \, dy \right] \quad . \quad (9)$$

$$= \frac{8\pi V m_0^4 c^5}{h^3} \left[-\frac{x^3}{3} + f(x) \right] . \quad . \quad . \quad . \quad . \quad . \quad . \quad (9a)$$

As long as x is small (i. e., $p_0 << m_0 c$), $f(x)$ may be readily evaluated by integration in series,

$$[f(x)]_{x<} = \frac{1}{3} x^3 + \frac{1}{10} x^5 - \frac{1}{56} x^7 \ldots,$$

$$E_K = \frac{8\pi V m_0^4 c^5}{10 h^3} x^5 \left(1 - \frac{5}{28} x^2 \ldots \right) . \quad . \quad . \quad (10)$$

Substituting for x

$$E_K = \frac{8\pi V}{3 h^3 m_0} p_0^5 \left(1 - \frac{5}{28} \frac{p_0^2}{m_0^2 c^2} \ldots \right), \quad . \quad . \quad . \quad . \quad (10a)$$

$$= n V \frac{3}{40} \left(\frac{3}{\pi} \right)^{2/3} \frac{h^2 n^{2/3}}{m_0} \left[1 - \frac{5h^2}{112} \left(\frac{3}{\pi} \right)^{2/3} n^{2/3} \right], \quad . \quad (10b)$$

agreeing in the limit with (2) for n small.

The above expression may be used for $p_0 << m_0 c$, corresponding to $n << \frac{8\pi}{3} \left(\frac{m_0 c}{h} \right)^3$, or, substituting numerical values, $n << 5{\cdot}88 \times 10^{29}$. For stars of mass ·44 and ·85 that of the Sun, the value of n came out on the simple theory as about $1{\cdot}86 \times 10^{29}$ and $6{\cdot}9 \times 10^{29}$. The approximation given by series integration is thus inadequate, and it is necessary to use the complete expression for the integral

$$f(x) = \int_0^x (1+y^2)^{1/2} y^2 \, dy,$$

$$= \int_0^x (1+y^2)^{3/2} \, dy - \int_0^x (1+y^2)^{1/2} \, dy.$$

The second integral is known, and the first may be reduced by noting that

$$\frac{d}{dy} \{ y (1+y^2)^{1/2} \} = 4(1+y^2)^{3/2} - 3(1+y^2)^{1/2}.$$

The final result is

$$f(x)=\tfrac{1}{8}[x(1+x^2)^{1/2}(1+2x^2)-\log\{x+(1+x^2)^{1/2}\}]. \quad (11)$$

For x small this may be expanded (noting that the log is equal to

$$\int(1+x^2)^{-1/2}\,dx),$$

giving the result (10) on substitution in (9 *a*).

The complete expression for the total kinetic energy of the electrons thus becomes

$$E_K=\frac{8\pi V m_0^4 c^5}{h^3}[\tfrac{1}{8}x(1+x^2)^{1/2}(1+2x^2)-\tfrac{1}{3}x^3 - \log\{x+(1+x^2)^{1/2}\}], \quad (12)$$

with

$$x=\frac{p_0}{m_0 c}=\frac{1}{m_0 c}\left(\frac{3h^3 n}{8\pi}\right)^{1/3}.$$

The energy is less than that given by (2). In the limit when x is large ($x>>1$, $n>>5{\cdot}88\times10^{29}$),

$$(E_K)_{x>>1}=\frac{8\pi V m_0^4 c^5}{h^3}\frac{x^4}{4},$$

$$=\frac{2\pi V c}{h^3}p_0^4=nV\frac{3}{8}\left(\frac{3}{\pi}\right)^{1/3}hcn^{1/3}. \quad (12\,a)$$

These expressions may be compared with (10 *a*) and (10 *b*). They show that when n is large the mean kinetic energy increases as $n^{1/3}$ (instead of n^2). For a constant total number of electrons (nV constant), E_K then varies as $n^{1/3}$, as does also $-E_G$. When this is so there will obviously be no equilibrium under the conditions imposed.

The Equilibrium Condition.

If the conditions are such that an equilibrium state is possible, there will be a limiting density—"limiting" because the calculation refers to a sphere of uniform density at zero temperature. The limiting density is that corresponding to the value of n when

$$\frac{d}{dn}(E_K+E_G)=0. \quad (13)$$

It is more convenient, for the present application, to treat x, defined by (8), as the variable, so that the equilibrium condition becomes

$$\frac{d}{dx}(E_K+E_G)=0. \quad (14)$$

For the gravitational potential energy (as shown in I.) with $2{\cdot}5\ m_{\mathrm{H}}$ as the mean molecular weight of the material of the star,

$$\mathrm{E_G} = -\frac{3}{5}\frac{\mathrm{GM}^2}{\mathrm{M}^{1/3}}\left(\frac{4}{3}\pi n\right)^{1/3}(2{\cdot}5\ m_{\mathrm{H}})^{1/3}. \quad . \quad . \quad (15a)$$

Substituting $\left(\frac{8\pi}{3}\right)^{1/3}\frac{m_0 c x}{h}$ for $n^{1/3}$ from (8),

$$\mathrm{E_G} = 3^{1/3}\left(\frac{4\pi}{5}\right)^{2/3}\frac{1}{h}\mathrm{GM}^{5/3}m_{\mathrm{H}}^{1.3}m_0 c x. \quad . \quad . \quad (15b)$$

From (12) $\mathrm{E_K}$ may be written as

$$\mathrm{E_K} = \frac{8\pi \mathrm{V} m_0^4 c^5}{h^3} f_1(x).$$

Substituting $\mathrm{M}/(2{\cdot}5\ m_{\mathrm{H}}n)$ for V, and further substituting for n as above,

$$\mathrm{E_K} = \frac{3\mathrm{M}m_0 c^2}{2{\cdot}5\ m_{\mathrm{H}}}\frac{f_1(x)}{x^3}. \quad . \quad . \quad . \quad . \quad . \quad . \quad (16)$$

Using the values (15) and (16) in (14), the result is

$$\frac{d}{dx}\left[\frac{1}{x^3}f_1(x)\right] = 10^{1.3}\left(\frac{\pi}{3}\right)^{2/3}\frac{\mathrm{G}m_{\mathrm{H}}^{4/3}\mathrm{M}^{2/3}}{hc}. \quad . \quad (17)$$

Inserting numerical values,

$$\frac{d}{dx}\left[\frac{1}{x^3}f_1(x)\right] = \mathrm{F}(x) = 1{\cdot}483\times10^{-23}\mathrm{M}^{2/3}, \quad . \quad (18)$$

$$\mathrm{M} = 1{\cdot}751\times10^{34}[\mathrm{F}(x)]^{3/2}. \quad . \quad . \quad . \quad . \quad (18a)$$

$\mathrm{F}(x)$ is obtained by straightforward differentiation of $\frac{1}{x^3}f_1(x)$, where $f_1(x)$ is the bracketed quantity in (12). The final result is

$$\mathrm{F}(x) = \frac{1}{8x^3}\left[\frac{3}{x}\log\{x+(1+x^2)^{1/2}\} + (1+x^2)^{1/2}(2x^2-3)\right].$$
$$. \quad . \quad . \quad (19)$$

By means of equations (18*a*) and (19) the mass may be found corresponding to any value of x, and so to any limiting electron concentration. Since the mean molecular weight is about $2{\cdot}5\ m_{\mathrm{H}}$, the limiting density is given by

$$\rho_0 = 2{\cdot}5\ m_{\mathrm{H}}n = 4{\cdot}15\times10^{-24}n. \quad . \quad . \quad . \quad (20)$$

Numerical Results.

The method of procedure adopted is to calculate $F(x)$ for different values of x, from which a $F(x)$, x curve may be plotted. From this, using (18 a), an M, x curve may be derived. If desired, this may be converted into an M, n curve, using the relation

$$n=\left(\frac{8\pi}{3}\right)\left(\frac{m_0c}{h}\right)^3 x^3,$$

giving

$$n=5{\cdot}876\times10^{29}x^3 \quad \text{or} \quad x=1{\cdot}194\times10^{-10}n^{1/3}. \quad . \quad (21)$$

The full expression for $F(x)$ (19) is inconvenient to use when x is small. The expression may then be expanded, with the result

$$[F(x)]_{x<<1}=\frac{1}{5}x-\frac{1}{14}x^3+\frac{1}{24}x^5 \ldots . \quad . \quad . \quad (19a)$$

When x is small enough for the first term in the expansion to be sufficient, the same result is obtained as before, namely,

$$n=10^4\left(\frac{\pi}{3}\right)^3\frac{1}{h^6}G^3M^2m_H{}^4m^3, \quad . \quad . \quad . \quad (19a')$$

or, substituting numerical values from (18 a), (20), and (21),

$$\left.\begin{aligned} n&=2{\cdot}396\times10^{-37}M^2,\\ \rho&=9{\cdot}95\times10^{-61}M^2. \end{aligned}\right\} \quad . \quad . \quad . \quad . \quad (22)^*$$

The first two terms in (19 a) give $F(x)$ correct to less than 1 per cent. up to $x=\cdot5$, and form the most convenient expression for this range.

When x is large, as may be seen from (19),

$$\begin{aligned}[F(x)]_{x>>1}&=\frac{1}{8x^3}(2x^3-3x),\\ &=\cdot2500-\frac{3}{8x^2}. \quad . \quad . \quad . \quad . \quad (19b)\end{aligned}$$

This expression gives $F(x)$ correct to 1 per cent. for $x>10$. It indicates, moreover, the limiting mass for which an

* This is in agreement with Anderson's result. In I., as pointed out by Anderson, a slight numerical error was made, and the result was given as $n=2{\cdot}31\times10^{-37}M^2$. Correspondingly, the result for the maximum density, given as $\rho=3{\cdot}85\times10^5(M/M_s)^2$, should be $\rho=3{\cdot}977\times10^6(M/M_s)^2$, with the Sun's mass, M_s, taken as $2{\cdot}0\times10^{33}$.

equilibrium state can be attained under the conditions, namely, from (18 *a*),

$$M_0 = 1{\cdot}751 \times 10^{34} (\cdot 25)^{3/2},$$
$$= 2{\cdot}19 \times 10^{33}. \quad \ldots\ldots \quad (23)$$

TABLE I.

Corresponding values of x, $F(x)$, $\log_{10} n$, and $\log_{10} M$.

$$n = 5{\cdot}876 \times 10^{29} x^3,$$
$$M = 1{\cdot}751 \times 10^{34} [F(x)]^{3/2}.$$

x.	$F(x)$.	$\log_{10} n$.	$\log_{10} M$.
·1	·0200	26·7690	31·6947
·2	·0394	27·6720	32·1364
·3	·0581	28·2003	·3895
·4	·0756	·5753	·5609
·6	·1071	29·1036	·7879
·8	·1330	·4783	·9291
1·0	·1537	·7690	33·0233
1·5	·1887	30·2973	·1569
2	·2085	·6720	·2220
3	·2280	31·2003	·2801
4	·2366	·5753	·3042
5	·2410	·8660	·3162
6	·2436	32·1036	·3233
8	·2463	·4783	·3303
10	·2476	·7690	·3339
20	·2494	33·6720	·3385
40	·2498	34·5753	·3396
60	·2499	35·1036	·3399
100	·2500	·7690	·3401

The value obtained by Anderson for M_0 is $1{\cdot}37 \times 10^{33}$, so that the range of mass in which this particular type of equilibrium can occur is shown by this method to be considerably greater than that indicated by Anderson's approximate treatment.

A series of corresponding values of x and $F(x)$ calculated from (19), supplemented by (19 *a*) and (19 *b*), is shown in Table I. The relation required is that between n and M, related to x and $F(x)$ by (21) and (18 *a*). It is convenient

to use logarithms (base 10) when the following equations are obtained :

$$\log_{10} n = 29{\cdot}7690 + 3 \log x, \quad . \quad . \quad . \quad . \quad (24)$$

$$\log_{10} \mathrm{M} = 34{\cdot}2432 + \frac{3}{2} \log \mathrm{F}(x). \quad . \quad . \quad . \quad (25)$$

The conversion is then readily carried out. Corresponding values of n and M are shown in the last two columns of the table. It is unnecessary to give values for log M less than 32, as no stars are known of mass less than a tenth that of the Sun ($\log \mathrm{M}_s = 33{\cdot}3010$), and in any case, for stars of small mass, the approximate expression (22) will be sufficiently accurate. For any value of M the maximum value of $\log n$ can be found by interpolation, and from that

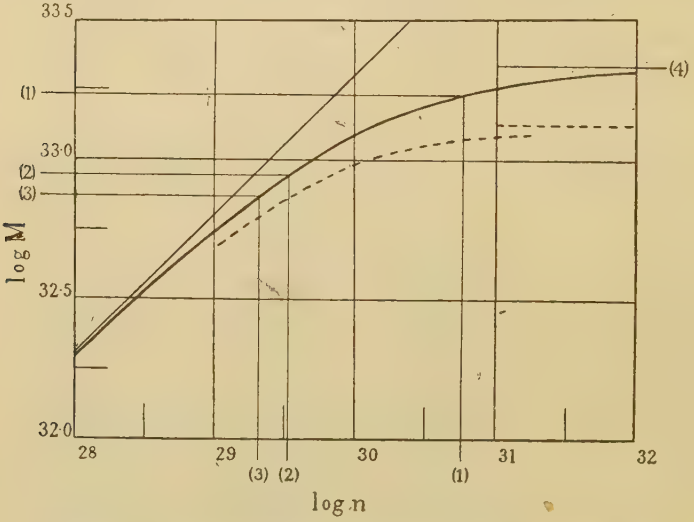

Variation of limiting electron concentration (n) with mass (M) in a sphere of uniform density.

(1) Sirus B	log M = 33·230	log n = 30·748
(2) o_2 Eridani B	log M = 32·944	log n = 29·524
(3) Procyon B	log M = 32·869	log n = 29·313
(4) Limiting M	log M_0 = 33·340	($\mathrm{M}_0 = 2{\cdot}19 \times 10^{33}$)

For the limiting density $\log \rho_0 = \log n - 24 + 0{\cdot}618$.
The straight line corresponds to the formula in which the relativity effect is neglected. The dotted curve gives Anderson's results.

the value of n. If the density is required it can be found from (20), while $\log \rho_0$ is given by

$$\log \rho_0 = \log n - 24 + {\cdot}6180. \quad . \quad . \quad . \quad . \quad (26)$$

The relation between $\log M$ and $\log n$ is shown by the curve in the figure. The "positions" of a number of stars are indicated. The straight line is the result found by the original approximation, in which the relativity effect was neglected (giving n varying as M^2). The main conclusion is that for stars for which this equilibrium can occur the limiting density is somewhat less than that calculated by Anderson, and that the "limiting mass" is larger; his results are indicated by the dotted line.

White Dwarfs.

The number of stars known to be of the white dwarf type is small, but this does not necessarily indicate that stars of very high density are uncommon. Dense stars of ordinary mass will have a small radius, and so will be faint objects unless they are near the Sun (on the stellar scale of nearness) or have a high-surface temperature. "Black dwarfs" (to use Fowler's term) would not be observed. According to Jeans *, four white dwarfs are known with certainty, but for one of these—the companion of the red giant *o* Ceti—he does not give any quantitative data. Procyon B is a possible white dwarf, but its spectral type is unknown. In the following table are collected the relevant observational data derived from Jeans †. Procyon B is included because its mass is known. The four columns give the spectral type, the absolute visual and bolometric magnitudes, and the mass in terms of the Sun's mass ($M_\odot$).

TABLE II.

Observational Data.

	Spectral Type.	$M_{vis.}$	$M_{bol.}$	$M/M_\odot$.
Sirius B	A 7	11·3	11·2	·85
o_2 Eridani B	A 0	11·2	10·8	·44
Procyon B	—	16	—	·37
Van Maanen's star	F	14·3	14·3	—

* J. H. Jeans, 'Astronomy and Cosmogony,' p. 63 (Camb. Univ. Press, 1928).

† *Loc. cit.* p. 59. I am indebted to Prof. Eddington for informing me that the value ·21 given for the mass of o_2 Eridani B in his 'Internal Constitution of the Stars' is based on an earlier determination of the orbit, and that the value ·44 is presumably the more trustworthy. Also to Sir James Jeans for confirming the value ·44.

From these observational data deductions may be made as to other characteristics of the stars. From the spectral type the surface temperature (T_e) may be estimated, and from the effective temperature and the absolute magnitudes the radius of the star. The following formulæ are given by Jeans for the radius in terms of that of the sun (r/r_s denoted by R):—

$$\log R = -0{\cdot}2\, M_{bol.} - 2 \log T_e + 8{\cdot}53, \quad . \quad . \quad (27a)$$

$$\log R = -0{\cdot}2\, M_{vis.} + \frac{5880}{T_e} - 0{\cdot}01. \quad . \quad . \quad . \quad (27b)$$

It is further possible to calculate the total radiation of energy in ergs per second (E),

$$\log E = -0{\cdot}4\, M_{bol.} + 35{\cdot}52. \quad . \quad . \quad . \quad . \quad (28)$$

TABLE III.

Deduced Characteristics of Sirius B and o_2 Eridani B.

	M/M_s.	T_e.	R.	E′.	ρ.	ρ_0 calc.
Sirius B	·85	8,000	·0312	·0065	$3{\cdot}97\times10^4$	$2{\cdot}3\times10^7$
o_2 Eridani B...	·44	11,200	·0187	·0185	$9{\cdot}55\times10^4$	$1{\cdot}4\times10^6$

The amount of radiation per gram (E′) is a quantity of great interest:

$$\log E' = \log E - \log M,$$
$$= \log E + \log (M_s/M) - \log M_s,$$
$$= -0{\cdot}4\, M_{bol.} + 2{\cdot}22 + \log (M_s/M). \quad . \quad (29)$$

(The sun's mass is taken as $2{\cdot}0 \times 10^{33}$ grams.)

The mean density is given by

$$\rho = \frac{3M}{4\pi r^3} = \left(\frac{M}{M_s}\right)\left(\frac{r_s}{r}\right)^3 \frac{3M_s}{4\pi {r_s}^3},$$
$$= (M/M_s)\,(1/R)^3 \rho_s = 1{\cdot}42\,(M/M_s)\,(1/R)^3. \quad . \quad . \quad (30)$$

The values given in Table III. have been calculated from these equations. It may be noted that for Sirius B the radius deduced from the relativity shift is ·03, in remarkable agreement with the value ·0312 calculated in the way indicated. (In general the values are not significant to more than two figures.) The available data for Procyon B and Van Maanen's Star are insufficient for the calculation

of ρ or E′; these stars will be discussed later. The value of M/M_s is included in the table, and also the value of the limiting density, ρ_0, calculated as already described.

The calculated limiting densities are considerably greater than those obtained by the simple formula (19 *a*) (used in I.), which gives for stars of the mass of Sirius B and o_2 Eridani B the values $\rho = 2{\cdot}8 \times 10^6$ and $7{\cdot}5 \times 10^5$. The order of magnitude of the difference for stars of different mass will be apparent from the figure.

The calculated radiation per gram (E′) of o_2 Eridani B is about 10 times greater than the value given by Jeans. This will be discussed later. The mean density for Sirius B is somewhat smaller than that usually given (about 5×10^4). This results from the use of a slightly larger value for the radius. Taking the relativity shift value ($\mathfrak{R} = {\cdot}03$), the mean density comes out as $4{\cdot}5 \times 10^5$.

Mean Molecular Weight.

The mean molecular weight has been taken as $2{\cdot}5\, m_{\mathrm{H}}$. This is the value for completely ionized atoms of lead $\left(\frac{207{\cdot}2}{82+1}\right)$. For atoms of lower atomic number the value is slightly smaller, and for those of high atomic number, larger. Jeans derives a value $2{\cdot}6\, m_{\mathrm{H}}$ on the assumption, for which there is strong evidence, that in many stars atoms of the atomic number equal to that of uranium, and even higher, are present. In condensed stars of the type considered, however, most of these atoms will have been transformed into atoms of an inert type, and the estimate $2{\cdot}5\, m_{\mathrm{H}}$ is probably sufficiently accurate. In any case, a small change will not affect the numerical results appreciably.

It might be thought that the change of mass of the electron would produce a not negligible effect, but it may readily be shown that the effect will be very small. Let m be the mass of an electron with momentum p. The molecular weight becomes $2{\cdot}5\, m_{\mathrm{H}} + \mu$, where

$$2{\cdot}5\, m_{\mathrm{H}} + \mu = m_{\mathrm{H}} \left(2{\cdot}5 + \frac{m - m_0}{m_{\mathrm{H}}}\right).$$

Now

$$m^2(1-\beta) = m_0^2,$$

$$\beta = \frac{p}{mc} = \left(\frac{p}{m_0 c}\right)\frac{m_0}{m}$$

$$\frac{m-m_0}{m_0}=\left[1+\left(\frac{p}{m_0c}\right)^2\right]^{1/2},$$

$$2{\cdot}5\,m_{\mathrm{H}}+\mu=m_{\mathrm{H}}\left[2{\cdot}5+\frac{1}{1845}\left\{1+\left(\frac{p}{m_0c}\right)^2\right\}^{1/2}\right]. \quad . \quad . \quad . \quad . \quad (31)$$

From (8) the maximum momentum is given by

$$p_0=\left(\frac{3h^3n}{8\pi}\right)^{1/3},$$

so that

$$\frac{p_0}{m_0c}=\frac{h}{m_0c}\left(\frac{3}{8\pi}\right)^{1/3}n^{1/3},$$

$$=1{\cdot}194\times10^{-10}n^{1/3}. \quad . \quad . \quad . \quad (32)$$

For an electron concentration $n=10^{33}$ (corresponding to a density greater than 10^9) the maximum molecular weight is

$$2{\cdot}5\,m_{\mathrm{H}}+\mu=m_{\mathrm{H}}(2{\cdot}5+{\cdot}0065). \quad . \quad . \quad . \quad (31a)$$

The correction is thus quite negligible for all the densities which come into consideration.

Mean Density.

In the foregoing treatment the star has been idealized as having a uniform density. This seems legitimate when the aim has been to obtain an estimate of the maximum density under gravitational-kinetic equilibrium. In an actual star, however, the density will not be uniform, even in the condensed limit. When n is small the energy per unit volume is proportional to $n^{5/3}$ (eq. 10 *b*), and when n is large, to $n^{4/3}$ (eq. 12 *a*). Since the pressure is proportional to the energy per unit volume, and the density is proportional to n, the following relations hold between the pressure and density :—

$$n\ll5{\cdot}9\times10^{29}, \quad \rho\ll2{\cdot}4\times10^6, \quad p=\kappa\rho^{5/3}, \quad . \quad (33\,a)$$

$$n\gg5{\cdot}9\times10^{29}, \quad \rho\gg2{\cdot}4\times10^6, \quad p=\kappa\rho^{4/3}. \quad . \quad (33\,b)$$

In an ideal condensed star the distribution will thus be polytropic, the relation between pressure and density obeying the relation $p=\kappa\rho^{\gamma}$. The distributions in polytropic stars for a number of values of γ (or its equivalent n', defined by $\gamma=1+1/n'$) have been worked out by Emden. The results are quoted by Eddington *. Table IV. gives the ratio of the

* A. S. Eddington, 'The Internal Constitution of the Stars,' p. 89 (C. U. P. 1926).

maximum (central) to the mean density. Uniform density corresponds to $n' = 0$.

This table certainly indicates that the maximum mean density may be considerably less than the maximum central density, and it might seem that all that is necessary to convert the previously calculated results for limiting densities to mean densities is to divide by the appropriate ratio. There are a number of other factors, however, which have to be taken into consideration. The gravitational energy of a star is given by *

$$E_G = -\frac{3}{5-n'} G \frac{M^2}{r} \quad . \quad . \quad . \quad (34)$$

For uniform density the coefficient is 3/5, the value used (eq. 15 *a*). For $\gamma = 5/3$ the factor becomes 6/7, so that for a given M the calculated n would be increased. The whole

TABLE IV.

Ratio of Maximum to Mean Density in Polytropes.

γ	∞	5/3	3/2	7/5	4/3
n'	0	3/2		5/2	3
ρ_0/ρ	1	6·00	11·4	24·1	54·4

calculation, however, is based on the assumption that n is uniform, and different averaging processes would have to be carried out in deriving expressions for the gravitational and kinetic energies in terms either of n_0 (the central electron concentration) or the mean n. Some rough calculations indicate that the values derived for the limiting concentrations approximate to those for n_0; but a much more elaborate investigation would be necessary if the variation of density were to be properly taken into account. The indications are that the values obtained for the limiting density approach those for the limiting central density, and that the limiting mass may be slightly changed; that Sirius B still falls within the range for which gravitational-kinetic equilibrium can occur; and that the limiting mean densities may be smaller than those calculated approximately in the ratios suggested by the values in Table IV. These results, however, are somewhat uncertain, and for the present the calculations are left in the form which is strictly appropriate for the case of the homogeneous sphere.

* Eddington, *loc. cit.* p. 87.

Van Maanen's Star and Procyon B.

Van Maanen's Star is of great interest, as it is the smallest star known, being about the same size as the earth. From the data in Table II. the radius may be calculated (eq. 27), the result being R = ·00955, taking the surface temperature as 7000 corresponding to an F-type star. The mass is unknown, and since the star is not a binary component, there is no method available by which it may be estimated. It is, however, possible to calculate *compatible* values of the mass (giving the mean density) and of the radiation per gram (E′) from the known data. From (29),

$$\log E' = -5{\cdot}72 + 2{\cdot}22 + \log (M_s/M),$$

$$E'(M/M_s) = 3{\cdot}162 \times 10^{-4}. \quad . \quad . \quad . \quad . \quad (35)$$

Table V.

Compatible Values for Van Maanen's Star.

$T_e = 7000.$ $R = {\cdot}00955.$

M/M_s.	E′.	$10^{-6}\rho$.	$10^{-6}\rho_0$ calc.
·2	·0016	·33	·19
·4	·0008	·65	1·14
·6	·0005	·98	3·7
·8	·0004	1·30	13·1
1·0	·0003	1·63	104

In Table V. are given compatible values of M/M_s, ρ, and E′, together with the calculated ρ_0 for each value of the mass. Incidentally, this table gives the values of ρ_0 for a range of masses.

As will be seen from the above table, the values which Jeans suggests as a pure guess * for M/M_s and E′—·2 and ·00055—are not compatible with each other. The interesting point which emerges, however, is that unless the numerical results of the equilibrium theory are very wide of the mark owing to the essential factors being ignored, a lower limit for the mass of Van Maanen's Star can be roughly estimated. The mean density cannot be greater than the calculated limiting density, and it is probably several times smaller.

* J. H. Jeans, 'The Universe Around Us,' p. 310 (C. U. P. 1929).

From this it is possible to draw the following conclusions for Van Maanen's Star :—

$$M/M_s > \cdot 4, \quad \rho > 650{,}000, \quad E' < \cdot 0008.$$

For Procyon B the spectral type is unknown, though it is probably M or K *. It is, however, of interest to examine how far the star approaches the condensed type if a reasonable value of the surface temperature is assumed. For assumed temperatures of 3000 (M type) and 4000 (K type) the estimated correction † to convert $M_{vis.}$ to $M_{bol.}$ may be applied, and using (27), (29), and (30), the following results are obtained :—

TABLE VI.

Compatible Values for Procyon B.

$M/M_s = \cdot 37$. $\quad \rho_0$ calc. $= \cdot 84 \times 10^6$.

T_e.	$M_{bol.}$	R.	ρ.	E'.
3000	14	·056	$2 \cdot 4 \times 10^3$	·001
4000	15·5	·018	$1 \cdot 1 \times 10^5$	·0003

Of course nothing definite can be deduced from these results, as in the case of Van Maanen's Star. They simply serve to show that unless the surface temperature is considerably greater than 3000, Procyon B does not approach the limiting condensed state, the mean density being much smaller than that of other white dwarfs.

Generation of Energy.

Some of the more important observed and deduced data for the three white dwarfs about which most is known are collected together, for convenience in comparison, in Table VII. The total energy radiated per second is symbolized by E, the energy per gram by E'.

As was to be expected, the calculated limiting density ρ_0 is considerably greater than the "observed" mean density. The polytrope ratios (Table IV.) suggest that the maximum mean density may be something approaching 50 times smaller than ρ_0 for Sirius B, and 6 times smaller for

* J. H. Jeans, 'Astronomy and Cosmogony,' p. 128.
† *Ibid.* p. 46.

o_2 Eridani B. If these ratios are approximately correct, o_2 Eridani B may be said to approach the limiting condensed state fairly closely, while Sirius B is still far removed from it. If the observational data (Table II.) and the essentials of the equilibrium theory are correct, Van Maanen's Star is certainly the most dense that is known, though it is impossible to say how nearly it approaches the condensed limit.

If the observational data are correct, again, there is for stars of this type no simple relation between the mass and luminosity—as is shown by the absolute bolometric magnitude of o_2 Eridani B being smaller than that of Sirius B, although its mass is smaller. The radiation per gram, moreover, does not decrease steadily with the mass of the star, as had been suggested *.

TABLE VII.

Observed and Deduced Data for White Dwarfs.

	$M/M_\odot$.	T_e.	R.	ρ.	ρ_0 calc.	E.	E'.
Sirius B	·85	8,000	0312	40,000	23×10^6	$1{\cdot}1\times10^{31}$	0065
o_2 Eridani B	·44	11,200	·0187	95,000	$1{\cdot}4\times10^6$	$1{\cdot}6\times10^{31}$	·0185
Van Maanen's Star .	>·4	7,000	·0095	>650,000	$>1{\cdot}1\times10^6$	$6{\cdot}4\times10^{29}$	<·0008

According to Jeans's hypothesis, which, in spite of its speculative nature, certainly satisfies most of the conditions, the energy generation in stars is to be traced to electron-proton annihilation occurring in hyper-uranium atoms as a result of one of the extra-nuclear electrons of the atom falling into the nucleus. In completely ionized stars of the white dwarf type this process could not occur, so that the small radiation per gram of these stars is in complete accordance with the hypothesis. The radiation would be mainly due to the atoms in the outer layers of the star, so that there is not necessarily any simple relation between either the mass or the mean density and the amount of radiation per gram. It does none the less remain peculiar that o_2 Eridani B, which approaches the condensed state, should have a much higher surface temperature than Sirius B, and that it should generate more energy per gram. The material available in this connexion, however, is too slight to permit of any inductive generalizations being made.

* J. H. Jeans, 'The Universe Around Us,' p. 310.

The Fermi Statistics of Electron Gas at Lower Densities.

The densities of white dwarfs are very much greater than those of other stars, in which the densities are too low and the temperatures too high for the electron gas to approach the condensed state. According to Jeans's theory of stellar evolution (outlined in I.), the tenanted portions of the Russell temperature-luminosity diagram correspond to stable states in which the pressures exceed considerably the perfect gas-pressures. There will be a range of stability for each successive stage of ionization of the atoms, and this, on the liquid-star hypothesis, corresponds to the "jamming" of the incompletely-ionized atoms. The difficulty about this hypothesis is that the size which must be attributed to the atoms is very much greater than that indicated by other evidence. Now, with the Fermi statistics the pressure is always greater than that of a perfect gas, and it is interesting to note that there will be a maximum deviation corresponding to each stage of ionization. When with increasing temperature there is an increase in the number of electrons through ionization, there will be a deviation from the perfect gas relation between pressure and number of molecules. This deviation will decrease as the temperature increases, and will increase again when the next stage of ionization will increase. The deviations required, however, are much greater than those indicated by the Fermi statistics. This may be illustrated by taking a particular case and making the most favourable estimates. To ensure stability at the centre of the star, according to Jeans, the pressure must be at least 1·107 times the normal pressure *. The pressure of electron gas is given by

$$p = nk\mathrm{T}\left\{1 + \frac{1}{16\times 2}\frac{nh^3}{(\pi mk\mathrm{T})^{3/2}}\cdots\right\}. \quad . \quad . \quad . \quad (36)$$

Inserting numerical values

$$p = nk\mathrm{T}\left\{1 + 3{\cdot}62\times 10^{-17}\frac{n}{\mathrm{T}^{3/2}}\cdots\right\}. \quad . \quad . \quad . \quad (37)$$

Taking ρ as $2{\cdot}5\ nm_{\mathrm{H}}$, Table VIII. gives the corresponding values of T, n, and ρ for the pressure to exceed the normal by 10 per cent.

In stars generally, for a given central temperature the central density is of order of ten times less than that in

* J. H. Jeans, 'Astronomy and Cosmogony,' p. 141.

the table. For the sun * the central density is about 140, and the temperature can hardly be less than 40×10^6. This gives

$$p = nk\mathrm{T}(1 + 0{\cdot}48 \times 10^{-2}). \quad . \quad . \quad . \quad . \quad (38)$$

The pressure is thus about $\frac{1}{2}$ per cent. above normal instead of the required 10 per cent. It would seem, therefore, that unless there are other parts of the theory requiring modification, a simple application of the Fermi statistics is unable to remove the difficulties, although it does lead to deviations from the perfect gas laws of the required type.

TABLE VIII.

Corresponding Values for the Pressure to exceed normal by 10 per cent.

T.	n.	ρ.
10^3	$2{\cdot}76 \times 10^{18}$	$1{\cdot}145 \times 10^{-5}$
10^4	$2{\cdot}76 \times 10^{21}$	$1{\cdot}145 \times 10^{-2}$
10^5	$2{\cdot}76 \times 10^{24}$	$1{\cdot}145 \times 10$
10^6	$2{\cdot}76 \times 10^{27}$	$1{\cdot}145 \times 10^4$

Conclusion.

It is generally agreed that the dense dwarf stars represent an advanced stage of stellar evolution. It is reasonable to suppose that the *white* dwarf stage, corresponding to high surface temperature, will be a comparatively short one, and since the stars are small, it is probable that most condensed stars are too faint to be observed. From the mass luminosity relation, moreover, even treating this as a purely empirical generalization, the masses of condensed stars will in general be small. There is therefore a strong probability that stars of the type in which the gravitational kinetic equilibrium discussed in this paper is of importance are much more numerous than is suggested by the number of known examples. For these the theory may be said to account in a general way for the order of magnitude of the densities deduced from the observational data.

For more normal stars the application of the Fermi statistics shows that there will be an appreciable deviation from the perfect gas laws for the electron gas. Although the deviations will be of the kind required in Jeans's theory

* *Ibid.* p. 104.

of stability, they are not nearly large enough. It would seem, therefore, either that the theory as to the conditions for stability requires modification, or that there are factors involved which are at present unrecognized.

Summary.

In a previous paper the conclusion was reached that there was a limiting density for stars in which the atoms were completely ionized, varying as the square of the mass of the star. The limiting state occurs when the decrease in gravitational energy on contraction is equal to the increase in the total kinetic energy of the electron gas. In the treatment the relativity change of mass with velocity was neglected. Some approximate calculations by Anderson indicate the general effect of this change of mass, which necessitates a modification of the previous conclusions when the mass of the star becomes comparable with that of the sun.

In the present paper the effect of the relativity change of mass is worked out with more rigour for the idealized case for a sphere of uniform density. For spheres of increasing mass the limiting density varies at first as the square of the mass, and then more rapidly, there being a limiting mass ($2{\cdot}19 \times 10^{33}$) above which the gravitational kinetic equilibrium considered will not occur. Tables and curves are given showing the relation between mass and limiting density.

It is shown that the distribution of density in condensed stars will be polytropic, and rough estimates are made of the ratio of the central to the mean density.

The observational and deduced data for known white dwarfs are considered in some detail. The density of Sirius B is well below the limit calculated, while that of o_2 Eridani B approaches it. The theory enables a lower limit for the mass and density of Van Maanen's Star to be roughly estimated. The observational, deduced, and calculated data for these three stars, and also for Procyon B, are given in tables.

The deduced data indicate that the generation of energy per gram in known dense stars is not simply related to the mass of the star.

The application of the Fermi statistics to the electron gas in normal stars is briefly discussed in connexion with Jeans's theory of stability. There will be deviations from the perfect gas laws of the type required, but they are about twenty times too small to satisfy the stability conditions.

Physics Department,
The University, Leeds.
December 1929.

LXXXVIII. *Second Order Expressions for the Potentials of a Sphere.* *By* D. B. Mair*.

1. THE measure ds of a timelike interval in the gravitational field of the sun being given in terms of polar coordinates by

$$ds^2 = -e^{\lambda}dr^2 - e^{\mu}(r^2 d\theta^2 + r^2 \sin^2\theta\, d\phi^2) + e^{\nu}dt^2$$

Θ being the Newtonian potential of the sun (treated as a non-rotating sphere of perfect fluid, symmetrical about its centre), zero at infinity and negative elsewhere, and L being the product of the sun's mass and the gravitation constant, it is known that, to the first power of L, the set of values

$$\lambda = -2\Theta \qquad \mu = -2\Theta \qquad \nu = 2\Theta$$

give the potentials in matter and in the void, and that the set

$$\lambda = 2L/r \qquad \mu = 0 \qquad \nu = -2L/r$$

give the potentials in the void. The object of this paper is to extend the second set of expressions to matter, and to extend both sets of expressions to the second power of L for matter and the void.

2. In a reference system in which the sun is at rest the elements of the energy tensor are

$$T_{11} = pe^{\lambda} \qquad T_{22} = pe^{\mu}r^2 \qquad T_{33} = pe^{\mu}r^2\sin^2\theta \qquad T_{44} = (\rho - p)e^{\nu}$$

$$T = \rho - 4p$$

The field equations

$$H_{\alpha\beta} \equiv G_{\alpha\beta} - \tfrac{1}{2}g_{\alpha\beta}G + \kappa T_{\alpha\beta} = 0$$

become in terms of $\lambda\,\mu\,\nu$, a dash denoting differentiation with respect to r,

$$H_{11} \equiv \frac{e^{\lambda-\mu}-1}{r^2} - \frac{\mu'+\nu'}{r} - \frac{\mu'}{4}(\mu'+2\nu') + \kappa p e^{\lambda} = 0$$

$$H_{22} \equiv r^2 e^{\mu-\lambda}\left\{ -\frac{\mu''+\nu''}{2} + \frac{\lambda'-2\mu'-\nu'}{2r} + \tfrac{1}{4}(\lambda'\mu' + \lambda'\nu' - \mu'^2 - \mu'\nu' - \nu'^2)\right\} + \kappa p r^2 e^{\mu} = 0$$

* Communicated by the Author.

$$H_{44} \equiv e^{\nu-\lambda}\left\{\frac{1-e^{\lambda-\mu}}{r^2}+\mu''+\frac{3\mu'-\lambda'}{r}+\frac{\mu'}{4}(-2\lambda'+3\mu')\right\}$$
$$+\kappa(\rho-p)e^{\nu}=0$$

H_{33} repeats H_{22} and all other equations $H_{\alpha\beta}$ are identities. Along with these we have $G=\kappa T$ or

$$H \equiv e^{-\lambda}\left[\frac{2(e^{\lambda-\mu}-1)}{r^2}-2\mu''-\nu''+\frac{2\lambda'-6\mu'-2\nu'}{r}\right.$$
$$\left.+\tfrac{1}{2}\{(\lambda'-\nu')(2\mu'+\nu')-3\mu'^2\}\right]-\kappa T=0$$

by which we may replace any one of the three.

3. As these equations contain the pressure p we must take account of the equations of matter

$$T^{\beta}_{\alpha\beta}=0$$

For $\alpha=1$ this is

$$p'+\tfrac{1}{2}\rho\nu'=0$$

while the other equations are identities. This with the field equations constitute the equations that have to be satisfied.

As the field equations we take

$$H_{11}=0 \qquad H_{11}-\frac{e^{\lambda-\mu}}{r^2}H_{22}=0 \qquad e^{\lambda}H=0$$

The four equations whose solution we seek are thus

$$J_1 \equiv -\frac{\mu'+\nu'}{r}+\frac{e^{\lambda-\mu}-1}{r^2}-\tfrac{1}{4}\mu'(\mu'+2\nu')+\kappa p e^{\lambda}=0$$

$$J_2 \equiv \frac{\mu''+\nu''}{2}-\frac{\lambda'+\nu'}{2r}+\frac{e^{\lambda-\mu}-1}{r^2}$$
$$+\tfrac{1}{4}(-\lambda'\mu'-\lambda'\nu'-\mu'\nu'+\nu'^2)=0$$

$$J_3 \equiv -2\mu''-\nu''+\frac{2\lambda'-6\mu'-2\nu'}{r}+\frac{2}{r^2}(e^{\lambda-\mu}-1)$$
$$+\tfrac{1}{2}\{\lambda'-\nu')(2\mu'+\nu')-3\mu'^2\}-\kappa T e^{\lambda}=0$$

$$J_4 \equiv p'+\tfrac{1}{2}\rho\nu'=0$$

4. We first seek a solution of the first order in L, neglecting powers of L. J_1 gives

$$\lambda=\mu+r(\mu'+\nu') \quad . \quad . \quad . \quad . \quad . \quad (4,1)$$

With this value of λ J_2 becomes an identity, and J_3 becomes

$$\nu'' + \frac{2\nu'}{r} = \kappa T \quad . \quad . \quad . \quad . \quad . \quad (4, 2)$$

Since the Newtonian potential Θ is given when the density is taken as $T \equiv \rho - 4p$ by

$$\Theta'' + \frac{2\Theta'}{r} = 4\pi\chi T = \tfrac{1}{2}\kappa T \quad . \quad . \quad . \quad (4, 3)$$

in which χ is the gravitation constant, equation (4, 2) shows that ν is 2Θ, and the most general first order solution is thus

$$\lambda = \xi + r\xi' + 2r\Theta' \qquad \mu = \xi \qquad \nu = 2\Theta \quad . \quad (4, 4)$$

ξ being such as to make $\xi\,\xi'\,\lambda'$ continuous at the boundary of the sun, and otherwise at our disposal.

5. As second order solution we assume

$$\left.\begin{aligned} \lambda &= \xi + r\xi' + 2r\Theta' + \chi - \psi \qquad \mu = \xi + \chi - \psi + \omega \\ \nu &= 2\Theta + 2\psi - \chi \end{aligned}\right\} \quad (5, 1)$$

$\chi\,\psi\,\omega$ being second order quantities to be now determined. Substitution of these expressions in the equations of article 3 gives, to the second order,

$$K_1 \equiv -\left(\frac{\psi'}{r} + \frac{\omega'}{r} + \frac{\omega}{r^2}\right) + \tfrac{1}{4}\xi'^2 + \xi'\Theta' + 2\Theta'^2 + \kappa p = 0$$

$$K_2 \equiv \frac{1}{2}\left(\psi'' - \frac{\psi'}{r} + \omega'' - \frac{2\omega}{r^2}\right) + 2\Theta'^2 - \frac{r}{4}(\xi' + 2\Theta')(\xi'' + 2\Theta'') = 0$$

$$K_3 \equiv -\left(\chi'' + \frac{2\chi'}{r}\right) - 2\left(\omega'' + \frac{3\omega'}{r} + \frac{\omega}{r^2}\right) + \tfrac{3}{2}\xi'^2 + 6\xi'\Theta' + 4\Theta'^2 + r(\xi' + \Theta')(\xi'' + 2\Theta'') - \kappa T(\xi + r\xi' + 2r\Theta') = 0$$

$$K_4 \equiv p' + \rho\Theta' = 0$$

6. Integration of the equation $2K_2/r = 0$ gives

$$\psi' + \omega' + \frac{\omega}{r} = \frac{r}{4}(\xi' + 2\Theta')^2 - 4r\Phi \quad . \quad . \quad (6, 1)$$

in which

$$\Phi' = \frac{\Theta'^2}{r} \quad . \quad . \quad . \quad . \quad . \quad . \quad (6, 2)$$

The use of this in equation K_1 gives

$$\kappa p = -4\Phi - \Theta'^2 \quad . \quad . \quad . \quad . \quad . \quad (6,3)$$

whence by differentiation and the use of equation (4, 3)

$$\kappa p' = -\frac{4\Theta'^2}{r} - 2\Theta'\Theta'' = -\kappa T\Theta' \quad . \quad . \quad (6,4)$$

To the second order this is equation K_4, which is thus included in the other three and need not be considered further.

Integration of the equation $r^2K_3=0$ gives

$$\chi' + 2\left(\omega' + \frac{\omega}{r}\right) = \frac{\Psi}{r^2} \quad . \quad . \quad . \quad . \quad (6,5)$$

in which

$$\Psi' = r^2\left(\tfrac{3}{2}\xi'^2 + 6\xi'\Theta' + 4\Theta'^2\right) + r^3(\xi' + \Theta')(\xi'' + 2\Theta'') - \kappa T r^2(\xi + r\xi' + 2r\Theta')$$

$$= \tfrac{1}{2}(r^3\xi'^2)' + (r^3\xi'' + 2r^2\xi')\Theta' - \xi r^2\kappa T - r^3\kappa T\Theta' \quad . \quad (6,6)$$

7. The density T of the sun is assumed to be a function of the distance r from the centre. Let it be given by

$$\tfrac{1}{2}\kappa T = \frac{L}{a^3}\left\{3A_1 + 4A_2\frac{r}{a} + \ldots + (q+2)A_q\left(\frac{r}{a}\right)^{q-1}\right\} \quad (7,1)$$

in which a is the sun's radius. Since L is the sun's mass multiplied by $\chi \equiv \kappa/8\pi$

$$L = \int_0^a \tfrac{1}{2}\kappa T r^2\, dr = \int_0^a dr\,\frac{L}{a}\Sigma A_m(m+2)\left(\frac{r}{a}\right)^{m+1} = L\Sigma A_m$$

so that

$$\Sigma A_m \equiv A_1 + A_2 + \ldots + A_q = 1 \quad . \quad . \quad (7,2)$$

The differential equation for Θ gives for Θ_M in matter

$$(r^2\Theta'_M)' = \tfrac{1}{2}r^2\kappa T = \frac{L}{a}\Sigma A_m(m+2)\left(\frac{r}{a}\right)^{m+1}$$

$$\Theta'_M = \frac{L}{a^2}\Sigma A_m\left(\frac{r}{a}\right)^m$$

$$\Theta_M = \frac{L}{a}\Sigma A_m\frac{1}{m+1}\left(\frac{r}{a}\right)^{m+1} + B$$

and for Θ_V in the void

$$\Theta_V = \frac{C}{r}$$

Determining the constants so that Θ and Θ' are continuous at the boundary of the sun, we have

$$\Theta_V = -\frac{L}{r} \quad . \quad . \quad . \quad . \quad . \quad . \quad . \quad . \quad . \quad . \quad (7,3)$$

$$\Theta_M = \frac{L}{a}\Sigma A_m \left\{ \frac{1}{m+1}\left(\frac{r}{a}\right)^{m+1} - \frac{m+2}{m+1} \right\} \quad . \quad (7,4)$$

8. By equation (6, 2) these expressions for Θ give for Φ' in the void and in matter

$$\Phi'_V = \frac{L^2}{r^5}$$

$$\Phi'_M = \frac{L^2}{a^5}\Sigma A_m A_n \left(\frac{r}{a}\right)^{m+n-1}$$

in which Σ means that both m and n are to be summed from 1 to q. Integration gives

$$\Phi_V = -\frac{L^2}{4r^4} \quad . \quad . \quad . \quad . \quad . \quad . \quad . \quad . \quad . \quad . \quad (8,1)$$

$$\Phi_M = \frac{L^2}{a^4}\Sigma A_m A_n \frac{1}{m+n}\left(\frac{r}{a}\right)^{m+n} + \frac{L^2}{a^4}C_1 \quad . \quad (8,2)$$

In Φ_V the integration constant is zero because $r\Phi$ is zero at infinity. The value of the constant C_1 is given by the continuity of Φ at the sun's boundary, and is

$$C_1 = -\Sigma A_m A_n \left(\frac{1}{m+n} + \frac{1}{4}\right) \quad . \quad . \quad . \quad (8,3)$$

Equations (6, 3) and (8, 2) give

$$\kappa p = -4\Phi - \Theta'^2$$

$$= \frac{L^2}{a^4}\Sigma A_m A_n \left(1 + \frac{4}{m+n}\right)\left\{1 - \left(\frac{r}{a}\right)^{m+n}\right\} \quad . \quad (8,4)$$

9. The quantity ξ is at disposal. We give it the value

$$\xi = -2\Theta$$

in matter and in the void. Equation (6, 6) then becomes

$$\Psi' = 2r^2\kappa T\Theta - 2r^2\Theta'^2$$

so that

$$\Psi'_{V} = -\frac{2L^2}{r^2} \quad . \quad . \quad . \quad . \quad . \quad . \quad . \quad . \quad . \quad . \quad . \quad (9,1)$$

$$\Psi'_{M} = \frac{2L^2}{a^2}\Sigma A_m A_n \left[\left(\frac{2m+4}{n+1}-1\right)\left(\frac{r}{a}\right)^{m+n+2} - \frac{(2m+4)(n+2)}{n+1}\left(\frac{r}{a}\right)^{m+1}\right] \quad (9,2)$$

and by integration

$$\Psi_{V} = \frac{2L^2}{r} + \frac{L^2}{a}C_2 \quad . \quad . \quad . \quad . \quad . \quad . \quad . \quad . \quad . \quad . \quad (9,3)$$

$$\Psi_{M} = \frac{2L^2}{a}\Sigma A_m A_n \left[\left(\frac{2m+4}{n+1}-1\right)\frac{1}{m+n+3}\left(\frac{r}{a}\right)^{m+n+3} - \frac{2n+4}{n+1}\left(\frac{r}{a}\right)^{m+2}\right] \quad (9,4)$$

In Ψ_M the integration constant is zero because Ψ/r^2 is finite at the origin. The value of the constant C_2 is given by the continuity of the Ψ at the sun's boundary and is

$$C_2 = -6\Sigma A_m A_n\left(1+\frac{1}{m+n+3}\right) \quad . \quad . \quad (9,5)$$

10. Writing

$$\Omega' = \omega' + \frac{\omega}{r}$$

we have from (6, 1) and (6, 5)

$$\psi'_{V} = -\Omega'_{V} + \frac{L^2}{r^3}$$

$$\psi'_{M} = -\Omega'_{M} - \frac{4L^2}{a^3}\Sigma A_m A_n \frac{1}{m+n}\left(\frac{r}{a}\right)^{m+n+1} - \frac{4L^2 r C_1}{a^4}$$

$$\chi'_{V} = -2\Omega'_{V} + \frac{2L^2}{r^3} + \frac{L^2 C_2}{ar^2}$$

$$\chi'_{M} = -2\Omega'_{M} + \frac{2L^2}{a^3}\Sigma A_m A_n \left[\left(\frac{2m+n}{n+1}-1\right)\frac{1}{m+n+3}\left(\frac{r}{a}\right)^{m+n+1} - \frac{2n+4}{n+1}\left(\frac{r}{a}\right)^{m}\right]$$

Integrating these equations we have in the void

$$\psi_V = -\Omega_V - \frac{L^2}{2r^2}$$

$$\chi_V = -2\Omega_V - \frac{L^2}{r^2} - \frac{L^2 C_2}{ar}$$

the integration constants being zero because ψ and χ vanish at infinity. The expressions for ψ_M χ_M in matter need not be written down. Each has an integration constant, and by means of them we make ψ χ continuous at the sun's boundary.

The quantity ω is at our disposal. It and its first derivative must be made continuous at the sun's boundary. That done we have values of ψ χ ω, and therefore of λ μ ν, that satisfy the differential equations in matter and in the void, and are continuous together with their first derivatives across the boundary. Hence they give the values of the potentials to the second power of L.

11. From these values we have in the void, from equation (5, 1)

$$\lambda = \frac{L}{r}\left(2 - \frac{L}{a}C_2\right) - \frac{L^2}{2r^2} - \Omega$$

$$\mu = \frac{L}{r}\left(2 - \frac{L}{a}C_2\right) - \frac{L^2}{2r^2} + \omega - \Omega$$

$$\nu = -\frac{L}{r}\left(2 - \frac{L}{a}C_2\right)$$

$$e^{\lambda} = 1 + \frac{L}{r}\left(2 - \frac{L}{a}C_2\right) + \frac{3L^2}{2r^2} - \Omega$$

$$e^{\mu} = 1 + \frac{L}{r}\left(2 - \frac{L}{a}C_2\right) + \frac{3L^2}{2r^2} + \omega - \Omega$$

$$e^{\nu} = 1 - \frac{L}{r}\left(2 - \frac{L}{a}C_2\right) + \frac{2L^2}{r^2}$$

The simplest treatment of ω is to make it zero everywhere, which makes λ and μ equal. We may also take for ω_V a series in negative powers of r. The third and higher powers of r introduce these powers in the expressions for λ μ ν, and are of no particular interest. We shall take

$$\omega_V = \frac{L^2}{a^2}\left(D\frac{a}{r} + E\frac{a^2}{r^2}\right)$$

to which corresponds in matter

$$\omega_{\mathrm{M}} = \frac{\mathrm{L}^2}{a^2}\left\{2\mathrm{D}+3\mathrm{E}-(\mathrm{D}+2\mathrm{E})\frac{r}{a}\right\}$$

These give in the void

$$\Omega = \frac{\mathrm{L}^2\mathrm{E}}{2r^2} \qquad \omega-\Omega = \frac{\mathrm{L}^2}{a^2}\left\{\mathrm{D}\frac{a}{r}+\tfrac{1}{2}\mathrm{E}\left(\frac{a}{r}\right)^2\right\}$$

and

$$e^{\lambda} = 1+\frac{\mathrm{L}}{r}\left(2-\frac{\mathrm{LC}_2}{a}\right)+\frac{\mathrm{L}^2}{r^2}\left(\tfrac{3}{2}-\tfrac{1}{2}\mathrm{E}\right)$$

$$e^{\mu} = 1+\frac{\mathrm{L}}{r}\left(2-\frac{\mathrm{LC}_2}{a}+\frac{\mathrm{LD}}{a}\right)+\frac{\mathrm{L}^2}{r^2}\left(\tfrac{3}{2}+\tfrac{1}{2}\mathrm{E}\right)$$

$$e^{\nu} = 1-\frac{\mathrm{L}}{r}\left(2-\frac{\mathrm{LC}_2}{a}\right)+\frac{2\mathrm{L}^2}{r^2}$$

In these expressions C_2 is given by equation (9, 5), and D and E are at our disposal. These are second order expressions to which the first set of values mentioned in article 1 have been extended.

12. The quantity ξ of expression (4, 4) being at disposal we now give it the value zero in the void. Since

$$\lambda' \equiv r(\xi''+2\Theta'')+2\xi'+2\Theta'$$

is to be continuous at the boundary ξ'' must be discontinuous to balance the discontinuity of Θ''. We take

$$\xi_{\mathrm{M}} = -\mathrm{Z}\frac{\mathrm{L}}{a}\left(\frac{r}{a}-1\right)^2 \quad . \quad . \quad . \quad . \quad (12, 1)$$

$$\mathrm{Z} = \Sigma(m+2)\mathrm{A}_m$$

which makes $\xi\ \xi'\ \lambda'$ continuous.

The values in matter of certain expressions of equation (6, 6) are

$$(r^3\xi''+2r^2\xi')\Theta' = \frac{2\mathrm{L}^2}{a^2}\Sigma\mathrm{A}_m\mathrm{A}_n\left[-3(n+2)\left(\frac{r}{a}\right)^{m+3}+\left(\frac{r}{a}\right)^{m+2}\right]$$

$$-r^2\xi\kappa\mathrm{T} = \frac{2\mathrm{L}^2}{a^2}\Sigma\mathrm{A}_m\mathrm{A}_n(m+2)(n+2)$$

$$\left[\left(\frac{r}{a}\right)^{m+3}-2\left(\frac{r}{a}\right)^{m+2}+\left(\frac{r}{a}\right)^{m+1}\right]$$

$$-r^3\kappa T\Theta' = -\frac{2L^2}{a^2}\Sigma A_m A_n (n+2)\left(\frac{r}{a}\right)^{m+n+2}$$

$$\tfrac{1}{2}r^3\xi'^2 = \frac{2L^2}{a^2}\Sigma A_m A_n (m+2)(n+2)$$

$$\left[\left(\frac{r}{a}\right)^5 - 2\left(\frac{r}{a}\right)^4 + \left(\frac{r}{a}\right)^3\right]$$

Integrating the sum of the first three and adding the fourth we have

$$\Psi_M = \frac{2L^2}{a}\Sigma A_m A_n (n+2)$$

$$\left[-\frac{1}{m+n+3}\left(\frac{r}{a}\right)^{m+n+3} + \frac{m-1}{m+4}\left(\frac{r}{a}\right)^{m+4} - \frac{2m+2}{m+3}\left(\frac{r}{a}\right)^{m+3}\right.$$

$$\left. + \left(\frac{r}{a}\right)^{m+2} + (m+2)\left\{\left(\frac{r}{a}\right)^5 - 2\left(\frac{r}{a}\right)^4 + \left(\frac{r}{a}\right)^3\right\}\right] \quad (12,2)$$

The integration constant is zero because Ψ/r^2 is finite at the origin.

Since in the void ξ and T are zero equation (6, 6) gives

$$\Psi_V = \text{const} = \frac{L^2}{a}C_2 \quad . \quad . \quad . \quad . \quad (12,3)$$

and the continuity of Ψ at the sun's boundary gives for the value of C_2

$$C_2 = \Sigma A_m A_n 2(n+2)\left(-\frac{1}{m+n+3} - \frac{5}{m+4} + \frac{4}{m+3}\right) \quad (12,4)$$

13. By the help of equations (8, 1) (8, 2) and (12, 1) equation (6, 1) gives

$$\psi'_M = -\Omega'_M + \frac{L^2}{a^3}\Sigma A_m A_n$$

$$\left[\left(1-\frac{4}{m+n}\right)\left(\frac{r}{a}\right)^{m+n+1} - 2(m+2)\left\{\left(\frac{r}{a}\right)^{n+2} - \left(\frac{r}{a}\right)^{n+1}\right\}\right.$$

$$\left. + (m+2)(n+2)\left\{\left(\frac{r}{a}\right)^3 - 2\left(\frac{r}{a}\right)^2 + \frac{r}{a}\right\}\right] - \frac{4L^2C_1 r}{a^4}$$

$$. \quad . \quad . \quad (13,1)$$

$$\psi'_V = -\Omega'_V + \frac{3L^2}{r^3} \quad . \quad . \quad . \quad . \quad . \quad . \quad . \quad . \quad . \quad . \quad . \quad (13,2)$$

and by the help of (12, 2) and (12, 3) equation (6, 5) gives

$$\chi'_{\mathrm{M}} = -2\Omega'_{\mathrm{M}} + \frac{2\mathrm{L}^2}{a}\Sigma \mathrm{A}_m \mathrm{A}_n (n+2)$$

$$\left[-\frac{1}{m+n+3}\left(\frac{r}{a}\right)^{m+n+1} + \frac{m-1}{m+4}\left(\frac{r}{a}\right)^{m+2} - \frac{2m+2}{m+3}\left(\frac{r}{a}\right)^{m+1} \right.$$

$$\left. + \left(\frac{r}{a}\right)^{m} + (m+2)\left\{\left(\frac{r}{a}\right)^{3} - 2\left(\frac{r}{a}\right)^{2} + \frac{r}{a}\right\}\right] \quad . \quad (13, 3)$$

$$\chi'_{\mathrm{V}} = -2\Omega'_{\mathrm{V}} + \frac{\mathrm{L}^2 \mathrm{C}_2}{ar^2} \quad . \quad . \quad . \quad . \quad . \quad . \quad . \quad . \quad . \quad (13, 4)$$

The integration of these equations gives in the void

$$\psi_{\mathrm{V}} = -\Omega_{\mathrm{V}} - \frac{3\mathrm{L}^2}{2r^2} \quad . \quad . \quad . \quad . \quad . \quad (13, 5)$$

$$\chi_{\mathrm{V}} = -2\Omega_{\mathrm{V}} - \frac{\mathrm{L}^2 \mathrm{C}_2}{ar} \quad . \quad . \quad . \quad . \quad (13, 6)$$

the integration constants being zero because ψ and χ vanish at infinity. In matter integration gives expressions that we need not write down. The integration constants are determined by making ψ and χ continuous at the sun's boundary. ω being supposed so chosen as to satisfy the continuity conditions, we have in $\psi\, \chi\, \omega$ a set of values that satisfy the differential equations in matter and in the void and also the continuity conditions. Hence the values of $\lambda\, \mu\, \nu$ expressed in terms of $\psi\, \chi\, \omega$ by equations (5, 1) give the values of the potentials everywhere.

These expressions furnish the extension to the second power of L of the second set of values mentioned in article 1.

14. If ω is given the same values as in article 11 we have in the void

$$\left.\begin{aligned} e^{\lambda} &= 1 + \frac{\mathrm{L}}{r}\left(2 - \frac{\mathrm{LC}_2}{a}\right) + \frac{\mathrm{L}^2}{r^2}\left(\frac{7}{2} - \frac{\mathrm{E}}{2}\right) \\ e^{\mu} &= 1 + \frac{\mathrm{L}^2}{ar}(\mathrm{D} - \mathrm{C}_2) + \frac{\mathrm{L}^2}{2r^2}(3 + \mathrm{E}) \\ e^{\nu} &= 1 - \frac{\mathrm{L}}{r}\left(2 - \frac{\mathrm{LC}_2}{a}\right) - \frac{\mathrm{L}^2}{r^2} \end{aligned}\right\} \quad . \quad (14, 1)$$

If D and E are chosen to make μ zero the other two expressions are

$$\left.\begin{aligned} e^{\lambda} &= 1+\frac{L}{r}\left(2-\frac{LC_2}{a}\right)+\frac{5L^2}{r^2} \\ e^{\nu} &= 1-\frac{L}{r}\left(2-\frac{LC_2}{a}\right)-\frac{L^2}{r^2} \end{aligned}\right\} \quad . \quad . \quad (14, 2)$$

the value of C_2 being given by equation (12, 4).

15. It is well known that the values used for the potentials in the expression

$$ds^2 = (1-2L/r)\,dt^2-(1-2L/r)^{-1}\,dr^2-r^2\,d\theta^2-r^2\sin^2\theta\,d\phi^2$$

satisfy the differential equations in the void exactly. This is however not sufficient to prove them true potentials. To prove that it would be necessary to discover the complementary values of the potentials in matter, and to show that the two sets, along with their first derivatives, are continuous across the boundary of the matter. While some variation in the values given in article 14 for the potentials in the void can be obtained by varying the value of ξ of article 12, we have been unable to find a variation of ξ that makes the values in question true to the second power of L, and we see no reason to believe that these values are true beyond the first power of L.

LXXXIX. *Reducing Observations by the Method of Minimum Deviations.* *By* E. C. Rhodes, *D.Sc., Reader in Statistics, University of London* *.

THE writer recently was desirous of smoothing out the fluctuations in the series of figures set out below. A parabola was fitted by the method of Least Squares. The accompanying diagram shows clearly the effect of this smoothing.

The result was not considered altogether satisfactory. The plus and minus deviations occurred practically in three sets ; a set of minus, then a set of plus, then a set of minus. It was considered that the parabola was a bad fit. Two reasons suggested themselves for this: first, the original

* Communicated by Sir J. J. Thomson, O.M., F.R.S.

data from which the series was obtained did not involve absolutely random fluctuations ; second, the parabola might

Series.		Parabola (by Least Squares).	Deviations.
x.	*y.*		
−8	+28	−21	+49
−7	−39	− 8	−31
−6	−40	+ 2	−42
−5	− 1	+11	−12
−4	+23	+18	+ 5
−3	+34	22	+12
−2	+25	25	0
−1	+40	25	+15
0	+43	24	+19
1	+29	21	+ 8
2	+14	15	− 1
3	+12	8	+ 4
4	−16	− 2	−14
5	−14	−13	− 1
6	−46	−26	−20
7	−68	−42	−26
8	−24	−59	+35

Fig. 1.

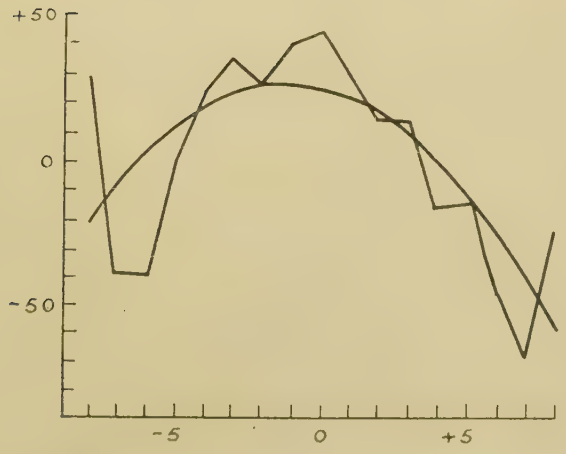

not be the best curve for use in smoothing. As to the first, it was definitely known that the original data, which were

observations at equal time-intervals, were subject to periodic fluctuations of varying intensity and changing phase, as well as to random variations. As to the second, there was no virtue in the parabola, as such, but associated series were reasonably represented by parabolas. It was therefore decided to concentrate on the first consideration, which meant that although we had obtained the parabola of best fit by the criterion of least squares, yet it might not really be the best parabola which would smooth out the fluctuations in the series. This led us to the question of what other methods of fitting there were available, and Edgeworth's description of the use of medians in this connexion led to the attempt to fit by the method of Minimum Deviations. This method may be briefly described. Suppose the equation to the parabola is

$$y = a_0 + a_1 x + a_2 x^2,$$

and the given y's are $y_{-8}, y_{-7}, \ldots y_{-1}, y_0, y_1, \ldots y_8$, then instead of, as in the method of Least Squares, making

$$\sum_{x=-8}^{+8} (a_0 + a_1 x + a_2 x^2 - y_x)^2$$

a minimum, we make

$$\sum_{x=-8}^{+8} | a_0 + a_1 x + a_2 x^2 - y_x |$$

a minimum.

His description of the method and his arguments in its favour are briefly summarized in Bowley's 'Edgeworth's Contributions to Mathematical Statistics,' pp. 103 *et seq.* (1928), and are exposed by Edgeworth in the 'Philosophical Magazine,' xlvi. (1923), xxv. (1888). Unfortunately, Edgeworth confined himself in the working of the method to a reliance on a diagram (he used as illustrations the problem of two variables), which means in practice a rather laborious piece of work, and apparently did not notice that the method could be applied in a more simple manner, without any need to rely on the position of straight lines in relation to one another, although at one stage in his argument he touched on this simplification. The writer, finding Edgeworth's method cumbrous, especially when he intended to use the method over and over again on different series, sought a simplification, which it is hoped will be of use to others, especially as there are many series which involve fluctuations which cannot on *à priori* grounds be

considered altogether adventitious, and where therefore the method of Least Squares does not strictly apply.

The simpler method is as follows:—Suppose we are dealing with a series of deviations, say, involving three unknowns,

$$A_1u+B_1v+C_1w+D_1,\quad A_2u+B_2v+C_2w+D_2,\ldots$$
$$\ldots A_nu+B_nv+C_nw+D_n,$$

and we want to find values of u, v, w which make

$$\sum_{s=1}^{n} | A_su+B_sv+C_sw+D_s |$$

a minimum. First, find for what values of v and w the expression is a minimum when u is given by

$$-\frac{B_rv+C_rw+D_r}{A_r},$$

i.e. find a local minimum point in the plane

$$A_ru+B_rv+C_rw+D_r=0,$$

where r is any one of the values s from 1 to n. This reduces the problem to one involving two variables only, *i.e.* what values of v and w will make

$$\sum_{t=1}^{n-1} | E_tv+F_tw+G_t |$$

a minimum, where the E's, F's, G's are obtained from the A's, B's, C's, D's. To solve this, find for what value of w the expression is a minimum when v is given by

$$-\frac{F_pw+G_p}{E_p},$$

i.e. find a local minimum point in the line

$$E_pv+F_pw+G_p=0,$$

where p is any one of the values of t from 1 to $n-1$. This reduces simply to the problem of finding a weighted median. The process is repeated until we arrive at a stage when we find that the local minimum in the plane

$$A_lu+B_lv+C_lw+D_l=0$$

is the point where the planes

$$A_mu+B_mv+C_mw+D_m=0 \quad \text{and} \quad A_nu+B_nv+C_nw+D_n=0$$

meet it, and where the local minimum in the plane

$$A_m u + B_m v + C_m w + D_m = 0$$

is the point where the planes

$$A_n u + B_n v + C_n w + D_n = 0 \quad \text{and} \quad A_l u + B_n v + C_n w + D_n = 0$$

meet it, and the local minimum in the plane

$$A_n u + B_n v + C_n w + D_n = 0$$

is the point where the planes

$$A_l u + B_l v + C_l w + D_l = 0 \quad \text{and} \quad A_m u + B_m v + C_m w + D_m = 0$$

meet it. Then this point of intersection of these three planes is the true minimum point, and the values u, v, w obtained from solving these equations make

$$\sum_{s=1}^{n} | A_s u + B_s v + C_s w + D_s |$$

a minimum.

In the case of two variables, where a diagram is used by Edgeworth to illustrate the argument, the process is simply to proceed along one line until we arrive at the point on the line for which the values of the variables make the expression a minimum, this being a point of intersection with another line. Then proceed along this new line until we arrive at the mininum point on this line, which is a point of intersection of this second line with a third. Then proceed along this third line until we get to the minimum point, which will give another line. This goes until we reach the stage where the qth line leads to the $q+1$th and the $q+1$th leads to the qth again. The required values of the variables are given by the intersection of these qth and $q+1$th lines. The description of the process may appear to make it complicated, but in practice this is not so. In the first place, in tracing the course of these lines to the minimum point we are getting closer and closer to this point very quickly, and one or two attempts are alone necessary in practice. Further, in any problem we can start with a particular line which we suspect is near the heart of the mystery by getting some crude approximation to the minimum or by other considerations, and from this line there is probably little distance to go to the minimum.

The accompanying example will indicate the method and the amount of labour involved. The problem is to fit a parabola to the data on p. 975 by this method.

(1) Deviations.	(2)	(3)	(4) Values of a_2.	(5) a_2 in order.	(6) Coefficient of a_2 in (3).	(7) Sums.
$a_0-8a_1+64a_2-28$	$-4a_1+48a_2-5$	$36a_2-9{\cdot}8$	$+0{\cdot}3$	$-4{\cdot}3$	14	14 380
$a_0-7a_1+49a_2+39$	$-3a_1+33a_2+62$	$24a_2+58{\cdot}4$	$-2{\cdot}43$	$-3{\cdot}3$	6	20 366
$a_0-6a_1+36a_2+40$	$-2a_1+20a_2+63$	$14a_2+60{\cdot}6$	$-4{\cdot}3$	$-3{\cdot}8$	4	24 360
$a_0-5a_1+25a_2+1$	$-a_1+9a_2+24$	$6a_2+22{\cdot}8$	$-3{\cdot}8$	$-2{\cdot}7$	6	30 356
$a_0-4a_1+16a_2-23$	0	0		$-2{\cdot}45$	4	34 350
$a_0-3a_1+9a_2-34$	a_1-7a_2-11	$-4a_2-9{\cdot}8$	$-2{\cdot}45$	$-2{\cdot}43$	24	58 346
$a_0-2a_1+4a_2-25$	$2a_1-12a_2-2$	$-6a_2+0{\cdot}4$	$+0{\cdot}1$	$-2{\cdot}2$	6	64 322
$a_0-a_1+a_2-40$	$3a_1-15a_2-17$	$-6a_2-13{\cdot}4$	$-2{\cdot}2$	$-2{\cdot}0$	21	88 316
a_0-43	$4a_1-16a_2-20$	$-4a_2-15{\cdot}2$	$-3{\cdot}8$	$-1{\cdot}62$	50	138 292
$a_0+a_1+a_2-29$	$5a_1-15a_2-6$	0		$-1{\cdot}58$	66	204 242
$a_0+2a_1+4a_2-14$	$6a_1-12a_2+9$	$6a_2+16{\cdot}2$	$-2{\cdot}7$	$-1{\cdot}4$	14	218 176
$a_0+3a_1+9a_2-12$	$7a_1-7a_2+11$	$14a_2+19{\cdot}4$	$-1{\cdot}4$	$-1{\cdot}3$	36	254 162
$a_0+4a_1+16a_2+16$	$8a_1+39$	$24a_2+48{\cdot}6$	$-2{\cdot}0$	$-0{\cdot}7$	84	338 126
$a_0+5a_1+25a_2+14$	$9a_1+9a_2+37$	$36a_2+47{\cdot}8$	$-1{\cdot}3$	$+0{\cdot}1$	6	344 42
$a_0+6a_1+36a_2+46$	$10a_1+20a_2+69$	$50a_2+81{\cdot}0$	$-1{\cdot}62$	$+0{\cdot}3$	36	380 36
$a_0+7a_1+49a_2+68$	$11a_1+33a_2+91$	$66a_2+104{\cdot}2$	$-1{\cdot}58$			
$a_0+8a_1+64a_2+24$	$12a_1+48a_2+47$	$84a_2+61{\cdot}4$	$-0{\cdot}7$			

From the diagram (fig. 1) we might suspect that the parabola would go through the point $x=-4$, $y-23$. We therefore start by taking $a_0-4a_1+16a_2-23=0$, and obtain col. (2) by substituting for a_0. Considering col. (2), the diagram again suggests that the parabola might go through the point $x=1$, $y=29$; we therefore substitute for a_1 in col. (2) from $5a_1-15a_2=6$, which gives col. (3). Col. (3) gives us values of a_2 from which we can obtain the weighted median, col. (5) shows the values of a_2 in order, col. (6) the corresponding coefficients of a_2 in col. (3) without sign, and col. (7) shows the sums of these coefficients starting from the top and bottom of col. (6) respectively. The best value of a_2 is $-1{\cdot}58$. This is the value corresponding to 66 in col. (6); the sum of col. (6) from the top to 66 is greater than the sum from the bottom to 14 (the figure below 66), the sum of col. (6) from the top to 50 (the figure above 66) is less than the sum from the bottom up to (66).

Thus we are led to the expression $11a_1+33a_2+91$ in col. (2). The local minimum of the series of col. (2) in the line $5a_1-15a_2=6=0$ is the point in this line where it intersects $11a_1+33a_2+91=0$. We now substitute in col. (2) the value of a_1 obtained from $11a_1+33a_2+91=0$. This gives a new col. (3) and new values of a_2, and an examination of these gives the best. The work is set out below.

(3)	(4)	(5)	(6)	(7)	
	Values of a_2.	a_2 in order.	Coefficients of a_2 in (3).	Sums.	
$60a_2+28{\cdot}1$	$-0{\cdot}4$	-3	26	26	372
$42a_2+86{\cdot}8$	$-2{\cdot}07$	$-2{\cdot}7$	12	38	346
$26a_2+79{\cdot}5$	-3	$-2{\cdot}08$	18	56	334
$12a_2+32{\cdot}3$	$-2{\cdot}7$	$-2{\cdot}07$	42	98	316
0		$-1{\cdot}93$	10	108	274
$-10a_2-19{\cdot}3$	$-1{\cdot}93$	$-1{\cdot}90$	28	136	264
$-18a_2-18{\cdot}5$	$-1{\cdot}0$	$-1{\cdot}74$	24	160	236
$-24a_2-41{\cdot}8$	$-1{\cdot}74$	$-1{\cdot}67$	28	188	212
$-28a_2-53{\cdot}1$	$-1{\cdot}90$	$-1{\cdot}58$	30	218	184
$-30a_2-47{\cdot}4$	$-1{\cdot}58$	$-1{\cdot}37$	10	228	154
$-30a_2-40{\cdot}6$	$-1{\cdot}35$	$-1{\cdot}35$	30	258	144
$-28a_2-46{\cdot}9$	$-1{\cdot}67$	$-1{\cdot}1$	24	282	114
$-24a_2-27{\cdot}2$	$-1{\cdot}1$	$-1{\cdot}0$	18	300	90
$-18a_2-37{\cdot}5$	$-2{\cdot}08$	$-0{\cdot}4$	60	360	72
$-10a_2-13{\cdot}7$	$-1{\cdot}37$	$+4{\cdot}4$	12	372	12
0					
$12a_2-53{\cdot}3$	$+4{\cdot}4$				

This gives the best $a_2=-1{\cdot}67$ from $7a_1-7a_2+11=0$.

We now substitute in the original col. (2) the value of a_1 from $7a_1-7a_2+11=0$ and get the following series. In what follows col. (5) is dispensed with, it is not really necessary to rewrite the values of a_2, and all the figures are not written in col. (7). Again, in the determination of the weighted median we are not really particular in what order the values of a_2 are written, except in the immediate neighbourhood of the median itself.

(3)	(4)	(6)	(7)	
	Values of a_2.	Coefficients of a_2 in order of a_2.	Sums.	
$44a_2+1{\cdot}3$	$-0{\cdot}03$	18	18	
$30a_2+66{\cdot}7$	$-2{\cdot}22$	8	26	
$18a_2+66{\cdot}1$	$-3{\cdot}7$	8	34	
$8a_2+25{\cdot}6$	$-3{\cdot}2$	30	64	
0		12	76	
$-6a_2-12{\cdot}6$	$-2{\cdot}1$	6	82	
$-10a_2-5{\cdot}1$	$-0{\cdot}51$	12	94	
$-12a_2-21{\cdot}7$	$-1{\cdot}8$	30	124	
$-12a_2-26{\cdot}3$	$-2{\cdot}2$	44	168	192
$-10a_2-13{\cdot}9$	$-1{\cdot}39$	10	178	148
$-6a_2-0{\cdot}4$	$-0{\cdot}07$	18		138
0		10		120
$8a_2+26{\cdot}4$	$-3{\cdot}3$	60		110
$18a_2+22{\cdot}9$	$-1{\cdot}27$	6		50
$30a_2+53{\cdot}3$	$-1{\cdot}78$	44		44
$44a_2+73{\cdot}7$	$-1{\cdot}68$			
$60a_2+28{\cdot}1$	$-0{\cdot}4$			

This gives the best $a_2=-1{\cdot}68$ from $11a_1+33a_2+91=0$.

This stage illustrates the procedure in the case of two variables. Starting from the original col. (2), involving a_1 and a_2, we find the local minimum on the line

$$5a_1-15a_2-6=0$$

is at the intersection of this with

$$11a_1+33a_2+91=0.$$

The local minimum along

$$11a_1+33a_2+91=0$$

is at the intersection of this with

$$7a_1-7a_2+11=0.$$

The local minimum along

$$7a_1-7a_2+11=0$$

is at the intersection of this with

$$11a_1+33a_2+91=0.$$

Therefore the values of a_1 and a_2 obtained from

$$7a_1-7a_2+11=0 \quad \text{and} \quad 11a_1+33a_2+91=0$$

will make the series in col. (2) when summed without regard to sign a minimum.

Returning to our problem, we have found that starting from

$$a_0-4a_1+16a_2-23=0,$$

we are led to

$$a_0+7a_1+49a_2+68=0 \quad \text{and} \quad a_0+3a_1+9a_2-12=0.$$

Now start from col. (1) again, substituting

$$a_0=-3a_1-9a_2+12;$$

we get a new col. (2) :—

(2)
$-11a_1+55a_2-16$
$-10a_1+40a_2+51$
$-\ 9a_1+27a_2+52$
$-\ 8a_1+16a_2+13$
$-\ 7a_1+\ 7a_2-11$
$-\ 6a_1\qquad -22$
$-\ 5a_1-\ 5a_2-13$
$-\ 4a_1-\ 8a_2-28$
$-\ 3a_1-\ 9a_2-31$
$-\ 2a_1-\ 8a_2-17$
$-\ a_1-\ 5a_2-\ 2$
0
$a_1+\ 7a_2+28$
$2a_1+16a_2+26$
$3a_1+27a_2+58$
$4a_1+40a_2+80$
$5a_1+55a_2+36$

In dealing with this we may use the information already acquired and try substituting for a_1 in col. (2) from

$$4a_1+40a_2+80=0,$$

which comes from

$$a_0 + 7a_1 + 49a_2 + 68$$

of col. (1). This substitution gives us a new col. (3), from which we obtain the median a_2, which is the intersection of

$$4a_1 + 40a_2 + 80 = 0 \quad \text{with} \quad -10a_1 + 40a_2 + 51 = 0.$$

Substituting in col. (2) the value of a_1 from this last equation gives a new col. (3), from which the median a_2 is the intersection of this line with

$$4a_1 + 40a_2 + 48 = 0.$$

Thus we have arrived at the fact that the local minimum in

$$a_0 + 3a_1 + 9a_2 - 12 = 0$$

is where this meets

$$a_0 + 7a_1 + 49a_2 + 68 = 0 \quad \text{and} \quad a_0 - 7a_1 + 49a_2 + 39 = 0.$$

Now repeat the process from col. (1). Starting with a substitution of

$$a_0 = -7a_1 - 49a_2 - 68,$$

we get a new col. (2) :—

Col. (2).

$$\begin{array}{r}
-15a_1 + 15a_2 - 96 \\
-14a_1 \qquad - 29 \\
-13a_1 - 13a_2 - 28 \\
-12a_1 - 24a_2 - 67 \\
-11a_1 - 33a_2 - 91 \\
-10a_1 - 40a_2 - 102 \\
-\ 9a_1 - 45a_2 - 93 \\
-\ 8a_1 - 48a_2 - 108 \\
-\ 7a_1 - 49a_2 - 111 \\
-\ 6a_1 - 48a_2 - 97 \\
-\ 5a_1 - 45a_2 - 82 \\
-\ 4a_1 - 40a_2 - 80 \\
-\ 3a_1 - 33a_2 - 52 \\
-\ 2a_1 - 24a_2 - 54 \\
-\ a_1 - 13a_2 - 22 \\
0 \\
a_1 + 15a_2 - 44
\end{array}$$

Obtain from this col. (2) a value of a_1 from

$$14a_1 + 29 = 0,$$

which has been obtained from

$$a_0 - 7a_1 + 49a_2 + 39 = 0.$$

This gives the best a_2 from the intersection of

$$14a_1+29=0 \quad \text{with} \quad -6a_1-48a_2-97=0.$$

Using this last equation to give a_1 for substitution in col. (2), we arrive at the best a_2 from the intersection of this with

$$14a_1+29=0.$$

Thus the local minimum on

$$a_0+7a_1+49a_2+68=0$$

is where this meets

$$a_0-7a_4+49a_2+39=0 \quad \text{and} \quad a_0+a_1+a_2-29=0.$$

The field has now been narrowed down, and we find, when we get a new col. (2) from col. (1) by substituting

$$a_0=7a_1-49a_2-39,$$

that the local minimum in the plane

$$a_0-7a_1+49a_2+39=0$$

is where this meets

$$a_0+a_1+a_2-29=0 \quad \text{and} \quad a_0+7a_1+49a_2+68=0.$$

With the information available at this stage there is no wasted labour involved; in fact, we merely verify the statement. It follows now that the local minimum on

$$a_0+a_1+a_2-29=0$$

is where this meets

$$a_0+7a_1+49a_2+68=0 \quad \text{and} \quad a_0-7a_1+49a_2+39=0.$$

If the actual work is done, we find ourselves with a repetition of work previously done. This marks the end of the working of the new procedure, and we find that the best values of a_0, a_1, a_2 to render the original series a minimum when summed without regard to sign are those obtained by solving

$$a_0-7a_1+49a_2+39=0,$$

$$a_0+\ a_1+\ \ a_2-29=0,$$

$$a_0+7a_1+49a_2+68=0,$$

which give

$$a_0=32^5/_6, \quad a_1=-2^1/_{14}, \quad a_2=-1^{16}/_{21}.$$

The table below shows again the original series and the smooth values from this parabola obtained by the method of Minimum Deviations.

A diagram (fig. 2) showing this parabola with the original data, when compared with fig. 1, will indicate clearly the

Series.		Parabola (by Minimum Deviations).	Deviations.
x.	*y.*		
−8	+28	−63	+91
−7	−39	−39	0
−6	−40	−18	−22
−5	− 1	− 1	0
−4	+23	+13	+10
−3	+34	+23	+11
−2	+25	+30	− 5
−1	+40	+33	+ 7
0	+43	+33	+10
1	+29	+29	0
2	+14	+22	− 8
3	+12	+11	+ 1
4	−16	− 4	−12
5	−14	−22	+ 8
6	−46	−43	− 3
7	−68	−68	0
8	−24	−96	+72

Fig. 2.

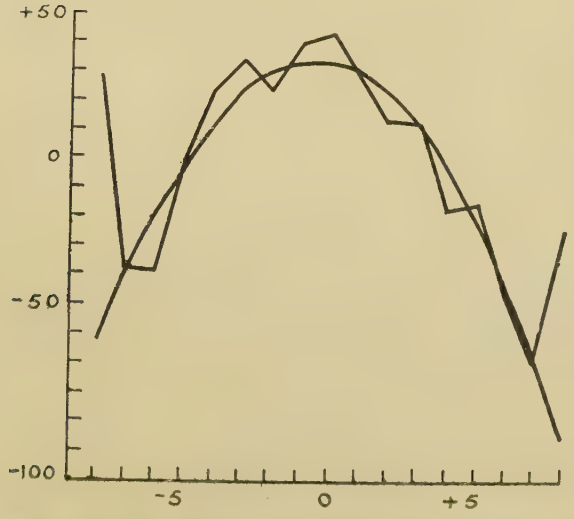

difference between the two parabolas obtained by Least Squares and Minimum Deviations as smooths of the original series. The second parabola is much more satisfactory. A glance at the diagrams and at the table of deviations

shows the important part of the two values of y associated with $x=+8$ and $x=-8$. The importance of these compared with the other y's has been exaggerated in the method of Least Squares ; this method has forced the parabola to pay too much attention to these values and to neglect its duty towards the other observations. In the method of Minimum Deviations these large deviations are not given undue prominence, with the result that the parabola adequately describes the remaining observations.

The exposition above might appear to make the procedure laborious. Undoubtedly it is more so than the method of Least Squares. But the labour would have appeared less if one had been content to illustrate with an example involving only two variables. On the other hand, the illustration here shown indicates how the method can be used with three variables ; and it has the advantage of being derived from a problem met with in the course of an investigation, with the accompanying illuminating diagrams, which call attention to the necessity for alternative methods, to that of Least Squares, where fluctuations are not random.

Pressing the advantages of this method further, it is not restricted to problems where the deviations involve only linear functions of the variables. Theoretically there is nothing to prevent the method from being extended to the case of a general problem of minimizing

$$\sum_{s=1}^{n} | f_s(u, v, w) | .$$

Here we choose a particular deviation, say $f_r(u, v, w)$, equate this to zero and find u in terms of v, w, and get a new series:

$$\sum_{t=1}^{n-1} | F_t(v, w) | ,$$

from which we choose, say $F_p(v, w)$, and get a series involving only one variable. In practice the working would depend on the simplicity or otherwise of the functions f, but in certain cases the method can be applied without a great deal of labour, and gives a great advantage over the method of Least Squares, which can only be used in such cases in a modified manner, where the original foundation for the justification for the method of Least Squares now disappears. For instance, the curve $y=Bx^a$ crops up as a theoretical method of describing data in a variety of ways. When the method of Least Squares is used for fitting this curve, the computer resorts to a trick and fits the line

$$\log y = a \log x + \log B$$

to the data, using as his variables $\log x$ and $\log y$; thus virtually asserting that the deviations of the logarithms of the original y's from the logarithms of the y's of the curve follow the normal law, instead of the deviations of the original y's from the y's of the curve. But in a comparatively simple case like this the method of minimum deviations may be used with fair ease. The method may be illustrated by the working on the data below, which relate to production (x) and price (y) of corn in the United States (Warren and Pearson, 'Inter-relationships of Supply and Price,' 1928, p. 188).

x.	y.	x.	y.
68	192	113	77
75	135	113	93
79	169	114	86
81	141	116	86
85	116	118	89
90	123	118	89
93	103	119	99
94	123	120	106
96	120	120	109
96	101	120	82
97	109	121	85
98	130	122	79
100	102	123	79
102	105	123	96
103	91	124	90
107	121	133	93
108	114	137	60
109	94	140	66
110	100	147	93
112	82		

A plot of these associated values of x and y suggests that a useful start would be given by taking $x = 110$, $y = 100$ as satisfying the equation $y = Bx^a$. From this we get $B = 100/110^a$. Substituting this value we get a series of deviations:

$$192 - 100\left(\frac{68}{100}\right)^a,$$

$$135 - 100\left(\frac{75}{110}\right)^a,$$

$$169 - 100\left(\frac{79}{100}\right)^a,$$

$$\vdots$$

From these we may obtain values of a by equating each to zero, and from these values of a we must pick out the best to make the sum of the deviations a minimum. At this stage the work is slightly different from that in the simpler case of a linear function considered first above and dealt with by Edgeworth. Suppose that we have obtained the values of a as described above, and suppose now they are arranged in order of size, and that the corresponding deviations are also so arranged. Take the general case where $B = y_r/x_r^a$, and we have :

$$\begin{array}{c|c} a_1 & y_1 - y_r\left(\frac{x_1}{x_r}\right)^a, \\ a_2 & y_2 - y_r\left(\frac{x_2}{x_r}\right)^a, \\ a_3 & y_3 - y_r\left(\frac{x_3}{x_r}\right)^a, \\ a_4 & y_4 - y_r\left(\frac{x_4}{x_r}\right)^a \\ \vdots & \vdots \end{array}$$

where $a_1 < a_2 < a_3 \ldots < a_n$.

Now suppose that of these a's, arranged in order, a_s is that which makes

$$\mathop{\mathrm{S}}_{t} \left| y_t - y_r\left(\frac{x_t}{x_r}\right)^a \right|$$

a minimum, then the deviations in series above which occur before the sth will be negative and those after the sth will be positive. If we put $a = a_s + \alpha$, where α is small and positive, the sum of the deviations may be written

$$\left(y_r\left(\frac{x_1}{x_r}\right)^{a_s+\alpha} - y_1\right) + \left(y_r\left(\frac{x_2}{x_r}\right)^{a_s+\alpha} - y_2\right) + \ldots + \left(y_r\left(\frac{x_s}{x_r}\right)^{a_s+\alpha} - y_s\right)$$
$$+ \left(y_{s+1} - y_r\left(\frac{x_{s+1}}{x_r}\right)^{a_s+\alpha}\right) + \ldots,$$

and if we put $a_s = a_s - \alpha$ where α is small and positive, the sum of the deviations may be written

$$\left(y_r\left(\frac{x_1}{x}\right)^{a_s-\alpha} - y_1\right) + \left(y_r\left(\frac{x_2}{x_r}\right)^{s^{-\alpha}} - y_2\right) + \ldots$$

$$+\left(y\left(\frac{x_{s-1}}{x_r}\right)^{a_s-\alpha}-y_{s-1}\right)+\left(y_s-y_r\left(\frac{x_s}{x_r}\right)^{a_s-\alpha}\right)$$

$$+\left(y_{s+1}-y_r\left(\frac{x_{s+1}}{x_r}\right)^{a_s-\alpha}\right)+\ldots$$

If we express

$$\left(\frac{x_t}{x_r}\right)^{a_s+\alpha}=\left(\frac{x_t}{x_r}\right)^{a_s}\left(1+\alpha\log\left(\frac{x}{x_r}\right)\right),$$

we see that since a_s makes the expression a minimum

$$\sum_{t=1}^{s}\left(\frac{x_t}{x_r}\right)^{a_s}\log\left(\frac{x_t}{x_r}\right)>\sum_{t=s+1}^{n}\left(\frac{x_t}{x_r}\right)^{a_s}\log\left(\frac{x_t}{x_r}\right)$$

and

$$\sum_{t=1}^{s-1}\left(\frac{x}{x_r}\right)^{a_s}\log\left(\frac{x^t}{x_r}\right)<\sum_{t=s}^{n}\left(\frac{x_t}{x}\right)^{a_s}\log\left(\frac{x_t}{x_r}\right).$$

Thus the "weights" to be used for finding the weighted median a are

$$\left(\frac{x_t}{x_r}\right)^{a_s}\log\left(\frac{x_t}{x_r}\right)$$

for values of t from 1 to n, and are proportional to

$$x_t^{a_s}\log\left(\frac{x_t}{x_r}\right).$$

Unfortunately, these weights to be used to determine a_s involve a_s itself, but we can get approximations to the weights by taking weights proportional to

$$y_t\log\left(\frac{x_t}{x_r}\right),$$

replacing $x_t^{a_s}$ by y_t. Or we can see at a glance at the table of the a's in order that the value required will be nearly $a=-1$, and we can take the weights proportional to

$$\log\left(\frac{x}{x_r}\right)\Big/x_t.$$

Either of these will lead to the correct result, for we can always check these results by using the value of a_s so found to work out the correct weights and verify that our a_s is really the weighted median. In any other problem of curve fitting by this method a similar difficulty will arise, and can be overcome by some such device as described above.

Proceeding then with our illustration, we get values of a, arrange them in order, weight them, and get the weighted average.

Values of a.	a's in order.	$\left(yt\log\frac{x_t}{x_r}\right)$. Weights.	Sums.		$\left(\log\left(\frac{x_t}{x_r}\right)\Big/ x_t\right)$. Weights.	Sums.	
− 1·35	−10	1	1		1	1	
− ·78	− 9	1	2		1	2	
− 1·58	− 7	1	3		1	3	
− 1·12	− 6	1	4		1	4	
− ·5	− 4	1	5		1	5	
− ·98	− 2·8	2	7		2	7	
− ·1	− 2·7	1	8		1	8	
− 1·31	− 2·32	6	14		7	15	
− 1·34	− 2·28	4	18		4	19	
− ·07	− 2·28	3	21		3	22	
− ·7	− 2·28	7	28		5	27	
− 2·28	− 2·11	4	32		4	31	
− ·2	− 1·72	7	39		7	38	
− ·6	− 1·70	4	43		3	41	
+ 1	− 1·66	3	46		3	44	
− 6	− 1·66	3	49		3	47	
− 7	− 1·58	24	73		18	65	
+ 6	− 1·35	40	113		34	99	
...	− 1·34	7	120		6	105	
−10	− 1·31	8	128		7	112	
− 9	− 1·12	19	147	136	16	128	123
− 2·7	− ·98	11	158	117	10	138	107
− 4	− ·8	5	163	106	4	142	97
− 2·8	− ·78	22		101	22		93
− 1·66	− ·7	6		79	6		71
− 1·66	− ·6	3		73	3		65
− ·1	− ·5	13		70	13		62
+ ·7	− ·3	5		57	4		49
+ ·91	− ·3	8		52	6		45
− 2·28	− ·2	12		44	9		39
− 1·70	− ·2	4		32	4		30
− 2·28	− ·1	3		28	3		26
− 2·11	− ·1	8		25	8		23
− ·3	− ·07	6		17	6		15
− ·8	+ ·7	4		11	3		9
− ·3	+ ·91	4		7	3		6
− 2·32	+ 1	3		3	3		3
− 1·72	+ 6	0		0	0		0
− ·2							

Thus the best a is $-1{\cdot}12$ obtained from $x=81$, $y=141$.

Now we start again by taking $B=141/81^a$. This gives us another series of a's, from which we deduce the best a is $-1{\cdot}26$, obtained by the intersection of $141=B\,81^a$ with $85=B\,121^a$. Further, we find when we start from $85=B\,121^a$

that we arrive again at $141 = B\,81^a$. Therefore $a = -1{\cdot}2610$, $B = 35967$ are the a, B which make a minimum, the sum of the deviations $192 - B\,68^a$, etc., when the signs are ignored.

		Minimum Deviation.		Least Square. Logs.	
x.	y.	Curve.	Deviation.	Curve.	Deviation.
68	192	176	+16	168	+24
75	135	155	−20	150	−15
79	169	145	+24	141	+28
81	141	141	0	137	+ 4
85	116	133	−17	130	−14
90	123	124	− 1	123	0
93	103	118	−15	118	−15
94	123	117	+ 6	117	+ 6
96	120	114	+ 6	114	+ 6
96	101	114	−13	114	−13
97	109	112	− 3	112	− 3
98	130	111	+19	111	+19
100	102	108	− 6	109	− 7
102	105	105	0	106	− 1
103	91	104	−13	105	−14
107	121	99	+22	101	+20
108	114	98	+16	100	+14
109	94	97	− 3	99	− 5
110	100	96	+ 4	98	+ 2
112	82	94	−12	96	−14
113	77	93	−16	95	−18
113	93	93	0	95	− 2
114	86	92	− 6	94	− 8
116	86	90	− 4	92	− 6
118	89	88	+ 1	90	− 1
118	89	88	+ 1	90	− 1
119	99	87	+12	89	+10
120	106	86	+20	89	+17
120	109	86	+23	89	+20
120	82	86	− 4	89	− 7
121	85	85	0	88	− 3
122	79	84	− 5	87	− 8
123	79	83	− 4	86	− 7
123	96	83	+13	86	+10
124	90	82	+ 8	85	+ 5
133	93	75	+18	78	+15
137	60	73	−13	76	−16
140	66	71	− 5	74	− 8
147	93	67	+26	71	+22
	Sum (Deviations)^2.....		6339		6244

The table above shows for comparison the values of y from the curve

$$y = 35967x^{-1\cdot2610},$$

just obtained by the method of Minimum Differences, with the original y's, also the values of y from the curve

$$y = 19083x^{-1\cdot1220},$$

obtained by Warren and Pearson (*loc. cit.*) by fitting a straight line to the logarithms of the x's and y's, and the original y's, with deviations.

It is interesting to compare the sum of the squares of the deviations, 6244 against 6339; and if it is felt in a case of this kind that the deviations were purely fortuitous, then the method of Least Squares on the logarithms of the originals gives a curve which is a better approximation to the true Least Square curve than the method of Minimum Deviations, and, in a sense, we may regard the preceding work as justifying the use of the Least Square Method in fitting a straight line to the logarithms of the original figures. But there is another point of view; if there is no more justification for the idea that the sums of the squares of the deviations from the fitting curve should be a minimum than there is for the idea that the sum of the deviations from the fitting curve, signs being ignored, should be a minimum, then the work here and that by Warren and Pearson bear comparison in an important particular, viz. the value of a. In the work done by these authors the important part related to this value, and we see that two different methods of reconciling the original data to a function of the form $y = Bx^a$ lead to results which are approximately equal, but which really differ by about 10 per cent. of their values, viz. $-1\cdot122$ and $-1\cdot261$, difference $\cdot139$. These considerations indicate clearly that not too great a reliance may be placed on the absolute exactitude of such a figure when calculated by one of these methods.

The writer has used the method of Minimum Deviations in the case of 2 and 3 variables where the deviation function is linear, and in the case where the deviations are obtained from $y = Bx^a$. There are simpler problems than those illustrated here, where the method would not require such labour, *e. g.* fitting a hyperbola to a few observations; and it would be of interest if other workers would try this method, and make comparisons with results obtained by the method of Least Squares.

XC. *An X-ray Investigation of the Copper-Antimony System of Alloys.* *By* E. Vyron Howells, *M.Sc.* (*Wales*) *and* W. Morris-Jones, *M.A.*, *M.Sc.*, *F.Inst.P.* (*Physics Department, University College, Swansea*)*.

Introduction.

THE investigation described in this paper was undertaken with the object of determining the crystal structure of the Copper-Antimony Alloys. The structure of one member of the series—Cu_3Sb—had already been determined by Morris Jones and Evans [1], but the crystal structures of the complete system were unknown†. An X-ray examination of the system seemed, therefore, well worth carrying out, especially as the results of such a study should, in addition, serve to verify information concerning the metallurgy of the system obtained by thermal and micrographical methods.

The metallurgy of the copper-antimony system has engaged the attention of many workers. The most complete investigation is that of Sir H. C. Carpenter [2], published in 1913. As a result of his work, Carpenter drew up the equilibrium diagram given in fig. 1, and this is the diagram taken as the basis of comparison in the research described below. The diagram shows the existence at normal temperatures of the following constituents :—

(i.) The α phase, a region of solid solution of antimony in copper up to 7 per cent. by weight of antimony.

(ii.) The γ phase, extending between the composition 30 per cent. to 39 per cent. by weight of antimony ; the latter limit being at the composition Cu_3Sb.

(iii.) The intermetallic compound Cu_2Sb.

(iv.) The ε phase, consisting of a region of slight solution of copper in antimony.

* Communicated by W. Morris-Jones, Senior Lecturer in Physics, University College, Swansea.

† *Note added.*—Since the completion of the present investigation, in September 1929, a paper on the Copper-Antimony Alloys by Westgren, Hagg, and Erikson has appeared (*Zeit. für Phys. Chem.* B. iv. pt. 6, August 1929). Their results agree very satisfactorily with those of the present work.

At temperatures higher than 430° C. a phase β is formed ; but below this temperature the alloy assumed the character of the γ phase.

Previous investigators of this system of alloys had concluded from micrographical, thermal, and other data that, if copper can hold antimony in solution, the degree of solubility was very small, and in no case did it exceed 0·4 per cent. by weight of antimony ; whereas Carpenter, as his diagram shows, found that antimony is soluble in copper to the extent of 4 atoms per cent.—which is slightly over 7 per cent. by weight of antimony.

Fig. 1.

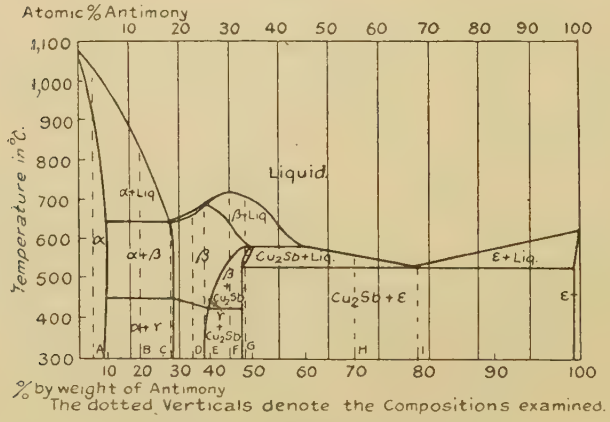

Carpenter's equilibrium diagram.

In agreement with previous workers Carpenter found, on the other hand, that antimony could hold very little copper in solution, and that the degree of solubility did not exceed 0·5 per cent. by weight of copper.

An earlier equilibrium diagram due to Guertler [3] showed copper and antimony to be completely insoluble in each other. In addition, there was no phase in this diagram corresponding to the γ phase of Carpenter.

In the course of the present X-ray investigation a study was therefore made of the crystal structure of the regions of solid solution at the copper and antimony ends of the diagram. The crystal structure of the compound Cu_2Sb was also investigated, and an examination made of the character of the β and the γ phases.

Preparation of the Alloys.

The copper used in making the alloys was of electrolytic origin, while the antimony was of 99·916 per cent. purity. In making the alloys the copper was placed in a salamander pot, under a layer of charcoal, and melted in a wind-furnace. The antimony, which melts at a much lower temperature, was then introduced quickly in small quantities, and the whole was well stirred with a carbon

TABLE I.

Alloy.	Composition per cent. Cu by weight.	Density grams. per c.c.	Crystal structure.	Dimensions of the unit-cell in Å.U.
Copper	100	8·93	Face-centred cubic.	a_0 —3·610
A	96	8·75	Face-centred cubic.	a_0 —3·644
B	80	8·26	Mixture of face-centred cubic and hexagonal close-packed lattices.	a_0'—3·670 a_0''—2·728 c_0''—4·288
C	70	8·34	Hexagonal close-packed lattice.	a_0 —2·728 c_0 —4·288
D	65	8·64	Hexagonal close-packed.	a_0 —2·752 c_0 —4·326
E	61	8·66	Hexagonal close-packed.	a_0 —2·766 c_0 —4·348
F	55	8·30	Mixture of hexagonal close-packed and simple tetragonal lattices.	a_0'—2·766 c_0'—4·348 a_0''—4·029 c_0''—6·140
G	51	8·42	Simple tetragonal.	a_0 —4·029 c_0 —6·140
H	30	7·45	Mixture of simple tetragonal and face-centred rhombohedral lattices.	a_0'—4·020 c_0'—6·126 a_0''—6·235
I	20	7·02	Mixture of simple tetragonal and face-centred rhombohedral lattices.	a_0'—6·024 c_0'—6·133 a_0''—6·240
Antimony ..	0	6·62	Face-centred rhombohedral.	a_0 —6·235 angle 87° 24′

rod. To ensure homogeneity of each ingot the pot was replaced in the furnace and the alloy re-heated to a temperature above its melting-point.

The compositions of the alloys were determined electrolytically by estimation of the copper content, and the densities found by the specific gravity bottle method. To make certain that the alloys were in a definite state of

equilibrium the specimens were subjected to prolonged periods of annealing, at temperatures given in the equilibrium diagram.

In all nine alloys were prepared. Their compositions and densities are given in Table I.

Experimental Method.

The crystal structures of the alloys were investigated by the X-ray powder method. Details of the apparatus used in the present investigation and the precaution observed to ensure the accuracy of measurements have been described in previous papers [1] and [4]. Following the experimental procedure there outlined, the accuracy of the measurements in the present investigation may be estimated as within $\frac{1}{4}$ to $\frac{1}{6}$ of 1 per cent.

To simplify as far as possible the examination of the powder photographs only the K_α radiation of copper was used, the K_β radiation being absorbed by a thin nickel filter placed at the point of entry of the beam into the camera. One or two of the strong lines due to the K_β radiation could not be eliminated, though they were considerably reduced in intensity. Occasionally a line due to the L_α radiation of tungsten was also present on the film ; this happened after the tube had been used for some time, and was due to the slow deposition of tungsten on to the target as the filament slowly volatilized.

Results.

The X-ray data supplied by the films of copper, of alloys of A to I, and of antimony are given in Tables II. to XII. The first column in each case gives the radiation producing the reflexion, the values taken for the wavelength being :—

K_α (copper).	1·540 Å.U.
K_β ,,	1·389 Å.U.
L_α (tungsten).	1·484 Å.U.

The second column of the Tables gives the Miller indices of the reflecting planes, and the third column the intensities of the lines on the films. The symbol (St.) denotes strong ; M. (medium) ; W. (weak) ; and V.W. (very weak).

The plane spacings deduced from measurements on the films are tabulated in the fourth column, while the calculated spacings for the structure found are given in column

five. The composition, density, crystal structure, and the dimensions of the unit-cells for the nine alloys and for the two end elements copper and antimony are given in Table I.

Fig. 2 gives the crystal structure data found for the system.

The α Phase.

According to the equilibrium diagram (fig. 1) the α phase consists of a solid solution of antimony in copper up

Fig. 2.

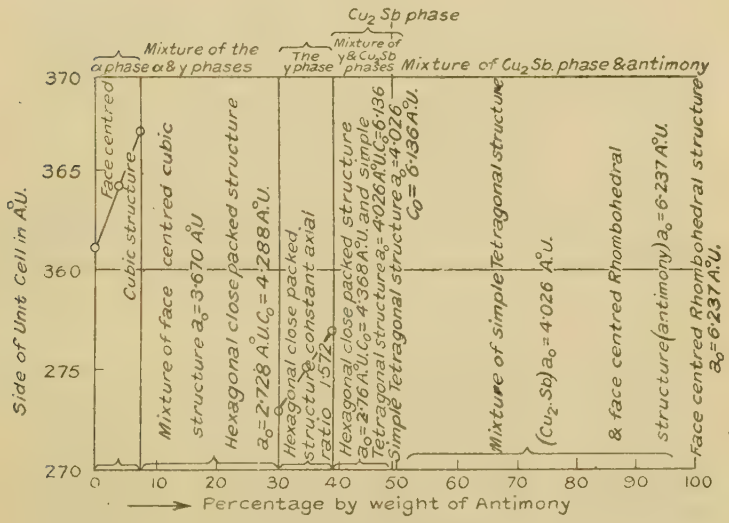

Crystal structure data for the Cu–Sb alloys.

to over 7 per cent. by weight of antimony. As the atomic diameters of copper and antimony are 2·54 Å.U. and 2·87 Å.U. respectively, a change in the lattice constant of copper would therefore be expected on the introduction of antimony, the solution of antimony causing an expansion of the copper lattice, but accompanied by no change in the type of lattice.

Table II. gives the data supplied by films for electrolytic copper. The films, as was to be expected, gave the well-known pattern of lines associated with the face-centred

cubic structure of copper. The side of the unit-cell deduced from these lines was $a_0 = 3{\cdot}610$ Å.U.—in agreement with the values obtained by other workers.

TABLE II.

Pure Copper.

Radiation.	Plane.	Intensity.	Observed d/n.	a_0.	Calculated d/n.
$K\beta$	111	W.	2·085 Å.U.	3·611 Å.U.	2·084 Å.U.
$K\alpha$	111	St.	2·084	3·610	2·084
$K\alpha$	100 (2)	St.	1·807	3·614	1·805
$K\alpha$	110 (2)	St.	1·275	3·610	1·275
$K\alpha$	311	St.	1·087	3·610	1·087
$K\alpha$	111 (2)	M.	1·041	3·606	1·042
$K\alpha$	100 (4)	M.	·902	3·608	·902
$K\alpha$	331	St.	·828	3·610	·828

Structure : face-centred cubic.
Dimensions of the unit-cell : $a_0 = 3{\cdot}610$ Å.U.

The crystal structure of the α phase was investigated by the aid of alloys A and B, and the data obtained from measurements on the films are given in Tables III. and IV.

TABLE III.

Alloy " A."—Composition 96 per cent. copper, 4 per cent. antimony. (The α phase.)

Radiation.	Plane.	Intensity.	Observed d/n.	Calculated d/n.
$L\alpha$ (tungsten)....	111	W.	2·102 Å.U.	2·104 Å.U.
$K\alpha$	111	St.	2·106	2·104
$K\alpha$	100 (2)	St.	1·827	1·822
$K\alpha$	110 (2)	St.	1·291	1·289
$K\alpha$	311	St.	1·097	1·099
$K\alpha$	111 (2)	M.	1·048	1·052

Structure : face-centred.
Dimensions of the unit-cell : $a_0 = 3{\cdot}644$ A.U.

It was found that alloy A (Table III.) produced lines on the film conforming to the face-centred cubic structure of copper, but there was a distinct displacement of the lines, indicating a definite increase in the size of the unit-cell, due to the antimony in solution. As there were no

other lines present on the films, it was evident that this alloy lay within the α phase. The 4 per cent. antimony in solution caused an expansion of the copper lattice from $a_0=3{\cdot}610$ Å.U. to $a_0=3{\cdot}644$ Å.U.

The films of alloy B, 80 per cent. copper, 20 per cent. antimony (Table IV.), on the other hand, contained lines of both the α and the γ phases, showing that the limit of solubility of antimony in copper is below this composition in antimony. The value of the lattice constant gives therefore the dimensions of the face-centred structure

TABLE IV.

Alloy "B."—Composition 80 per cent. copper, 20 per cent. antimony. (The Eutectic Mixture $\alpha+\gamma$.)

Radiation.	Plane.	Intensity.	Observed d/n.	Calculated d/n.
K_β	$10\bar{1}0$	W.	2·364 Å.U.	2·363 Å.U.
K_α	0002	M.	2·173	2·144
*K_α	111	St.	2·121	2·116
K_α	$10\bar{1}1$	St.	2·073	2·069
*K_α	100	M.	1·832	1·834
K_α	$10\bar{1}2$	M.	1·600	1·588
K_α	$11\bar{2}0$	W.	1·364	1·364
*K_α	110	M.	1·298	1·298
K_α	$10\bar{1}3$	M.	1·233	1·223
K_α	$20\bar{2}1$	M.	1·153	1·151
*K_α	311	W.	1·104	1·104
K_α	0004	W.	1·081	1·072

Mixture of face-centred cubic lattice of side $a_0=3{\cdot}670$ Å.U. and a hexagonal close-packed lattice of sides :—

$$a_0=2{\cdot}728 \text{ Å.U.}$$
$$c_0=4{\cdot}288 \text{ Å.U.},$$

corresponding to an axial ratio 1·572.

NOTE.—Lines of the face-centred cubic lattice of the α phase are marked with an asterisk (*).

at the limit of the α phase. This value was found to be 3·670 Å.U., showing a further expanison of the lattice from that of alloy A.

As stated above, the addition of 4 per cent. by weight of antimony to pure copper expands the unit-cell from $a_0=$ 3·610 Å.U. to 3·644 Å.U. If this increase follows a linear law with solution of antimony, as is the case with most solid solutions, then the side of the unit-cell increases by

·0085 Å.U. per 1 per cent. by weight of antimony. At the limit of solution the total expansion is from 3·610 Å.U. to 3·770 Å.U.—*i.e.*, ·06 Å.U. A simple calculation therefore fixes the boundary of the solid solution at 7 per cent. by weight of antimony. This agrees almost exactly with the result given by Carpenter, who stated that the upper limit of the α phase was slightly over 7 per cent. by weight of antimony.

The γ Phase.

According to the equilibrium diagram the γ phase is a homogeneous phase, extending between the compositions 30 per cent. and 39 per cent. by weight of antimony. The phase, however, does not exist at temperatures above 430° C., for, on heating the alloy above the segregation line in the diagram, a definite change has been found to take place and another phase β is formed. In Carpenter's diagram the boundary of the γ phase on the antimony side coincides with the composition Cu_3Sb.

In the examination of the crystal structure and character of the γ phase the five alloys B, C, D, E, and F were used ; of these the alloy B, as indicated by the diagram (fig. 1), was a composition in the eutectic mixture $\alpha+\gamma$; C, D, and E were compositions in the γ phase itself, E corresponding to the composition Cu_3Sb ; while F was a composition in the eutectic mixture $\gamma+Cu_2Sb$.

The films of alloy B contained lines of both the α and the γ phases. The crystal structure data for this alloy, obtained by an examination of the films, corresponded with the dimensions of the structures at the adjoining boundaries of the α and the γ phases. The lines corresponding with the γ phase in alloy B conformed to a crystal structure of the hexagonal close-packed class. The dimensions of the unit-cell are :—

$a_0=2·728$ Å.U. and $c_0=4·288$ Å.U., corresponding to an axial ratio 1·572 (Table IV.).

Lines corresponding to a hexagonal close-packed lattice only were present on the films of alloy C, the dimensions of the lattice (see Table V.) being the same as those obtained from the γ phase lines of alloy B. Starting from the copper end of the diagram, the γ phase can then be considered to commence near the composition 70 per cent. by weight of copper.

Table V.

Alloy "C."—Composition 70 per cent. copper, 30 per cent. antimony. (The γ Phase.)

Radiation.	Plane.	Intensity.	Observed d/n.	Calculated d/n.
K_β	$10\bar{1}0$	V.W.	2·361 Å.U.	2·363 Å.U.
K_α	$10\bar{1}0$	V.W.	2·375	2·363
K_α	0002	M.	2·170	2·144
K_α	1011	St.	2·076	2·069
K_α	$10\bar{1}2$	M.	1·600	1·588
K_α	$11\bar{2}0$	M.	1·364	1·364
K_α	$10\bar{1}3$	M.	1·232	1·223
K_α	$11\bar{2}2$	M.	1·153	1·151
K_α	$20\bar{2}1$	W.	1·149	1·139
K_α	0004	V.W.	1·080	1·072
K_α	$20\bar{2}2$	V.W.	1·035	1·035
K_α	$10\bar{1}4$	V.W.	·982	·976
K_α	$20\bar{2}3$	V.W.	·911	·911
K_α	$21\bar{3}1$	V.W.	·871	·874
K_α	$11\bar{2}4$	V.W.	·844	·844

Structure: close-packed hexagonal.
Dimensions of the unit-cell: $a_0 = 2·728$ Å.U.
$c_0 = 4·288$ Å.U.,
corresponding to an axial ratio 1·572.

Table VI.

Alloy "D."—Composition 65 per cent. copper, 35 per cent. Antimony. (The γ Phase.)

Radiation.	Plane.	Intensity.	Observed d/n.	Calculated d/n.
K_β	$10\bar{1}0$	W.	2·364 Å.U.	2·383 Å.U.
K_α	0002	M.	2·185	2·163
K_α	$10\bar{1}1$	St.	2·093	2·088
K_α	$10\bar{1}2$	W.	1·610	1·602
K_α	$11\bar{2}0$	M.	1·376	1·376
K_α	$10\bar{1}3$	M.	1·239	1·231
K_α	$11\bar{2}2$	M.	1·161	1·161
K_α	$20\bar{2}1$	W.	1·147	1·149
K_α	$20\bar{2}2$	V.W.	1·045	1·044
K_α	$20\bar{2}3$	V.W.	·917	·918
K_α	$21\bar{3}1$	V.W.	·878	·882
K_α	$11\bar{2}4$	V.W.	·850	·851

Structure: hexagonal close-packed.
Dimensions of the unit-cell: $a_0 = 2·752$ Å.U.
$c_0 = 4·326$ Å.U.,
corresponding to an axial ratio 1·572.

Only lines of the γ phase were present, also on the films of alloy E. The data for this alloy are given in Table VII. The plane spacings derived from these lines again satisfied a hexagonal close-packed arrangement ; but, in this case, the sides calculated for the unit cell are :—

$$a_0 = 2{\cdot}766 \text{ Å.U. and } c_0 = 4{\cdot}348 \text{ Å.U.},$$

TABLE VII.

Alloy " E " (Cu_3Sb).—Composition 61 per cent. Cu, 39 per cent. Sb. (The γ phase.)

Radiation.	Plane.	Intensity.	Observed d/n.	Calculated d/n.
K_α	$10\bar{1}0$	M.	2·400 Å.U.	2·395 Å.U.
K_α	0002	M.	2·181	2·177
K_α	$10\bar{1}1$	St.	2·096	2·098
K_α	$10\bar{1}2$	M.	1·610	1·610
K_α	$11\bar{2}0$	M.	1·382	1·383
K_α	$10\bar{1}3$	M.	1·240	1·240
K_α	$20\bar{2}0$	W.	1·195	1·197
K_α	$11\bar{2}2$	M.	1·167	1·167
K_α	$20\bar{2}1$	W.	1·149	1·154
K_α	0004	V.W.	1·088	1·088
K_α	$20\bar{2}2$	V.W.	1·043	1·049
K_α	$10\bar{1}4$	V.W.	·989	·990
K_α	$20\bar{2}3$	W.	·920	·923
K_α	$21\bar{3}1$	W.	·882	·886
K_α	$11\bar{2}4$	V.W.	·853	·856
K_α	$21\bar{3}2$	V.W.	·832	·836
K_α	$10\bar{1}5$	V.W.	·817	·817

Structure : hexagonal close-packed.
Dimensions of the unit cell : $a_0 = 2{\cdot}766$ Å.U.
$c_0 = 4{\cdot}348$ Å.U.,
corresponding to an axial ratio 1·572.

corresponding to an axial ratio 1·572, showing an expansion of the lattice with increase of antimony content. Alloy E, as already pointed out, corresponds to the composition Cu_3Sb, and a more detailed account of it will be given at a later stage. The films of alloy F contained a mixture of lines due to the γ phase and to the alloy Cu_2Sb. Table VIII. gives the data for this alloy. The lines of the γ phase conformed to a hexagonal close-packed structure—the dimensions of the

Table VIII.

Alloy " F."—Composition 55 per cent. copper, 45 per cent. antimony. (Eutectic mixture $\gamma + Cu_2Sb$.)

Radiation.	Plane.	Intensity.	Observed d/n.	Calculated d/n.
K_α	101	V.W.	3·382 Å.U.	3·369 Å.U.
K_α	001 (2)	V.W.	3·058	3·070
K_β	111	V.W.	2·612	2·584
K_α	110	V.W.	2·831	2·849
L_α (tungsten)	111	M.	2·596	2·584
*K_β	$10\bar{1}0$	M.	2·357	2·395
K_α	111	W.	2·568	2·584
*K_α	0002	V.W.	2·193	2·177
*K_α	$10\bar{1}1$	W.	2·104	2·098
K_α'	112	M.	2·088	2·088
K_α	001 (3)	V.W.	2·045	2·046
K_α	100 (2)	M.	2·016	2·015
L_α (tungsten)	201	V.W.	1·903	1·914
K_α	201	M.	1·879	1·914
K_α	103	V.W.	1·836	1·825
K_α	121	V.W.	1·727	1·729
K_α	101 (2)	V.W.	1·682	1·684
*K_α	$10\bar{1}2$	V.W.	1·614	1·610
K_α	001 (4)	W.	1·537	1·535
K_α	203	V.W.	1·444	1·436
K_α	104	W.	1·431	1·434
*K_α	$11\bar{2}0$	V.W.	1·383	1·383
K_α	100 (3)	V.W.	1·338	1·343
K_α	112 (2)	V.W.	1·289	1·292
K_α	130	V.W.	1·270	1·274
K_α	131	W.	1·246	1·247
K_α	102 (2)	V.W.	1·219	1·221
*K_α	$20\bar{2}0$	W.	1·197	1·197
K_α	105	W.	1·173	1·175
*K_α	$11\bar{2}2$	W.	1·166	1·167
K_α	115	W.	1·125	1·129
*K_α	$20\bar{2}2$	V.W.	1·044	1·049
K_α	112 (2)	V.W.	1·039	1·044
K_α	100 (4)	V.W.	1·004	1·007

Mixture of a hexagonal close-packed lattice of dimensions :
$a_0 = 2·766$ Å.U.
$c_0 = 4·348$ Å.U.
} axial ratio 1·572 and a simple tetragonal lattice of dimensions :—

$a_0 = 4·029$ Å.U.
$c_0 = 6·140$ Å.U.
} corresponding to axial ratio 1·524.

unit-cell being in exact agreement with those obtained from alloy E. As the dimensions of the unit-cell calculated from the films of alloy F, which exists in the eutectic mixture $\gamma + Cu_2Sb$, are identical with those obtained from films of alloy E (composition Cu_3Sb), which contains lines of the γ phase only, it follows that the boundary of the γ phase on the antimony side of the diagram is near the composition Cu_3Sb. This statement confirms the result of Carpenter.

To complete the examination of the γ phase it was considered that information should be obtained from the films of an alloy existing well inside the phase. Such an alloy was alloy D, of composition 35 per cent. by weight of antimony. A hexagonal close-packed lattice was found to be the arrangement for this alloy also, the dimensions of the unit-cell being $a_0 = 2{\cdot}752$ Å.U. and $c_0 = 4{\cdot}326$ Å.U., corresponding to an axial ratio 1·572. As was expected, this unit-cell is intermediate in size between the unit-cells for alloys C and E.

The results obtained from the films of alloys B, C, D, E, and F all point to the fact that the γ phase is a region of solid solution, crystallizing in a close-packed hexagonal structure, the dimensions of the unit cell increasing from

$$\left.\begin{aligned} a_0 &= 2{\cdot}728 \text{ Å.U.} \\ c_0 &= 4{\cdot}288 \text{ Å.U.} \end{aligned}\right\} \text{ to } \left\{\begin{aligned} a_0 &= 2{\cdot}766 \text{ Å.U.} \\ c_0 &= 4{\cdot}348 \text{ Å.U.} \end{aligned}\right.$$

with increase of antimony content. For all these alloys the axial ratio remained constant at 1·572. This result is of interest, as it shows that the hexagonal cell, like a cubic cell, expands proportionally in all directions when a solid solution is formed having this structure. If, as shown in fig. 2, the expansion of the hexagonal lattice of the γ phase follows a linear relationship with composition of antimony, and if one boundary of the γ phase is fixed at the Cu_3Sb composition, a simple calculation gives the other boundary to be at the composition 71 per cent. by weight of copper. On the other hand, by using the films of alloys B and C this boundary was found to be near 70 per cent. by weight of copper.

These results indicate that the boundary of the γ phase on the copper side is somewhere in the region of 70 per cent. by weight of copper, and on the antimony side at the composition Cu_3Sb (*i. e.*, 39 per cent. by weight of

antimony). These are also the limits of the phase found by Carpenter.

The crystal structure and lattice dimensions of the alloy Cu_3Sb had already been determined by Morris-Jones and Evans [1], who assigned to it a hexagonal close-packed lattice, the dimensions of the unit-cell being $a_0 = 2{\cdot}777$ Å.U., and the axial ratio 1·572. From consideration of these values and of the density of the alloy they found that half a molecule of Cu_3Sb was associated with the cell. Many films of long exposures were taken to see whether the above unit was a sub-unit of a larger cell, but they did not detect the presence of any additional lines which would suggest such a cell. Proceeding then as if the alloy Cu_3Sb was a composition in a region of solid solution Morris-Jones and Evans placed two mean atoms of mass $\frac{1}{4}$ of that of the Cu_3Sb molecule at the coordinates (000) and $(\frac{1}{3}, \frac{2}{3}, \frac{1}{2})$. This procedure enabled them to calculate the intensities of the lines on the films, and they found that the calculated intensities agreed very well with the observed intensities. As a result of their work Morris-Jones and Evans intimated that Cu_3Sb may not be a true compound, but an alloy in a range of solid solution.

In the present investigations the observations from the films of Cu_3Sb corroborated the work of Morris-Jones and Evans. The plane spacings calculated from the films of alloy E and given in Table VII. satisfied a close-packed hexagonal unit-cell, the dimensions being $a_0 = 2{\cdot}766$ Å.U., and the axial ratio 1·572, agreeing to $\frac{1}{3}$ of 1 per cent. with the results of these workers.

If two mean atoms were placed at the coordinates given by these investigators the shortest inter-atomic distance was 2·700 Å.U., agreeing very well with 2·705 Å.U., the mean diameter of the copper and antimony atoms. There were no lines on any of the films which did not satisfy a hexagonal structure or would suggest a bigger cell.

In the present investigation no crystal structure data were discovered to indicate the existence of a definite compound at the composition Cu_3Sb. It appears that the alloy Cu_3Sb is just a composition in the range of solid solution γ, which extends from 30 to 39 per cent. by weight of antimony. The boundary of the γ phase on the antimony side happens to coincide with the composition Cu_3Sb, and the limit of the expansion of the hexagonal

lattice is at this composition. The work of Morris-Jones and Evans [1], which has been confirmed, is therefore explained.

TABLE IX.

Alloy "G."—Composition 51 per cent. copper, 49 per cent. antimony. (The Cu_2Sb Phase.)

Radiation.	Plane.	Intensity.	Observed d/n.	Calculated d/n.
K_α	101	V.W.	3·382 Å.U.	3·369 Å.U.
K_β	001 (2)	V.W.	3·071	3·070
K_α	111	V.W.	2·609	2·584
K_α	110	W.	2·854	2·849
L_α (tungsten)	102	V.W	2·418	2·442
K_α	111	W.	2·584	2·584
K_α	102	V.W.	2·435	2·442
K_α	112	St.	2·088	2·088
K_α	001 (3)	V.W.	2·048	2·046
K_α	100 (2)	M.	2·016	2·015
K_α	201	W.	1·879	1·914
K_α	103	V.W.	1·836	1·825
K_α	121	V.W.	1·729	1·729
K_α	101 (2)	V.W.	1·684	1·684
K_α	001 (4)	V.W.	1·537	1·535
K_α	203	V.W.	1·444	1·436
K_α	104	M.	1·433	1·434
K_α	110 (2)	M.	1·424	1·424
K_α	100 (3)	V.W.	1·338	1·343
K_α	111 (2)	V.W.	1·289	1·292
K_β	102 (2)	V.W.	1·219	1·221
K_α	130	V.W.	1·271	1·274
K_α	131	W.	1·246	1·247
K_α	102 (2)	W.	1·218	1·221
K_α	105	M.	1·174	1·175
K_α	115	M.	1·124	1·127
K_α	112 (2)	V.W.	1·041	1·044
K_α	100 (4)	V.W.	1·004	1·007
K_α	120 (2)	V.W.	·897	·901

Structure : simple tetragonal.
Dimensions of the unit-cell : $a_0 = 4·029$ Å.U.
$c_0 = 6·140$ Å.U.
corresponding to an axial ratio 1·524.
Two molecules of Cu_2Sb to the unit-cell.

It may also be pointed out that the resistivity curve of Stephens and Evans [5] for the copper-antimony alloys shows only a slight increase in resistivity over the range

30 to 40 per cent. by weight of antimony corresponding to the γ phase.

The Cu_2Sb *Phase.*

The alloy Cu_2Sb has a characteristic purple-lilac colour and is extremely brittle. Its metallurgical and physical properties all point to the fact that it is a definite compound, existing at the composition represented by the formula.

TABLE X.

Alloy "H."—Composition 30 per cent. copper, 70 per cent. antimony. (Eutectic mixture Cu_2Sb and Sb.)

Radiation.	Plane.	Intensity.	Observed d/n.	Calculated d/n.
K_α	100 (2)	M.	3·110 Å.U.	3·111 Å.U.
*K_α	110	W.	2·822	2·843
*K_α	111 ⎫ 211 ⎭	M.	2·609	2·579 ⎫ 2·637 ⎭
K_α	110 (2)	W.	2·252	2·250
K_α	221	W.	2·155	2·159
*K_α	112	M.	2·086	2·084
*K_α	001 (3)	V.W.	2·032	2·042
*K_α	100 (2)	W.	2·008	2·010
K_α	112	V.W.	1·874	1·880
K_α	320	V.W.	1·777	1·755
*K_α	121	V.W.	1·720	1·725
K_α	100 (4)	V.W.	1·554	1·555
*K_α	110 (2)	V.W.	1·424	1·422
K_α	210 (2)	V.W.	1·418	1·416
K_α	332	V.W.	1·369	1·385

Mixture of a simple tetragonal lattice of dimensions : a_0=4·020 Å.U. c_0=6·126 Å.U. corresponding to an axial ratio 1·524, and a face-centred rhombohedral lattice of antimony a_0=6·235 Å.U. and angle 87° 24′.

NOTE.—The lines of the simple tetragonal lattice of Cu_2Sb are denoted by an asterisk (*).

In the course of the present work X-ray photographs were taken of this phase (i.) to establish its crystal structure, and (ii.) to discover whether a region of solid solution exists on either side of the Cu_2Sb composition.

The crystal structure of the phase was deduced from the measurements of the films of the alloys F, G, H, and I, and

the X-ray data for these alloys are recorded in Tables VIII., IX., X., and XI. The composition of alloy C corresponds to the pure compound. These films showed that Cu_2Sb crystallizes in a simple tetragonal arrangement, the dimensions of the unit-cell being constant within the range of accuracy claimed for the measurements. This

TABLE XI.

Alloy " I."—Composition 20 per cent. copper, 80 per cent. antimony. (Eutectic mixture $Cu_2Sb + Sb$)

Radiation.	Plane.	Intensity.	Observed d/n.	Calculated d/n.
K_α	100 (2)	M.	3·113 Å.U.	3·114 Å.U.
*K_α	111 211	V.W.	2·607	2·581 2·639
K_α	110 (2)	W.	2·255	2·251
K_α	221	W.	2·158	2·161
*K_α	112	W.	2·086	2·086
*K_α	001 (3)	V.W.	2·044	2·044
*K_α	100 (2)	V.W.	2·011	2·012
K_α	111 (2)	W.	1·883	1·882
K_α	320	W.	1·772	1·763
K_α	100 (4)	V.W.	1·558	1·557
K_α	210 (2)	W.	1·418	1·418
*K_α	110(2)			1·422
K_α	332	W.	1·370	1·386
K_α	431	V.W.	1·262	1·262
K_α	100 (5)	V.W.	1·244	1·245
*K_α	131			1·246

Mixture of a simple tetragonal lattice of dimensions :—
$a_0 = 4{\cdot}024$ Å.U. } corresponding to an axial ratio of 1·524, and a face-
$c_0 = 6{\cdot}133$ Å.U. } centred rhombohedral lattice of dimensions $a_0 = 6{\cdot}240$ Å.U. and angle 87° 24′.

NOTE.—The lines of he simple tetragonal lattice of Cu_2Sb are denoted by an asterisk (*).

structure accounted for all the reflexions produced by the crystal planes. The dimensions of the unit-cell deduced from the films of the alloys of F, G, H, and I, are :—

F. $a_0 = 4{\cdot}029$ A.U., $c_0 = 6{\cdot}140$ A.U.
G. $a_0 = 4{\cdot}029$ Å.U., $c_0 = 6{\cdot}140$ Å.U.
H. $a_0 = 4{\cdot}024$ Å.U., $c_0 = 6{\cdot}133$ Å.U.
I. $a_0 = 4{\cdot}020$ Å.U., $c_0 = 6{\cdot}126$ Å.U.

corresponding to an unvarying axial ratio $c = 1{\cdot}524$.

The maximum fluctuation in the values of the lattice constants is within the range of experimental error, being less than $\frac{1}{4}$ of 1 per cent. This close agreement between the values of the lattice from the four alloys, which include the actual compound and compositions on either side of it, shows that the lattice structure is of unvarying dimensions. Cu_2Sb has therefore a unique structure, and the constancy of the unit-cell obtained from the alloys F, G, H, and I shows that neither copper nor antimony is soluble in it.

The mean values taken for the sides of the fundamental cell are

$$a_0 = 4{\cdot}026 \text{ Å.U.}$$
$$c_0 = 6{\cdot}136 \text{ Å.U.}$$

corresponding to an axial ratio $c = 1{\cdot}572$.

The reflexions from the tetragonal faces, combined with the density of the compound, *i. e.*, 8·42 gms. per c.c., showed that two Cu_2Sb molecules are associated with the unit-cell. The Laue symmetry for Cu_2Sb was not determined, as we failed to obtain an isolated crystal of any size. However, the powder photograph shows that the unit-cell is obviously simple tetragonal, and the body-centre space-groups are thus excluded. To determine the space-group and atomic arrangement further measurements with single crystals are needed. The crystal structure and size of unit-cell determined in the present investigation were quoted by Stephens [6] in a paper dated April 1929.

Antimony.

Carpenter, in his investigation of the antimony end of the diagram found that an alloy containing 0·98 of an atom per cent. of copper was inhomogeneous even after prolonged annealing, being an eutectic mixture of Cu_2Sb and antimony crystals. From a study of this alloy Carpenter states that the solubility of copper in antimony does not exceed one atom per cent., and he has drawn the solubility line at this composition, which is 0·5 per cent. by weight of copper. This phase of solution Carpenter called the " ε " phase.

A solution of 0·5 per cent. of copper in antimony should produce a slight but measurable change in the dimensions of the antimony cell—the change to be expected in this case being a contraction due to the smaller copper atom.

The antimony end of the diagram was therefore examined by taking photographs of pure antimony and of the alloys H and I (composition 70 per cent. and 80 per cent. by weight of antimony), to see whether any contraction took place. The data obtained from these films are given in Tables X., XI., and XII.

The crystal structure of pure antimony has already been determined by James and Tunstall [7], and Ogg [8] by spectrometer methods. In each case, the element was found to have a face-centred rhombohedral structure of

TABLE XII.

Pure Antimony.

Radiation.	Plane.	Intensity.	Observed d/n.	Calculated d/n.
K_α	100 (2)	St.	3·110 Å.U.	3·111 Å.U.
K_α	211	M.	2·634	2·637
K_α	110 (2)	M.	2·252	2·250
K_α	221	M.	2·155	2·159
K_α	111	W.	1·881	1·880
K_α	320	M.	1·776	1·755
K_α	100 (4)	W.	1·554	1·555
K_α	210 (2)	W.	1·418	1·416
K_α	332	W.	1·369	1·385
K_α	431	W.	1·263	1·261
K_α	100 (5)	V.W.	1·246	1·245
K_α	432	V.W.	1·195	1·203

Structure: Face-centred Rhombohedral.
Dimensions of the Unit Cell:—a_0=6·235 Å.U.
Angle of the Rhombohedron=87° 24′.

side a_0=6·200 Å.U., the angle between the sides being 86° 58′.

The only powder method of analysis for antimony is that of Persson and Westgren [9]; they recently found the same structure, but in this case the side was 6·226 Å.U. and the angle 87° 24′.

The present investigation corroborated the face-centred rhombohedral structure of these workers, the side of the unit-cell being A_0=6·235 Å.U. and the angle of the structure 87° 24′ (Table XII.). This result agrees to within $\frac{1}{7}$th of 1 per cent. with that of Persson and Westgren, and the value of the angle is identical.

The films of alloys H and I contain lines satisfying both the simple tetragonal structure of Cu_2Sb and a face-centred rhombohedral structure. As would be expected, the intensity of the two sets of lines on these films varied with the composition of the alloy, the Cu_2Sb lines being more intense for alloy H than for alloy "I," while the antimony lines were less intense.

For alloys H and I the sides of the rhombohedron are respectively 6·235 Å.U. and 6·240 Å.U., the angle being constant at 87° 24′ (Tables X. and XI.). The unit-cell of alloy H is identical in dimensions with that of pure antimony, whereas that of alloy "I" agrees to less than $\frac{1}{10}$th of 1 per cent. The slight deviation in the side of this cell for alloy "I" is a very small expansion, which comes within the range of error of the measurements. These results, therefore, show no measurable contraction in the volume of the antimony cell. The X-ray investigation of the antimony end of the diagram gives therefore no evidence of the existence of the region of solution "ε," but indicates that the compound Cu_2Sb forms an eutectic mixture with antimony.

Having determined the crystal structure of the phases of the copper-antimony system, stable at normal temperatures, it would be of interest at this juncture to examine the evolution of the crystal structures as we proceed along the equilibrium diagram (fig. 1).

Starting from the copper end of the diagram, on adding up to 7 per cent. by weight of antimony the copper cell expands from 3·610 Å.U. to 3·670 Å.U. without departing from its face-centred cubic structure, this region being a range of solid solution of antimony in copper. As the antimony content increases from 7 per cent. to 30 per cent. by weight (*i. e.*, the eutectic range $\alpha+\gamma$), the face-centred cubic close-packing gradually transforms into the next simplest arrangement—hexagonal close-packing—until, at 30 per cent. by weight of antimony, the whole structure of the alloy is close-packed hexagonal.

At this point the γ phase begins. If the addition of antimony is continued, the unit-cell of this hexagonal structure in turn expands, and the copper-antimony solid solution γ, having this crystal structure, exists up to the limit of the expansion at the composition Cu_3Sb.

If further antimony is added (the eutectic range $\gamma+$

Cu_2Sb) a definite compound Cu_2Sb is formed, having a characteristic tetragonal lattice. As the dimensions of the tetragonal cell remain constant, Cu_2Sb does not form any solid solution with either of the end elements—copper and antimony. From the composition Cu_2Sb to 100 per cent. antimony we have, as the X-ray investigation shows, a mixture of the simple tetragonal lattice of Cu_2Sb and the face-centred rhombohedral lattice of antimony.

The β Phase.

To complete the examination of the system an attempt was made to determine the crystal structure of the β phase, which exists at temperatures above 430° C. To obtain a β-phase alloy a composition within the β phase was maintained at a temperature well over 500° C. for some time, and then quenched. Carpenter experienced great difficulty in obtaining quenched specimens of the β phase for microscopic examination, as the alloy almost always cracked or pulverized. This, however, was an advantage in the present case for the obtaining of powdered photographs.

Although a long exposure was given to the photograph the films obtained for the alloy contained only a few weak lines which were also to be found on the films of the γ phase. The number of lines was not sufficient to draw any conclusions as to the crystal structure of the β phase. However, according to Carpenter, the basis of the β phase is Cu_3Sb, and this alloy has been found in the present investigation to possess a hexagonal structure.

Summary.

An X-ray investigation of the crystal structure of the copper-antimony alloys has been carried out, and the results discussed with respect to the equilibrium diagram of the system.

Nine alloys were prepared, and their composition and densities were determined. X-ray powder photographs were taken, and the crystal structures of the alloys studied.

The α-phase alloys were found to possess a face-centred cubic structure, the dimensions of the elementary cell varying from 3·610 Å.U. to 3·670 Å.U. at the limit of

solution of antimony in copper. This limit was fixed at 7 per cent. by weight of antimony.

The γ phase had a close-packed hexagonal structure, the unit-cell expanding from $a_0 = 2{\cdot}728$ Å.U. to $a_0 = 2{\cdot}766$ Å.U. with increase of antimony content, while the axial ratio for the cells remained constant at 1·572. The γ phase extended from 70 per cent. by weight of copper to the composition Cu_3Sb, *i. e.*, 61 per cent. by weight of copper. The work of Morris-Jones and Evans on the crystal structure of Cu_3Sb was confirmed, no evidence being found for the existence of the larger cell required if the alloy was a chemical compound. The γ phase is a region of solid solution. The structure of the alloys within the eutectic range $\alpha + \gamma$ on the diagram was a mixture of the face-centred cubic and the hexagonal lattice of the α and γ phases.

The Cu_2Sb phase possessed a tetragonal crystal structure, the unit-cell being of unvarying dimensions. The cell contains two molecules of Cu_2Sb, with $a_0 = 4{\cdot}026$ Å.U. and axial ratio 1·524. The structure of the alloys in the range $\gamma + Cu_2Sb$ on the diagram consisted of a mixture of the lattices of these two phases.

No trace of the solid solution phase "ε" could be detected at the antimony end of the diagram. The crystal structure of the alloys of composition from Cu_2Sb to antimony was a mixture, in varying proportions, of the tetragonal structure of Cu_2Sb and the face-centred rhombohedral structure of antimony. The dimensions of the unit-cell of the rhombohedral lattice of antimony were found to be $a_0 = 6{\cdot}235$ Å.U., and the angle of the structure 87° 24′.

Owing to the small number of lines on the films of the β phase alloy, no conclusions could be drawn as to the structure of this phase.

Omitting the "ε" phase, Carpenter's equilibrium diagram has been verified for those constituents stable at normal temperatures, and the crystal structures of the alloys, extending over the whole range of composition, have been determined.

In conclusion, we are under obligation to Professor E. J. Evans for facilities for carrying out this investigation, and for his interest during its progress.

References.

(1) Morris-Jones and Evans, Phil. Mag. iv. p. 1302 (Dec. 1927).
(2) Carpenter, H. C., *Zeit. für Metallkunde*, iv. p. 300 (1913).
(3) Guertler, *Zeit. Anorg. Chem. SI.* p. 418 (1906).
(4) Grime and Morris-Jones, Phil. Mag. vii. p. 1113 (June 1929).
(5) Stephens and Evans, Phil. Mag. viii. no. 48 (July 1929).
(6) Stephens, Phil. Mag. viii. no. 50, p. 286 (September 1929).
(7) James and Tunstall, Phil. Mag. xl. p. 233 (August 1920).
(8) Ogg, Phil. Mag. xlii. p. 163 (1921).
(9) Persson and Westgren, *Zeit. für Phys. Chem.* cxxxvi. p. 208 (September 1928).

January 1930.

XCI. *A Method of Investigating the Higher Atmosphere.* *By* E. H. Synge *.

REGULAR balloon observations of the upper atmosphere, as may be seen from the tables in any book on meteorology, do not extend beyond 20 km., at which height the density is from $\frac{1}{12}$ to $\frac{1}{14}$ that at sea-level. The density is falling rapidly at this point, and it is improbable that balloon observations could be carried to a much greater altitude. They must certainly fail long before that interesting region is attained, at about 50 km., where the density is about $\frac{1}{1000}$ that at sea-level and the pressure similar to that at which electrical discharge in vacuum tubes takes place most readily. It is quite probable that the ionization of the lower atmosphere may be controlled by conditions here, so that a means of recording variations in the atmosphere at these altitudes might be of considerable importance to meteorologists. So far as the writer is aware the only method suggested for obtaining records at such altitudes has been that of sending up powerful rockets, loaded with apparatus, which, after recording the conditions at the height reached, would descend to the earth by means of parachutes †. The difficulties of this method are numerous and obvious, and it does not seem that any attempt has been made to obtain records in this way. The following method, on quite different lines, is, however,

* Communicated by the Author.

† R. H. Goddard, "A Method of Reaching Extreme Altitudes," Smithsonian Misc. Collections, vol. lxxi. no. 2 (1921).

available to determine certain properties and variations of the upper atmosphere, as far as a density from $\frac{1}{1000}$ to $\frac{1}{10,000}$ that at sea-level. Nearly all the apparatus required exists in sufficient quantity; there are no formidable technical difficulties to be surmounted; and the theory appears quite unassailable.

The method depends on the scattering of light by the molecules of a gas; for a gas of constant composition this scattering is proportional, to a high approximation, to the density of the gas, and inversely proportional to the fourth power of the wave-length of the light. Thus, supposing the composition of the atmosphere to be unchanged at the heights investigated, its density at these heights will be known, after making various corrections, if we can project a sufficiently strong beam of light to allow of the light scattered in a given region being detected and measured by photo-electric apparatus after collection by a large reflector.

The sky of night is, of course, by no means perfectly dark, and even if we select the darkest part of the sky on a clear moonless night as a background, the light scattered by the beam of a single searchlight at any considerable height will be quite imperceptible to the eye. For instance; taking figures for the searchlight from Glazebrook's 'Dictionary of Applied Physics'; for the molecular scattering from Schuster and Nicholson's 'Optics'; and for the sky from Russell, Dugan, and Stewart's 'Astronomy,' it appears that, at a height of 30 km., where we may suppose the density to be about $\frac{1}{50}$ that at sea-level, the light scattered from the beam of a 36-inch searchlight, with the most powerful arc, will only add about 1 part in 200 to the brightness of the darkest part of the sky. This proportion, although perfectly imperceptible to the eye, can be detected by photo-electric apparatus, which is sensitive to a difference of 1 part in 1000.

This is the case of a single searchlight, but the method involves the concentration of a large number of searchlights upon the same region in the upper atmosphere. The effect is additive. In the case considered, if a single searchlight enables a reading to be made with a probable error of 10 per cent., then ten searchlights will reduce the probable error to about 1 per cent. This leaves out of account various important considerations—for instance, the steadiness of the arcs and the absorption of the light by

the atmosphere in its double journey, first from the searchlights to the region of the upper atmosphere under investigation, and afterwards from this region to the collecting reflector. The latter effect, which differs for various wave-lengths, will usually be much more complicated if the emitting and receiving stations are at a low altitude. A table in Schuster and Nicholson's 'Optics,' 3rd ed. p. 321, makes this very evident. Figures are given which compare the observed mean, the observed clear-day readings, and the theoretical molecular scattering for Washington and Mount Wilson. The variation of the clear-day observations from the mean is about four times as great at the lower station as at Mount Wilson. At both stations clear-day observations differ very little from the calculated values for the short wave-lengths, which produce far the greatest effect on the photo-electric cell, so that even at a low altitude observations of this sort would require trifling corrections only, for atmospheric variations on clear days.

With regard to the steadiness of the arc, the high intensity Sperry arc is only moderately steady. Its intensity, however, appears to be a function of the current passing through the arc *, and if this is known for the moment of observation the correction could be made at once. When a number of searchlights are employed together the irregularities would tend to neutralize one another, and this, the more effectively, the more numerous were the searchlights. Probably the total current used per second with a large assemblage of searchlights would hardly vary at all, and the amount of any small variation would indicate the necessary correction with sufficient accuracy.

Some remarks are necessary as to the collecting reflector and the design of photo-electric cell required. A parabolic mirror about 1 metre in diameter would seem well suited to the case, but it should be made with considerably greater care than an ordinary searchlight reflector, in which errors amounting to a divergence of 1° beyond theory are usual †. The error here should not exceed a few minutes of arc, and the mirror should be silvered on the face, as the dispersion of the glass and irregularities of two surfaces instead of one are no doubt responsible for the large error in the ordinary

* "Colour and Spectral Composition of certain High-Intensity Searchlight Arcs," Bur. Stand. Tech. Pap. no. 168 (1920).

† Glazebrook's 'Applied Physics,' vol. iv. pp. 521, 522.

reflector. A focal length of about 1 metre would be suitable. With such a reflector a photo-electric cell-window of a little less than 2 cm. in diameter placed at the focus would admit light from a circle of the sky about 1° in diameter. In the approximate result given for a height of 30 km. it was supposed that the beam of the searchlight made an angle of about 60° with the horizontal, and that the axis of the receiving reflector made a similar angle with the horizontal. We can give an approximate figure for the amount of light entering the cell under these circumstances. No unit of photo-electric activity seems to be in use, but the photo-electric effectiveness depends so largely on the wave-length, blue light being more than 30 times as effective as yellow light for a potassium cell *, that it is pointless to give a value for the light in ergs without specifying the wave-length. But making the necessary calculations, it appears that the light entering the cell from a single searchlight in the given circumstances may be taken as approximately equivalent in photo-electric activity to 10^{-5} or $1{\cdot}5 \times 10^{-5}$ ergs of yellow light per second. The light from the night sky, which comes jointly from a faint zodiacal light spread over the whole sky, although strongest near the ecliptic; from a permanent auroral effect; from the stars, which contribute about a sixth part of the whole; and, finally, from the light scattered in the atmosphere by all these, may probably be taken as about the same in composition (practically speaking, in blueness), as the light scattered from the searchlight, and we may set it as photo-electrically equivalent to 2×10^{-3} or 3×10^{-3} ergs of yellow light per second entering the cell. These amounts are quite sufficient in themselves to allow of an accuracy to the degree mentioned. The light, however, which passes through the window diverges at an angle of 60°, and as the photo-electric surface is not sensitive to yellow light beyond 10^{-7} erg per sq. cm. per sec. the cell must be rather flatter than is usual. If the sensitive surface is 2 cm. distant from the cell-window, the concentration would be sufficient. By making the reflector larger, and the window proportionately larger, the depth of the cell can be increased in the same proportion, and the total current will be increased in the square of this proportion.

* H. S. Allen, 'Photoelectricity,' p. 273.

A cell with so large a window is not suited for giving direct readings to the degree of accuracy aimed at, but the method of a substituted beam, on a similar principle to that outlined by the authors of 'Photographic Photometry' (Oxford University Press), seems adequate to ensure the required accuracy.

The question of a substituted equivalent beam appears essential to the method, and as it presents various difficulties it may be discussed here. The principle is very simple. The searchlight or searchlights are simultaneously occulted, and at the same time an equivalent light whose strength is known enters the cell. When this light is exactly equivalent in its effect to the light collected from the searchlight, the needle of the galvanometer will remain steady. And thus the strength of the light coming from the searchlight can be calculated from the strength of the known light, which is regulated by crossed optical wedges.

For accurate results, however, the lights should be exactly equivalent. They should have the same composition and strike the cell at the same angles. It is this which presents difficulties here, since the composition of the light from the searchlights as it reaches the receiving mirror varies according to the conditions of the atmosphere.

The most simple plan for meeting the difficulty might be the following:—A frame carrying some narrow strips of aluminium ribbon, painted white on the side facing the mirror and black on the other side, is suspended between the sky and the reflector. A beam is made up with a composition approximately the same as that reaching the reflector from the searchlight under the actual conditions. This beam is divided by mirrors, and the divided parts are each passed along the aluminium strips, with which they make small angles. A proportion of the light diffused from the strips strikes the mirror at the proper angles to bring it into the cell. The strength of the beam, before division, is regulated by passage through crossed optical wedges, and the effect on the photo-electric cell can be made approximately identical with the effect of the searchlights. The composition of the equivalent beam with the proper proportions of the various wave-lengths does not present any great difficulty. The source of light can be a standard incandescent wire. A spectrum of this is formed by a prism, and there is an arrangement of narrow shutters or flat pins which can be pushed down in the focal plane of

the spectrum, so as to cut off the desired portions of various wave-lengths; the beam is then reconstituted by reverse passage through a prism, passes through the optical wedges, is divided as described, and switched on at the same instant as the searchlights are occulted. The energy value and photo-electric value of different portions of the spectrum of the wire being supposed known, tables could be made out showing the proper amounts of each wave-length to be cut out for different conditions of the atmosphere, and the latter can be determined by observation on certain bright standard stars. The corrections would be much more complicated for a low-altitude station than for Mount Wilson, but they would not be so difficult as they appear at first sight. In practice they would take on a routine character. One would not, of course, determine the absolute density of the atmosphere directly in this way. To do this, one could compare the effect at the height under investigation with that at a height within the range of balloon observation. But we are far less concerned with the absolute density of the atmosphere at any height than with its variation from day to day, and the method suggested gives us the means of ascertaining this with great simplicity, to the degree of accuracy we are aiming at, say 1 part in 100.

If investigations of the atmosphere at very great heights were attempted (of course, with a great assemblage of searchlights) the general brightening of the atmosphere due to secondary and tertiary scattering from the beams would have to be allowed for. For an altitude where the density was $\frac{1}{100}$ that at sea-level, this effect would equal about $\frac{1}{20}$ that of the direct scattering reaching the cell. Where the density was $\frac{1}{10,000}$ it might equal $\frac{1}{2}$ that of the direct scattering. To eliminate this effect the receiving reflector would be turned a little aside from the spot under investigation, and the difference recorded by the cell when the beams were all on, and all occulted, would measure this effect, which could then be allowed for in the determination when the reflector was turned directly on the spot. A theoretical calculation would give the proper composition for the substituted beam, which would be required to measure the secondary and tertiary scatterings. It is, of course, only necessary to have a quite approximately correct composition of the substituted beam, *i. e.*, the beam

which is diffused from the aluminium ribbons, but it is important to know its relative photo-electric value in any arrangement.

If it were intended to carry out regular observations on the density of the atmosphere at a height of 50 km. (density about $\frac{1}{1000}$ that at sea-level) a permanent assemblage of several hundred searchlights would be required. It would also be necessary to have some electrically controlled mechanism by which the observer at the receiving station could simultaneously occult the whole assemblage, about 30 km. distant. This offers no great difficulty, and since all the belligerent nations in the late war have many thousands of searchlights on their hands, the investigations could be carried out by their meteorological departments without any great outlay.

In such an assemblage it would be simplest to keep all the searchlight reflectors permanently fixed in the same direction, while the observer with his collecting reflector followed the course of their combined beam from kilometre to kilometre of altitude, choosing times for his observations when no bright star lay within the 1° circle whose light enters the photo-electric cell.

It is possible, of course, that the daily variations in density at 50 km. may be small, or that they may not be immediately related to the weather, in which case the method would only have an abstract scientific interest; but it is at least equally possible that the variations may be considerable and rapid, and may bear closely upon conditions in the lower atmosphere; and if so, the method might prove an important one in meteorology. It is certainly a simple and direct one, at all events for stations at high altitudes.

XCII. *Measurements of Sound-Velocities in Air, Oxygen, and Carbon Dioxide at Temperatures from* 900° *C. to* 1200° *C., with special reference to the Temperature-Coefficients of Molecular Heats. By* Dr. F. E. King *and* Prof. J. R. Partington *.

THE present communication gives the results of measurements of sound-velocities at higher temperatures than those previously used, except in the case of air, for which

* Communicated by the Authors.

measurements up to 1300° C. have been published. The method used and the way in which the results were calculated agree with those previously described (Shilling, Phil. Mag. iii. p. 273 (1927); Partington and Shilling, Phil. Mag. vi. Suppl. p. 920 (Nov. 1928)).

It was stated in the second reference (pp. 928 and 932) that the piston and central furnace tube of the most recent type of apparatus were of Pythagoras porcelain, and that these measurements were discontinued owing to fracture of the piston. A new piston was obtained, and, after fitting, was dried by passing dry air through the furnace, the temperature being gradually raised to a red heat. After drying, a series of measurements was made with air at room temperature, in which the value of the tube constant previously found, viz. 0·00136, was confirmed (*op. cit.* p. 937). An opportunity was also taken to recalibrate the valve oscillator against the standardized steel bar, when the value previously found was confirmed.

The experiments with air were continued with rising temperatures, and the values of the wave-lengths at temperatures above 900° were measured as an additional check on the apparatus. These values were in agreement with those previously found, as will be seen by comparing the velocities given in Table I. with those previously published.

The temperature of the furnace was maintained during the night, when the dynamo was not running, by using the 240-volt D.C. mains. On account of the higher voltage economical running was arranged by putting the furnace windings in series, instead of in parallel, the change-over being made by a large double-throw switch. In this way undue cooling of the furnace was prevented when the dynamo was shut off, but as the current was now the same in all windings the ends of the furnace now tended to cool off somewhat on account of the greater radiation losses there. When the dynamo was put in operation, with the windings in parallel, a uniform temperature throughout the working length of the tube was rapidly attained by suitable manipulation of the resistances.

A few measurements had been made, and a temperature of 1100° C. reached, when one of the end platinum windings fused. As this occurred overnight, when the resistances were in series, the whole furnace cooled rapidly. After removing some of the lagging, it was found that the cause of the breakdown was the penetration of a little of the outside lagging of bauxite to the surface of the outer winding, causing fusion of the platinum. At the same time the

sudden cooling had caused fracture of the central furnace tube. It was therefore necessary entirely to dismantle the whole furnace and erect it again.

A new tube was available, and the apparatus was re-assembled with every precaution against breakdown of the tube or platinum windings. It was clear, however, that there was considerable risk of breakdown at the higher temperatures used, and in order to economize time and thus minimize risk, apparatus for the delivery of the three gases used in a pure and dry condition was arranged. The constant of the new tube was determined, and found to be 0·00137. The procedure adopted was, when the furnace had reached a desired temperature, to pass each gas in turn through the furnace tube until analysis of the issuing gas showed that all air or foreign gas had been displaced, and measurements were then made with all the gases at this temperature. This was carried as far as 1200°, when it was noticed that gas was not issuing from the exit, and investigation showed that the new tube had also cracked. Since the assembly of another apparatus will be a lengthy operation, the results so far found, up to 1200°, are now published. The properties of the Pythagoras porcelain showed that, although small pieces would withstand very high temperatures and soften only superficially in the oxy-coal gas-flame, lengths of two metres were liable to sudden and unexpected fracture at temperatures in the neighbourhood of 1100°–1200° *.

The results of the sound-velocity measurements are presented in tables, those in Table I. being for air. The two sets of figures refer to the two furnaces used. The good agreement between these results and those previously found is apparent when they are plotted against temperature. The new points fall reasonably closely on both sides of the smooth curve derived from the previous values (*op. cit.* p. 933), thus confirming the latter. Since the earlier results were from

* In this connexion we wish to draw attention to the fact that after full inquiries we were unable, at the time the experiments were made, to obtain any material of English make which was suitable for the furnace tubes. After some delay we obtained specimens of material from a firm recommended to us, but they were in forms unsuitable for testing, and we were informed that the material could not be supplied in tubes which could be used under the conditions contemplated. It seems necessary to mention this in view of some communications on the subject which appeared since our experiments were completed ('Chemistry and Industry,' June 21 and July 5, 1929). One of the most difficult problems in this work is that of obtaining a suitable material for the tubes.

a continuous series of measurements made throughout the whole temperature range, and extend to higher temperatures than the present, they are probably to be preferred, and hence no calculations of molecular heats have been made from the present velocities.

TABLE I.

Sound-velocities in Air.

Temperature °C.	Velocity m./sec.	Temperature °C.	Velocity m./sec.
939	691·4	1025	715·6
975	702·8	1074	729·9
864	670·8	1069	727·2
932	690·9	1119	739·5
1017	712·0	1167	750·4
1048	721·1	—	—

TABLE II.

Oxygen. Sound-velocities and Molecular Heats.

Temperature °C.	Velocities m./sec.		C_v.	C_p.	C_p/C_v.
	Observed.	Interpolated.			
959	664·1	663·3	5·319	7·306	1·3736
1024	679·8	680·0	5·350	7·337	1·3715
1052	686·7	687·1	5·356	7·343	1·3710
1085	695·6	695·4	5·369	7·356	1·3701
1139	708·8	708·7	5·394	7·381	1·3684
1171	716·7	716·4	5·411	7·398	1·3673

Table II. contains the results with oxygen. The observed velocities in the second column were plotted against the temperatures, and the values in column three found by graphical interpolation. The molecular heats and their ratio were calculated exactly as before. The last decimals

are of no real significance in these values but are included for purposes of comparison.

In calculating the results for carbon dioxide the method of correcting for the presence of 0·5 per cent. of air in the gas used differs from that employed by Shilling (*op. cit.* p. 293). In the latter it appears that the correction was determined by simple proportion from the measured velocities of sound in the carbon dioxide containing 0·5 per cent. of air and the velocity in pure air. The method now adopted is to calculate the molecular heat of the impure gas (C_v^I in the

TABLE III.

Sound-velocities and Molecular Heats for Carbon Dioxide.

Temperature °C.	Carbon dioxide + 0·5 per cent. of air.		Pure carbon dioxide.			
	Velocity m./sec.	C_v^I.	C_v.	C_p.	C_p/C_v.	Velocity m./sec.
15	265·01	6·732	6·741	8·782	1·3028	264·83
100	300·36	7·087	7·098	9·110	1·2835	300·13
200	336·30	7·524	7·536	9·536	1·2654	336·04
300	368·00	7·974	7·989	9·983	1·2496	367·72
400	397·70	8·220	8·236	10·228	1·2419	397·40
500	424·64	8·544	8·561	10·551	1·2324	424·31
600	449·90	8·829	8·848	10·837	1·2248	449·55
700	472·70	9·316	9·336	11·325	1·2131	472·34
800	495·26	9·555	9·576	11·564	1·2076	494·89
900	516·55	9·850	9·873	11·861	1·2014	516·16
1000	537·39	10·032	10·058	12·046	1·1977	536·97

Tables III. and IV.), using the appropriate constants, and to correct for the presence of the 0·5 per cent. of air by the mixture rule. The derivation of the sound-velocities in pure carbon dioxide from the corrected values of C_v thus obtained is simply the reverse of the usual calculations. The corrections for the earlier determinations have therefore been repeated, and the results are given in Table III., the values in which have been calculated from the velocities V′ in Shilling's paper (Table VII.), which, when the tube correction has been applied, appear in column two in Table III. in the present paper. A comparison with Shilling's table will show that the differences between the corrected and

uncorrected figures are smaller than those given by the previous method of calculation, and this has resulted in some small modification in the corresponding values of the molecular heats. The present corrected values are closer to the values obtained by Dixon, to which reference was made in Shilling's paper (p. 293). Five-figure logarithms were used in the calculations, and a fifth figure has been included

TABLE IV.

Sound-velocities in Carbon Dioxide + 0·5 per cent. of Air.

Temperature ° C.	Velocity m./sec.	C_v^I.	Temperature ° C.	Velocity m./sec.	C_v^I.
946	526·05	9·973	1081	552·63	10·374
1020	541·83	9·982	1135	562·49	10·614
1050	546·98	10·211	1178	571·24	10·575

TABLE V.

Sound-velocities and Molecular Heats. Pure Carbon Dioxide.

Temperature ° C.	C_v.	Velocities m./sec.		C_v.	C_p.	C_p/C_v.
		Calculated.	Interpolated.			
946	9·997	525·64	525·60	10·005	11·993	1·1987
1020	10·005	541·40	540·40	10·230	12·218	1·1944
1050	10·233	546·56	546·40	10·272	12·260	1·1936
1081	10·400	552·19	552·35	10·369	12·357	1·1918
1135	10·640	562·04	562·70	10·491	12·479	1·1895
1178	10·601	570·81	570·80	10·601	12·589	1·1875

in order to show how the corrected and uncorrected values compare. The last figure, however, has no real significance.

The new values for carbon dioxide, uncorrected, are given in Table IV., whilst Table V. contains the figures for the pure gas, corrected for the presence of air as explained above. In Table V. the velocities obtained from the corrected values in column three by interpolation are given in

column four, and from these the values of C_v, C_p, and C_p/C_v were calculated.

The values for oxygen and carbon dioxide at each hundred degrees from 900° to 1200°, to two decimal places, are given in Table VI. The values for oxygen and carbon dioxide are in good agreement with those previously found at 900 and 1000°.

TABLE VI.

Molecular Heats of Oxygen and Carbon Dioxide.

Temperature °C.	Oxygen.		Carbon dioxide.	
	C_v.	C_p.	C_v.	C_p.
900	5·30	7·29	9·90	11·89
1000	5·33	7·32	10·18	12·17
1100	5·37	7·36	10·42	12·41
1200	5·42	7·40	10·57	12·66

The authors desire to acknowledge the receipt of a grant from the Government Grant Committee of the Royal Society, which has defrayed part of the expense of the research. One of the authors (F. E. K.) also wishes to acknowledge the receipt of a grant from the Department of Scientific and Industrial Research.

Chemistry Department,
East London College,
University of London.

XCIII. *The Magnetic Characteristics of Nickel.*

By F. TYLER*, *B.Sc.*†

DURING the last thirty or forty years a large number of investigations on the magnetic properties of materials have been carried out, and extensive experimental data have been accumulated. Recently great advances have been made on the theoretical side, and for diamagnetism and paramagnetism a considerable amount of work has been done in

* In receipt of a maintenance grant from the Department of Scientific and Industrial Research.

† Communicated by Prof. R. Whiddington, F.R.S.

correlating experiment and theory. For ferromagnetism the correlation has not been carried so far. In view of the many interesting points which arise in connexion with ferromagnetism, it seems desirable to consider how far the experimental results are in conformity with the various theories, and to discuss the significance of the data in the light of them. In this paper the magnetic characteristics of nickel, particularly in the neighbourhood of the Curie point, will be considered from this point of view, the data for nickel being the most reliable amongst those on ferromagnetics.

Theoretical Magnetization Curves.

According to the classical treatment of magnetism given by Langevin in 1905 and extended by Weiss in 1907, paramagnetic behaviour generally (including ferromagnetism) should be determined by the following equations :

$$\frac{\sigma}{\sigma_0} = \coth a - \frac{1}{a}, \quad . \quad . \quad . \quad . \quad . \quad . \quad (1)$$

$$H = H_e + NI, \quad . \quad . \quad . \quad . \quad . \quad . \quad . \quad (2)$$

$$a = \frac{\mu H}{kT}, \quad . \quad . \quad . \quad . \quad . \quad . \quad . \quad . \quad (3)$$

where σ is the specific intensity of magnetization, σ_0 the saturation intensity, and N the coefficient of the "molecular field" (postulated by Weiss to account for ferromagnetism, and for deviations from the simple Curie law shown by many paramagnetics). When the external field is zero ($H_e = 0$), the possibility arises of a substance becoming spontaneously magnetized if N is positive, and by a graphical method curves showing the relation between this magnetization and temperature can be obtained. (This magnetization corresponds to the extrapolated saturation value for zero external field at the particular temperature.) These curves are usually drawn so as to represent $\frac{\sigma}{\sigma_0}$ as a function of $\frac{T}{\theta}$, where θ is the Curie temperature.

This treatment assumes that any orientation of the magnetic carriers with respect to the field is possible. According to the quantum theory, however, only certain discreet orientations (or rather discreet values of the resolved moment) are possible, and a knowledge of these is to be obtained from a study of the Zeeman effect. The magnetic moment in the field direction is given by mg (Bohr magnetons), where

$m = j, j-1, j-2, \ldots\ldots -j$. ($j$ is the inner quantum number.)

The expression $\frac{\mu H}{kT}\cos\theta$ appearing in Langevin's treatment then becomes

$$\frac{jg\mu_B H}{kT}\cdot\frac{m}{j} = \frac{mg\mu_B H}{kT} \quad (\mu_B = 1 \text{ Bohr magneton}).$$

Now, the number of atoms whose moment resolved parallel to the field is $mg\mu_B$ is proportional to

$$e^{\frac{mg\mu_B H}{kT}} = e^{mgh}\left(\text{putting } h = \frac{\mu_B H}{kT}\right),$$

and hence for the mean resolved magnetic moment of the assembly

$$\bar{\mu} = \sum_{-j}^{j} e^{mgh}\cdot mg\mu_B \Big| \sum_{-j}^{j} e^{mgh},$$

whence

$$\frac{\sigma}{\sigma_0} = \frac{1}{j}\sum_{-j}^{j} e^{mgh}\cdot m \Big| \sum_{-j}^{j} e^{mgh}. \quad \ldots\ldots \quad (4)$$

This is the function which must replace the classical expression for $\frac{\sigma}{\sigma_0}$ appearing in (1).

The limiting quantum case is that in which the magnetic elements can only set themselves either parallel or anti-parallel with the field which occurs when the magnetic moment of the carriers is 1 Bohr magneton ($jg=1$). Under these circumstances (4) reduces to the form

$$\frac{\sigma}{\sigma_0} = \tanh a. \quad \ldots\ldots \quad (5)$$

With this relation in place of (1) magnetization temperature curves can be obtained as before. The classical curve may be considered as the limiting quantum curve for $j \to \infty$.

An essential point which emerges from the foregoing discussion is that while the reduced magnetization temperature curves for the Weiss-Langevin theory should be the same for all substances, a series of curves are possible on the quantum theory, the form of the curves depending on the quantum state of the elementary carriers under consideration. These curves will now be discussed in relation to the experimental results.

Experimental Results.

The saturation values for ferromagnetics below the Curie point have been given by several investigators. Weiss *, in collaboration with Onnes (1910), determined the saturation intensity of nickel, iron, cobalt, and magnetite down to 20° K.,

Fig. 1.

Spontaneous magnetization curves.

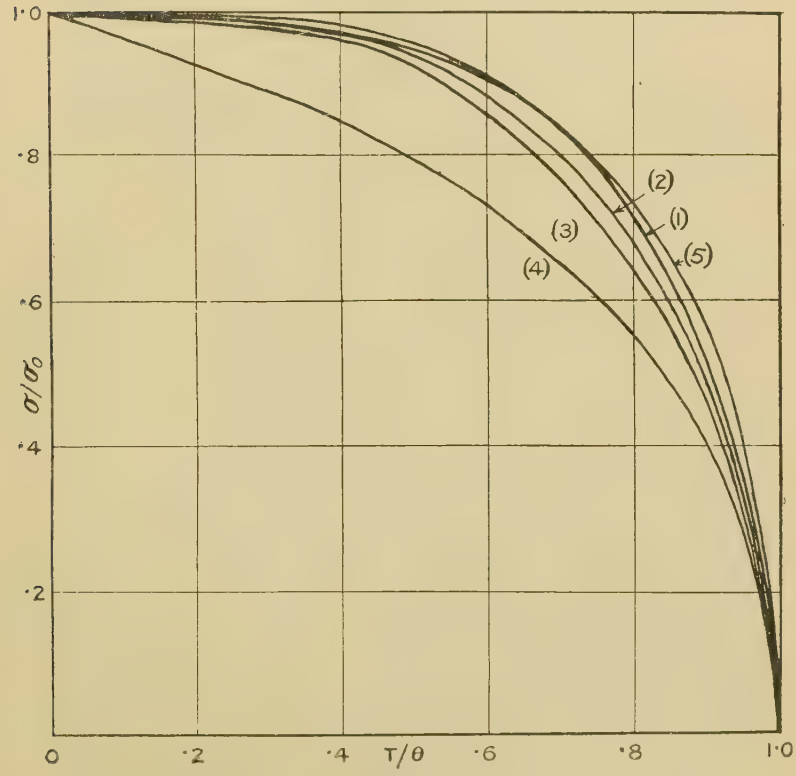

(1) Quantum theoretical curve for 1 μ_B.
(2) „ „ „ 2 μ_B.
(3) „ „ „ 3 μ_B.
(4) Classical curve (Langevin).
(5) Experimental curve for nickel (Weiss & Forrer).

* P. Weiss and H. K. Onnes, *Comptes Rendus*, cl. pp. 686-687 (1910).

the method being based on the measurement of the maximum couple exerted on an ellipsoid of the material supposed isotropic. For temperatures above 0° C. the most satisfactory results for nickel are those recently given by Weiss and Forrer * ; these results will be used in constructing a " corresponding state " curve for this metal. The values of σ are obtained by extrapolating the (σ, H) curves to zero field. The saturation intensity σ_0 at absolute zero can also be found by extrapolation, and hence from Weiss's magnetic isothermals $\frac{\sigma}{\sigma_0}$ may be obtained as a function of $\frac{T}{\theta}$. The value of θ adopted is that obtained by Weiss from experiments on the magnetic-caloric effect. The resulting experimental corresponding state curve is shown in fig. 1 together with the theoretical curves discussed above. Included in fig. 1 are also theoretical curves for the cases of 2 and 3 μ_B.

From fig. 1 it will be seen that the experimental results fit reasonably closely with the 1 μ_B curve ; there is an appreciable divergence from the 2 and 3 μ_B curves, whilst there is little or no correspondence between the experimental and classical curves.

The quantum theory treatment of ferromagnetism thus gives a much more satisfactory representation of the facts for nickel than the older theory, if it is assumed that the carriers have a moment of $1\mu_B$. There are, however, still slight discrepancies between the theoretical and experimental curves to be considered, as may be seen from the figure. The non-conformity of the two curves is most pronounced in the region just below the Curie point, the experimental values being appreciably higher than the theoretical. This may be attributed to a number of reasons; but perhaps the chief reason lies in the uncertainty of the experimental curve in this region due to the difficulty of obtaining reliable extrapolated values for the quasi-saturation moment.

Magnetization near the Curie Point.

In order to circumvent the uncertainty due to extrapolation in the curves for zero external field in the neighbourhood of the Curie point, it was decided to compare the theoretical and experimental curves giving the relation between $\frac{\sigma}{\sigma_0}$ and $\frac{T}{\theta}$ for an external field of a few thousand

* P. Weiss and R. Forrer, *Annales de Physique*, X^e Serie, Tome v. p. 153 (1926).

gauss. The experimental curves are obtainable directly from results; the theoretical curves, however, require more detailed consideration.

When the carriers have a moment of 1 μ_B, the quantum theory gives the following equations:

$$\frac{\sigma}{\sigma_0} = \tanh a, \quad . \quad . \quad . \quad . \quad . \quad . \quad . \quad . \quad (6)$$

$$a = \frac{\mu H}{kT} = \frac{\sigma_0 H}{RT}, \quad . \quad . \quad . \quad . \quad . \quad . \quad . \quad (7)$$

$$H = H_e + N\frac{\rho\sigma}{m}. \quad . \quad . \quad . \quad . \quad . \quad . \quad . \quad (8)$$

Substituting for H in (7),

$$a = \frac{\sigma_0}{RT}\left(H_e + \frac{N\rho\sigma}{m}\right)$$

$$= \frac{\sigma_0}{RT}\cdot H_e + \frac{N\rho\sigma_0^2}{mRT}\cdot\frac{\sigma}{\sigma_0}. \quad . \quad . \quad . \quad . \quad (9)$$

Now θ, the Curie temperature, is given by

$$\theta = \frac{\sigma_0^2 N\rho}{mR}. \quad . \quad . \quad . \quad . \quad . \quad . \quad . \quad (10)$$

Hence, using (10), (9) becomes

$$a = \frac{\sigma_0 H_e}{RT} + \frac{\theta}{T}\cdot\frac{\sigma}{\sigma_0},$$

or, rewriting,

$$\frac{\sigma}{\sigma_0} = \frac{T}{\theta}\cdot a - \frac{H_e\sigma_0}{R\theta}$$

$$= \frac{a}{\theta}\left(T - \frac{H_e\sigma_0}{Ra}\right). \quad . \quad . \quad . \quad . \quad (11)$$

From (11) it follows that the state of a substance in an external field H_e and at a temperature T is the same as if the substance were subject solely to the intrinsic field, and at a slightly lower temperature, viz., $T - \frac{H_e\sigma_0}{Ra}$. A consideration of this fact then enables the desired curves to be obtained from the appropriate corresponding temperature curves, without the uncertainty inherent in the usual graphical treatment. (This uncertainty is due to the fact that the term $\frac{H_e\sigma_0}{Ra}$ appearing in (11) is far too small to be represented with precision on a diagram.)

The experimental and theoretical curves thus obtained for $H_e = 10{,}000$ gauss are shown in fig. 2. There is no coincidence between the two curves, although they are sensibly parallel. The rélative position of the two curves depends on the choice of θ, and it is found that by a judicious selection of the value of the Curie temperature the curves can be made to coalesce satisfactorily for a wide range below the Curie point; though whatever the value of θ chosen, the

Fig. 2.

Magnetization curves for $H_e = 10{,}000$ gauss.

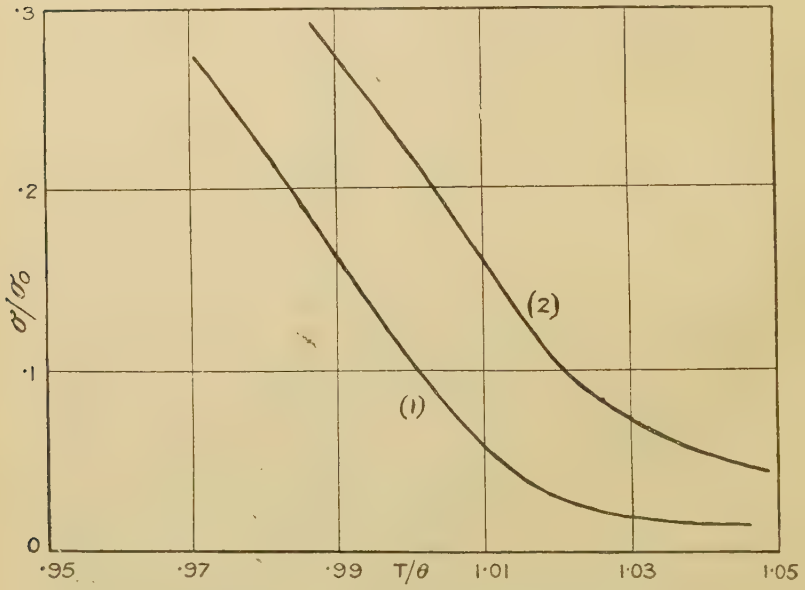

(1) Quantum theoretical curve for $1\mu_B$.

(2) Experimental curve for nickel (Weiss & Forrer).

experimental curves always lie above the theoretical for values of $T > \theta$.

Now, it is well known that there are wide discrepancies in the values of θ as given by different investigators. This is partly due to variation of θ with the chemical purity of the material, but from the observations on material of a high degree of purity it seems fairly certain that the value of θ as derived from observations on the ferromagnetic properties of a substance is materially different from the value obtained

from the paramagnetic properties by extrapolation of the $\left(\frac{1}{\chi}, \mathrm{T}\right)$ curves. Forrer * has recently discussed the significance of the ferromagnetic and paramagnetic Curie points, which in the case of nickel differ by about 16°C. He points out that in this immediate region there is still some effect due to hysteresis, and it is only above the upper point that the substance loses entirely its ferromagnetic properties and becomes truly paramagnetic. If this higher value of θ is employed in dealing with the magnetization curves, then a satisfactory agreement can be obtained for a considerable range below the Curie point.

A problem closely associated with the magnetization values in the vicinity of the Curie point is the variation of specific heat of a ferromagnetic body. Thermodynamical considerations predict a sudden decrease in the specific heat at the Curie point, the magnitude depending on $\frac{d\sigma^2}{d\mathrm{T}}$ in the immediate neighbourhood. In the classical case for values of T just less than θ the following approximate relation holds :

$$\frac{\sigma}{\sigma_0} = \sqrt{\frac{5}{3}\left(1 - \frac{\mathrm{T}}{\theta}\right)}, \quad . \quad . \quad . \quad . \quad . \quad (12)$$

whence

$$\left[\frac{d\left(\frac{\sigma}{\sigma_0}\right)^2}{d\left(\frac{\mathrm{T}}{\theta}\right)}\right]_{\mathrm{T}=\theta} = \frac{5}{3}.$$

The corresponding relation for the quantum theory case when the carriers have a moment of $\mathrm{I}\,\mu_{\mathrm{B}}$ is

$$\frac{\sigma}{\sigma_0} = \sqrt{3\left(1 - \frac{\mathrm{T}}{\theta}\right)}, \quad . \quad . \quad . \quad . \quad . \quad (13)$$

giving

$$\left[\frac{d\left(\frac{\sigma}{\sigma_0}\right)^2}{d\left(\frac{\mathrm{T}}{\theta}\right)}\right]_{\mathrm{T}=6} = 3.$$

These values, $\frac{5}{3}$ and 3, are the extreme values, and it would be expected *à priori* that the experimentally-obtained magnitude would not lie outside these limits ; a value close

* R. Forrer, *Comptes Rendus*, clxxxviii. pp. 1242-1244 (May 6, 1929).

to 3 would be expected. From Weiss and Forrer's results a graph giving the relation between $\left(\frac{\sigma}{\sigma_0}\right)^2$ and $\frac{T}{\theta}$ can be drawn ; from this it is found that

$$\left[\frac{d\left(\frac{\sigma}{\sigma_0}\right)^2}{d\left(\frac{T}{\theta}\right)}\right]_{T=\theta} \doteqdot 5.$$

This value is considerably higher than the extreme upper limit indicated by theoretical considerations.

Heisenberg's * recent theory of ferromagnetism essentially gives a satisfactory interpretation of the Weiss molecular field. This he shows may arise from the interchange interaction of the electrons outside closed groups in the atoms in the lattice. Equations are deduced similar to those appearing in the quantum modification of Weiss's theory for the $I\,\mu_B$ case. The main differences are that an I^3 term is introduced into the expression for the internal field, and that the quantity corresponding to N is dependent on the temperature. Although the expressions are admittedly approximations, the closeness of approximation should be greatest at fairly high temperatures, and it seemed of interest to carry out a calculation from them as to the variation of magnetization near the Curie point. They do actually give a value for

$$\left[\frac{d\left(\frac{\sigma}{\sigma_0}\right)^2}{d\left(\frac{T}{\theta}\right)}\right]_{T=\theta}$$

materially greater than 3, but it is doubtful whether much significance can be attached to the result on account of the limited applicability of the formulæ resulting from some of the subsidiary assumptions made in the treatment of the problem.

Above the Curie Point.

The magnetic data for nickel above the Curie point are as tabulated below :—

	Temp. range °C.	C.	θ.	C_M.	p.
$Ni\beta_1$	412–900	·0056	645	·325	8·02
$Ni\beta_2$	900–	—	—	·403	8·96

* W. Heisenberg, *Zeits. für Physik*, xlix. p. 619 (1928).

The p values given in the last column are computed from the Curie constant appearing in the Weiss-Curie law as follows :—

$$p = \frac{\sigma}{1123{\cdot}5} = \frac{\sqrt{3\mathrm{R}\mathrm{C}_\mathrm{M}}}{1123{\cdot}5} = 14{\cdot}07\ \sqrt{\mathrm{C}_\mathrm{M}}.$$

If the carriers have not all the same magnetic moment, then the Weiss magneton number (p) deduced from C_M is a root-mean square value $p = \sqrt{\bar{p}^2}$.

Now, in his investigations on ferromagnetics at low temperatures, Weiss deduced with reasonable certainty that the gramme-molecular moment of nickel extrapolated to zero temperature corresponded to a p value of 3. (For carriers of different moments the p value observed at low temperature will be an arithmetic mean $p = \bar{p}$.)

Weiss attempted to account for the discordance between the p values at high and low temperatures by supposing that there were carriers with moments of 3 and 8 whose relative number changed gradually as the temperature rose (there being no discontinuity in the quasi-saturation curve). The investigations above the Curie point, however, show that the magnetic properties usually occur discontinuously, and, further, if they are of considerable magnitude, that they are usually associated with changes in the crystalline structure.

Stoner * has shown that both the results can be accounted for on the basis of the atomic theory of magnetism without the necessity in general of assuming a change in the constitution of the substance. He supposes that there are groups of atoms in the crystals, and that the magnetic properties are due to ions which have the same moment as those found from measurements on paramagnetic solutions and solid salts. Thus for nickel he considers groups of five Ni atoms, and suggests that the effective ions with μ_B values constituting the group to be

$$\mathrm{Ni}^{++}(2), \qquad \mathrm{Ni}^{+}(1), \qquad 3\,\mathrm{Ni}(0).$$

This gives a p value for low temperatures ($p = p$) of 3 to agree with the observed value of 3, and for high temperatures ($p = \sqrt{\bar{p}^2}$) the calculated p value is 8·2 against the observed value of 8·0 for Niβ_1. With the change in crystal structure in passing from Niβ_1 to Niβ_2 the constitution of the group changes which he suggests is now

$$\mathrm{Ni}^{++}(2), \qquad 2\,\mathrm{Ni}^{+}(1), \qquad 2\mathrm{Ni}(0).$$

* E. C. Stoner, Leeds Phil. Soc. i. p. 55 (1926).

This gives a calculated p value of 9·1, the observed value being 8·96.

Discussion.

In view of the preceding discussion of the corresponding temperature curves for nickel, it may reasonably be supposed that the magnetic state of nickel is governed by the relation expressed in equation (5), implying that the magnetic moment of the elementary carriers is $1\,\mu_B$. This assumption satisfactorily correlates the magnetization values below the Curie point, although there are a few uncertain features in the immediate neighbourhood of the Curie point: this region, however, presents a separate problem of its own. In order to account for the p value of 3 at low temperatures, it may be assumed that there are groups of 5 carriers, three of which have a moment of $1\,\mu_B$; this would give the necessary Weiss magneton value of 3. Little, however, can be said about the *nature* of the carriers. It has been seen that Weiss and Stoner, in discussing the magnetic data for nickel, definitely attribute the ferromagnetic properties of the metal to ions. The recent thermoelectric observations of Dorfmann *, however, seem to indicate that it is the free or conduction electrons which play the role of the elementary magnets. The jump in the specific heat at the Curie point may be written $\Delta_\theta C_a$ per atom, and this will be made up of $\Delta_\theta C_i$ due to the positive ions and $\Delta_\theta C_e$ due to the conduction electrons: *i. e.*,

$$\Delta_\theta C_a = \Delta_\theta C_i + n\Delta_\theta C_e,$$

where n = number of conduction electrons per atom.

$\Delta_\theta C_a$ is measured calorimetrically, and $\Delta_\theta C_e$ is obtained from the sharp change in the thermoelectric magnitude $T\frac{d^2E}{dT^2}$ at the Curie point. These latter measurements were of the same order of magnitude—implying that the conduction electrons are responsible for the ferromagnetism of nickel. Further, on substituting the value of $\Delta_\theta C_e$ into the quantum theory expression for the jump in the specific heat at the Curie point, viz.

$$\Delta_\theta C_m = \frac{5}{2}k \cdot \frac{j(j+1)}{j^2+j+\frac{1}{2}},$$

the j value obtained was approximately $\frac{1}{2}$. This is to be

* J. Dorfmann and R. Jaanus, Pt. I.; J. Dorfmann and I. Kikoin, Pt. II., *Zeits. für Physik*, liv. pp. 277-296 (1929).

expected if the carriers are free electrons, for then $l=0$ and $j=s=\frac{1}{2}$. Also for free electrons $g=2$, and hence they have an associate magnetic moment of $1\mu_B$—a fact in accordance with the previous discussion. To account for the p value of 3 at low temperatures, a concentration of 60 per cent. of free electrons to atoms is necessary. Above the Curie point, considering an electron, the p value can be obtained from Hund's expression :

$$p = 4{\cdot}97g\sqrt{j(j+1)}$$

by putting $g=2$ and $j=\frac{1}{2}$. The value of p then obtained is 8·6. To account for the observed p values of 8·02 and 8·96 an electron concentration of approximately 80 per cent. (at the Curie point Dorfmann finds 78 per cent.) and 110 per cent. respectively is necessary. Under these circumstances the necessary facts can readily be accounted for.

On the free electron explanation of ferromagnetism, however, it is difficult to realise why ferromagnetism should be restricted to the metals iron, nickel, and cobalt, and certain alloys and compounds (though this objection might also be raised against Heisenberg's theory) ; the majority of the metals would be expected to share the characteristic properties of ferromagnetics, such metals as silver and copper manifesting them to a high degree. Further, Pauli has shown by applying the Fermi statistics to the assembly of free electrons in the alkali metals, that the slight residual paramagnetism shown by these metals can be satisfactorily accounted for. Far from producing marked ferromagnetic properties, free electrons appear to be responsible for a slight paramagnetism. Thus the nature of the carriers in a ferromagnetic body still remains an outstanding problem.

Summary.

Quantum and classical theory curves for the variation of the spontaneous magnetization with temperature below the Curie point are obtained and compared with the experimental results for nickel. Curves corresponding to large external fields are also considered.

The comparison shows that the variation of $\frac{\sigma}{\sigma_0}$ with $a=\left(\frac{\mu H}{kT}\right)$ is closely given by a tanh curve, indicating that the carriers have a moment of 1 Bohr magneton ($j=\frac{1}{2}$, $g=2$). There seem to be anomalies in the variation in magnetization close to the Curie point.

The magnetic data for temperatures above the Curie point are also discussed. It is possible to explain most of the magnetic characteristics by supposing that the carriers are free electrons whose numbers may vary, as suggested by Dorfmann's work on the variation of thermoelectric properties of nickel at the Curie point. There are, however, several objections to this hypothesis. No definite conclusions can be drawn until the relation between conduction electrons and interaction electrons is more fully worked out.

In conclusion I wish to express my indebtedness to Dr. E. C. Stoner for his valuable advice and constructive criticism.

Physics Department,
University of Leeds.

XCIV. *The Turbulence in front of a Body moving through a Viscous Fluid.* *By* N. A. V. Piercy, *D.Sc.*, *and* E. G. Richardson, *B.A.*, *Ph.D.*, *D.Sc.* *

A PREVIOUS paper † relating to the generation of the large-scale turbulence in the wake of a circular cylinder moving through air at considerable Reynolds' numbers, incidentally showed the front stagnation point to be a region of maximum turbulence. Similar exploration near the front stagnation point of an aerofoil ‡ gave the same result. In both cases the unsteadiness of flow was damped out in the subsequent motion of the fluid.

The matter is of some interest in the theory of aerodynamics, if this instability is an essential feature of all stagnation points, because of its relation to an aspect of the stability of fluid motion in cylindrical layers studied by Kelvin, Rayleigh, and G. I. Taylor. According to a well-known analogy, "the varying centrifugal force of the different layers of fluid plays the part of gravity (in a fluid of variable density), and the resulting condition for stability is that the square of the circulation must increase continuously in passing from the inner to the outer cylinder, just as the density of a fluid under gravity must decrease continuously with height in order that it may be in stable

* Communicated by the Authors.
† Phil. Mag. vi. p. 970 (1928).
‡ Aero. Res. Comm. R. & M. no. 1224 (1928).

equilibrium"*. So far as this simple feature of rotating fluids may find reflexion in the varying flow round a body in a stream, one might expect instability in a limited region surrounding the stagnation point where the stream-lines are convex to the axis and the pressure decreases outwards along a normal, and stability farther round the shoulder of the body where those conditions are reversed.

Both cases of motion that we have so far examined accord with these expectations, but both leave in doubt a question as to whether the instability observed may be a consequence of fluctuation in the circulation round the body. With the aerofoil the circulation had a large average value depending on lift, while in the case of the circular cylinder, although the average circulation was zero, it might conceivably have had a periodic value due to the large-scale eddies shed asymmetrically from the rear.

At Prof. Taylor's suggestion, we therefore explored the region in front of a cylinder of good "stream-line" section—

Fig. 1.

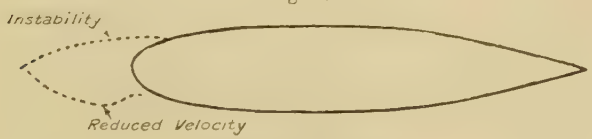

Section of strut.

an aeroplane strut—arranged with its axis of symmetry parallel to the wind. The shape of the section, given in fig. 1, and the Reynolds's number employed, 4×10^4, using maximum width across the stream to specify length, ensured that insignificant eddying only was shed from the tail, so that the periodic circulation round the cylinder, if any, was very small.

The strut was arranged in a two-dimensional fashion between the walls of the 4-ft. wind-channel working at 42 ft./sec. in the Aerodynamical Laboratory at East London College, and the hot-wire method employed in comparing the velocity fluctuation at any point near the body with that in the undisturbed stream was essentially the same as described in the earlier paper referred to.

Along the various lines that were explored round the nose of the cylinder measurements were made of the average value of the velocity as well as of its relative amplitude, and

* Taylor, Phil. Trans. Roy. Soc. A, ccxxiii. pp. 291 & 327 (1923).

from this information fig. 2 has been prepared, which shows above the symmetrical axis contours of equal galvanometer response to velocity amplitude, and below the axis iso-average-velocity curves. The numbers attached to the amplitude contours give the amplitude in terms of its value at a distance in the stream, while those attached to the curves of average velocity give the average velocity in terms of its undisturbed value.

The question may be raised to what extent the magnitude of the temperature fluctuations set up in the hot-wire by fluctuations of velocity are influenced by the mean velocity round which these fluctuations take place. The calibration curve of a hot-wire in a steady wind shows (*a*) at low

Fig. 2.

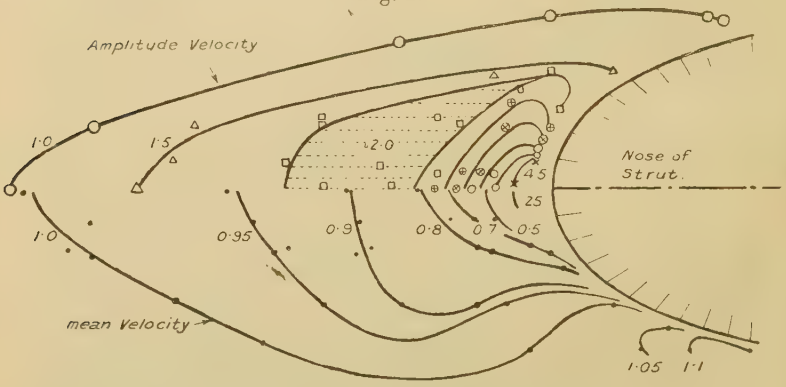

Contours of mean velocity and velocity amplitude.

velocities an almost parabolic drop of resistance, merging into (*b*) a linear drop at high velocities. Anywhere over this second region a given change of velocity will produce an approximately constant change of resistance; in other words, a linear relation between the response of a vibration galvanometer and the fluctuation of velocity might be looked for.

Investigations have been in hand to test this point practically, in which hot-wires have been oscillated at various amplitudes approximately in S.H.M., both in stagnant air and in an air-stream. In some of these the wires have been oscillated in close proximity to a smooth brass surface. An early opportunity will be taken to describe in detail the results obtained, but it has been found that, although abnormal response occurs at low speeds, yet easily within

the limits of the mean velocities measured in the present investigation (fig. 2), the relation between velocity amplitude and galvanometer reponse at constant frequency is linear and independent of the mean velocity.

Conclusion.

Fig. 2 shows a considerable area of instability extending upstream a distance about one quarter of the length of the strut section and roughly covering the area for which the mean velocity is sensibly reduced below its value in the undisturbed stream. The broken lines in fig. 1 show to scale the extent of the disturbance. The disturbance is quickly damped out over the shoulder of the strut.

Within the area explored, velocity amplitude increases rapidly as the stagnation point is approached. We therefore conclude that front stagnation points in general are centres of maximum turbulence.

XCV. *Experiments on the Apparent Deviation from Ohm's Law for Metals at High Current Densities.* *By* H. Monteagle Barlow, *Ph.D.**

Introduction.

A NUMBER of experimental investigations have been made to test the validity of Ohm's law for a metallic conductor carrying a current of very high density †. All of these attempts, with the exception of a recent one by Bridgman, indicate that any departure from Ohm's law, if it exists at all, is exceedingly small, even at densities as large as 10^7 amp. per sq. cm. Prof. Bridgman, however,

* Communicated by the Author.

† (*a*) Clerk Maxwell, J. D. Everett, and A. Schuster, Brit. Assoc. Rep. pp. 36–63 (1876).

(*b*) E. Lecher, *Sitzber. Wien Akad.* cxvi. (2 *a*) i. p. 49 (1907).

(*c*) H. Rausch von Traubenberg, *Phys. Zeits.* xviii. p. 75 (1917).

(*d*) F. Wenner, Phys. Rev. (2) xv., p. 531 (1920).

(*e*) P. W. Bridgman, Proc. Am. Acad. Arts & Sci. lvii. no. 6, p. 131 (1922), and a preliminary report in Proc. Nat. Acad. Sci. vii. p. 299 (1921).

See also J. J. Thomson, 'The Corpuscular Theory of Matter,' p. 54 (1907); W. F. G. Swann, Phil. Mag. xxviii. p. 467 (1914); K. T. Compton, Nat. Acad. Sci. Proc. xii. p. 548 (1926), and H. Margenau, *Zeits. f. Physik*, lvi. p. 259 (1929).

claims to have observed and measured a definite increase in the effective resistance of gold and silver films to currents of the order 10^6 amp. per sq. cm., and this after eliminating errors due to rise of temperature.

The method of investigation adopted by Bridgman is exceedingly ingenious. Measurements were made by passing a large direct current and a small audible frequency

Fig. 1.

alternating current through the metal film at the same time. The P.D. between the ends of the film was balanced in a simple bridge circuit first with a moving coil galvanometer and then with a pair of telephones. The balancing resistances were exactly the same for the alternating current and the direct current until the density reached about 10^5 or 10^6 amp. per sq. cm., but after this small differences were observed.

This result naturally suggests that at very high current densities the curve representing the relation between the P.D. across the ends of the film and the current through it at constant temperature is no longer a straight line, but has a slightly increasing slope in accordance with the fact that the alternating current P.D. was greater than the corresponding direct current P.D. Thus in fig. 1 the D.C. balance gives a resistance at the point W represented by the slope of the straight line OW, whereas the A.C.

Fig. 2.

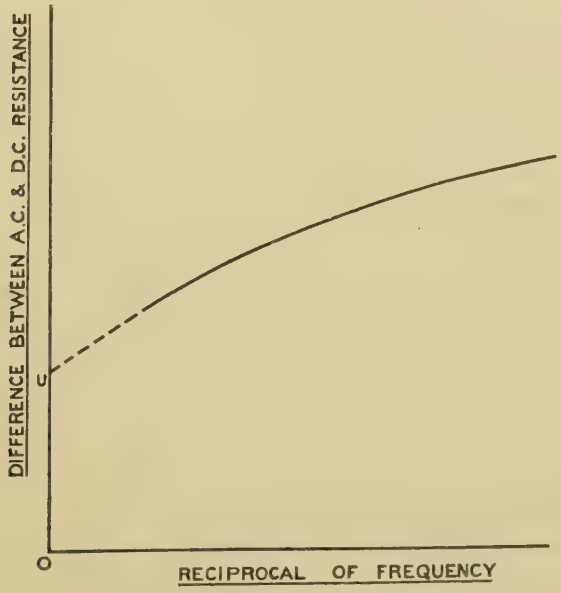

balance gives a resistance at the same point represented by the slope of the line MWN, which is a tangent to the curve at W.

Bridgman noticed that this apparent deviation from Ohm's law was a function of the frequency of the alternating current, and became smaller as the frequency was increased. He concluded that this effect was due to the periodic heating and cooling of the film with the alternating current. To eliminate the error introduced in this way he made a series of measurements with a given current density and different frequencies from 3750 periods per

sec. down to 320 periods per sec., plotted the difference between the A.C. and the D.C. resistance against the reciprocal of the frequency, and extrapolated to zero or infinite frequency (see fig. 2). The assumption was made that at very high frequencies the heating and cooling effect would become negligible, so that a true measure of the deviation from Ohm's law was given by the intercept OU on the curve.

So far as the magnitude of the alternating current was concerned, Bridgman did not find that this affected the apparent deviation over a range of ten- or twenty-fold. The average alternating current used was about 0·02 amp., being about one-thirtieth part of the maximum direct current employed.

To test the genuineness of the observed effect, an experiment was made with two different rates of flow of the cooling water traversing the surface of the film. With constant direct current the steady rise of temperature was 40 per cent. greater in one case than in the other. When the difference between the A.C. and D.C. settings in cm. of the bridge wire were plotted against the reciprocal of the frequency, it was found that the two curves appeared to extrapolate to the same value, indicating that the effect as measured by the intercept on the vertical axis was independent of temperature *.

Although there was a marked change in the rise of temperature of the film for specimens of different width, this seemed to bear no relation to the extrapolated difference between the A.C. and D.C. resistance expressed as a percentage of the initial resistance.

On the other hand, the thickness of the film was an important factor and conductors of gold leaf $16{\cdot}7 \times 10^{-6}$ cm. thick gave a percentage deviation some seven times as much as the corresponding percentage deviation for gold leaf only 8×10^{-6} cm. thick. This variation of the effect with thickness was far more than could possibly be accounted for by errors in observation and seems to the author to have an important significance.

* It is not quite clear whether the result would have been the same had the difference between the A.C. and D.C. resistances been plotted instead of the difference between the slide-wire readings. At the higher temperature the steady current resistance of the film must have been greater, so that the balance-point on the slide wire would be in a new position, and a given displacement would no longer correspond with the same change in resistance

Experimental Work.

(*a*) *Description of Apparatus.*

The following experiments were carried out with the object of confirming Bridgman's observations. The same method of investigation was employed, but certain refinements were introduced to obtain a higher degree of accuracy.

A four-valve audible frequency amplifier was used in conjunction with the telephone receiver, so that the A.C. balance of the bridge could be made effectively with very much smaller alternating currents. The frequency range employed was from 1000 to 14,000 cycles per sec.

The diagram of connexions for the bridge is shown in fig. 3. A Eureka slide wire 274 cm. long, and having a

Fig. 3.

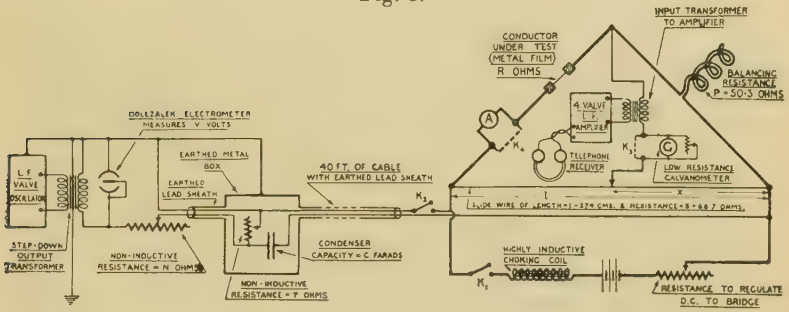
INPUT TRANSFORMER TO AMPLIFIER
CONDUCTOR UNDER TEST (METAL FILM) R OHMS
BALANCING RESISTANCE P = 50·3 OHMS
4 VALVE L.F. AMPLIFIER
TELEPHONE RECEIVER
LOW RESISTANCE GALVANOMETER
DOLEZALEK ELECTROMETER MEASURES V VOLTS
L.F. VALVE OSCILLATOR
EARTHED METAL BOX
EARTHED LEAD SHEATH
40 FT. OF CABLE WITH EARTHED LEAD SHEATH
SLIDE WIRE OF LENGTH l = 274 CMS. & RESISTANCE = S = 66·7 OHMS.
STEP-DOWN OUTPUT TRANSFORMER
NON-INDUCTIVE RESISTANCE = N OHMS
CONDENSER CAPACITY = C FARADS
NON-INDUCTIVE RESISTANCE = T OHMS
HIGHLY INDUCTIVE CHOKING COIL
RESISTANCE TO REGULATE D.C. TO BRIDGE

resistance of 66·7 ohms, was used, the only sliding contact in the bridge being the tapping-point to which the detector system was connected. Thus, only out-of-balance currents passed through this contact, which consisted of a very narrow ebonite trough filled with mercury, through which the wire was free to slide. The conductor under test was a thin metal film, in some cases of gold either 5×10^{-6} cm. or 9×10^{-6} cm. thick, and in others of platinum $16{\cdot}5 \times 10^{-6}$ cm. thick, whilst the balancing resistance P was a non-inductively wound Eureka wire of 50·3 ohms. The cross-section of every conductor, with the exception of the metal film under test, was sufficiently large to make special cooling devices unnecessary with the currents employed. The A.C. was derived from a valve oscillator, and a 25-mfd. condenser in the supply leads prevented the D.C. from getting back along these leads. A large inductance coil in

the D.C. supply wires was used to choke back the A.C. For the detector it was found best to connect the moving coil galvanometer in series with the primary of the transformer attached to the amplifier.

One of the important points in the investigation was to determine how the apparent departure from Ohm's law was affected by the magnitude of the A.C. through the film. With this in mind great care was taken to prevent direct induction from the valve oscillator, which was placed 40 feet away from the bridge and connected to it by a cable having an earthed lead sheath. The output from the oscillator was applied first to a step-down transformer on the secondary of which the voltage was measured with a Dolezalek electrometer, and then passed through a system of non-inductive resistances forming a potential

Fig. 4.

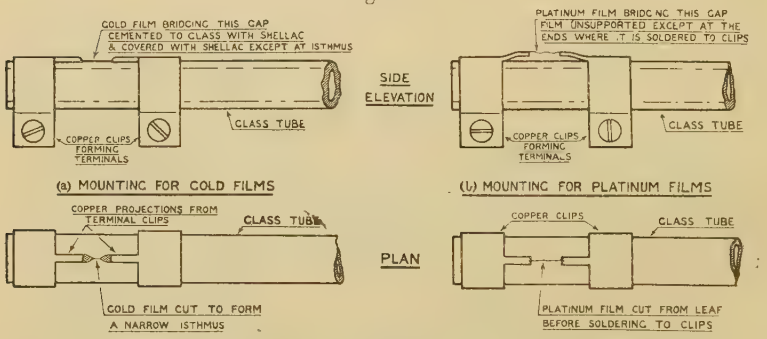
GOLD FILM BRIDGING THIS GAP CEMENTED TO GLASS WITH SHELLAC & COVERED WITH SHELLAC EXCEPT AT ISTHMUS
PLATINUM FILM BRIDGING THIS GAP FILM UNSUPPORTED EXCEPT AT THE ENDS WHERE IT IS SOLDERED TO CLIPS
SIDE ELEVATION
CLASS TUBE
COPPER CLIPS FORMING TERMINALS
(a) MOUNTING FOR GOLD FILMS
(b) MOUNTING FOR PLATINUM FILMS
COPPER PROJECTIONS FROM TERMINAL CLIPS
PLAN
COPPER CLIPS
GOLD FILM CUT TO FORM A NARROW ISTHMUS
PLATINUM FILM CUT FROM LEAF BEFORE SOLDERING TO CLIPS

divider, so that the current flowing away to the bridge was reduced to a very small value. The oscillator and its accessories were enclosed in earthed metal boxes as shown in the diagram. With this arrangement it was not possible to detect any trace of A.C. in the bridge circuit when the key K_2 connecting to the supply cable was open.

A low resistance moving coil milli-ammeter was joined in series with the metal film to measure the direct current passing through it. This instrument was short-circuited during the measurements.

Various methods of mounting the metal foils under test were tried. With the gold films it was not found possible to improve on Bridgman's arrangement. They were cemented to the outside of a glass tube with shellac dissolved in alcohol (see fig. 4 (*a*)). In some cases a

stream of pure distilled water flowing across the film at right angles to its length was used for cooling, but the author found that the water had a tendency to boil, causing irregular variations in the resistance of the film and noises in the telephone receiver. Much steadier conditions were obtained with no special cooling device apart from the surrounding air, and the current densities reached, about 3×10^{-6} amp. per sq. cm., were not far short of those possible with the flowing water.

Attempts were made to employ liquid-air cooling, but with gold this was unsuccessful on account of a change in structure at the reduced temperature. Experiment showed that only platinum would withstand immersion in liquid air and return to its original condition when brought back to room temperature. A very narrow strip of platinum was cut from the leaf and soldered to copper terminals mounted on a glass tube (see fig. 4 (*b*)). The film was entirely unsupported except at its ends, and formed an arched bridge at room temperature, so that the contraction, when immersed in liquid air, could take place without restriction. Tests on these platinum conductors were also made in absolute alcohol and air at room temperature, the natural convection currents in the cooling medium being relied upon to dissipate the heat. With platinum the current densities reached were comparatively small, but the apparent deviation from Ohm's law was large enough to measure accurately. In order to make a comparison between the observations it was essential not to submit the film to any treatment that caused a permanent change in its properties. Thus great care had to be taken to immerse the film in the liquid air gradually.

(*b*) *Procedure in making the Measurements.*

The galvanometer was short-circuited with the link K_3, and then both D.C. and A.C. were admitted to the bridge by closing keys K_1 and K_2. A balance was first made with the telephones, and if, after opening the link K_3, the galvanometer showed a deflexion, the slider was re-set for the D.C. balance. Generally the observations were repeated several times before recording them. The voltage output and frequency of the valve oscillator were also noted, together with the resistances and capacity in the wires connecting to the bridge. This enabled the A.C.

through the conductor under test to be calculated. Representing the constants of the circuit by symbols as indicated in fig. 3, it is easy to show that the alternating current I_a through the metal film is given by :—

$$I_a = \frac{QV}{\left(P+R\right)\sqrt{\left(Q^2+\frac{1}{\omega^2C^2}\right)\left(\frac{N+r}{r}\right)^2+2QN\left(\frac{N+r}{r}\right)+N^2}},$$

where

$$Q=\frac{(R+P)S}{R+P+S} \quad \text{and} \quad \omega=2\pi \text{ (frequency)}.$$

Fig. 5.

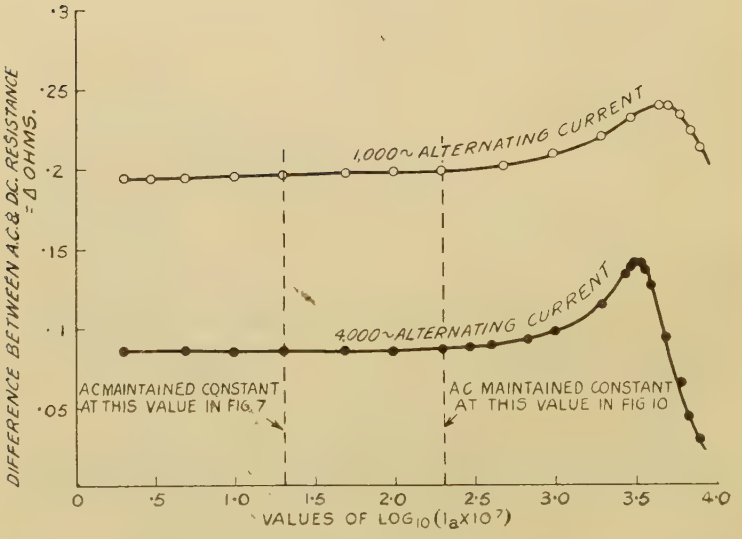

Platinum film, $16{\cdot}5\times10^{-6}$ cm. thick. Section $2{\cdot}47\times10^{-7}$ cm.^{2}
Film immersed in absolute alcohol at room temperature.
Constant direct current $=0{\cdot}024$ amp. $=0{\cdot}97\times10^5$ amp. per cm.^{2}

The value of the D.C. was obtained by removing the link K_4 across the milli-ammeter, which was in series with the film.

For each specimen preliminary tests were made with a small D.C., and under these conditions the balance position as shown by the galvanometer always agreed exactly with the balance position obtained with the telephones.

If x_1 and x_2 represent the distances from the balance point to the right-hand end of the slide wire (see fig. 3) for the direct current and alternating current respectively, then the difference between the A.C. and D.C. resistances of the conductor under test is given by :

$$\Delta = Pl\left(\frac{x_1 - x_2}{x_1 x_2}\right)$$

where l = total length of the slide wire.

Fig. 6.

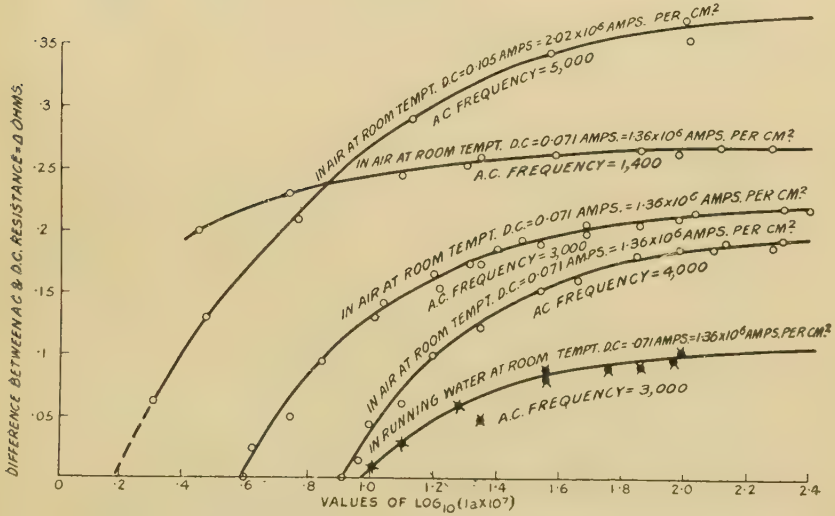
DIFFERENCE BETWEEN A.C. & D.C. RESISTANCE = Δ OHMS.
·35
·3
·25
·2
·15
·1
·05
0
·2
·4
·6
·8
1·0
1·2
1·4
1·6
1·8
2·0
2·2
2·4
VALUES OF LOG10(1a x 10⁷)
IN AIR AT ROOM TEMPT. D.C = 0·105 AMPS = 2·02 x 10⁶ AMPS. PER CM.²
A.C. FREQUENCY = 5,000
IN AIR AT ROOM TEMPT. D.C = 0·071 AMPS. = 1·36 x 10⁶ AMPS. PER CM.²
A.C. FREQUENCY = 1,400
IN AIR AT ROOM TEMPT. D.C = 0·071 AMPS. = 1·36 x 10⁶ AMPS. PER CM.²
A.C. FREQUENCY = 3,000
IN AIR AT ROOM TEMPT. D.C = 0·071 AMPS. = 1·36 x 10⁶ AMPS. PER CM.²
A.C. FREQUENCY = 4,000
IN RUNNING WATER AT ROOM TEMPT. D.C = ·071 AMPS = 1·36 x 10⁶ AMPS. PER CM.²
A.C. FREQUENCY = 3,000

Gold film 9×10^{-6} cm. thick. Section $= 5{\cdot}2 \times 10^{-8}$ cm.^{2}

All the measurements were made with relatively small alternating currents, so that the D.C. balance was not appreciably altered by interrupting the A.C. supply.

(c) *Experimental Results.*

The curves figs. 5 and 6 show the manner in which the observed difference between the A.C. and D.C. resistances of the metal film varied with the magnitude of the alternating current passing through the film. The logarithm of the current has been plotted in order to cover the range within a reasonable space. The smallest alternating current that could be used to give sufficiently reliable

results was 2×10^{-7} amp., and the largest employed was 8×10^{-4} amp., the latter representing about one-thirtieth part of the D.C., this relative value being roughly the same as that used by Bridgman throughout his work.

It will be seen that in the case of platinum there was a curious increase in the difference between the A.C. and D.C. resistances for comparatively large alternating currents, but there was no indication that the effect would

Fig. 7.

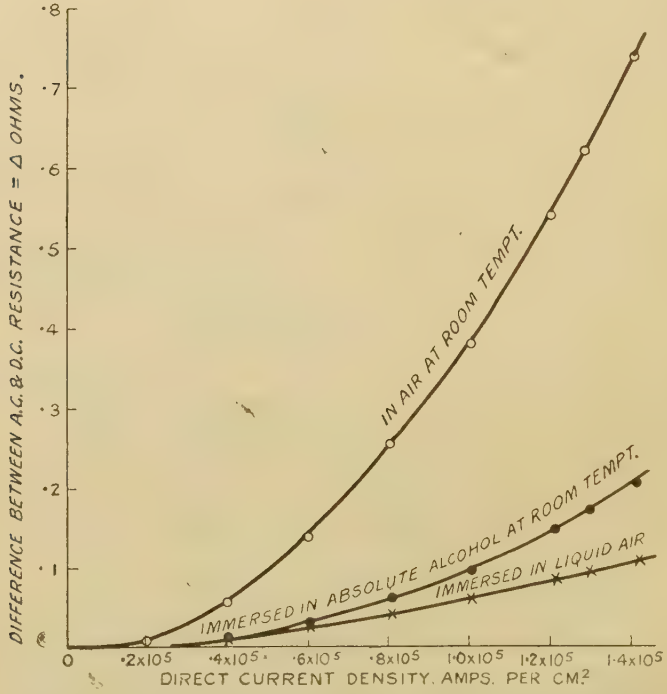

Platinum film $16{\cdot}5\times10^{-6}$ cm. thick. Section $2{\cdot}47\times10^{-7}$ cm.²
Constant A.C. $=2\times10^{-6}$ amp. $=8{\cdot}1$ amp. per cm.² Frequency $=4000$.

ultimately disappear with the smallest currents employed. On the other hand, with the gold film the difference between the A.C. and D.C. resistances became zero in some cases within the range of measurement, and in others showed definite signs of rapidly approaching that value at the lower end of the scale.

Fig. 7 refers to the platinum film with various cooling media, and shows the difference between the A.C. and D.C

resistances as a function of the direct-current density. The A.C. had a value of about 2×10^{-6} amp. throughout this test, and the frequency was kept constant at 4000. Assuming a temperature coefficient of resistance for platinum of $36{\cdot}5 \times 10^{-4}$, a calculation was made for the rise in temperature of the film. It was found that this rise in temperature was always directly proportional to the measured difference between the A.C. and D.C. resistances, suggesting that if the heating effect of the current could be completely eliminated there would be no apparent deviation from Ohm's law.

In attempting to deduce figures for the difference between the A.C. and D.C. resistances at infinite frequency

Fig. 8.

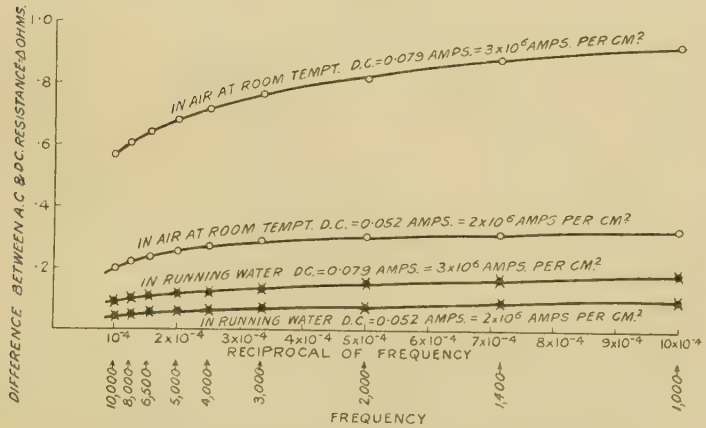
DIFFERENCE BETWEEN A.C. & D.C. RESISTANCE-OHMS.
1·0
·8
·6
·4
·2
IN AIR AT ROOM TEMPT. D.C.=0·079 AMPS.=3x10⁶AMPS. PER CM.²
IN AIR AT ROOM TEMPT. D.C.=0·052 AMPS.=2x10⁶AMPS PER CM.²
IN RUNNING WATER D.C.=0·079 AMPS.=3x10⁶ AMPS. PER CM.²
IN RUNNING WATER D.C.=0·052 AMPS.=2x10⁶ AMPS PER CM.²
10⁻⁴ 2x10⁻⁴ 3x10⁻⁴ 4x10⁻⁴ 5x10⁻⁴ 6x10⁻⁴ 7x10⁻⁴ 8x10⁻⁴ 9x10⁻⁴ 10x10⁻⁴
RECIPROCAL OF FREQUENCY
10,000 8,000 6,500 5,000 4,000 3,000 2,000 1,400 1,000
FREQUENCY

Gold film 5×10^{-6} cm. thick. Section $= 2{\cdot}5 \times 10^{-3}$ cm.²
Constant A.C. $= 2 \times 10^{-5}$ amp. $= 800$ amp. per cm.²

the curves shown in figs. 8, 9, and 10 were obtained. The highest frequency employed by Bridgman was 3750, whereas in the author's experiments with gold measurements were made at 14,000 frequency.

The platinum film was, unfortunately, broken before the frequency was taken above 5000, but the results (fig. 10) serve to show the influence of the different cooling media. The effect of frequency is very much greater in air at room temperature than in liquid air.

The A.C. was kept as nearly as possible constant during these tests, having the value 2×10^{-5} amp. for the platinum

film, 2×10^{-5} amp. for one of the gold films, and 3×10^{-5} amp. for the other gold film.

It will be seen that all the curves bend over rapidly towards the origin, and any extrapolation is subject to serious error.

The specimen of gold to which the curves shown in fig. 8 refer was cut from a specially thin part of the leaf (estimated at about 5×10^{-6} cm. thick), and it was possible in this case to reach a current density of about 3×10^{6} amp./cm.^{2} with only the surrounding air for dissipating

Fig. 9.

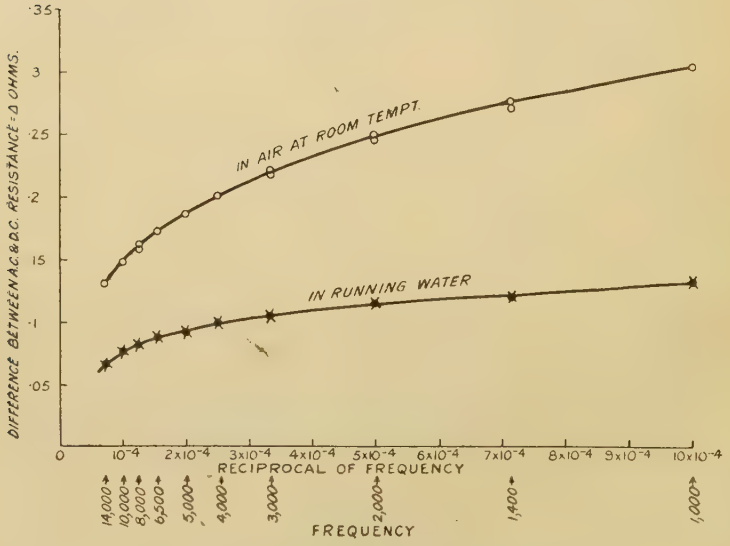

Gold film 9×10^{-6} cm. thick. Section $5{\cdot}2\times10^{-8}$ cm.^{2}
Constant D.C. $=0{\cdot}0707$ amp. $=1{\cdot}36\times10^{6}$ amp. per cm.^{2}
Constant A.C. $=3\times10^{-5}$ amp. $=577$ amp. per cm.^{2}

the heat. With a stream of distilled water for cooling, and the same current density, the difference between the A.C. and D.C. resistances was very much smaller.

Bridgman produced his curves with a straight line from the point corresponding to a frequency of 3750 to the vertical axis. Evidently this leads to entirely erroneous results, and, in any case, would give different values for the intercept on the vertical axis with the same current density when using natural air cooling and water cooling.

Conclusion from Experiments.

The foregoing observations prove that Ohm's law is rigidly true for a gold conductor carrying a current of density 2×10^6 amp. per sq. cm., and leave little room for doubt that the law is equally true at 3×10^6 amp. per sq. cm.

Fig. 10.

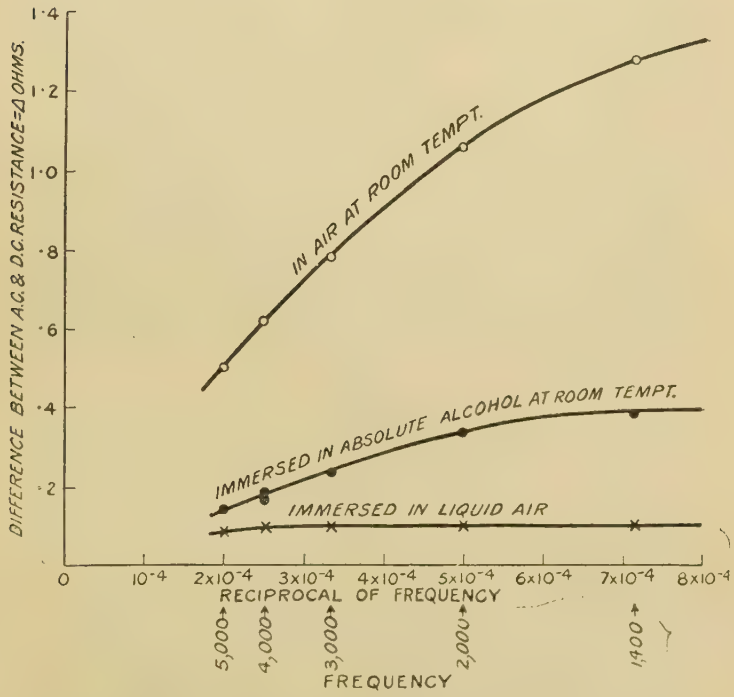

Platinum film $16{\cdot}5 \times 10^{-6}$ cm. thick. Section $2{\cdot}47 \times 10^{-7}$ cm.^{2}
Constant D.C. $= 0{\cdot}032$ amp. $= 1{\cdot}3 \times 10^5$ amp. per cm.^{2}
Constant A.C. $= 2 \times 10^{-5}$ amp. $= 81$ amp. per cm.^{2}

The same conclusion is indicated for platinum at a current density of $1{\cdot}3 \times 10^5$ amp. per sq. cm.

Discussion of Results.

Suppose that a curve (fig. 11) is plotted giving the change of P.D. across the metal film for various direct currents passing through it. The gradient of this curve

OMWN increases, due to the rising temperature with increase of current.

Now let a small A.C. be superposed on the D.C. If the frequency were sufficiently low, the corresponding alternating potential variations would be expected to follow the static characteristic, that is, along the line MWN.

Fig. 11.

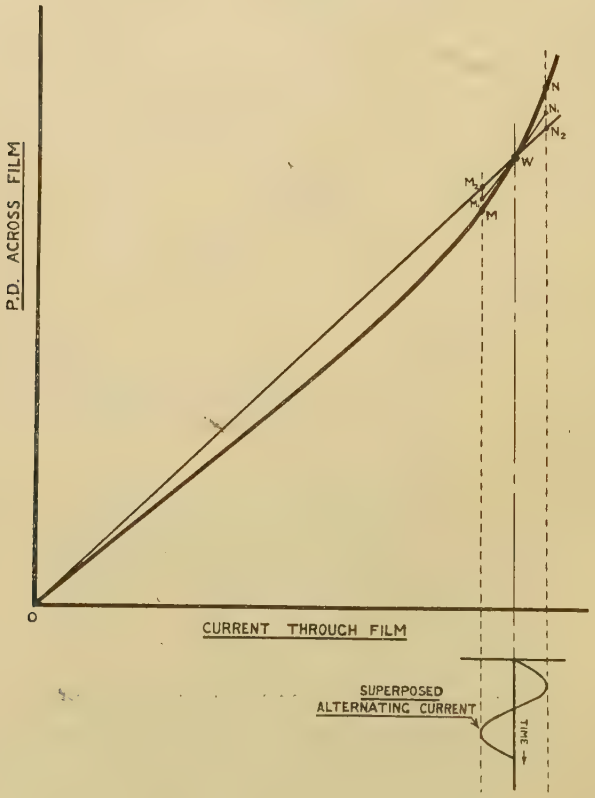

Assuming that Ohm's law is strictly true, then the higher the frequency the more nearly will the potential variation approximate to the straight line through W from the origin, that is, M_2WN_2. For audible frequencies such as can be employed in these experiments, the alternating potential variation probably follows some curve such as M_1WN_1.

Again, the smaller the value of the alternating current the less it will influence the temperature of the conductor, so that the A.C. balance of the bridge is brought nearer to the D.C. balance. Bridgman, in analysing his experiments, assumed a sinusoidal variation of resistance with the alternating current. The author's observations on the effect of decreasing the magnitude of the A.C. suggest that Bridgman's hypothesis does not really represent the facts. During the tests the conductor was necessarily always at a higher temperature than its surroundings, and any reduction in current tended to produce a fall in temperature which was more rapid than the corresponding rise accompanying an increase of current.

In all cases the more efficient the cooling the smaller the difference between the A.C. and D.C. resistance.

As one would expect, it was only possible to get a minimum sound in the telephones for the A.C. balance, and this minimum was always sharper the less the values of the direct and alternating currents. Moreover, the A.C. balance was greatly improved by immersing the conductor in a good cooling medium such as water or liquid air.

In conclusion, the author desires to express his thanks to Prof. W. C. Clinton for placing the apparatus in the Pender Laboratory at his disposal.

University College, London.
February, 1930.

XCVI. *Notices respecting New Books.*

Speech and Hearing. By Dr. Harvey Fletcher. [Pp. xv+331, with 154 figures.] (New York: D. van Nostrand Co.; London: Macmillan & Co. 1929. Price 21*s.* net.)

FIFTEEN years ago a systematic investigation of speech and hearing was commenced in the Research Laboratories of the Bell Telephone System with a view to obtain data upon which to base the design of telephone apparatus. The investigation was planned on a comprehensive scale, and is still far from finished; as it has proceeded, many new problems requiring investigation have arisen. The investigation commenced with a study of the

constitution of speech in order to establish a description of average speech and to ascertain to what extent intelligibility was affected by small variations and imperfections in speech. A necessary adjunct was a study of the human ear and its mechanical operation.

As the investigation progressed the necessity of the design of better and more precise instruments than were already available became apparent. The problem of obtaining a reliable record of a complex sound was solved by means of electrical apparatus consisting of condenser, microphone, amplifier, and a special oscillograph. Apparatus was designed by means of which sound-waves can be converted into electrical form and reconverted again to sound with the least possible distortion. There are many examples in this book of beautiful experimental technique which emphasize the wide applications of the thermionic valve in acoustic problems.

For the measurement of the degree of precision with which speech sounds can be recognized and differentiated an essentially perfect reproduction system was employed which could be deteriorated step by step until the faults became noticeable; an estimate was made of the degree of dissatisfaction produced by measured imperfections.

The volume is divided into four parts. Part I. is devoted to speech, including the mechanism of speaking and the characteristics of speech waves. Many examples of speech waves, in the form of photographic oscillograms, are given. Part II. deals with the physical properties of musical sounds and of noise. Part III. is concerned with hearing; it includes an account of the mechanism of hearing, limits of audition, minimum perceptible differences in sound, and the methods by which acuity of hearing may be tested. Part IV. is entitled perception of speech and music; it is devoted mainly to the methods of measuring the recognition of speech sounds and to the effects of intensity changes of frequency distortion and of other types of distortion and of noise and deafness upon the recognition of speech sounds.

It is of interest to note that many of the instruments devised in connexion with these researches have found important commercial applications. "A surprising number of modern acoustical accomplishments have come about through the use of slightly modified forms of apparatus which was originally developed for these investigations. Modern phonographic records are produced with an electrical transmitter which was developed in the very early stages of these studies; and radio broadcasting has grown up around this same 'microphone.' The reproducing equipment of the modern phonograph and of the radio were predicated directly upon these investigations; and talking motion pictures owe their success and much of their apparatus to this same source."

Dr. Fletcher is to be congratulated upon such a fascinating account of an important series of investigations.

The Life and Work of Sir Norman Lockyer. By T. Mary Lockyer and Winifred L. Lockyer, with the assistance of Prof. H. Dingle and contributions by Dr. Charles E. St. John; Prof. Megh Nad Saha, F.R.S., Sir Napier Shaw, F.R.S., Prof. H. N. Russell, the Rev. J. Griffith, Sir Richard Gregory, and Prof. A. Fowler, F.R.S. [Pp. xii+474, with 17 plates.] (London: Macmillan & Co. 1928. Price 18*s.* net.)

The first half of this volume consists of a general biography of Sir Norman Lockyer, written by Prof. Dingle from material compiled by Lady Lockyer and Miss Lockyer. It presents the main facts of Lockyer's life, but as a biography it is singularly unsatisfying. The narrative is unrelieved by a single anecdote, and contains few extracts from letters written by Lockyer. It presents to us Lockyer the scientist, but not Lockyer the man.

The second portion consists of chapters contributed by several writers in appreciation of Lockyer's astronomical, archæological, and general scientific work. Of Lockyer's wholehearted and unselfish devotion to the cause of science, and of his far-sighted realization of the importance of scientific education and research to the industry and commerce of the country, there can be no denial. Science owes much to him for his unsparing advocacy of its importance for national advancement. Lockyer will also be remembered as the founder and first editor of 'Nature,' which he nursed with persistent devotion through a long period of struggle. It is difficult to realize at the present time that for thirty years this publication was not a financial success.

Lockyer's astronomical work is a curious mixture of grain and chaff. We can see now what was of permanent value in it and what was not, but it is more than doubtful whether Lockyer himself would have appraised his work in the same way. He was very prone to advance theories on incomplete and inconclusive evidence, and he therefore failed to influence current astronomical thought as he otherwise might have done. His laboratory work was of greater importance than his speculations, and his studies of the spectra of elements under varying conditions are of permanent value.

National Physical Laboratory. Collected Researches. Vol. xxi. 1929. (His Majesty's Stationery Office. Price £1 2*s.* 6*d.*)

The researches brought together in this volume have, with one exception, appeared in the 'Proceedings of the Royal Society,' 'The Philosophical Magazine,' and other journals during the last three or four years. Members of the Electrical Department of the National Physical Laboratory and the Radio Research Board have contributed papers dealing with problems connected with the propagation of radio waves, the attenuation due to the resistance of the earth, errors in direction-finding, and measurements on waves received from the upper atmosphere. Several

papers included in this collection have an indirect bearing on wireless waves—piezo-electric quartz resonator, improved cathode ray-tube, and the measurement of inductances and capacities. The first paper gives a detailed description of the new standard of mutual inductance constructed at the National Physical Laboratory for presentation to the Japanese Government, the former standard having been destroyed in the 1923 earthquake.

Dipolmoment und Chemische Struktur. Herausgegeben von Prof. Dr. P. Debye. Leipziger Vorträge. 1929. Kartoniert R.M. 9. (Verlag von S. Hirzel in Leipzig.)

In Prof. Debye's recently published book on Polar Molecules a considerable number of experimental results on the determination of molecular moments are given and compared with the calculations derived from the theoretical formulæ. These include the work of Errera on the molar polarization of free molecules and the relation between dissymmetry and chemical structure; Sänger on the determination of electric moments for gases and vapours using the temperature effect, and the polarization of mixtures; and Höjendahl's experiments to establish the connexion between the arrangement of atoms and the dissymmetry measured by the electric moment. Their later researches and those of Wolf, Ebert, and others are brought together in the present volume. Estermann's paper on the application of the molecular ray method for the measurement of molecular polarization is of special interest. The first experiments of this kind were undertaken by Wrede on the alkali salts. Estermann has developed and improved the experimental arrangements, and applied the method to a number of organic compounds. This collection of experimental data will be of service in keeping research workers in touch with the recent developments in the study of chemical structure, based upon Debye's dipole theory.

Einführung in die Wellenmechanik, Louis de Broglie. Übersetzt von Rudolf Peierls. Geb. R.M. 13.80. (Akademische Verlagsgesellschaft, m.b.H., Leipzig.)

The development of wave mechanics has proceeded at a rapid rate during the last three or four years, and notable contributions have been made by de Broglie, Schrödinger, and others. This volume gives an orderly and systematic account of the new mechanics, the theoretical basis for the understanding of atomic phenomena. In the preface the author has reproduced the paper read at the Glasgow meeting of the British Association. The subject is presented in the order of its development—the earlier dynamical theories, the analogy between dynamics and optics, the association of wave propagation with the motion of a particle, and the derivation of the Schrödinger differential equation of the wave function. Examples of wave motion are given in the case of

vibrating strings and membranes, rectangular and circular, followed by the determination of energy levels for the rotator, the harmonic oscillator, and the hydrogen atom whose eigen functions are the polynomials of Legendre, Hermite, and Laguerre. The experiments of G. P. Thomson on the diffraction of cathode rays through metal films are described in detail, and show close agreement with the wave mechanical theory. Brief reference is made to the work of Rupp, who has investigated this problem by photographic and electrical methods. Recent experiments on the relative intensities of the Stark components in hydrogen also show a remarkable agreement with Schrödinger's theoretical calculation. No better introduction to the study of wave mechanics can be recommended to students of modern physics, who require a clear exposition of the new theory and its application to atomic problems. An English translation would deservedly bring the book within the reach of a wider circle of readers.

XCVII. *Proceedings of Learned Societies.*

GEOLOGICAL SOCIETY.

[Continued from p. 864.]

January 22nd, 1930.—Prof. J. W. Gregory, LL.D., D.Sc., F.R.S., President, in the Chair.

THE following communication was read :—

'The Geology of some Salt-Plugs in Laristan (Southern Persia).' By John Vernon Harrison, B.Sc., F.G.S.

The area under consideration is contained in the rectangle between lat. 27° and lat. 28° 20′ N. (85 miles) and between long. 54° 20′ and long. 57° E. (175 miles). The two main towns are Bandar Abbas and Lar.

Much of this district is covered by normally folded rocks which range in age from Ordovician to Recent, and reach an aggregate thickness of as much as 25,000 feet. The lowest 1000 feet are chiefly shales and sandstones. From Carboniferous to Middle Miocene there are about 13,000 feet of strata which are mainly limestones. The silt, sand, and conglomerate of the Mio-Pliocene together reach a thickness of 11,000 feet. The only general angular unconformity occurs high in the Mio-Pliocene. On the north and east the frontal part of the nappes overrides and ploughs into the normally folded rocks.

South and west of the line of nappes the normal folds have been invaded by plugs of salt, which have brought up quantities of

gypsum and blocks of sedimentary and igneous rocks. The extrusive salt has come to the surface at different times, from Oligocene to late Mio-Pliocene. The intrusive salt-masses, sheathed with autochthonous sediments tilted around them, form in some cases brightly coloured mountains of very striking and characteristic appearance.

Where the sedimentary sheath has been broken or removed by erosion, tongue-like masses of salt and gypsum have moved outwards from the salt dome, and these are described as salt-gypsum 'glaciers'. Erosion has sometimes entirely removed the soluble upper portions of a salt-plug and left a corrie-like valley in a limestone hogback. In such a case the corrie-floor is covered with a layer of the insoluble material which has accompanied the salt to the surface.

This jumbled assemblage of rocks is designated the Hormuz Series. They comprise fœtid dolomites and limestones, dark calcareous shales, red sandstone and shale, variegated shales and sandstones, and igneous rocks which range from granite-porphyry to basalt, all more or less epidotized. Dr. G. M. Lees first found Cambrian trilobites in the dark shales, and since then other geologists have discovered them in several other localities. The Hormuz Beds are believed to lie directly on the salt which has brought them to the surface, so that the salt and gypsum of the salt-plugs must be older than Middle Cambrian.

The formation of the salt-plugs is attributed to tangential forces acting on Cambrian salt, which, on account of its comparative plasticity, has acted as something analogous to an igneous magma in its behaviour.

February 21st, 1930.—Prof. J. W. Gregory, LL.D., D.Sc., F.R.S., President, in the Chair.

In dealing in his Anniversary Address with the Geological History of the Pacific Ocean, the President remarked that widespread faith in the unity and permanence of the Pacific Ocean has been based on many features, such as its simple trigonal form, its marginal earthquake-zone, its volcanic girdle, and its coastal structure. The theory was rejected by Huxley in his Presidential Address to this Society in 1870. The view that the Pacific Basin is the hollow left when the moon was torn away from the Earth is untenable, as the moon is 37 times too big and 20 per cent. too heavy. The standard geological theory of the origin of the Pacific is that of Suess, who inferred, from the parallelism of the surrounding mountains, its unity of origin, and from the widespread marine Triassic rocks on the coasts, its Triassic age.

The geological evidence indicates, not a persistent Pacific Ocean, but a succession of variable narrow seas separated by land, and frequently with a predominant trend of west and east. Thus in the Lower Cambrian the *Olenellus* Sea on the north was separated from the *Redlichia* Sea on the south-west; in the Middle Cambrian one

sea spread from the Himalaya to the Rocky Mountains, and an arm of it in the Upper Cambrian overspread Eastern Australia. The whole of the Southern Pacific from New Zealand to South America may have been land, for the only Cambrian in South America was an arm of the Atlantic.

The Ordovician of Pupiao in Southern China has 'scarcely any trace of an American element', the fauna there is European. China and Western America had no direct marine connexion.

In the Devonian Period the East Indies and the China Sea were occupied by a land that extended into the Western Pacific and bounded the sea by which the European fauna reached South-Eastern China and Tongking. In the Middle Devonian the sea with the *Flabellites* fauna lay along western South America and in the valleys of the Amazon and Mississippi; but it did not reach Australia, where, in Upper Devonian times, the Chemung fauna of New York invaded New South Wales. The absence of this fauna from Asia and California shows the separation of the north-western and south-eastern Pacific seas.

The Carboniferous had the same separation of the Asiatic and West American marine faunas, and evidence of land is given by *Gigantopteris*, a member of the Gondwana flora, which is found in Southern and Eastern China and in Texas, and doubtless entered both from a Pacific land.

The Trias has a wide range around parts of the Pacific, but was deposited in separate seas—an Arctic Ocean with a gulf to British Columbia; the western end of a South European sea which reached Venezuela and Southern California; the eastern end of the same sea which extended past the Himalaya to New Zealand. It is represented in New Zealand by a distinct province in a gulf, and not the opening to a Pacific Ocean. Evidence of Transpacific lands in the Trias is given, according to F. von Huene, by the affinities of the Triassic reptiles of South America to those of India.

The Jurassic was the time of the main development of the Pacific Continent of Haug. The Liassic Sea of the North Pacific was separated from the contemporary seas in Central and South America. The Malm fauna of Chile ranged westwards to the Himalaya, but was different from that of the North Pacific and the European fauna in the Antillean region. The Pacific region in Upper Jurassic times, according to Uhlig, was occupied by faunas of four geographical provinces.

In the Cretaceous shallow water connected California and India, while later a land separated the Senonian fauna of California and Japan from that of Chile and New Zealand. The North Pacific was crossed by the giant Sauropods in their range between Mongolia and Montana, and a land-route in a suitable latitude was used thrice later by large quadrupeds. The South Pacific was crossed in the Cretaceous Period by reptiles that migrated between South America and Asia, as the route by way of North and Central America was not then available. Lands west of America allowed the diffusion of the Dakota flora (Turonian) southwards to the Argentine.

In the Kainozoic Era Transpacific lands seem to have lasted until the Oligocene or early Miocene, since the alligator, various reptiles, amphibia, insects, crayfish, land-mollusca, primitive mammals, etc., indicate routes of migration across the tropical and warm temperate zones. Land-plants show the same, for Asa Gray pointed out how much is common to the floras of China and to those of the southern humid areas of the United States. *Gordonia*, one of the plants with this distribution, helps to fix the date of the migration, as it has recently been discovered in the Miocene strata of the Rocky Mountains.

The occurrence of similar animals and plants on opposite sides of the southern oceans has been explained by their origin in a northern land or by their independent evolution. The northern monopoly of evolution is opposed by the theory of Ernst Schwarz of the southern origin of the mammals, and the evidence of the development of numerous animals and plants in the southern lands. The evidence of parasitology renders the alternatives to the spread of some animals across the Southern Pacific, according to Launcelot Harrison, 'merely grotesque'.

The life of the Pacific islands, according to many authorities, can only be explained by the existence of extensive Pacific lands on which developed a Eu-Pacific fauna and flora. These lands must have been connected with Polynesia and Australia, and were probably united to the former extension of the Andes to the north-west of Peru; according to Steinmann, his Chimu-andes extended to Hawaii and Polynesia, and were cut off from South America at the end of the Eocene Period.

The coral-islands and the circum-Pacific river-systems also constitute evidence in favour of a subsidence of the Pacific area in the Middle and Upper Kainozoic Eras.

The evidence of the sedimentary rocks that the crust subsides to amounts up to 50,000 feet is opposed to that extreme form of isostasy which denies the possible uplift of an ocean-floor. The arguments in favour of that view, based on a sub-oceanic heavy stratum, as proved by the distribution of igneous rocks, gravity observations, and the speed of earthquake-waves, rest on assumptions so doubtful that geologists should be guided by the direct geological evidence.

February 26th, 1930.—Prof. E. J. Garwood, M.A., Sc.D., F.R.S., President, in the Chair.

The following communication was read:—

'The Glaciation of Western Edenside and Adjoining Areas, and the Drumlins of Edenside and the Solway Basin.' By Sydney Ewart Hollingworth, M.A., B.Sc., F.G.S.

The first part of this paper deals with the glaciation and deglaciation of Western Edenside and of the eastern and north-

eastern parts of the Lake District. In the lowland areas the threefold sequence[1] of Early Scottish, Lake District–Edenside, and late Scottish glaciations is recognized. Almost the whole of the deposits are referable to the maximum of the second or main glaciation. At that time, Edenside acted not merely as a reservoir into which ice moved from the surrounding high ground, but was, with the latter, part of one vast area of accumulation. A great flood of ice travelled anti-clockwise around the northern end of the Lake District—first northwards towards the Solway, and then westwards and south-westwards into the Irish Sea Basin; it was joined en route by ice from the Lake District valleys. Other outlets were the Tyne Gap,[2] Stainmore, and the Lune Valley.

Some twenty stages in the retreat from the Eden back to the valley-glacier stage are recognized, those associated with the retreat from the Penrith Sandstone escarpment being particularly well defined. Although the ice in the lower ground received supplies from the hills throughout, movement during the later phases of the retreat was subordinate to decay, and in several areas the evidence suggests that lobes of ice died away *in situ* by progressive thinning.

The ice-fronts were, during the retreat, parallel to the trend of the drumlins over extensive areas. This unexpected result led to the study of the drumlins of the much wider area, embracing all Edenside and the Solway Basin, which forms the second part of the paper. It is shown conclusively that the drumlins were formed at the maximum of the Main or Lake District–Edenside glaciation and not—as has been frequently claimed for other areas—at a late stage. With rare exceptions, they show no evidence of modification by such transverse movements of ice as occurred during the phase of retreat. Even in the area south of the Solway that was covered by the Scottish Re-advance Ice, most of the drumlins are not due to that ice, but belong to the Lake District–Edenside maximum.

The existence is established of a parting or shed in the ground-ice of the low ground across Edenside near Appleby, from which the lower layers moved outwards, towards Stainmore and down Edenside, and a second similar shed near Carlisle, from which the ice moved eastwards and westwards. These ground-ice partings are independent of the position of the surface ice-sheds. When considered in conjunction with the boulder-dispersal, they imply extensive differential movements within the main body of the Edenside ice, and have important bearings on the movement of ice in general, and on glacial erosion.

Prof. W. T. Gordon exhibited a set of cellulose 'pulls' from coal-balls, on behalf of Mr. James Lomax, of Bolton. In doing so, he reminded Fellows that Mr. John Walton of

[1] & [2] See also F. M. Trotter, 'The Glaciation of Eastern Edenside, the Alston Block, & the Carlisle Plain,' Q. J. G. S. vol. lxxxv. (1929) pp. 549–612.

Manchester University and Dr. D. Koopmans of Heerlen had devised the process, and the former had given a description of the technique to the Society last session.[1] Since the discovery, several investigators had tried out the method, and the results obtained by Mr. Lomax represented some of the largest and best sections of coal-balls yet produced.

The essence of the process was the replacement of the matrix of the petrification by cellulose, and, in order to effect this, the surface of the fossil was smoothed and polished (the polish need only be a dull polish). If this surface was etched with hydrofluoric, hydrochloric, acetic, chromic, or other acid suited to the type of petrifaction, the etching produced a 'furry' surface, where the 'fur' was the insoluble part of the fossil and held together sufficiently well, so as not to crumble, when it was gently washed by immersion in water. The etching was continued to the extent desired, and, after washing and drying, a layer of cellulose in amyl acetate or cellulose acetate in acetone, or such other preparation as will give a cellulose film when it dries, was spread over the 'fur.' When thoroughly dry, the film could be stripped off, taking the 'fur' with it. In the case of plant-remains the 'fur' consisted, in part at all events, of carbon, and the cellulose was merely a new matrix replacing the old one of silica or calcite, etc. The film was then mounted in Canada balsam, or, as the specimens on exhibit, on paper, or on glass. One difficulty sometimes encountered was the presence of bubbles in the celluloid film.

Prof. Gordon further described a new technique which had been developed by Dr. B. F. Barnes & Mr. H. Duerden, of Birkbeck College. In it the cellulose film was made as in the Walton-Koopmans process; it was flattened by immersion in alcohol, then the back was coated with egg-albumen, and the whole laid on a glass slide. On hardening, the film was in close contact with the glass surface, and the cellulose was then removed by amyl acetate. Thus the original matrix was now replaced by egg-albumen, and the section rendered perfectly transparent. The process was completed by covering with Canada balsam and a cover-slip. This process will shortly be described by the two above-mentioned authors.

In conclusion, he said that it was possible to make fifty sections from 2 mm. thickness of material, and that a transverse, a longitudinal radial, and a longitudinal tangential section could be made at one and the same time by suitably squaring up the original specimen.

[1] Abstr. of Proc. No. 1189, December 13th, 1928, p. 16.

[*The Editors do not hold themselves responsible for the views expressed by their correspondents.*]